GIS-Based Models for Optimisation of Marine Cage Aquaculture in Tenerife, Canary Islands

Thesis submitted for the degree of
Doctor of Philosophy

by

OSCAR PÉREZ MARTÍNEZ

Institute of Aquaculture
University of Stirling
Stirling FK9 4LA
Scotland

ORIGINALITY STATEMENT

I declare that the work contained in this dissertation is my own, and where the work of others has been used it has been properly cited

....
Oscar Pérez Martínez

DEDICATION

To my family,
for their constant love and support.

To Patricia, my baby sister,
you make my days better..!!

To Tenerife,
..."mi tierra, mis raices"...

ACKNOWLEDGEMENTS

I would like to thank my supervisors Prof. Lindsay Ross and Dr. Trevor Telfer for their support, useful comments and criticism during this project. Also, I am grateful for their efforts in trying to understand and correct my "*Spanglish*", not an easy task..!!

I acknowledge, in alphabetical order, the following institutions and people for their contribution and help in the development of this project. CREPAD, for providing the NOAA-AVHRR satellites images and their assistance with the image processing. Dr Manuel Arbelo for his valuable suggestions and guidelines in the AVHRR satellite image processing. The Spanish Department of Maritime Climate (Departamento de Clima Marítimo) for providing the wave data. Tenerife Council (Excmo. Cabildo de Tenerife) for the valuable use of their CD-Map information.

This work was carry out as part of a European Community training project financed by the European Commission under the FAIR program (GT 973516).

I express my appreciation to Ei Lin Ooi, "*la china*", for her encouragement and support during the concluding parts of this project, and also, her invaluable help with the writing up.

I would like to thank my office-mates in the GIS lab (Philip Scot, Abdus Salam, Matias del Campo and Martin van Brakel) for their constant support, motivation, and for "*putting up*" with my moods, my music and me. I hope that you won't hate Jimi Hendrix for the rest of your life..!!. In addition, I would like to extent my gratitude to all my friends at the Institute of Aquaculture, our daily lunch-times were always a laugh..!!. I especially would like to thank my very best friend Ioannis Vatsos for his unconditional friendship, you made this place more easy going.

Abstract

This study focused on the optimisation of offshore marine fish-cage farming in Tenerife, Canary Islands. The main objective was to select the most suitable sites for offshore cage culture. This is a key factor in any aquaculture operation, affecting both success and sustainability. Moreover, it can solve conflicts between different coastal activities, making a rational use of the coastal space. Site selection was achieved by using Geographical Information Systems (GIS) based models and related technology, such as satellite images and Global Positioning System (GPS), to support the decision-making process. Three different cage systems were selected and proposed for different areas around Tenerife. Finally, a particulate waste distribution model (uneaten feed and faeces) was developed, also using GIS, for future prediction of the dispersive nature of selected sites. This can reduce the number of sites previously identified as most suitable, by predicting possible environmental impacts on the benthos if aquaculture was to be developed on a specific site.

The framework for spatial multicriteria decision analysis used in this study began with a recognition and definition of the decision problem. Subsequently, 31 production functions (factors and constraints) were identified, defined and subdivided into 8 submodels. These submodels were then integrated into a GIS database in the form of thematic layers and later scored for standardization. At this stage, the database was verified by field sampling to establish the quality of data used. The decision maker's preferences were incorporated into the decision model by assigning weights of relative importance to the evaluation under consideration. These, together with the thematic layers, were integrated by using Multicriteria Evaluation (MCE) and simple overlays to provide an overall assessment of possible alternatives. Finally, sensitivity analysis was performed to determine the model robustness. The integration, manipulations and presentation of the results by means of GIS-based models in this sequential and logical flow of steps proved to be very effective for helping the decision-making process of site selection in study. On the whole, this study revealed the usefulness of GIS as an aquaculture planning and management tool.

Cage systems that can withstand harsh environments were found to be suitable for use over a broader area of Tenerife's coastline. Thus, the more robust self-tensioned cage (SeaStation®) could be used over a greater area than the weaker gravity cages (Corelsa®). From the 228 km^2 of available area for siting cages in the coastal regions with depth of 50 m, the suitable area (sum of scores 6, 7 and 8) for siting SeaStation® cages was 61 km^2, while the suitable area for SeaStation® and Corelsa® cages was 49 and 37 km^2 respectively. Most of the variation between these three cage systems was found among the intermediate suitability scores. It was concluded that the biggest differences in suitable area among cage systems are between Corelsa® and SeaStation® systems, followed by differences between Corelsa® and OceanSpar® cages, and OceanSpar® and SeaStation® respectively. This variability was mostly located on the N and NNW of the island, where waves, both long and short-term, are higher.

List of Contents

List of Tables

List of Figures

Chapter 1

Introduction

1.1 GENERAL INTRODUCTION

As the world population increases, pressure on natural resources to maintain this growth also increases. Many of the natural resources on land and sea are already over-exploited or at their maximum production levels (Coll, 1991). Therefore, there is a need to increase existing food stocks by improving production technologies or by utilizing new resources.

In particular, the fishery sector is beginning to realise a rapid decrease in natural stocks. In the near future, the increase in fish demand will be greater than that available for capture. Therefore, it is necessary to find some alternative or complementary source to meet this deficiency. Aquaculture has become a realistic and practicable source of food protein, which may provide that extra supply of fish to fill the gap between demand and supply (Coimbra, 2001). Also, it will alleviate some of the pressure on the natural stocks.

For the last 40 years, world aquaculture has progressed from being a localised self-sufficient sector to become an important, well-structured and diverse industry. The growth of the sector has been driven by market demand, advances in scientific understanding of the life cycle and production environment of cultured species, and technological improvements of the culture systems (Roberts and Muir, 1995). However, this rapid expansion and development has increased the number of environmental concerns and questions about possible ecological impacts. Environmental managers and regulators have pointed out the necessity of minimising environmental impacts if productivity in the new industry is to be sustainable (Sowles *et al.*, 1994).

Aquaculture, as with any other economic activity which uses natural resources, depends upon inputs (e.g. water, seed, feed) and attendant processes (e.g. capacity of the environment to degrade wastes) to produce a final product for consumers (e.g. fish, mussels, shrimps). This interaction with the environment may have social, economic and environmental benefits such as; provision of food, employment, increase of income, improved nutritional and health, decreased pressure on natural stocks, etc. (Beveridge, 1996). On the other hand, interactions with the environment can also generate negative impacts. Wastes, which are generated by the farming activity and released into the environment, may have a negative effect on natural resources decreasing their quality and quantity. Consequently, farmed animals may be negatively affected by the degradation of the environmental conditions (e.g. generation of toxic substances such as hydrogen sulphide). Furthermore, an indirect consequence of waste impacts in the environment is the rise of a negative perception of aquaculture.

Quantities of aquacultural discharge are mainly dependent on husbandry, feeding technique, feed composition, digestibility, feed conversion ratio, site selection and system design (Tovar *et al.*, 2000). Complete reduction of these discharges are not possible for present culture systems, from both a technological and an economical point of view, therefore, they will have an impact on the environment. The extent of this environmental impact is a consequence of the type and amount of wastes produced as well as the biological, chemical and physical characteristics of the area (GESAMP, 1991). Some impacts such as enrichment of benthic and water column ecosystems have been extensively studied (Gowen *et al.*, 1989; Findlay and Watling, 1994; Gowen *et al.*, 1994; Hargrave, 1994; Troell and Berg, 1995), others for example, the genetic interaction between farmed and wild fish and the ecotoxicology of the many chemical compounds used in aquaculture are poorly understood.

In the particular case of marine cage fish farming, the most significant resources used are space, water, natural seeds (larvae and juveniles) and feed (Fig. 1.1). Space refers to the physical space which the cage or cages occupy in the water body, and this can affect boat traffic, fishing activities, local currents and sedimentation dynamics. Water is used for many purposes in cage culture, such as gas exchanges and waste dilution and dispersion. Increases in ammonia (NH_3), nitrite (NO_2) and nitrate (NO_3) from waste discharges lead to a decrease in water quality. The use of wild seeds in some parts of the world may have several negative effects on the natural populations if these are over-fished. Aquaculture feeds can represent 40-60% of the capital cost because the large amount required (Foster *et al.*, 1993), and normally all artificial diets are based on fishmeal in quantities of up to 60% of the dietary formulation (Shepherd and Bromage, 1995). Also, farmed fishes may consume some natural food decreasing its availability for wild stocks.

In the process of fish-cage production all the different wastes generated end within the environment (Fig. 1.1). The most important are uneaten feed, faecal pellets, urine and chemicals (Beveridge, 1996; Hennessy *et al.*, 1996). Biological pollutants such as escaped fishes and pathogens from farmed fish, may also have negative effects in the environment (Beveridge, 1996).

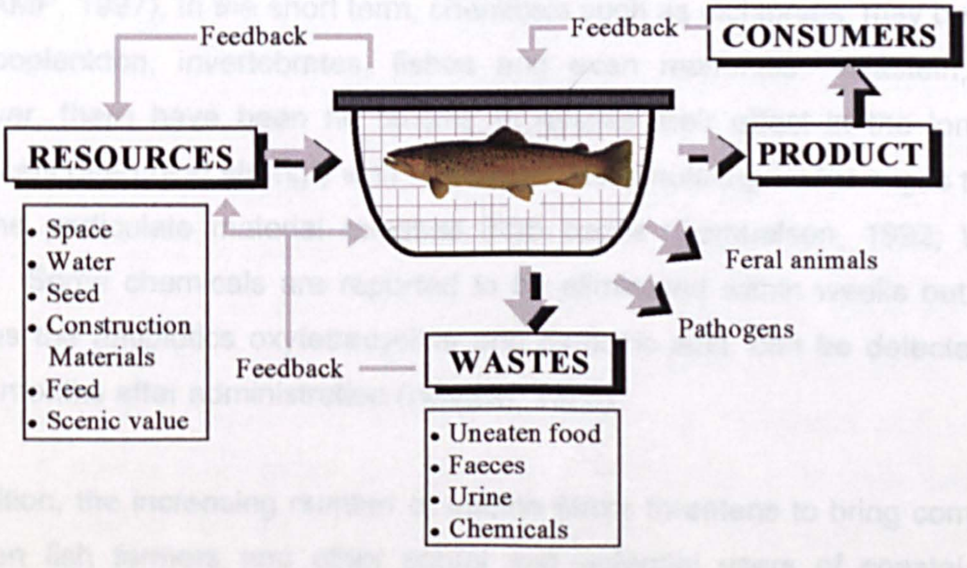

Fig. 1.1: Use of resources and wastes generation in cage aquaculture process (redrawn from Beveridge, 1996).

A high concentration of nutrients released to the environment may lead to eutrophication in closed water bodies with low water exchange rate. Nitrogen (N) and phosphorus (P) are the main nutrients that contribute to eutrophication, but recently there has been some concern about silicon (Si). Holby and Hall (1994) suggested that if there were a sustained imbalance in nutrient availability in terms of large quantities of N and P released from a farm relative to Si, favourable conditions would be created for the development of toxic dinoflagellate blooms.

Uneaten feed from floating cages settles mostly onto the sediments beneath, while faeces settle downstream adjacent to the cages. These organic materials greatly increase microbial production, changing the sediment chemistry and biology. The microbial activity gradually consumes the scarce oxygen, allowing anaerobic bacteria to colonise the sediments. The results of their metabolic processes are production of hydrogen sulfide, lactate, ammonia and methane (Beveridge, 1996). There may also be a built-up of facultative pathogens in heavily contaminated sediments under cages, acting as a disease reservoir (Philips and Beveridge, 1986).

Therapeutic chemicals are widely used for production management all over the world and their negative effects on the environment have only begun to be studied (GESAMP, 1997). In the short term, chemicals such as dichlorvos, may be toxic to the zooplankton, invertebrates, fishes and even mammals (Håstein, 1996). However, there have been no studies to assess their effect in the long term. Chemicals often bind strongly with sediments, accumulating under cages together with the particulate material released from cages (Samuelsen, 1992; Weston, 1996). Some chemicals are reported to be eliminated within weeks but others, such as the antibiotics oxytetracycline and oxolonic acid, can be detected up to seven months after administration (Håstein, 1996).

In addition, the increasing number of marine farms threatens to bring competition between fish farmers and other actual and potential users of coastal space. Therefore, to ensure a sustainable development of the aquaculture industry, there is a great need to allocate aquaculture to suitable locations (site selection) to resolve competing demands for coastal space, avoid undesirable impact on the environment, as well as ensuring the profitability of the operation (Kapetsky *et al.*, 1987; GESAMP, 1991; GESAMP, 1997).

1.2 AQUACULTURE SITE SELECTION

Aquaculture site selection is a key factor for the success and sustainability of a venture. The correct choice of site is vitally important since it can greatly influence economic viability by determining capital outlay, affecting running costs, rates of productions and mortality factors. Moreover, it can resolve conflicts between different coastal activities and users, such as fishing, tourism and local communities, making rational and sustainable use of the coastal space.

The management of aquaculture can been approached in a number of different ways. One strategy is to emphasise regulation of the quantity and/or quality of effluents. An alternative strategy is to emphasise the location of environments which are less sensitive to the type of perturbation aquaculture may generate in a particular place, in other words, site selection. The first approach is usually applied to existing farm-environments conflict, and normally employs limited environmentally focused criteria. The second approach often attempts to proactively avoid both the environmental impacts and resource user conflicts.

One of the pioneering countries in developing a management plan for aquaculture was Canada. The Canadian Ministry of Agriculture Fisheries and Food (MAFF) has recognised that siting of fish farms plays an important role in successful operations since the 1980's. MAFF developed factors and guidelines that have routinely been used for individual site assessments of salmon farming. Parameters used in the creation of environmental assimilative capability maps for salmon farming considered type of substrate, oceanographic conditions, upland conditions, marine algae and plankton, pollution and predators (Caine *et al.*, 1987). A further step taken by MAFF was to develop a scoring system for evaluating marine fish areas, based on a numerical rating scheme, ratings of "Poor", "Medium" and "Good" were assigned to final maps. Some areas were rated "Not Acceptable", where one or more individual parameters were overtly constraining, such as major pollution zones (Black, 1991).

Norway also attempted to integrate aquaculture licensing within a broader planning context in order to limit resources conflict. A programme called LENKA

(Nationwide Assessment of the Suitability of the Norwegian Coastal Zone and Rivers for Aquaculture) was developed from 1987 to 1990 as a modelling and accounting system for the allocation of estimated ability of the marine environment to absorb additional organic loading (Bergheim *et al.*, 1991; Ibrekk *et al.*, 1993). Besides the organic loading criteria, aquaculture was also licensed based on the potential for outbreak of diseases, pollution risk and potential location conflicts. The result assigned organic loading capacities to 500 geographically defined zones along the coast. A more recent programme called Modelling-Ongrowing fish farms-Monitoring (MOM) was developed to work in combination with the LENKA framework. MOM involves a more mathematical approach to modelling flushing rates and uses a number of features for different geographic scales. In macro-scale modelling, topography is the dominant feature used. As the scale increases, the effects of tidal action and river runoff become more important in determining flushing rates. MOM is designed to assess the effects of organic loading, and it helps in the determination of carrying capacity for a particular marine basin (Hansen *et al.*, 1997; Ervik *et al.*, 1997; Hansen *et al.*, 2001).

It is only comparatively recent that the rise in environmentalism world-wide has led to the development of new methods in coastal management, based on longer-term planning and more regional scales of investigation (Carter, 1988; Bartlett and Carter, 1990). The term *Integrated Coastal Zone Management* has been frequently used to refer to this type of coastal management. The primary objective of ICZM may be stated as being to "devise a framework within which Man may live harmoniously with nature" (Carter, 1988).

Clearly, coastal aquaculture should be developed within an ICZM plan and any proposed marine aquaculture plan or policy within an ICZM should integrate an adequate allocation system. Such a system should select the most suitable sites for aquaculture based on environmental, economical and social factors. In other words, selecting sites which may have the least environmental stress, maximum potential for species growth, minimum production costs and avoiding conflict with other users.

1.3 INTEGRATED COASTAL ZONE MANAGEMENT (ICZM)

The world coastline has traditionally attracted, and will increasingly attract, a very large proportion of the human population. At least 40% of the world's human population now live on or near the coast, and the proportion of coastal dwellers is increasing at a very much faster rate than that of the overall population (Carter, 1988). The shift of population to coastal areas taking place nowadays is comparable to the one from rural to urban areas which happened during the first half of 20th century in industrialised countries, and which is still happening in developing countries at present. This population shift brings about a growing demand for space by a great variety of competing and often incompatible uses, and consequently, an increased pressure on coastal resources. Traditional activities such as agriculture, stock raising, fisheries, ports, etc. have been joined at a growing rate by residential developments, tourism facilities, industries, quarries, sand and gravel pits for building material, hydrocarbon extraction, storage and processing, conventional and nuclear power plants, aquaculture, solid and liquid waste disposal, and multiple sources of recreation. Therefore, there is an urgent need to manage littoral zones carefully. A major review by the Organisation for Economic Co-operation and Development (OECD, 1993) pointed out the economic and environmental importance of coastal areas, which when combined with intense pressure on diverse coastal resources, make integrated planning a necessary component of coastal area management for this fragile ecosystem.

This urgent need for some kind of coastal management was given prominence at the United Nations Conference on Environment and Development (UNCED) in Rio de Janeiro in 1992, and was further developed at the World Coastal Conference in the Netherlands in 1993. From these meetings emerged the concept of Integrated Coastal Zone management (ICZM). It was suggested that every coastal nation should develop an ICZM structure appropriate to its needs.

An ICZM structure that works well should be an analytical process that advises governments on priorities, trade-offs, problems, and solutions and works toward democratically agreed objectives. It should employ a multidisciplinary approach, maintain a balance between protection and development and should provide mechanisms to reduce or resolve conflicts that may occur. A major objective is to overcome the consequences of an uncoordinated sequence of coastal development projects (such as aquaculture), which results in resource degradation and foreclosure of present and future options for resource use (Clark, 1996).

The development and approval of coastal aquaculture projects should be based on ICZM-type plans that identify resources and conflicts over their use. ICZM plans in aquaculture should also include the protection of coastal habitats for sustaining capture fisheries, supporting tourism, and maintaining a high level of ecological functions and diversity. Clark (1996) considered that projects that are in conflict with such plans should not be approved.

While development and implementation of ICZM policies is now an established concept and internationally recognised goal, the tools and methodologies for achieving such goals are still under development (Clark 1996; GESAMP, 1996b). It is clear, however, that for any management of the shore to be effective, it is necessary for the policies to be based on informed decision-making. This in turn requires ready access to appropriate, reliable and timely data and information, in suitable form for the task at hand (Urbanski, 1999). Since much of this information and data is likely to have a spatial component, Wright and Bartlett (2000) suggested that Geographical Information Systems (GIS) have relevance to this task, and have the potential to contribute to coastal management in a number of ways, these include;

- the ability to handle much larger databases to integrate and synthesise data from a much wider range of relevant criteria than might be achieved by manual methods,
- encouragement of the development and use of standards for coastal data definition, collection and storage, which promotes compatibility of data and processing techniques between projects and departments, as well as ensuring consistency of approach at any one site over time,
- the use of shared databases also facilitates the updating of records, and the provision of a common set of data to many different departments that might typically be involved in management of a single stretch of coast, and

- the efficient data storage and retrieval facilities characteristic of GIS offers the ability to model, test and compare alternative management scenarios, before a proposed strategy is imposed on the real-world.

1.4 GEOGRAPHICAL INFORMATION SYSTEMS (GIS)

Many technical definitions for GIS can be found in the literature, such a "... *an integrated system of computer hardware and software for entering, storing, retrieving, transforming, measuring, combining, subsetting and displaying spatial data that have been digitised and registered to a common co-ordinate system ...*" (Johnston, 1998). But more simply, a GIS is a "*tool*" for managing information of any kind according to where it is located, and hence, is a database with spatial co-ordinates where each piece of information has a precise location in space. The word tool is emphasised because it is a common mistake to think that GIS is a definitive answer to problems. GIS provide outputs from a range of input data, but does not intrinsically provide answers.

In the mid-1960s it was recognised that digital computers could be used quite effectively to map out and analyse the vast quantities of information being collected by Canada Land Inventory (Jones, 1998). The resulting statistical and cost-benefit analyses were used to develop management plans for large rural areas throughout the whole of settled Canada. One of the conclusions of this initial effort was that computerisation was going to be the best alternative for developing these management plans, in spite of the primitive computers of that time and their high cost. This new kind of "computerisation" was called the "geographic information system" (Wright and Bartlett, 2000).

Although the Canadian Geographical Information System can be regarded as having laid the foundations for many subsequent GIS, it was not in fact followed by a proliferation of similar systems. It was only from the late 1980s that GIS could claim to meet a significant proportion of the data-handling requirements of organisations concerned with geographical information (Jones, 1997), principally due to the recent technological advancements, in particular the increased availability and relative affordability of computer software and hardware. However, though the availability of the technology is a necessity, it is not a sufficient condition for its effective utilisation. To facilitate the take-up of GIS a number of institutional barriers must be overcome. Of particular importance in this respect is the need to take steps to promote the availability of digital data in forms that facilitate its use in a wide range of applications.

In recent years GIS have become of great significance for environmental planning and assessment. The main reason for this is the need to compare a great number of area-related data describing the affected natural resources and their sensitivity related to the effects of the action. Because GIS can be used to couple these types of data with their attributes and can be used to overlay them, it represents a highly efficient instrument for such planning tasks. Godschalk and McMahon (1992) label GIS as "revolutionary" in its potential to enhance the planning process itself.

Three of the fundamental questions that lie behind effective environmental management are, what is where?, why is it there?, and what would happen if?, lend themselves perfectly to the use of GIS-based analysis (Treweek, 1999). The latter author pointed out that it is not possible to describe, explain or predict ecosystem behaviour without knowing how ecosystem components are distributed in time and space or with respect to each other ("what is where?") and understanding the relationships and processes that explain their distribution and behaviour ("why is there?"). As well as requiring knowledge of spatial distribution and relationships, the ability to make reliable predictions ("what happen if?") often demands knowledge about temporal trends. Tackling these questions demands the very same spatial, analytical and predictive procedures that GIS are designed to facilitate, therefore GIS has an important relevance to address environmental and management problems.

GIS is thoroughly discussed by Aguilar-Manjarrez (1996), Burrough (1990), DeMers (1997), Jones (1997), Malczewski (1999), Nath *et al.* (2000) and Salam (2000) but in simple terms, GIS stores data according to two main attributes: (1) where? (the *locational attribute*), and (2) what? (the *thematic attribute*). Locational attributes are defined using co-ordinates which are stored digitally and GIS is therefore structured around a straightforward X, Y co-ordinate system to which a number of thematic layers of information can be referenced. Fig. 1.2 shows how different layers of thematic information relevant to a project might be built up, all referenced to a common X, Y co-ordinate system. Map features are defined using *topological data elements*; points, lines or areas (polygons). Attribute data are associated with these topologic data elements and provide descriptive data about them. GIS can therefore be used to store, manage and retrieve data to describe what entities or components are present in a study area and exactly where they are located in space and in relation to each other.

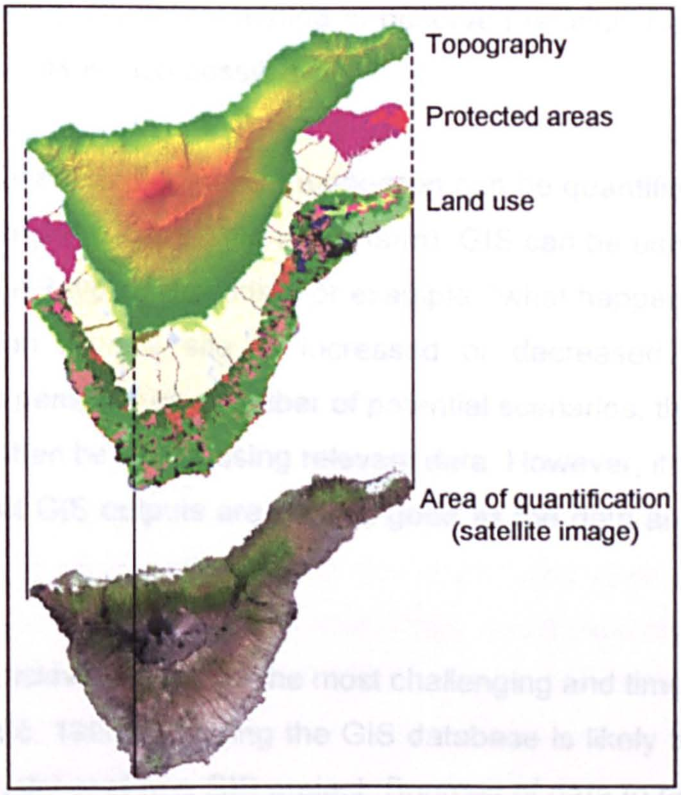

Fig. 1.2: A hypothetical GIS database structure.

Once created, the GIS database enhances data-handling capability and speeds up access to information for analytical purposes. Visual presentation of data layers (thematic maps) can facilitate recognition and/or understanding of potential relationships between different attributes, thereby ensuring that all relevant avenues of enquiry are explored and that suitable data have been collected in field study programmes.

As well as performing straightforward database query functions, GIS can also be used to explore functional relationships by querying data in different ways. GIS can be used to combined relevant thematic data layers and explore the possible relationships between them, often using overlaying functions ("how do these layers of information relate to each other?"). Statistical testing of observed relationships or correlation between thematic layers is also possible.

Finally, when relationships have been confirmed and responses can be quantified (e.g. the response of benthos to organic loads from a fish farm), GIS can be used to tackle the "what would happen if"? type questions. For example: "what happens to the benthos if fish production on the site is increased or decreased?". Theoretically, GIS can be used to generate any number of potential scenarios, the relative significance of which can then be tested using relevant data. However, it is very important to bear in mind that GIS outputs are only as good as the data and models on which they are based.

Database development has been acknowledged as the most challenging and time-consuming task (Lang, 1990; Budić, 1993). Creating the GIS database is likely to account for more than half of the total cost of a GIS project. Sources of data to be integrated in GIS are usually incredibly varied and may include existing paper or digital maps, satellite images, field surveys, aerial photographs, statistics, etc. In fact, one of the main advantages of using GIS is the ability use a variety of such data sources and interpret them on a "common platform". Decisions on what sources of data to use are fundamental to the development of GIS for environmental management. In particular, it is often necessary to decide what relative emphasis to place on field survey or remotely sensed data. The main advantage of using remotely sensed data is the ability to acquire spatially referenced information, which can be updated quickly, straightforwardly and often relatively cheaply. There are particular advantages for studies at the regional level, in areas where access for field survey is limited or difficult or where future monitoring is intended. Access to remotely sensed data has also made it considerably easier to develop regional approaches to natural resources management, which takes into account the wider geographical and temporal trends (Treweek, 1999). On the other hand, the use of remotely sensed data does require skills in interpretation and classification of images and field survey may be needed for helping image classification and later validation (Wilkinson, 1996).

Broad areas of environmental management in which the use of GIS has had demonstrable benefits are the assessment of cumulative ecological effects, environmental impact assessments, regional ecological studies, conflict resolution in land use planning, strategic ecological assessment, ecological mitigation planning and the assessment of landscape-scale effects:

- **GIS for cumulative effects assessment**

  Cumulative habitat loss is a problem for many species in many countries. GIS technology has made it considerably easier to quantify those spatial attributes of habitat distribution and organisation, which affect the value of an area to associated species and therefore, to recognise when unacceptable thresholds of habitat loss and fragmentation may have been reached (Wadwsworth and Treweek, 1999). Sebastini *et al.* (1989) used a GIS-based approach to trace the commutative loss of coastal wetlands as a result of development in a large study region. Other examples can be found in Bielecka *et al.* (1995), Lowry *et al.* (1995), Lehmann (1998) and Schippers *et al.* (1996).

- **GIS for Environmental Impact Assessment (EIA)**

  GIS has been used as a tool in scooping the EIA, deriving suitable study limits and generating appropriate impact scenarios and mitigation strategies as well as simply handling the relevant data and making them accessible (Johnston, 1998). Hassen and Prou (2001) give a good example of applying GIS for assessing potential aquacultural impacts due to nonpoint source loadings. Other examples are found in Perez *et al.* (2002) and Shukla *et al.* (1998).

- **GIS for mapping ecosystems**

  Ecosystem classification is used to derive homogeneous map units with predictable characteristics. Ecosystem mapping stratify the land base into map units based on information about environmental factors such as climate, geology, soils and vegetation. Digital maps generated from such GIS databases provide a spatial expression of ecosystem classifications that can be used to depict habitat, wildlife and other ecological resources in a standardised and directly comparable fashion. Examples of this type of applications can be found in Donnan and Davies (1996), Gold (1996), Lyon *et al.* (1987) and Plant (1998).

- **GIS for mapping habitat potential**
  Suitability maps can be useful for assessing habitat suitability, such as locations for fish farming. Suitability maps for a species can be assessed in various ways, for example a rating can be assigned based on professional experience or knowledge. If more detailed information is available, algorithms that rank habitats based on explicitly stated relationships between species life requisites and ecosystem units may be developed. Also, possible species distributions may be inferred by combining the knowledge of relationships between species and habitats in a straightforward way to limit interest survey areas, hence saving time and money. Examples of this type of applications can be found in Guo and He (1999), Pereira and Duckstein (1993) and William *et al.* (2000).

- **GIS for Strategic Ecological Assessment**
  Strategic ecological assessment has been promoted as a means of resolving conflicts in natural resource use at an early stage in land-use planning so that adverse ecological impacts can be avoided or reduced at source. This makes it possible to evaluate the likely consequences of different land-use strategies before they are implemented and also to test the effectiveness of alternative approaches to ecological mitigation (ecological mitigation planning). Impacts operating at different geographical and temporal scales can also be captured, quantified and compared relatively easily. Examples of this type of applications can be found in Budic (1994), Bushing (1997), Charnpratheep *et al.* (1997), Cochrane (1999), Gordon (1994), Hepner and Miller (1993), Schaller (1992) and Thumerer *et al.* (2000).

Despite its obvious potential benefits and the general favourable opinion, the use of GIS technology to manage environmental problems has a relatively recent history. In some countries, notably Canada and USA, EIA have been managed around GIS databases for some years. However, a review of GIS use for EIA by environmental consultants (Joao and Fonseca, 1996) confirmed that GIS were being used more for presentation of data results than they are for data analysis.

When considering the use of GIS for environmental management it is important to consider whether or not GIS will make the process more efficient, cost-effective and productive than more traditional methods. However, it is sometimes difficult to quantify benefits obtained by the use of GIS. For environmental management addressing relatively large or inaccessible areas, the cost of laborious survey can be prohibitive. In such circumstances, a GIS-based approach can be cheaper and more efficient than a traditional approach based on field survey. It can also open up opportunities for using alternative source data such as aerial photography or satellite imagery. On the other hand, the lack of readily available and affordable digital data means that a certain amount of hand digitising is very likely to be necessary, which is a laborious and time consuming task (Budic, 1994). In addition, mastering the technology itself requires time and intensive training to become familiar with the functions of GIS and learn about the logistics of exploiting its capabilities. Thus, the benefits of GIS technology are not attained immediately. The longer a GIS is used by an institution or individual, more potential it has to yield benefits.

There are several qualitative indications of the benefits of using GIS technology for management. Eason (1988) listed four categories of benefits; (1) cost reduction (staff savings and other direct cost savings such as space), (2) improved productivity, (3) improved support (improved information, decision support, expert assistance, computer aided support), and (4) organisation enhancement (new ways of integrating new business). On the other hand, quantitative data and methods on the benefits of using GIS are very rare. The U.S. Geological Survey (USGS) has developed a model for improving the quality of GIS cost/benefits studies (Gillespie, 1999) which focuses on the complexity of a GIS application as the key factor influencing the level of benefits. However, this technique is neither easy nor straightforward to use.

1.5 GIS IN THE COASTAL ZONE AND AQUACULTURE

Interest in applying GIS to the coast first emerged in the early and mid 1970s, at a time when GIS itself was still a very new technology. However, much of the earliest references are aspirational, rather than describing work in progress (Wright and Bartlett, 1999). In a historical perspective on the application of GIS to the coast conducted by Bartlett (1993a), the author concluded that the first "real" pioneering applications of GIS to the coast mostly focused on the ability of computers systems to store and retrieve data. In part, these early development of coastal GIS were frequently constrained by the hardware and software then available, and also by the generally low levels of awareness shown by potential users, regarding the functionality and capabilities of GIS (Green, 1987). Only in the late 1980s was an upsurge in the application of proprietary GIS packages to the coast (Wright, 1999).

The traditional home of GIS, in terms of managing, mapping and modelling spatial data and associated attributes, as well as spatial decision-making, has been in the land-based sciences and professions (Ricketts, 1992). Most commercial GIS are developed for land-based applications, and are built around cartographic metaphors, data models and fundamental paradigms optimised for conditions found in terrestrial environments. These paradigms and models are frequently poorly suited to coastal data, where boundaries between key variables are less easy to define. A much greater range of spatial scales and resolutions have to be considered, and there is a greater need to work in three spatial dimensions, where the temporal dimension is fundamental to many analyses (Wright and Goodchild, 1997). The limited widespread use of GIS in marine environments has also been blamed on the high cost of collecting and maintaining digital databases (Wright, 1999). However, satellite images are enabling capture of data over a wide area, and making the update of the database possible. Technological developments in this area have been incredibly rapid and the spatial, spectral and temporal resolution of satellite imagery is improving all the time.

There is a potential for GIS to contribute to costal management in a great variety of applications. Broadly, GIS applications in the coastal zone may be grouped into four categories; (1) inventory, (2) coastal change analysis, (3) risk assessment and (4) coastal resources survey and management.

In inventory applications, GIS can aid the sorting and rapid retrieval of data on the basis of location and other spatial relationships. The UK Integrated Coastal Zone Mapping Dataset (ICZMap) is a good example of this type of applications (Gomm, 2001). The aim of this work was to enable the integration of coastal data, referencing and recording information in a consistent framework. It was intended for this data to be accessed readily by users, to satisfy diverse and innovative coastal zone applications and services. Another national initiative is the SIGMAZAL project being developed by the Spanish government (Sanz, 1997; 1999) which is a marine geographical information system for management of the coastal and continental shelf resources.

GIS has been used for time series and change analysis applications, particularly in wetlands studies, but have also been widely applied to analysis of erosion, shoreline and mangrove forest changes. It is very common to make use of remote sensing data for these kinds of applications (Bartllet, 1993b).

As coastal population expands and land development near the coast increases, coastal problems will become intensified. Therefore, an understanding of the processes and hazards associated with these coastal regions is essential. Applying GIS to hazard assessment and risk mapping along coastal areas benefits communities by providing a basis for zoning, land-use planning and resource allocation. Some of the main coastal hazards that GIS technology is being applied to are: pollution (specifically oil spills; Abdel-Kader *et al.*, 1998), hurricanes (Hickey *et al.*, 1997), ice (Stringer, 1981), etc.

There are many and diverse applications of GIS in coastal resources survey and management applications. Within the leisure and recreation sectors, several examples exist where GIS has been used effectively in the assessment, development and management of coastal resources. Examples include the siting of shore-based facilities such as marinas (Fairfield, 1987), and the management of recreation activities in areas of fragile coastal dune systems (McGrath, 1990), as well as in the management of marine reserves (Bushing, 1997). GIS is also a major technology within the mining and oil exploration industries where it is harnessed to assist in the discovery, assessment and exploitation of resources (Jefferies-Harris and Selwood, 1991). Unfortunately, many of these applications remain relatively undocumented for reasons of commercial confidentiality.

Although it was not until the mid-1980s that any form of fisheries management GISs appeared, since then fisheries have likewise made use of GIS to assist in various fields, such as: predicting fish yield in reservoirs (De Silva *et al.*, 2001) and in marine protected areas (Maury and Gascuel, 1999); distribution of fish (Kulka, 2001), algae and seagrasses (Taranto *et al.*, 1997b) and holothurians (Taranto *et al.*, 1997a); habitat characterization and fisheries management (Andrew and O'Neill, 2000; Mckenzie *el al.*, 2000; Dunning *et al.*, 2000; Fouche *et* al., 1998) with special emphasis on fish (Rogers and Bergersen, 1996), oysters (Wilson *et al.*, 1999; Wilson *et al.*, 2000), clams (Rubec *et al.*, 1998) and lobsters (Anon, 1997); and spatial assessment of fish resources (Ardizonne *et al.*, 1998; Le Corre *et al.*, 1998; Corsi *et al.*, 1996) and cephalopod resources (Boyle *et al.*, 1998; Pierce *et al.*, 1998).

GIS has several advantages for aquaculture development programs. It not only provides a visual inventory of the physical, biological and economical characteristics of the environment, it also allows rational management without complex and time-consuming manipulations (Krieger and Mulsow, 1990). Despite this, the use of GIS in aquaculture has been very limited and only few studies are reported in the literature. Nath *et al.*, (2000) concluded that the little spread of aquaculture applications using GIS is due to: (1) a lack of appreciation of the benefits of such systems for this sector, (2) limited understanding about GIS principles and associated methodology, (3) inadequate administrative support to ensure GIS continuity among organisations, and (4) poor levels of interaction among GIS analyst, subject matter specialists and end users of the technology.

The first applications of GIS in aquaculture date from the late 1980's (Kapetsky *et al*, 1985; Kapetsky, 1987), since then, the use of GIS has been quite limited. At present, there are only about 50 literature references on the use of GIS in aquaculture. Despite this, GIS applications in aquaculture are surprisingly quite diverse, targeting a broad range of species (fish, crustacean and mollusc) as well as geographical scales, ranging from local areas (i.e. small bays, Ross *et al.*, 1993 and big bays, Scott and Ross, 1999), to sub-national regions (i.e. individual states/provinces, Aguilar-Manjarrez and Ross, 1995), to national (Salam and Ross, 2000) and continental (Aguilar-Manjarrez and Nath, 1998) expanses. They also vary with regard to the degree to which GIS outcomes have been used for practical decision-making (Nath *et al.*, 2000).

Several authors have extensibly documented the use of GIS in aquaculture (Meaden and Kapetsky, 1991; Kapetsky and Travaglia, 1995; Aguilar-Manjarrez, 1996; Ross, 1998; Nath *et al.*, 2000; Salam, 2000) and at present time, the extent of GIS applications in aquaculture include: site selection for target species such as fish (Grita, 1998; Alarcon and Villanueva, 2001; Benetti *et al.*, 2001), oysters (Chenon *et al.*, 1992), mussels (Krieger and Mulsow, 1990; Scott, 1998), clams (Arnold *et al.*, 1996; Arnold and Norris, 1998; Arnold *et al.*, 2000), scallop (Halvorson, 1997), shrimp (Salgado and Blanco, 2000; Alarcon and Villanueva, 2001) and seaweed (Brown *et al.*, 1999), environmental impact assessment (Thriscutt *et al.*, 1997; Fuchs *et* al., 1998; Gupta, 1998; Perez *et al.*, 2002), conflicts and trade-offs among alternate uses of natural resources (Angell, 1998; Biradar and Abidi, 2000), and consideration of the potential for aquaculture from the perspectives of technical assistance and alleviation of food security (Meaden and Kapestsky, 1991; Kapestsky, 1994; Kapestsky and Nath, 1996).

1.6 AIMS AND OBJECTIVES

The aim of this study was to select and optimise the most suitable sites for offshore marine fish-cage farming in Tenerife (Canary Islands) based on the use of GIS-based models and related technology (satellite images, GPS, etc.) to support the Coastal Zone Management decision-making process. To achieve this general aim, the following objectives were set:

- Identification of all the possible criteria that may influence the development of marine fish-cage culture within the context of a integrated coastal zone management (Chapter 3).
- Identifying the data sources for those criteria identified, gathering the required data, and finally entering this data into the GIS system to built up the database (Chapter 4).
- Database verification to control the quality of data used to help ensure reliable outcomes (Chapter 3 & 4).
- Selection of optimal cage systems for different locations around Tenerife (Chapter 5).
- Development of GIS-based models, for each cage design selected, for selection of most suitable sites for developing marine cage culture. (Chapter 3 & 5).
- Weight verification analysis to account for possible different points of view from different focus groups to the task of siting marine fish cages. Specifically developed questionnaires were used to obtain feed-back from these groups (Chapter 5).
- Development and integration of a particulate waste distribution model, so that areas which have been selected as the most suitable for siting of cages could benefit from a further study to quantify the dispersive nature of a site, and therefore, assist in predicting possible environmental impacts, as well as establishing the maximum desirable production of a site (Chapter 5).
- Sensitivity analysis to indicate what criteria are the most or least critical in determining the values of the output map. These critical maps indicate where most or least care may be taken in the input data in order to draw reliable conclusions from the output map, and also to assess the overall robustness of the model (Chapter 6).

Tenerife was chosen for study because it has very favourable environmental conditions for the culture of marine fish. It has clean, well-oxygenated waters, stable oceanic salinity and favourable temperatures for growth. The development of an aquaculture industry on the island could become a complementary sector to tourism and agriculture, which will diversify the island's economy. Also, it will provide a consistent fish supply, and hence, decrease the pressure on the already overexploited natural resources. In addition, because of the particular and fragile characteristic of islands, a rational and sustainable aquaculture management is needed. At present, there are no guidelines to follow, and this study was aimed to be the first of its kind on an island environment as whole.

Due to the small size of the island (2,036 km^2), overpopulation, and competition with tourism and agriculture, land availability in Tenerife is low. This pressure on the land is increasing with the growing local population and the developing tourism and agriculture industry. There are no lagoons available for aquaculture and the scarce bays are heavily used by tourism, which is the main source of income. Therefore, at present offshore cage culture seems like the most viable system for ongrowing fish farming.

The availability of suitable coastal areas for aquaculture and other coastal activities is diminishing due to land use conflicts and water quality degradation. Consequently, coastal areas are likely to be the scene of greater conflict in the future. In addition, the correct choice of site is vitally important since it can greatly influence economic viability, by determining capital outlay, affecting running costs, rates of productions and mortality factors. Therefore, the first prerequisite for sustainable aquaculture is an adequate aquaculture resource allocation system.

This study is based on extensive use of GIS because besides performing straightforward database functions, it can also be used to explore relationships by querying data in different ways combining relevant thematic data layers and exploring the possible relationships between them, using overlaying functions and more complex modelling structures. This allows exploration of sensitivities of the models and investigation of different scenarios, leading to optimisation of site location, exploration of visual and environmental impacts and estimation of sustainable production benefits.

Chapter 2

Study Area: Tenerife (Canary Islands)

2.1 THE CANARY ISLANDS

2.1.1 Geographical Location and Description

The Canary Archipelago, comprises of seven main islands and several minor ones and is located in the Eastern Central Atlantic Ocean between latitude 27.6°-29.5° N and longitude 18.2°-14.5° W. It is only 100 km from the north-western edge of the Africa continent (Fig. 2.1). The total area of the archipelago is 7501 km^2. The Canary Islands are the emerged parts of an important volcanic formation on the oceanic-continental transit of the Afro-Atlantic plate.

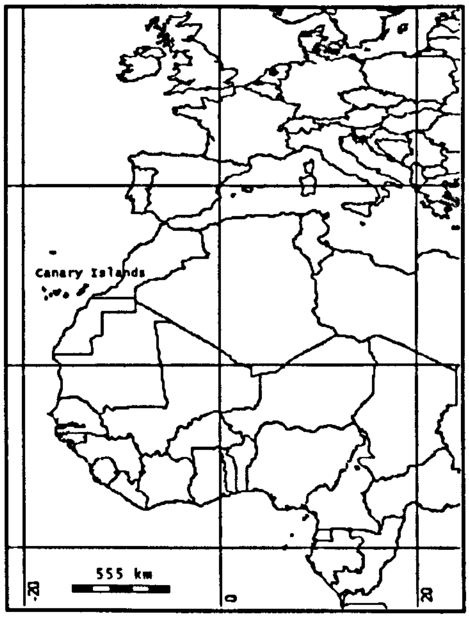

Fig. 2.1: Canary Islands location.

The Archipelago has been under the sovereignty of the Spanish government since the XV century and is divided into two provinces, Santa Cruz de Tenerife and Las Palmas. The former is constituted by the four most western islands, El Hierro, La Palma, La Gomera and Tenerife. The capital of this province is Santa Cruz de Tenerife, which is located on Tenerife island. Gran Canaria, Fuerteventura and Lanzarote form the second province. The capital of this province is located on Gran Canaria and is called Las Palmas de Gran Canaria (Fig. 2.2). The

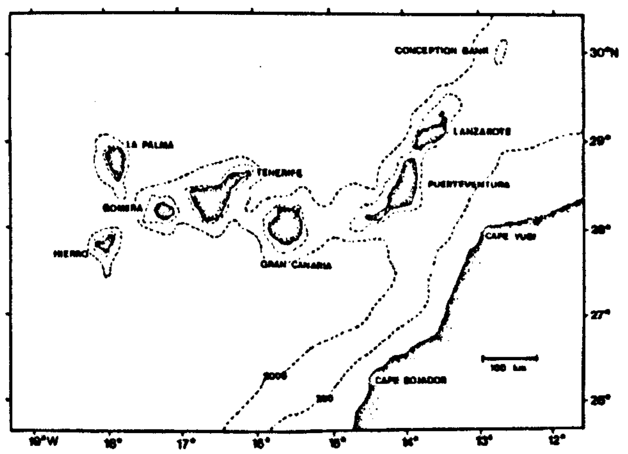

Fig. 2.2: Canary Island Archipelago and its two provinces.

population of the Archipelago is over 1,600,000 inhabitants, mainly concentrated in the two provincial capitals. To this must be added approximately 6,000,000 tourists who visit the islands annually.

From a geomorphology point of view, the Canary Islands can be divided into two different groups: the western and central islands (La Palma, El Hierro and La Gomera; Tenerife and Gran Canaria) and the eastern islands (Fuerteventura and Lanzarote) (Rodriguez *et al.*, 1993). The western and central islands are of volcanic origin from the Miocene and Holocene formations, together with more recent deposits. The rocks are varied and complex in nature and include lava flows and pyroclastics, basalt, trachytes and salic volcanic. The relief is rugged, with land rising to over 1000 m and steep slopes exceeding 30 per cent over more than half of the islands. The eastern islands, are where volcanic rocks of the classic series of the Canary volcanism (Miocene, Holocene and Pliocene in age), and non-volcanic igneous rocks (gabbros and syenites) are found. These are low altitude islands (<800 m), characterised by gentle slopes and wide plains, U-shaped valleys and abundant glacis, although there are some rugged areas and sharp mountain ranges.

2.1.2 Marine Environment

The Canary Archipelago emerged from the oceanic basin due to a successive overlay of volcanic material, forming an independent set of islands (except for Fuerteventura and Lanzarote which are considered to have originated from the same insular block). Their volcanic origin is responsible for the limited coastal shelf, and water depths of over 2,000 m can be reached very close to the shore. Around La Palma and El Hierro, the shelf is almost non-existent. On the other hand, the breadth of the shelf surrounding Fuerteventura and Lanzarote which were formed earlier, is much greater, reaching up to 30 km. The coast and seabed topography generally can be described as abrupt and highly uneven.

Both the particular oceanographic conditions and the bathymetry govern the marine environment in the Canaries. The oceanographic characteristics of the

Canary waters in general deviate greatly from that which is expected from its geographical location, typically classified as a subtropical zone. These differences are a consequence of the influence of the Canary Current, which brings to the Canaries colder waters than expected for its latitude. Primary production in the Canaries is very low due to the small continental shelf and also to the almost permanent water stratification, preventing nutrients from deeper waters from reaching the photic zone and being used by phytoplankton.

Temperature

The annual sea temperatures in the archipelago ranges between 16 and 24 °C. However, this is not homogeneous and, in any given period, differences of 2 °C can be found between the outer islands (Molina *et al.*, 1996; Morales-Matos and Pérez-González, 2000). The coldest waters are located around the eastern islands of Fuerteventura and Lanzarote due to the proximity of the African upwelling which "pumps" cold water to the surface.

The marine thermal structure of the superficial layer in the Canaries is characterized by the presence of two typical thermoclines; a superficial "seasonal thermocline", variable in its form and magnitude throughout the year, and a second more deep and stable "permanent thermocline". The seasonal thermocline varies because of strong annual rhythms in heating and wind strength. The period of strongest near surface stratification occurs in the summer (15 m depth) when insolation, but also wind forcing, is strongest. The situation differs from the temperate seas, where winter cooling coincides with strong winds. The time of maximum penetration of the surface mixed layer is in the winter and beginning of spring, with a depth of 100-150 m. The permanent thermocline is normally located between 600 and 800 m, however, as it is usually very weak it can be masked by the influence of Mediterranean water (Demetrio pers. comm.).

Salinity

The water salinity around the islands is constantly maintained, but there are differences among islands. In the same period, salinity values are in the range of 36-37 PSU between the outer islands in the archipelago (Molina *et al.*, 1996).

Winds

The large-scale mean atmospheric flow in the Canary Islands area is formed by the Trade Winds. During July-August the Azores High is at its northernmost position and the boundary of the trade winds is approximately between 32° N and 20° N. In autumn, the Azores High begins to move southward until it gains its southernmost position in winter (Pacheco and Hernández-Guerra, 1999).

The Canary Stream Current

The main large-scale oceanic flow in the Canary Islands is the Canary Current, which is the eastern boundary current of the North Atlantic subtropical gyre. The Canary Current is fed by the eastern branch of the Azores Current which turns southward east of Madeira Island (Stramma, 1984; Klein and Siedler, 1989; Fiekas *et al*. 1992). The Canary Current flows southward along the African coast and turns south-westward around 20° N contributing to the North Equatorial Current. This is the large-scale behaviour of the eastern subtropical gyre which, of course, presents considerable time and space variability. According to Stramma and Siedler (1988), the seasonal variability consists of a southward shift of the Azores Current, a northward shift of the North Equatorial Current, and the approach of the Canary Current to the African coast during summer.

The Canary Current is a slightly cold surface current that flows in the SSW direction, and is stronger in the top 200 m (Fiekas *et al.*, 1992). Outside of the archipelago the Canary Current has a mean velocity of 15 cms^{-1}, but when it passes between the island channels it may reach values of up to 25 cms^{-1} (Molina, 1996). This current is faster in the eastern islands, where the highest speeds have been measured in the corridors between the islands at up to 60 cms^{-1}.

Mesoscale phenomena

The Canary Islands lie in a transitional zone between the northwest African coastal upwelling region and the open ocean waters of the subtropical gyre. They present a barrier to the relatively weak equatorial flow of the Canary Current and to the flow of the Trade Winds, giving rise to a variety of mesoscale phenomena, such as eddies, intrusion of cold water filaments from the African coast and warm water tails (Fig. 2.3).

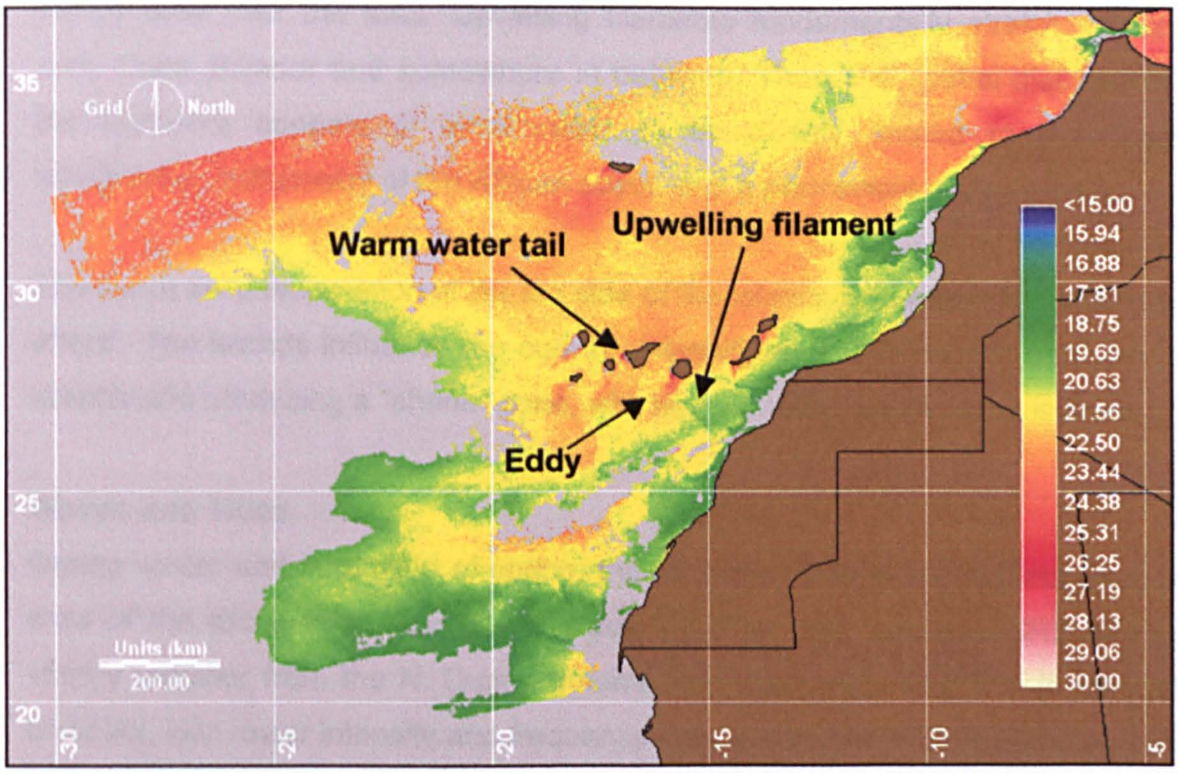

Fig. 2.3: Sea surface temperature (°C) derived from AVHRR-14 satellite image (16-07-1999).

Typical seasonal hydrographic conditions (Stramma and Siedler, 1988) are geographically altered by mesoscale circulation induced south of the islands. The main patterns associated with the islands are cyclonic and anticyclonic eddies downstream of the islands (60± 80 km in diameter), apparently caused by their effect as a topographic obstacle to the flow of the Canary Current (Arístegui *et al.*, 1992; Arístegui *et al.*, 1994). These eddies are present during all seasons, suggesting that the speed of the Canary Current is always sufficiently strong to develop eddies (Pacheco and Hernández-Guerra, 1999). These structures cause perturbations in the distribution of chemical species and in biological parameters (nutrients, metals, primary production, etc.).

The large-scale variation of the Trade Winds, which is coupled to the meridional shift of the Azores High, determines the strength and persistence of coastal upwelling along the African coast. Upwelling filaments stretching from the African coast into the islands characterize the pattern associated with the influence of the continental upwelling system over the ocean surrounding the islands (up to 300 km long). They are present only in summer and early autumn when strong Trade

Winds blow over the area. Upwelling filaments fundamentally stretch off Cape Jubi, Cape Bojador and somewhere in between. Thus, the spatial distribution of the filaments appears in most cases to be closely related to the coastal topography, bathymetry of the African coast, and a permanent cyclonic eddy.

The warm tail phenomenon at the lee side of the islands is due to the “island mass effect”. The islands influence the current, intensifying it as it passes between the islands and producing a "shade" zone, with warmer water south of the islands.

Waves and Tides

During winter and beginning of spring, the windward side is the highest exposed area of the archipelago due to the Trade Wind blowing from the NNE and the stormy weather from the N. During autumn, the main wave direction is also NE, however, with lower intensity and frequency than in summer. As a consequence of the sporadic W storm episodes, there are frequently some waves coming from the NW and SE with heights up to 10 m. During the end of spring and summer, the wave intensity decreases to average heights of 1 m.

In the Canaries, the tides are semidiurnal, with maximum fluctuations near 3 m. The tide wave moves towards the north, and when it collides with the Archipelago produces several phase lags due to the location and shape of the islands. Tidal currents have an enhancing or mitigating effect on the Canary Current, generating local anomalies.

Nutrients

The oceanic waters close to the Canary Islands have low amounts of nutrients in the euphotic zone, indicating the oligotrophic conditions of the archipelago waters (Braun *et al.*, 1982). A seasonal thermocline develops in oceanic areas, between 50 and 120 m, throughout most of the year, limiting the supply of nutrients to the surface layer (de León and Braun, 1973). Surface waters are mixed only during winter, allowing nutrients to reach their highest levels during late winter or early spring. However, these nutrients are quickly depleted through biological processes, returning to the former low productivity situation (Braun, 1980; Braun *et al.*, 1986).

Despite the general belief regarding the oligotrophic nature of the offshore waters of the Canary Islands, it has recently been disputed that the oligotrophic condition is the typical situation in this area. The mesoscale circulation in the Archipelago produces anticyclonic and cyclonic eddies south of the islands, the latter of which provide a supplementary source of cold, deep and nutrient enriched water (Basterretxea-Oyarzabal, 1994). Additionally, large upwelling filaments (up to 300 km long) extending from the African coast, together with atmospheric inputs affect the flow of nutrients and organic matter in the region (Davenport *et al.*, 1999).

Primary production

Although there is a lack of detailed seasonal biological studies in the Canary region, reported mean primary production and chlorophyll values are generally low throughout the year (De León and Braun, 1973; Braun and Real, 1984; Braun *et al.*, 1985; Fernández de Puelles and Gracía-Braun, 1989; Aristeguí *et al.*, 1989). Nevertheless, relatively high surface values (~0.5 mg Chl a m^{-3}) are reported from January to March (Aristeguí *et al.*, 1997), coinciding with the erosion of the thermocline. This enhancement is the result of nutrient enrichment of previously depleted surface waters, and therefore is more like the autumn bloom of temperate seas than the spring bloom. The close coupling between phytoplankton and grazers presumably prevents the accumulation of phytoplankton populations at surface (Arístegui, 1990). Thus, a weak late winter bloom is apparent during January and February, decreasing gradually towards spring and summer (Arístegui, 1997).

Marine flora and fauna

From a zoogeographic point of view, the Canaries are unique because its species composition in not what would be expected. For its geographical position, the archipelago belongs to the Mediterranean-Atlantic Region, but the Canary waters have a high presence of Mediterranean, as well as Antilles, African and Indopacific species. Within the archipelago there is species variation, both quantitative and qualitative, from the western to the eastern islands. For example, species with warmer water affinities occur predominately in the western islands while those with more temperate-water affinities are present in the eastern islands (Falcón *et al.*, 1996).

2.2 TENERIFE

Tenerife is located in the Atlantic Ocean, between the 28º and 29º North parallels and the 16º and 17º West meridians. It is the largest island of the Canary Archipelago with an area of 2,036 km^2, and has the longest coastline, at 398 km. The island is a triangular pyramid shape with a truncated apex at an altitude of 2000 m, from which the volcano Teide rises to 3,718 m. Fig. 2.4 shows a radar satellite image of Tenerife, where different vegetation zones, both natural and agricultural, are visible as areas of green and blue tones respectively. The purple and white areas are houses. The summit crater of Teide, clearly visible in the left centre of the image, contains lava flows of various ages and roughness that appear in shades of green and brown.

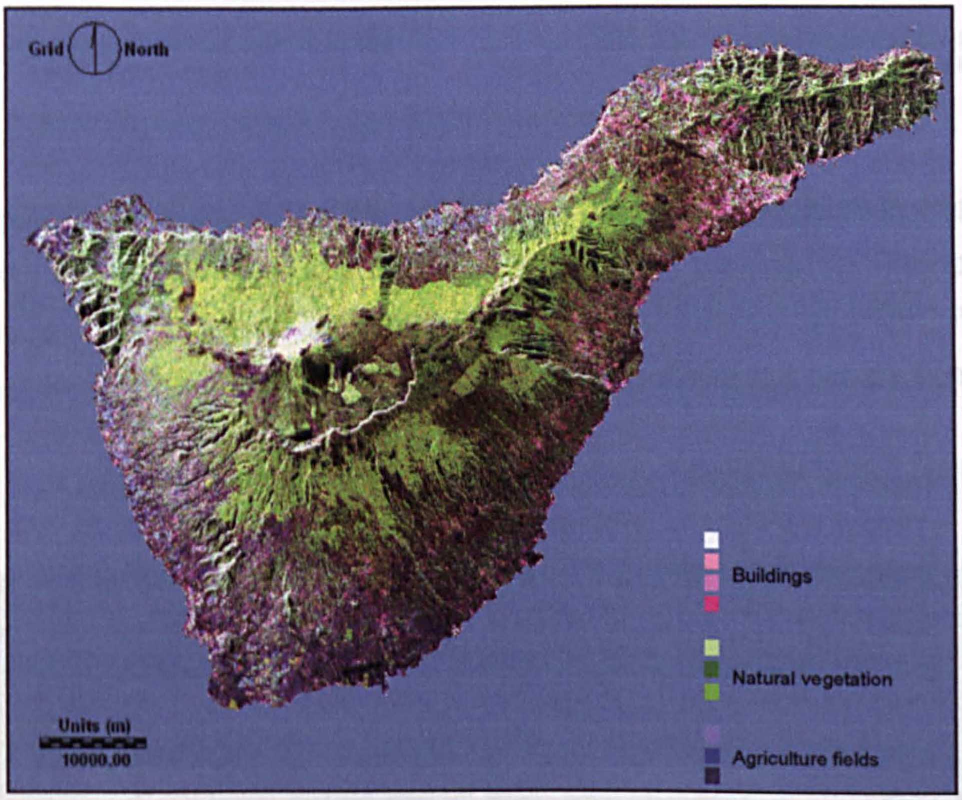

Fig. 2.4: SIR-C/X-SAR image of Tenerife taken August 10, 1995 (courtesy of Public Information Office Jet Propulsion Laboratory, California Institute Of Technology, National Aeronautics And Space Administration).

2.2.1 Population

The island's population has risen from 261,817 inhabitants in 1940 (128 inhabitants/km²) to 692,366 in 1999 (340 inhabitants/km²) (ISTAC, 2001). The cumulative annual growth rate during that period shows an increase of 2%, though in the last few years it has been reduced and now has similar levels to those of the rest of Spain. Fig. 2.5 shows the population progression in Tenerife for the last 11 years, and Fig. 2.6 indicates a generalized model of the predicted future population for the next 11 years.

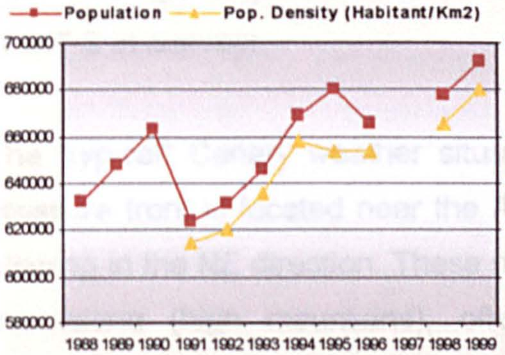

Fig. 2.5: Population evolution. Data obtained from ISTAC (2001).

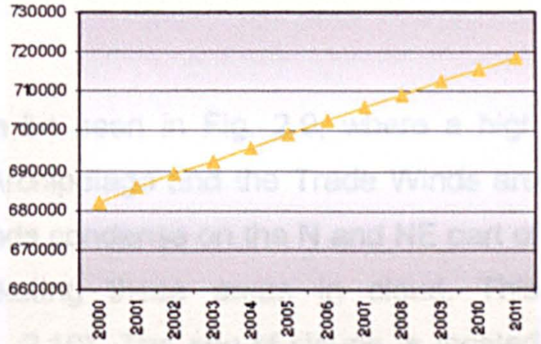

Fig. 2.6: Predicted population evolution. Data obtained from ISTAC (2001).

This population increase is not the same for all the Island's regions. In effect, the so-called metropolitan area (Santa Cruz de Tenerife, La Laguna, Puerto de la Cruz and Arona) has tripled its population in the same time period (Fig. 2.7). Fig. 2.8 shows the 31 municipalities and 743 population districts in to which Tenerife is divided.

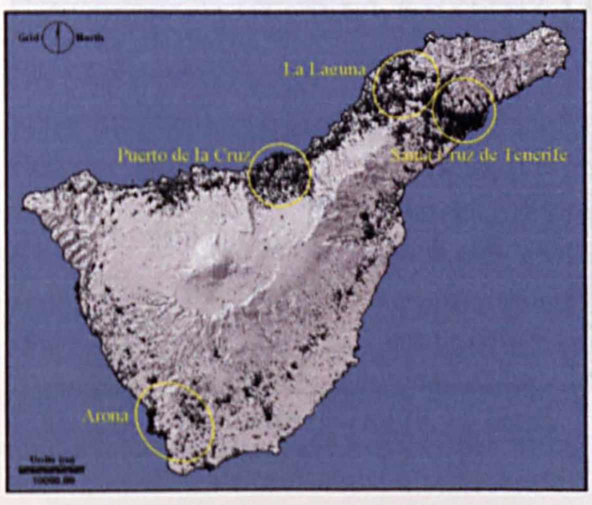

Fig. 2.7: Building density in Tenerife. Data obtained from CD-Map (1996).

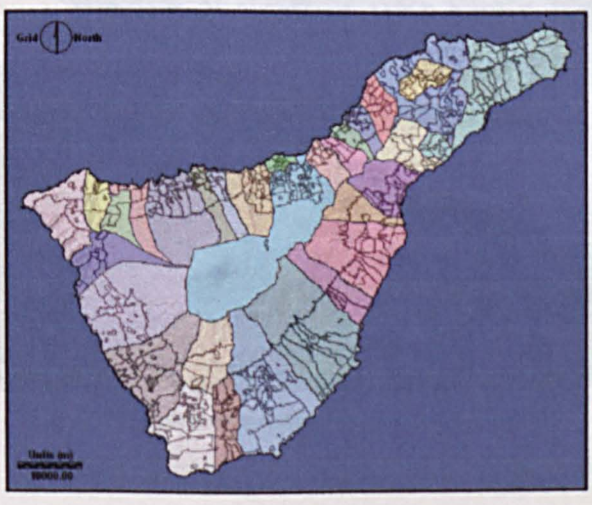

Fig. 2.8: Municipalities (in colour) and population districts (black lines) in Tenerife. Data obtained from CD-Map (1996).

2.2.2 Weather

Tenerife is known as the island of the "*eternal spring*" due to its mild, temperate and moderate weather throughout the year. Its subtropical situation, the presence of the trade winds, the topography of the island and the Canary current all contribute to this situation. There are no seasons of extreme cold or suffocating heat. Average temperatures fluctuate between 17º and 18º C in winter, up to 24º or 25º C in summer.

The "typical" Canary weather situation can be seen in Fig. 2.9, where a high pressure front is located near the Azores Archipelago and the Trade Winds are blowing in the NE direction. These moist winds condense on the N and NE part of the Island (high mountains), often blanketing these areas in cloud. This phenomenon is called "sea-of-clouds" (Fig. 2.10). The sea-of-clouds is located between approximately 600 and 1,800 m and provides a very important source of water, know as "horizontal rain". Its upper limit is determined by the circulation of high altitude winds, dry and warmer, which act as a barrier for the clouds to rise and go past the relief crossing to the south side of the island. However, sporadic atmospheric perturbations temporarily modify this so call "normal" situation generating diverse climatic variants, such as torrential rain, snow or strong winds.

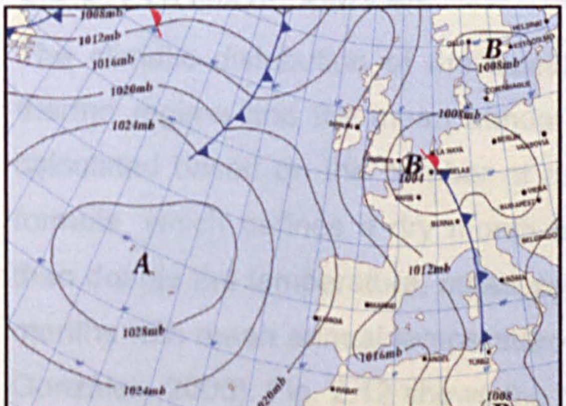

Fig. 2.9: Typical weather situation in the Canary Islands (Morales-Matos and Pérez-González, 2000).

Fig. 2.10: Cloud-sea in the north slope of Tenerife.

There is a great difference in climate between the northern windward and the leeward southern slopes (the Foehn effect). There are more sun hours per year in the S and more rain and humidity in the N. The southern slopes lie in a rain shadow, and temperature variance is largely controlled by incoming radiation because of the shelter from prevailing winds and paucity of cloud cover. Because of this, southern Tenerife experiences an altitude-induced environmental gradient from semi-desert at the coast rising to subalpine conditions on the mountains (Fig. 2.11). One significant divergence from this gradient takes place between 1500 and 1800 m, where cloud can develop in association with a weak temperature inversion caused by moist winds from the north west which blow around the island at this height. This produces a narrow zone of subtemperate climate.

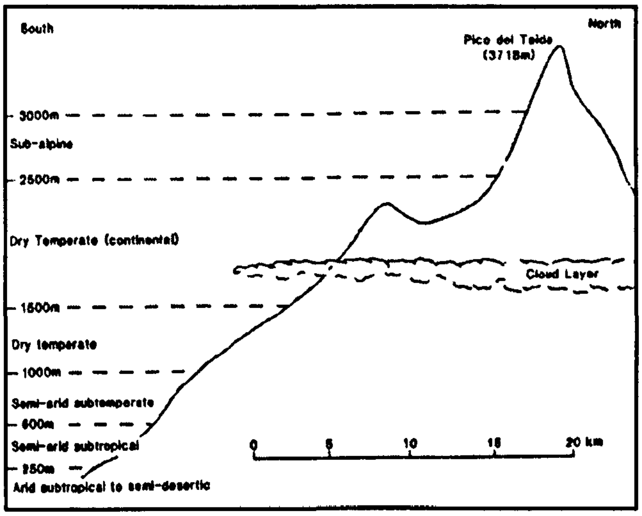

Fig. 2.11: Normal climatic division of the south slope in Tenerife (Jenkins and Smith, 1990)

2.2.2.1 CLIMATIC REGIONS

The climatic distribution of the island is dependent on two factors; the pluvio-thermo regime and the mean annual temperature. The pluvio-thermo regime is calculated based on the number of dry months (as determined by the Gaussen formula, which defines a dry month as one with rainfall, measured in mm, less than double the temperature, measured in degrees centigrade) and the number of months with mean annual temperature less than 8 °C (Morales-Matos and Pérez-Gonzâlez, 2000). Fig. 2.12 shows the climatic map for Tenerife island, from which five different climates can be identified:

Cold climate; mean annual temperature less than 10 °C, with annual precipitation between 400 and 800 L/m^2 and five dry months a year.

Chilly climate; mean annual temperature between 10 and 13 °C, with annual precipitation above 700 L/m^2 and no more than 4 dry months a year.

Temperate climate; mean annual temperature between 13 and 16 °C. Depending on the altitude and the slope it faces (north or south), the annual precipitation varies between 300 and 1100 L/m^2. The number of dry months varies between 3 and 7.

Temperate-warm climate; mean annual temperature between 16 and 19 °C annual precipitation between 200 and 600 L/m^2. The number of dry months is normally between 5 and 6.

Warm climate; mean annual temperature above 19 °C, annual precipitation less than to 350 L/m^2 and with more that 7 dry months a year.

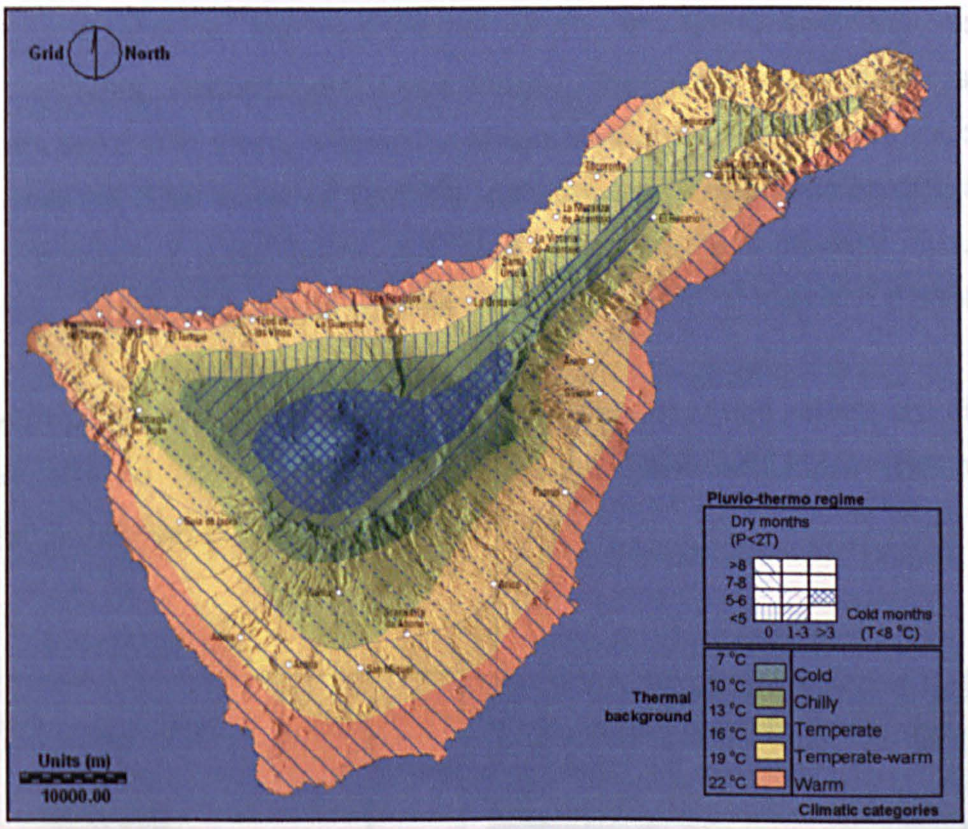

Fig. 2.12: Climatic map for Tenerife. Based on Morales-Matos and Pérez-González (2000).

2.2.3 Flora and Fauna

Despite its size (2034 Km^2), Tenerife has a surprisingly rich biological diversity due to its special climate. The rugged terrain of the island locally modifies the general weather conditions, generating a wide range of micro-climates. The combined action of all the different weather-related agents on the variety of volcanic materials has also led to a wide range of soil types. The influence of all these different factors has generated a whole variety of habitats that shelter many different communities of plants and animals, whose interactions constitute the outstanding ecosystems of Tenerife.

The abundance of micro-climates, and therefore, natural habitats, is clearly reflected in the rich and varied vegetation to be found on the island (1400 species of higher plants, including many species endemic to the Canary Islands (200) and to Tenerife (140)). A heritage of 140 plant species that are exclusive to Tenerife gives the island the greatest wealth of endemic species in the whole of Macaronesia (The Macaronesian region is the name of the group of five archipelagos located in the mid-oriental North Atlantic Ocean; the Azores, Madeira, Salvages, Canaries and Cape Verde). The fauna of the island is also highly interesting, with many endemic invertebrates and unique reptile, bird and mammal species. The fauna of Tenerife includes some 400 species of fish, 56 birds, 5 reptiles, 2 amphibians, 13 land mammals and several thousand invertebrates, along with several species of marine turtles, whales and dolphins

The vegetation of Tenerife can be divided into 6 major zones, which are directly related to altitude and slope (north or south). Their altitudinal and spatial distribution are shown in Fig. 2.13 and Fig. 2.14.

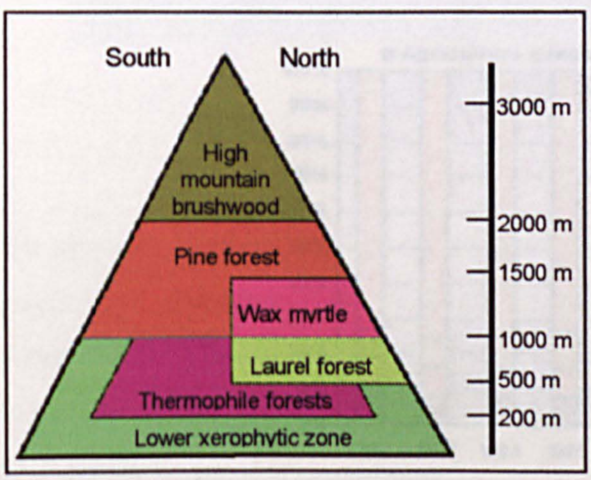

Fig. 2.13: Vegetation altitudinal distribution in Tenerife (Morales-Matos and Pérez-González, 2000).

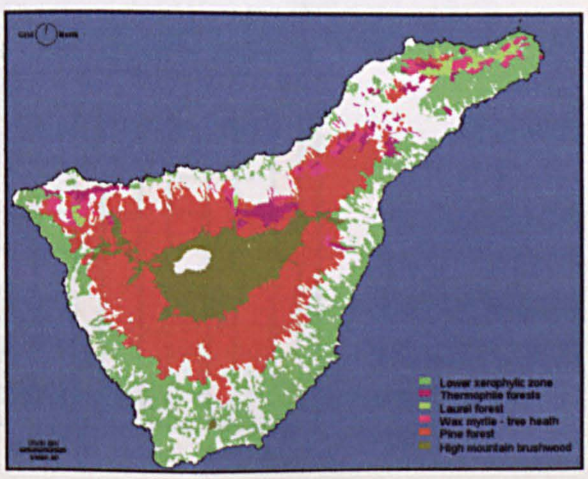

Fig. 2.14: Spatial distribution of vegetation in Tenerife. Data obtained from CD-Map (1996).

Therefore, it is not surprising that almost 45% of the island is protected by regulation in one way or another. Fig. 2.15 shows the spatial distribution and the category of the protected areas.

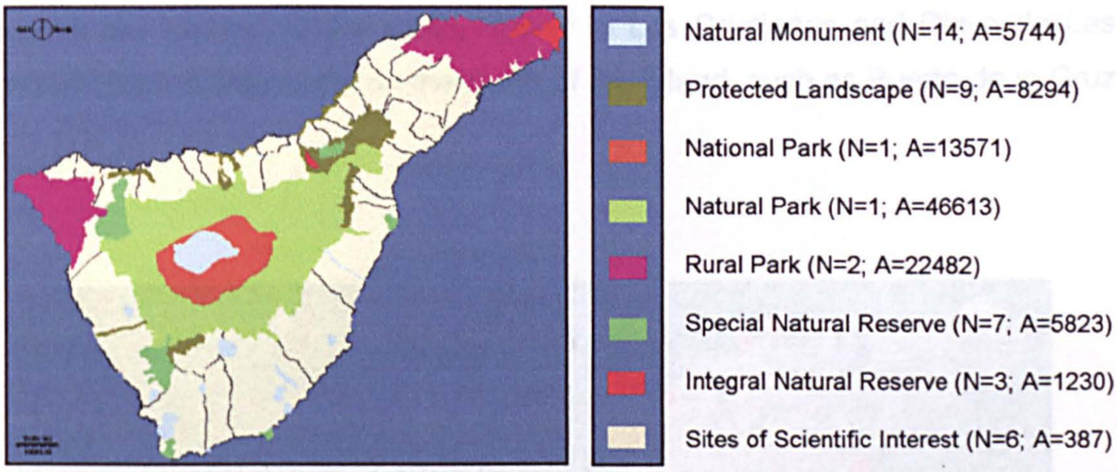

Fig. 2.15: Protected areas in Tenerife (N= number and A=area in Ha). Data obtained from CD-Map (1996).

2.2.4 Economy

The island's economy is more specialised than diversified, with tourism as the driving force. Other sources of income consist of port activity, for both commerce and the services sector, agriculture, livestock, fishing and, to a lesser extent the industrial sector, limited in practice to small processing centres for goods. Fig. 2.16 shows the percentages of occupation by each of the economic sectors.

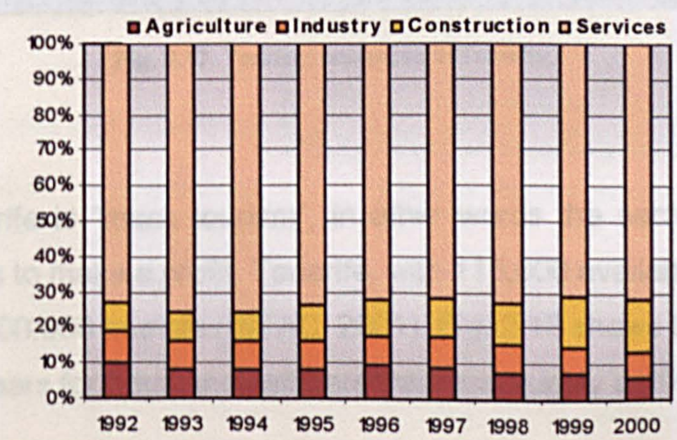

Fig. 2.16: Occupation in Tenerife by economic sectors from 1992 to 2000. Data obtained from ISTAC (2001).

2.2.4.1 Tourism

This is the island's most important economic sub-sector, and the activity which most influences the rest of the island economy. The hostelry and service sectors account for 60% of the GDP (ISTAC, 2001). Tenerife's most important tourist resources are located in the south, mainly in Los Cristianos and Playa de Las Americas, there is also some on the North of the Island, such as Puerto de la Cruz (Fig. 2.17).

Fig. 2.17: Tourism resources in Tenerife.

Tourism in Tenerife is "mass tourism", in other words the sector relies on high number of visitors to make a profit. Tenerife, with 115,000 available beds, annually receives over 2,300,000 tourists (ISTAC, 2001). Fig. 2.18 shows the evolution over a period of five years for hotel and self-catering beds supply and the percentage of occupation.

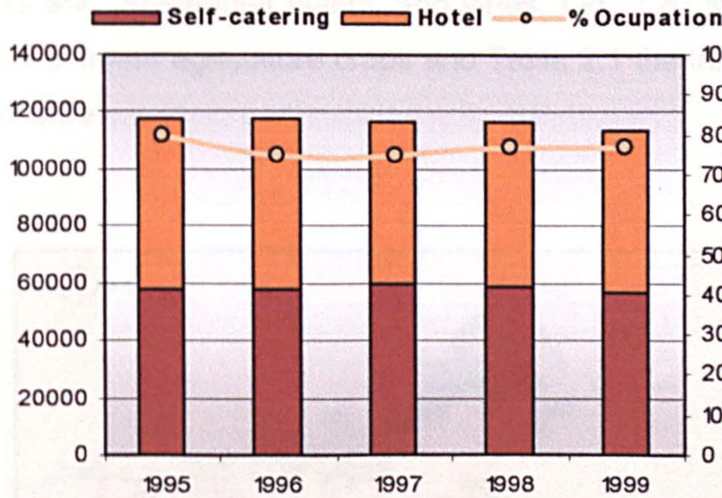

Fig. 2.18: Evolution of the hotel and self-catering beds supply and the percentage of occupation. Data obtained from ISTAC (2001).

2.2.4.2 AGRICULTURE

Agriculture accounts for less than 10% of GDP (ISTAC, 2001), but it makes an important contribution to the island, generating incalculable benefits, related to sustainability of the rural landscape and maintenance of cultural values. Bananas are the leading crop (Fig. 2.19), making Tenerife the leading producer in the Canary Islands. During the last few years, harvesting techniques have been improved, resulting in greater production and quality with a corresponding increase in profitability. The land area used for agriculture has been reduced from 71,849 Ha in 1993 to about 23,000 Ha presently (ISTAC, 2001). Annual production has stabilised at around 150,000 metric tonnes in recent years, after peaking at 200,000 tonnes in 1986 (ISTAC, 2001). Just over 90% of the crop goes to the Spanish domestic market. The next most important crop is tomatoes (with a production of 125,000 T), followed by

Fig. 2.19: Banana plantations in Tenerife.

potatoes, flowers and ornamental plants, and vines. Fig. 2.20 shows the spatial distribution of the different agriculture crops and Table 2.1 the land used over the past years in Tenerife.

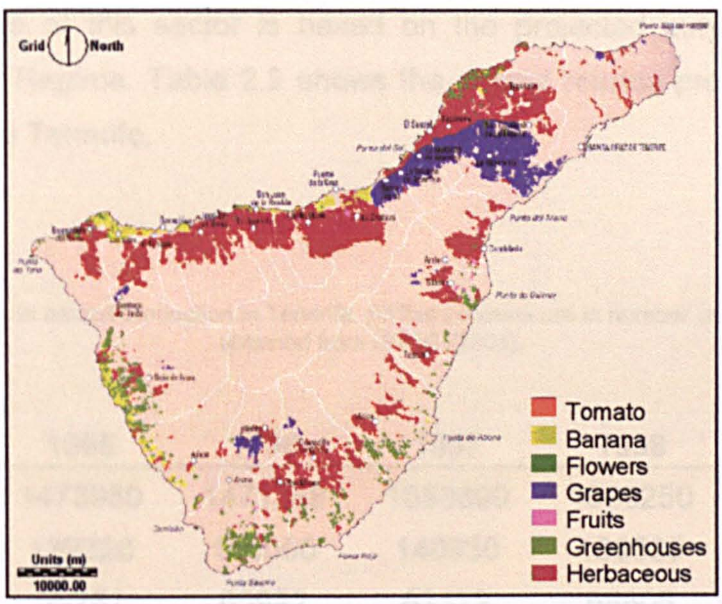

Fig. 2.20: Spatial distribution of the different agriculture crops in Tenerife. Data obtained form Morales-Matos and Pérez-González (2000)

Table 2.1: Land used (Ha) by the main agriculture crops from 1995-1999. Data obtained from ISTAC (2001).

	1995	1996	1997	1998	1999
Grapes	6657	7005	7326	7637	7741
Bananas	4186	4005	4041	4103	4141
Potatoes	3786	3960	3984	3809	3384
Tomatoes	1352	1401	1405	1382	1248
Avocados	300	284	270	234	233
Onions	155	142	140	141	111
Beans	132	137	143	144	92
Peppers	44	57	50	50	36
Cucumbers	32	28	29	21	13
Pineapples	2	2	2	1	1
Others	5736	5920	5478	5179	4537

2.2.4.3 ANIMAL REARING

Animal rearing on the Island is of great importance. Its production is mainly directed toward self-consumption and industrial products such as milk and cheese. This sector is growing due to the internal meat production deficit and the constant support from the regional administration, national government, and the EC. The promising future of this sector is based on the projected subsidies under the Special Supply Regime. Table 2.2 shows the animal rearing progress during the last few years in Tenerife.

Table 2.2: Trends in animal production in Tenerife. All five columns are in number of animals/year. Data obtained from ISTAC (2001).

	1995	1996	1997	1998	1999
Poultry	1473980	1471388	1653690	1688250	1689114
Rabbits	139320	150000	140930	139535	129000
Goats	56261	65992	67172	68805	72517
Pigs	31399	35072	28938	26776	26376
Cows	5499	5947	6038	6537	7628
Sheeps	3735	4325	4149	5183	7189

2.2.4.4 INDUSTRY AND COMMERCE

The island's size and the isolation are serious obstacles for development of the industrial sector. These explain why this sector only accounts for 9.80% of the GDP (ISTAC, 2001). The industry is mainly self-supply directed, with some exceptions such as the tobacco and the canned-fish industry, which are directed toward export markets. The most important industrial sectors are the food industry, electric power production, construction, tobacco and various sectors which cover internal demand. Commerce plays an important role in the economy of Tenerife, accounting for more than 16.60% of GDP (ISTAC, 2001). The extensive road network on the island, the two airports and the major harbours contribute to the development of the sector (Fig. 2.21).

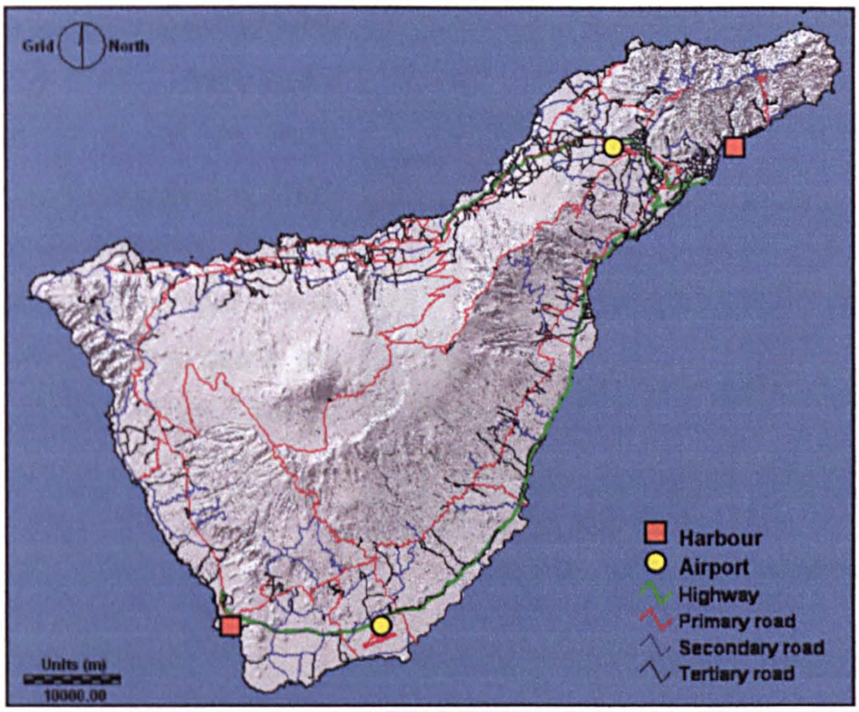

Fig. 2.21: Harbours, airports and road infrastructure in Tenerife. Data obtained from CD-Map (1996).

2.2.4.5 Fisheries

Fishing in Tenerife was a self-sufficient sector until the 1960, when the freezing industry was stabilised, communications between islands and the continent improved, and tourism proliferated (Luengo *et al.*, 1995). The excessive demand for sea-products is causing an over exploitation of most of the coastal resources, which is reaching alarming levels in Tenerife. Very damaging fishing techniques have been used for many years, even though they have been totally banned by the Government.

Most of the fishing effort in Tenerife is coastal, principally because of the coastal geomorphology and the reduced continental shelf. However, in the past few years efforts have been made to adapt the coastal fleet for pelagic fisheries such as tuna, sardine and mackerel. There are also other potential resources which have not yet been exploited due to inadequacy of the fleet, minimal infrastructure and lack of established markets for these products.

In Tenerife, the fishery sector is organised by the Fishermen's Association called "Cofradias". There are 11 of these associations on the island, and each of them has been assigned a specific area for fishing (Fig. 2.22). The names and number of boats for each Fisherman's Association are listed in Table 2.3. In Tenerife, 50% of the fishing boats are under 6 m in length and 80% of the boats are smaller than 9 m in length (Luengo *et al.*, 1995).

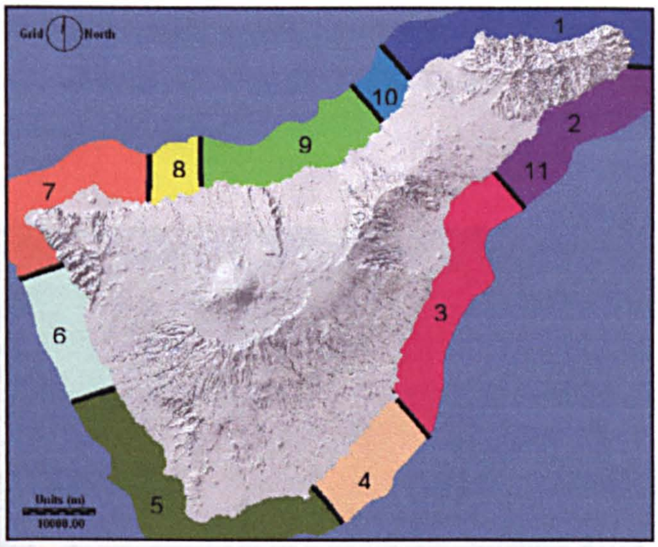

Fig. 2.22: Tenerife Fishermen's Associations. Data obtained from Luengo *et al.* (1995).

Table 2.3: Number of boats per Fishermen's Association (Marín and Luengo, 1998).

ID	Name	Total No. of boats
1	Ntra. Sra. de la Consolación	17
2	San Andres	28
3	Ntra. Sra. de la Candelaria	35
4	San Miguel de Tajao	14
5	Ntra. Sra. de las Mercedes	102
6	Ntra. Sra. de la Luz	67
7	San Roque de Isla Baja	37
8	San Marcos	31
9	El Gran Poder de Dios	37
10	Ntra. Sra. del Carmen	26
11	Sta. Cruz/A.P.A.B.A.T.	14
	TOTAL	447

Total fish captures in Tenerife are estimated to be 12,550 T/year (Luengo *et al.*, 1995), and they are separated into the following categories:

- Oceanic pelagic resources; these are migratory species which include the bigeye tuna, yellowfin tuna, barrilote (Fig. 2.23). These fisheries are estimated to be 6,050 T/year.

- Coastal pelagic resources; which include sardine, mackerel, blue jack mackerel, bogue, etc. This fishery is estimated to be 3,000 T/year. Fig. 2.24 shows the main fishing areas for these species.

Fig. 2.23: Oceanic pelagic resources.

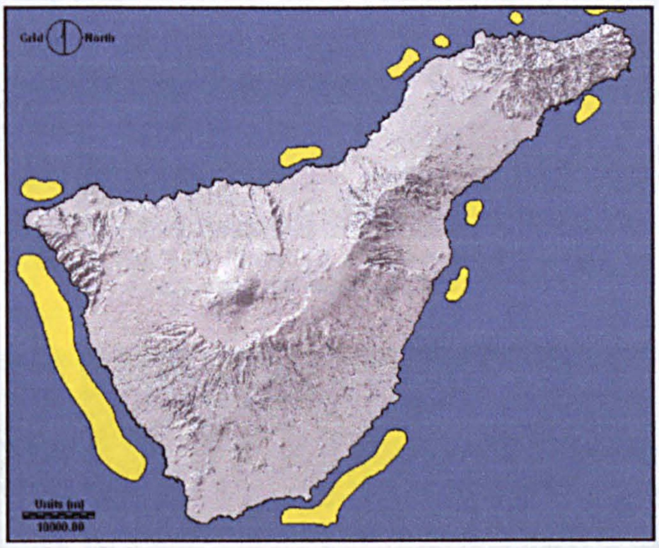

Fig. 2.24: Principal areas of coastal pelagic fishes. Data obtained from Marín and Luengo (1998).

- Littoral fisheries; the artesanal fleet (Fig. 2.25), targets more than 60 species of fish, some crustaceans and cephalopods. These fisheries are estimated to be 1400 T/year. Fig. 2.26 shows the main fishing areas. Fingerlings are used for live bait for some pelagic fisheries. Fig. 2.27 shows the fingerling accumulation areas. Spear-fishing, which is also included in the littoral fisheries category, is estimated to capture 2,100 T/year. Fig. 2.28 shows areas where spear-fishing is permitted.

Fig. 2.25: Artesian boat with dentex (*Dentex gibbosus*) and couch's sea bream (*Sparus pagrus).*

- Shoreline fisheries; include capture of crabs, limpets, abalone and sea snail. This fishery is very difficult to quantify and control. Fig. 2.29 shows the main locations for this fishery in the island.

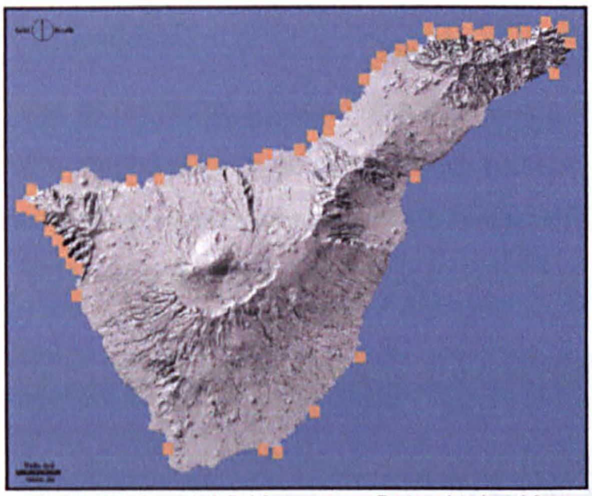

Fig. 2.26: Coastal fishing areas. Data obtained from Luengo *et al.* (1995).

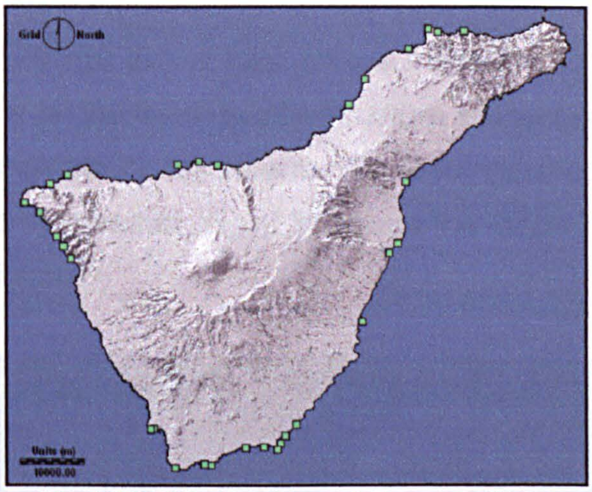

Fig. 2.27: Fingerling accumulation areas. Data obtained from Marín and Luengo (1998).

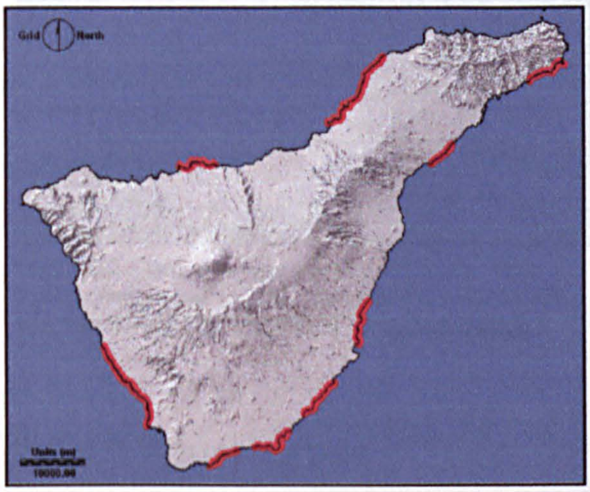

Fig. 2.28: Areas allocated for spear-fishing. Data obtained from Orden de 30 Octubre de 1996; Direccion General de Pesca and Orden Ministerial de 22 de Febrero de 1988.

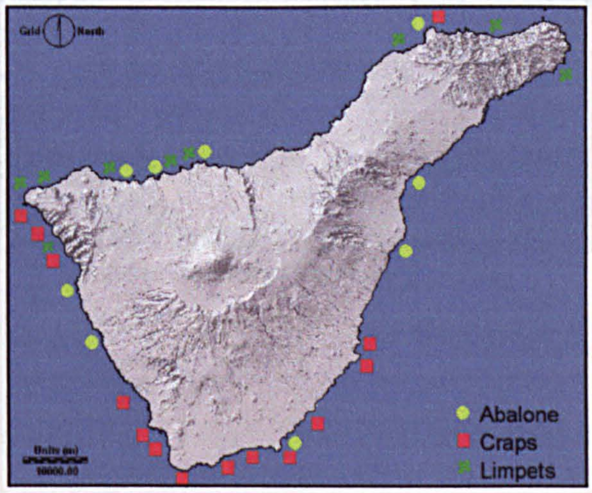

Fig. 2.29: Shore fisheries, ▲ crabs, ✕ limpets and • abalone. Data obtained from Luengo *et al.* (1995).

Until the 1970, fishing harbour infrastructure in Tenerife was limited to small, local and ancient piers located in fishing villages around the island (Luengo *et al.*, 1995). Since then, new refuges and ports have been built to improve and develop the fishing sector. Nowadays, ports in Tenerife can be classified into two main categories, fishing refuges and piers (Fig. 2.30). Fishing refuges are ports which allow access to medium-draught boats, while piers allow access to small boats. These are mostly old historic ports and the Fishermen's Association.

The freezing industry is a key factor to supporting the fishery sector. Pelagic fisheries totally rely on it to operate during the intensive and short season when schools of fish pass by close to the archipelago during their annual migration. On the other hand, littoral fisheries do not rely on the freezing infrastructure as most of the captures are sold locally to nearby markets or restaurants. Small refrigerated trucks are used when some transportation is needed. Fig. 2.31 shows the location of the two freezing infrastructure on the island.

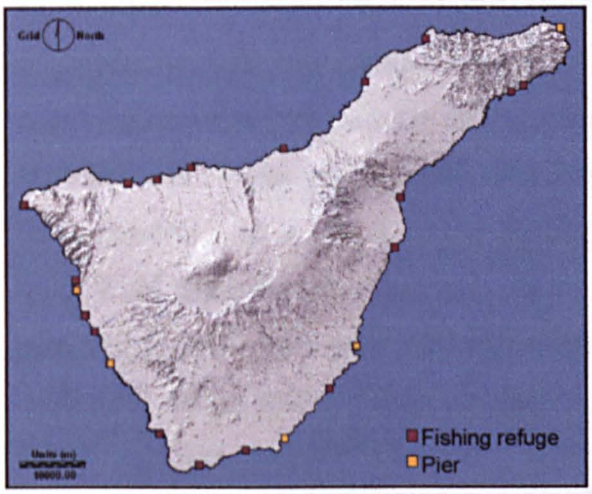

Fig. 2.30: Fishing refuges and piers. Data obtained from Luengo *et al.* (1995), Marín and Luengo (1998) and Morales-Matos and Pérez-González (2000).

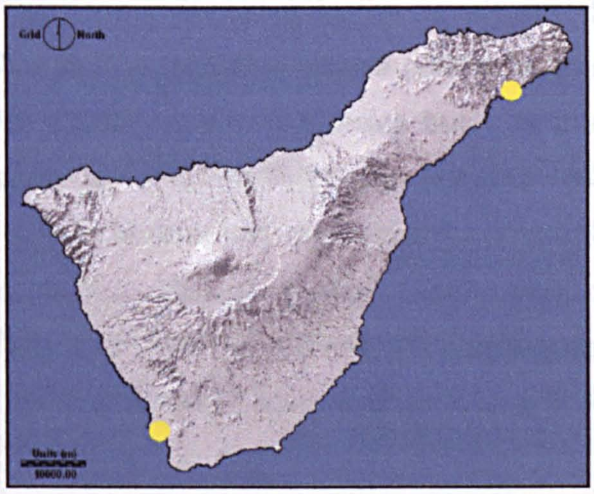

Fig. 2.31: Location of the freezing industry.

2.2.4.6 AQUACULTURE

Aquaculture in Tenerife may potentially be an additional industry to tourism, and could diversify the island's economic activities. Also, it may provide a constant fish supply and hence decrease some pressure on the natural resources. Tenerife has very favourable conditions for culture of marine fish because of its clean and well-oxygenated waters, favourable temperatures for growth (17-25 °C) and stable oceanic salinity (36-37 PSU). On the other hand, there are limiting factors such as scarce land availability, limited number of inlets and the lack of lagoons. An additional disadvantage is the oligotrophic nature of its waters, which makes the culture of filtering molluscs unviable. These disadvantages for aquaculture development in the island could be overcome in two ways; by using cage culture systems which can withstand the waves action, or by very intensive land-based installations which require very little land area.

In the Canaries, at the end of the 1970's the Technological Fisheries Centre (CTP) in Gran Canaria and the Canary Oceanographic Centre (COC) in Tenerife were the regions' pioneers in marine aquaculture. This interest in aquaculture was reflected in the first National Congress in Marine Culture (CONCUMAR, 1980) held in the Canaries. The congress pointed out the ideal conditions of the Canary Archipelago for culture of marine organisms, and identified potential for *Haliotis* sp., *Penaeus kerathurus, P. japonicus, Dicentrarchus labrax, Salmon salar, Anquilla anquilla* and *Psetta maxima*. One year later, in 1981, the first National Aquaculture Strategic Plan (NASP) was developed, encouraging the development of aquaculture in the Canary Islands. This plan recommended the culture of the same species mentioned by CONCUMAR (1980) plus new species such as the crustaceans *Palaemon serratus* and *Artemia sp*., and the fish *Solea vulgaris* and local species. As a result of the NASP, Gran Canaria commenced experimental culture of *Sparisoma cretense, Pagrus pagrus, Sparus aurata, Dicentrarchus punctatus* and *Penaeus sp*. In Tenerife, experimental culture of *Sparisoma cretense, Sarpa salpa, Diplodus sargus, Sparus aurata, Dicentrarchus labrax* and *Psetta maxima* was started.

The present aquaculture situation in Tenerife greatly differs from those initial high expectations, mainly due to the lack of governmental support and interest by the industry sector which was mostly orientated to the tourism. Very few species were properly studied to assess their farming potential, and nowadays the only species cultured on a commercial scale is seabream (*Sparus aurata*). Although *Sparus aurata* is an introduced species in Tenerife, its culture has proved very successful. In Tenerife, the growth cycle of *Sparus aurata* has been reduced to 10-12 months, compared with the 15-20 months needed in the Mediterranean (Cejas pers. comm.). At present there are only four cage farms on the island. They are all small-scale cage operations, growing seabream. However, there are several projects for new sites planned for the near future.

The COC in Tenerife (a governmental research institution) has on-going research for establishment of culture of local species. The COC has preliminarily highlighted some suitable areas for cage aquaculture without any detailed study (Luengo *at al*., 1995). Fig. 2.32 shows these areas, the location of the existing and planned fish farms and the location of the COC. Fig. 2.33 shows the existing four fish farms in Tenerife.

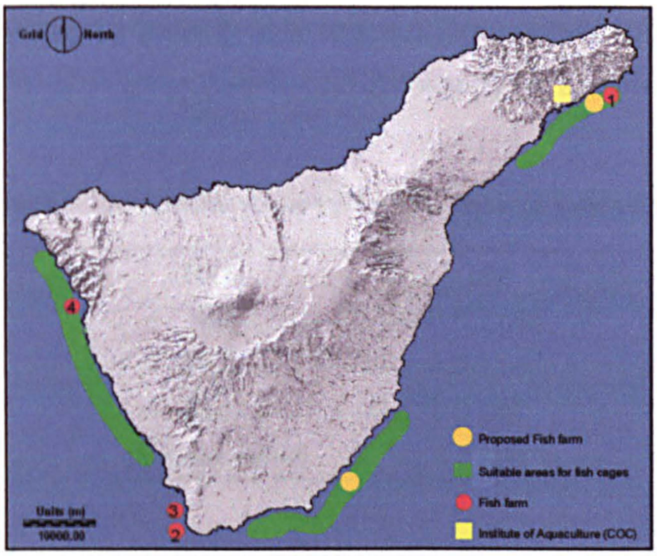

Fig. 2.32: Aquaculture in Tenerife.

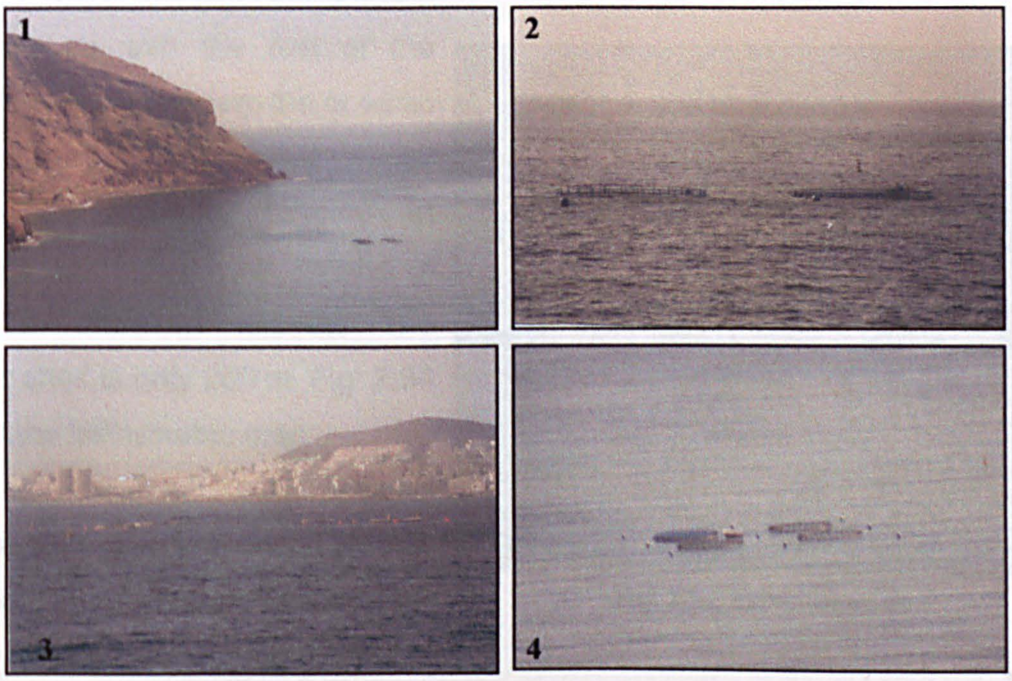

Fig. 2.33: Existing fish farms in Tenerife. Numbers refer to Fig. 2.32.

2.2.5 Marine Environment

Both the particular oceanographic conditions and the seabed morphology govern the marine environment in Tenerife. The most significant mesoscale phenomenon is the shedding of oceanic vortices downstream of the island (Wolansky *et al.*, 1984; Pattiaratchi *et al.*, 1986; Boyer *et al.*, 1987). Eddies, observed downstream of Tenerife, are a common mesoscale feature throughout the year (Arístegui, 1994; Arístegui, 1996; Molina, 1996). Tenerife waters are classified as "oceanic waters", making reference to their very low nutrient content (oligotrophic). Typical marine values in Tenerife for nutrients and chlorophyll-a are listed in Table 2.4.

Table 2.4: Typical water values for Tenerife (Escanez pers. comm.).

NO_3	0-0.5 µM
NO_2	0.01-0.02 µM
PO_4	0.02-0.04 µM
SiO_4	0.6-1.0 µM
Chlorophyll-a	0.2-0.3 mg/m^3

2.2.5.1 Bathymetry and Seabed

Tenerife, as with the rest of the Canaries, emerged from the oceanic basin due to the successive overlay of volcanic material, forming an independent island with depths of 2000 m between islands. The insular shelf is only 200 m. Fig. 2.34 shows the bathymetric map.

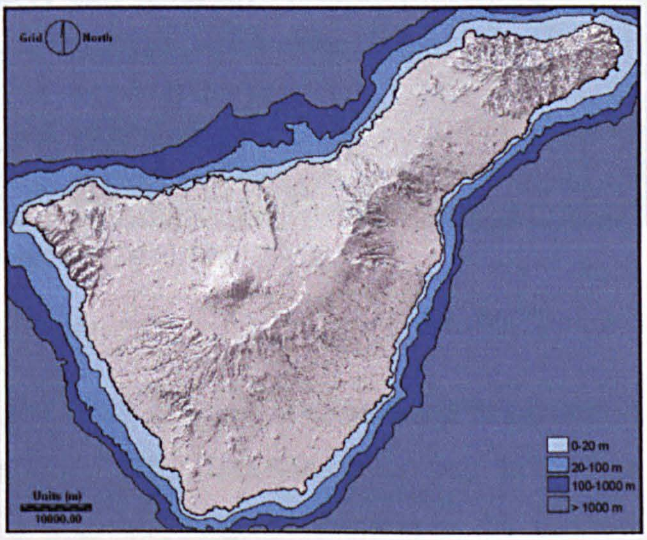

Fig. 2.34: Bathymetric map.

The seabed in Tenerife is broadly divided into three categories; sandy, rocky and algae seabed.

Sand beds are sunken beaches, either of black sand, of inorganic origin, produced by the erosion of the volcanic material, or of white calcareous sand, formed from the remains of marine animals. The substrata of these beds are not very stable, and vegetation only appears from 10 metres depth or in areas protected from currents, forming fields of seagrass (Fig. 2.35). Seagrasses, with their tangled rhizomes, serve to stabilize sediments and help protect the coastline from erosion. They provide food for a variety of important herbivores. The seagrasses themselves provide a platform for the growth of a rich assortment of attached algae and small animals, whose biomass may be almost as great as that of the seagrasses itself (Mann, 2000). Various species of fish and invertebrates obtain their food by grazing the epiphytic community. In addition, the seagrass beds act as refuges for many kind of animals, including the young stages of fish, protecting them from their predators. The net result is that seagrass beds contain many more fish and invertebrates than adjacent areas devoid of seagrasses and are clearly an important part of coastal ecosystems. *Cymodocea nodosa* is the most common and abundant seagrass species in the Tenerife (Alfonso-Carrillo and Gil-Rodriguez, 1980). This seagrass forms submarine monospecific meadows, or mixed populations with *Caulerpa prolifera*, generally located along the south-eastern coast of the island (Reyes *et al.*, 1995).

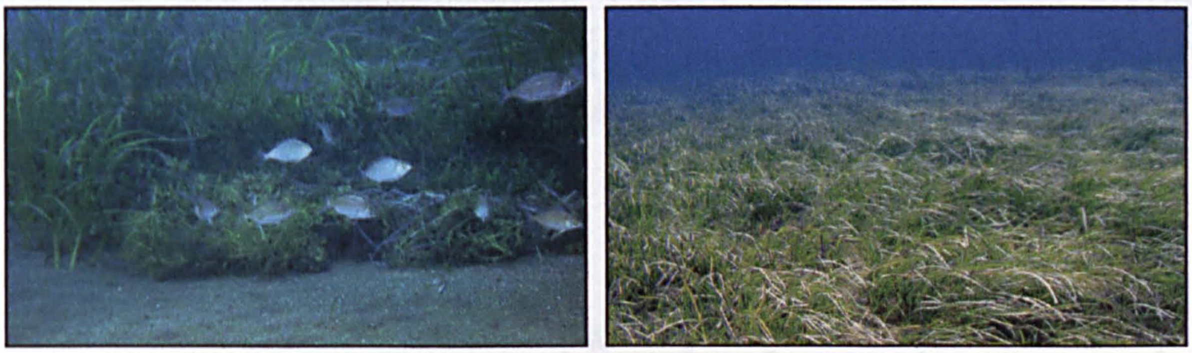

Fig. 2.35: Sandy seabed (Marín and Luengo, 1998).

Rocky seabeds are almost free from any cover due to the constant grazing action of the sea urchin *Diadema antillarum* (Fig. 2. 36). The sea urchin population has grown in size, becoming a pest and it is devastating some areas of the islands. The reason for this is the near extinction of their natural predators due to overfishing, such as parrot fish and sea-starts, producing an imbalance on the ecosystem. The rocky seabed is very poor in species diversity (Falcón *et al.*, 1996), with only a few dominant species present.

Fig. 2. 36: Rocky seabed (Baringo, 1999).

On algae beds (Fig. 2. 37), sunlight is responsible for the spatial distribution of the different species. Close to the surface there is a large amount of seaweed, and the brown alga *Cystoceira abies marina* is the most common. This habitat is the most diverse, with a wide range of vertebrate and invertebrate fauna.

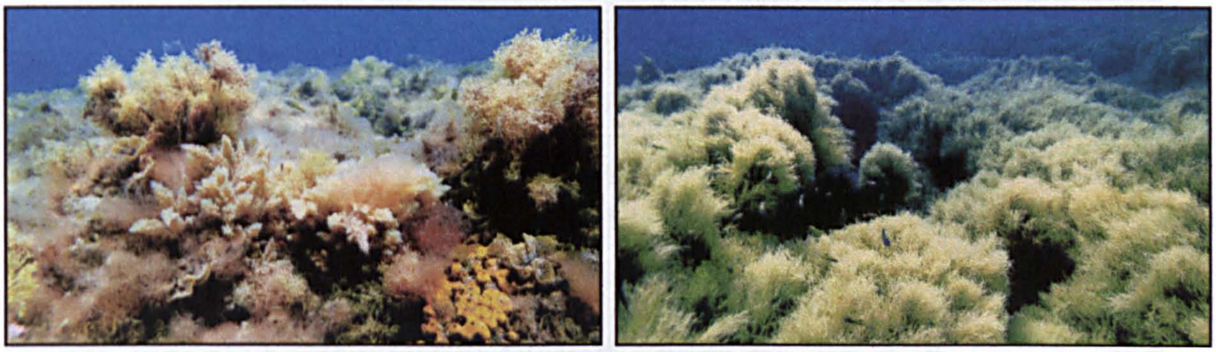

Fig. 2. 37: Algae seabed (Marín and Luengo, 1998).

2.2.5.2 Coast Line

Tenerife's coast line is characterized by its morphologic diversity, which is mostly the result of the volcanic nature of the island. Of its 398 kilometres of coast, 65% are cliffs (35% over 20 m and 30% 2-20 metres), around 12% is flat coast, another 16% are beaches (7% gravel, 3% gravel-sand and 6% sand) and 6% are man-made structures (Marín and Luengo, 1998).

There are notable morphological differences between the North, South, East and West coasts. The North coast combines spectacular sea-cliffs with an abrupt, uneven coast and some beaches. The beaches on this coast are made of black sand (basaltic volcanic material mainly), gravel or a combination of both (Fig. 2.38). By contrast, the South coast is characterised by gentle slopes, many beaches and smoother coastline. Some sea-cliffs are also present on this coast, but in smaller number and size. Beaches are made of whiter sand, from the acidic volcanic material present on this side of the island, gravel or a combination of both (Fig. 2.39).

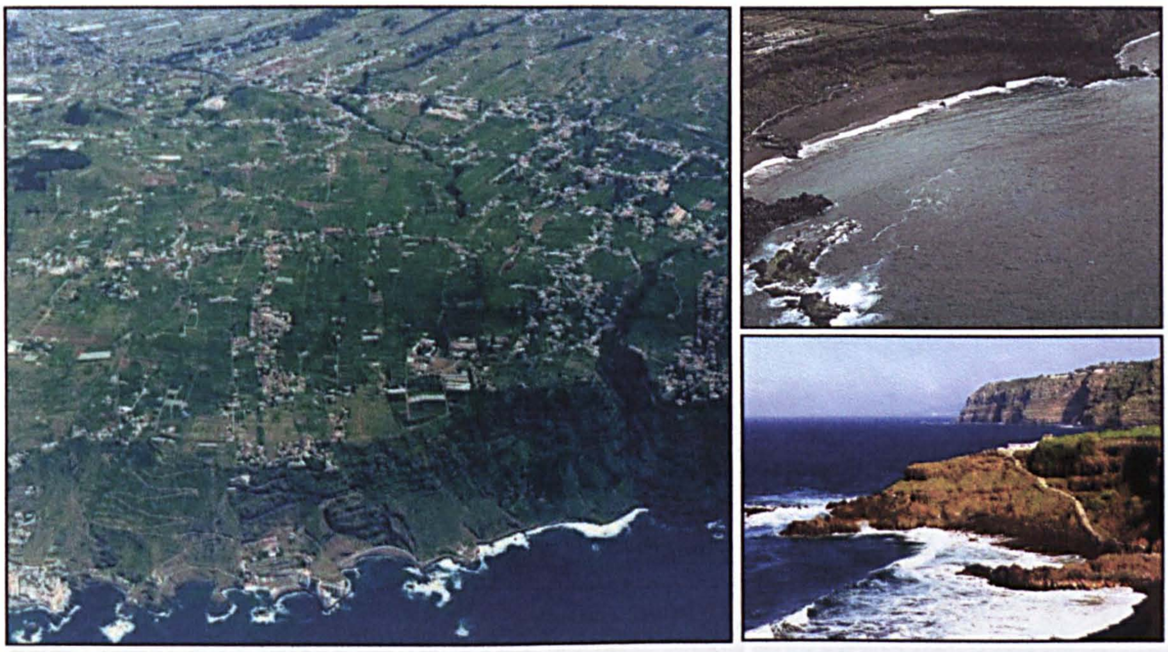

Fig. 2.38: Overview of Tenerife North coast (left), black sand beach (right top) and detail of the abrupt North coast with marine cliffs at the back of the images (right bottom). Aerial photograph obtained from CD-Map (1996) and beach photographs obtained from Official Spanish Beach Guide (2000).

Fig. 2.39: Overview of Tenerife South coast (left), white sand beach (right top) and detail of the gentle South coast (right bottom). Aerial photograph obtained from CD-Map (1996) and beach photographs obtained from Official Spanish Beach Guide (2000).

The East coast is the most abrupt and inaccessible side of the island. Most of this coast can only be accessed by boat or walking through very small pathways. This coast is characterised by its sea-cliffs and mountains that reach down to the shoreline. There are also some black sand beaches (Fig. 2.40).

Fig. 2.40: Overview of Tenerife East coast (left), detail of mountains reaching the East coast (right top), and black sand beach (right bottom). Aerial photograph obtained from CD-Map (1996) and beach photographs obtained from Official Spanish Beach Guide (2000).

The West coast can be classified as a transitional type of coast between the South and the North. The coast can be uneven like the North coast, having some spectacular cliffs, but at the same time, this coast is also characterised by gentle slopes and white sand beaches typical of the South. Black sand beaches are also found, but in a smaller number. The West coast has many very important sand beaches, most of which are artificial or have some breakwater structures to prevent sand being washed out by wave action and occasional storms. These structures also help sand accumulation (Fig. 2.41).

Fig. 2.41: Overview of Tenerife West coast (left), whitish sand beach (right top) and detail of the abrupt cliffs also present in this coast (right bottom). Aerial photograph obtained from CD-Map (1996) and beach photographs obtained from Official Spanish Beach Guide (2000).

Beaches

Beaches in Tenerife are a rare and fragile resource. The 600,000 local inhabitants of the island together with tourists are continually increasing the usage pressure on these beaches. Therefore, numerous artificial sand beaches have been built in the past years to respond to this demand. Fig. 2.42 shows the location of the most important beaches on Tenerife (natural and artificial).

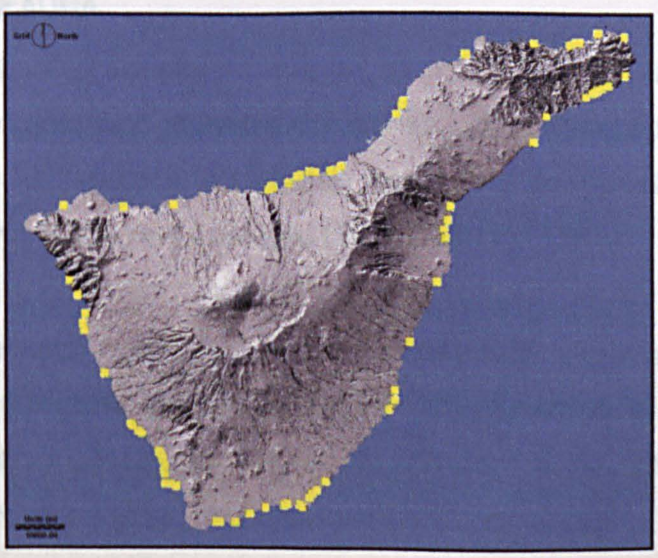

Fig. 2.42: The most important beaches in Tenerife. Data obtained from Official Spanish Beach Guide (2000).

Rocky platforms

These areas are shallow flat platforms, know in Tenerife as "rasas" or "bajas", that have been eroded on the coastline by sea action. They are of great importance, providing an unique habitat for many invertebrate and vertebrates species. These areas are catalogued as "*zoological interest sites*" due to their high biodiversity (Marín and Luengo, 1998). These areas are of great interest for coastal fisheries of invertebrates and fish of high commercial value. Fig. 2.43 shows the location of the main rocky platforms on the island.

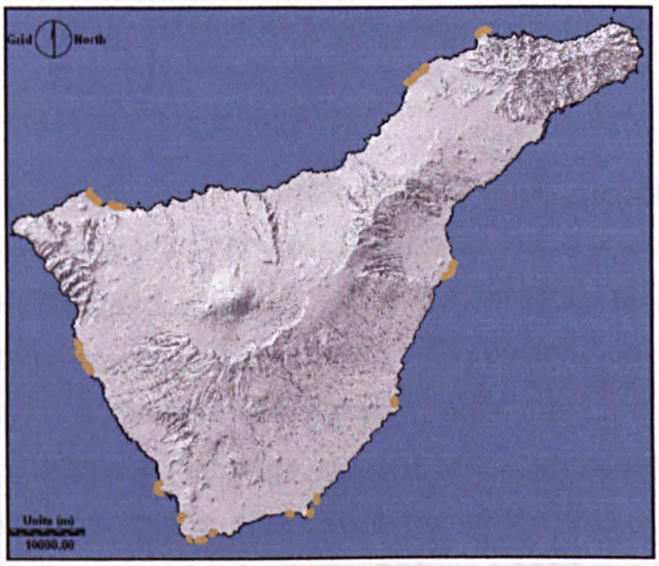

Fig. 2.43: Main rocky platforms location. Data obtained from CD-Map (1999) and Luengo *et al.* (1995).

2.2.5.3 MARINE FAUNA

The ichthyofauna of Tenerife is made up of elements from the Atlantic, Mediterranean, tropical and sub-tropical zones, and Macaronesia, giving it an enormous variety of species distributed according to substratum and depth (Falcon *et al.*, 1996; Marín and Luengo, 1998; Baringo, 1999).

The most abundant fish over rocky and algae seabeds are; wrasse (*Thalassoma pavo*), chromis (*Chromis limbatus*), parrot fish (*Sparrisoma cretense*), dusky grouper (*Epinephelus guaza*), comb grouper (*Mycteroperca rubra*), saupe (*Sarpa sarpa*), white bream (*Diplodus sargus*), Conger eel (*Conger conger*), Mediterranean moray eel (*Muraena helena* and *Lycodontis spp.*), blacktail comber

(*Serranus cabrilla* and *S. atricauda*), glasseye (*Priacanthus cruentatus*), scorpion fish (*Scorpaena spp*.), goldeneye perch (*Beryx spendens*) and wreckfish (*Polyprion americanus*).

Sand and stone beds are typified by dentex (*Dentex spp*.), Couch's sea bream (*Sparus pagrus*), common sea bream (*Pagellus spp*.), marmor bream (*Lithognathus mormyrus*), black bream (*Spondyliosoma cantharus*) and meagre (*Argyrosomus regius*).

On mud and sand beds red mullet (*Mullus spp*.), stingray (*Dasyatis pastinaca*), electric rays (*Torpedo spp*.), angel sharks (*Squatina spp*.), houndshark (*Mustellus mustellus* and *Galieorhinus gleus*) and morid cod (*Mora moro*) are found.

In the pelagic ecosystem, both coastal and oceanic pelagic species are represented. Among the oceanic species, some tropical tuna species can be found such as bigeye tuna (*Thunnus obesus*), yellowfin tuna (*Thunnus albacares*) and the skipjack tuna (*Katsumonus pelamis*), along with species from more temperate waters, like the Atlantic bluefin tuna and albacore. Also, there are some species of turtles such as the loggerhead (*Caretta caretta*) and a permanent population of pilot whales and dolphins on the southern coast of the island. These whales, measure 6 to 8 metres and weigh between 800 and 3000 kg, live in groups of between 10 and 200 (Baringo, 1999).

2.2.5.4 CURRENTS

Despite the numerous oceanographic studies based in the Canaries, little is known on coastal circulation (currents) around Tenerife. Molina *et al*. (1996) summarized the path of drifting buoys at several locations around the Island during different periods of time. Fig. 2.44 shows the most probable hypothetical surface current directions obtained by this study. In general, it can be seen that coastal currents are parallel to the shore, and in a clockwise direction. However, in some areas such, as the North of the island between Punta Teno and Anaga, and on the South between Punta Rasca and El Medano, there are insufficient data to confirm this pattern over a whole year. A southern current from Punta Teno to Punta Rasca has been found on several occasions.

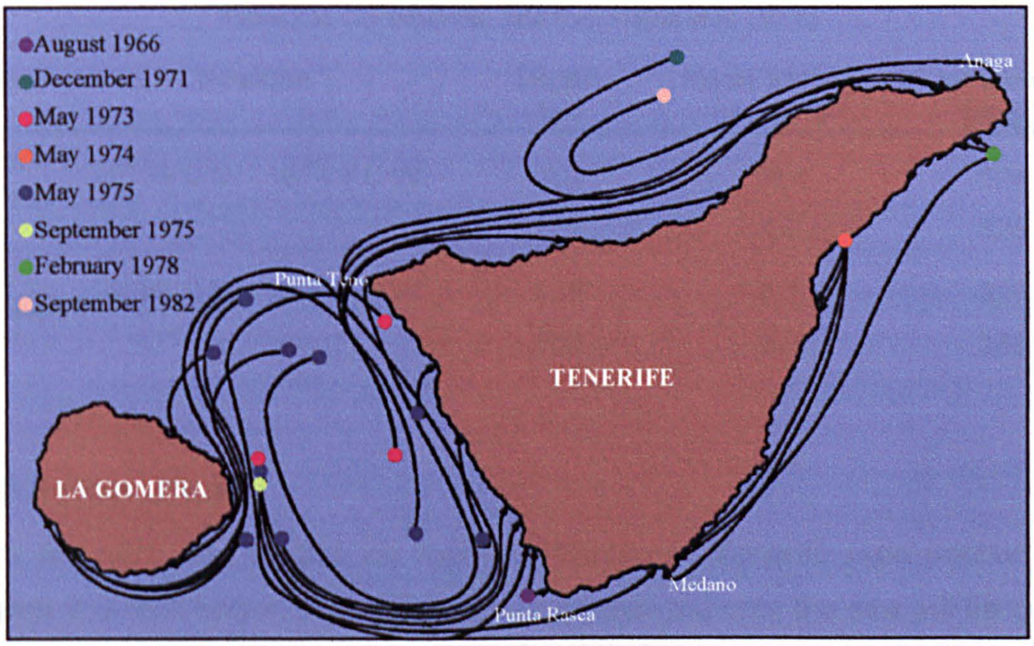

Fig. 2.44: Probable surface current directions (redrawn from Molina *et al.*, 1996).

Molina *et al.* (1996) deployed two current meters from December 1989 until January 1991 in the south-west coast of Tenerife (Fig. 2.45). Each current meter took readings at 15 minutes intervals at two different depths, approximately 150 m and 250 m. Table 2.5 provides information on the location, position, depth, mean velocity and mean direction for each current meter. At both locations, the mean current direction was practically constant and parallel to the coast. The mean current speed was notably faster in Playa San Juan than in Playa de Las Americas. However, during 10 days in April, the current at 139 m depth in Playa de Las Americas was constantly flowing South in direction, reaching velocities up to 52 cms^{-1}, which may be related to an eddy between the islands of la Gomera

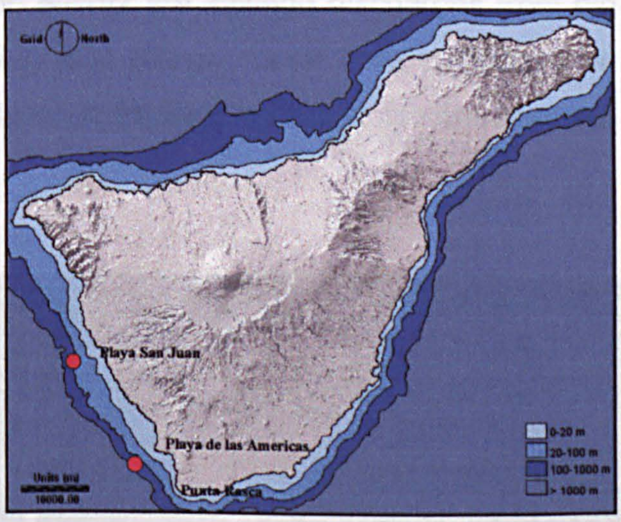

Fig. 2.45: Location of the two current-meter.

and Tenerife. In summer, the intensity of the eddy is magnified, therefore its lower limit moves south, towards Punta Rasca

Table 2.5: Current-meter data from Molina *et al.* (1996).

Location	Position	Depth (m)	Mean Velocity (cms^{-1})	Mean Direction (deg.)
Playa San Juan	28° 08' 0 N - 16° 49' 0 W	152	19.4	324
"	" "	277	4.7	325
Playa Americas	28° 03' 0 N - 16° 45' 0 W	139	3.1	350
"	" "	264	5.0	323

2.2.5.6 POLLUTION

There are very few studies on marine pollution in Tenerife (see section 4.6), however it is well known that any pollutant discharged onto the sea will be quickly diluted and removed because of the dynamic marine environment. Besides the petroleum refinery located in the capital Santa Cruz, there are no important industries or agriculture activities which could discharge any hazardous substances. The major marine pollution events are sewage discharges from big cities and tourism resources (Fig. 2.46) and stream runoff from torrential rain events (Fig. 2.47). Also, the main harbour in Santa Cruz possibly contributes to pollute the surrounding areas.

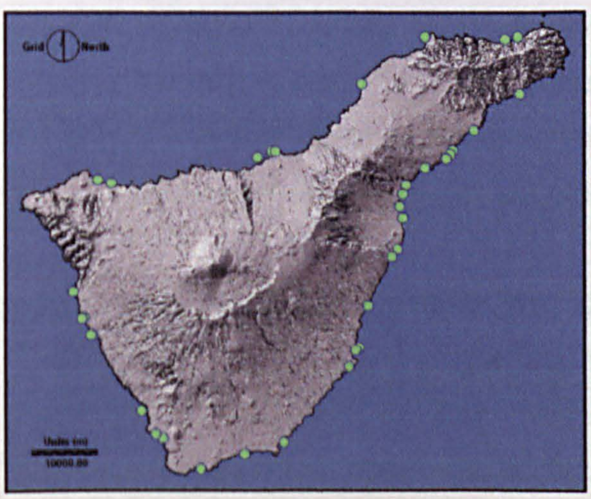

Fig. 2.46: Sewage pipelines. Data obtained from CD-Map (1996)

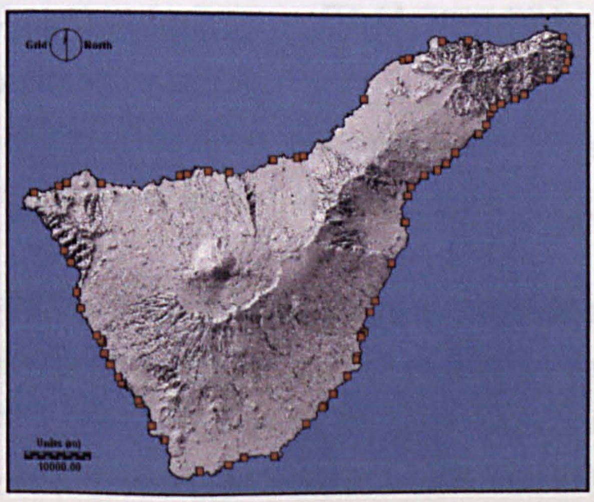

Fig. 2.47: Discharge points from major streams. Data obtained from CD-Map (1999) and Tenerife's topographic map 1:100,000.

Chapter 3

General Materials and Methods

3.1 GIS SOFTWARE AND HARDWARE

Two software packages were used throughout this project, IDRISI32 v1.1 and ERDAS IMAGE v8.3.1. Data processing and modelling was performed mostly with IDRISI32, while ERDAS was used for satellite image processing.

IDRISI32 for Windows (Clark Labs, USA) couples the extensive analytical capabilities of a GIS and an image processing system. It is a raster-based system, but vector files can be used and integrated. Raster files are named as "images". Each image consists of a defined number of rows and columns thus forming cells. These cells are stored as a sequence of numbers (byte, integer or real) representing values (vegetation class-codes, radiance values, etc.). In IDRISI32 cell values are allocated from the upper-left corner (row 0/column 0), then advances column by column and row by row (Fig. 3.1). Normally, the images are stored in binary units (one value after the other), but the simplest ASCII format (cell-values are stored one on each line) is also supported. Depending on the data type a value occupies a corresponding amount of memory. However, data can be compressed using simple RLC (run length compression) into packed binary. The compressed image requires 4 additional bytes, but images with large areas of the same values can show packing ratios of up to 1:100, and more.

	0	1	2	3	4
0	16	16	21	21	21
1	14	14	19	19	5
2	11	11	12	11	11
3	12	11	15	15	15

Fig. 3.1: Raster data in IDRISI32.

ERDAS IMAGE v8.3.1 (ERDAS Inc., USA) is a full suite of products for image mapping and visualisation, image processing for advanced remote sensing. This software is also a raster package that has been designed to integrate two data types into one system, raster and vector. The vector data structure is based on the ARC/INFO data model. Its raster file structure is the same as shown in Fig. 3.1.

All laboratory-based work was undertaken in the Geographical Information Systems and Applied Physiology Laboratory (GISAP) of the Institute of Aquaculture in Stirling University. The GIS software were operated on a DELL twin 400 MHz PII PC with 512 Mb RAM and 45 Gb hard disk. Display was via a 16 Mb Pormedia adaptor and a DELL 21" colour monitor. Digitising and scanning was done using a CalComp Drawingboard III table and a Hewlett-Packard flatbed scanner model ScanJet 3c, respectively. File and data backup systems comprise CDs, tape drives and a local networked server.

Spatial resolution in a GIS environment defines the level of detail at which geographic space is discretized (Jones, 1997). Fine spatial resolution means that the GIS and its data layers contain more detail, while coarse resolution means less detail. The size and complexity of the study area are key factors selecting the spatial resolution (DeMers, 1997). For a relatively small study area, detailed data sets are appropriate. As study areas increase in size, however, storage and processing of spatial data can become cumbersome. Expansion of a study area to a much larger area, therefore, would require vast storage space for data sets, as well as extreme patience with long processing times for managing them.

In this study, because spatial accuracy was of most concern, the GIS database was built based on the 10 by 10 pixel size of the Tenerife satellite image provide by CD-Map (1996). This pixel size, on one hand, will provide enough detail for the correct location of the cages, while on the other hand, maintaining images at a manageable size for analysis and storing purposes. Each image is composed of 8,322 columns and 6,868 columns (56 Mb).

3.2 GIS AND DECISION SUPPORT

Many of the types of decisions made by the public and private sector organizations often involve geographically related data and information, with multiple feasible alternatives, that are often conflicting and involving incommensurate evaluation criteria (Malczewski, 1999). The alternatives are usually evaluated by a number of individuals such as managers, decision makers, and interest groups. These individuals often have unique preferences with respect to the relative importance of evaluation criteria (Barredo, 1996). Accordingly, many real-world spatial planning and management problems involve multicriteria decision-making (MCDM). That is, given a set of alternatives and a set of decision criteria, decision-makers have to chose the best alternative. GIS-based techniques and procedures have an important role to play in analysing MCDM problems, as the technology offers unique capabilities for automating, managing, and analysing a variety of spatial data for decision making (Pereira and Duckstein, 1993).

Spatial multicriteria decision analysis can be though of as a process that combines and transforms geographical data (input) into a resulting decision (output) (Fig. 3.2). The MCDM procedures define the relationship between the input maps and the output map. The procedures involve the utilization of geographical data, the decision maker's preferences, and the manipulation of the data and preferences according to specified decision rules. The critical aspect of spatial multicriteria analysis is that it involves evaluation of geographical events (attributes) based on the criterion values and the decision maker's preferences with respect to a set of evaluation criteria. This implies that the results of the analysis depend not only on the geographical distribution of events but also on the value judgments of the decision-maker involved in process (Barredo, 1996).

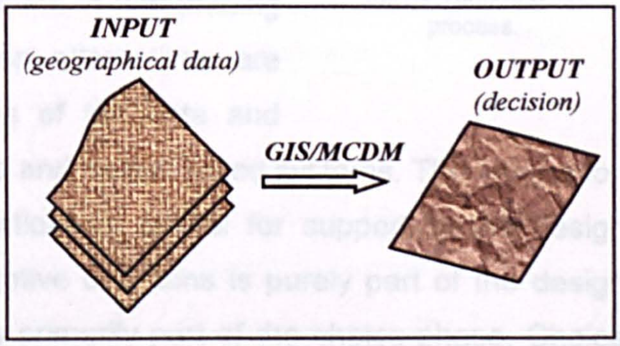

Fig. 3.2: Spatial multicriteria decision analysis: input-output perspective.

The ultimate aim of GIS is to provide support for making spatial decisions. There are a number of frameworks for analysis of the decision process (Raiffa, 1968; Brown *et al.*, 1974; Rietveld, 1980; Burrough, 1990; Goodwin and Wright, 1992; Kleindorfer *et al.*, 1993; Malczewski, 1999) but only Simon's (1960) generalization of the decision-making process is introduced due to its wide acceptance and simplicity. He suggested that any decision-making process can be structured into three major phases: *intelligence*, *design*, and *choice* (Fig. 3.3). During the intelligence phase, raw data are obtained, processed, and examined for clues that may identify opportunities or problems. The data acquisition, storage, retrieval, and management functions convert the real-world decision situation into the GIS database. This involves certain assumptions underlying a particular decision problem. Exploratory data analysis also plays a major role in the intelligence phase. The design phase involves inventing, developing, and analysing a set of possible solutions to the problem identified in the intelligence phase. Typically, a formal model is used to support decision makers in determining a set of alternatives. Spatial decision alternatives are derived by manipulation and analysis of the data and information stored in the GIS database and model-based systems. The integration of decision techniques and GIS functions is critical for supporting the design phase. While the generation of alternative decisions is purely part of the design stage, the evaluation of alternatives is primarily part of the choice phase. Choice involves selecting a specific alternative from those available. During this process each alternative is evaluated and analysed in relation to others in terms of a specified rule which is used to rank (order) the alternatives under consideration. These three stages do not necessarily follow a linear path from intelligence, to design, to choice. In fact, it is usually the case that at any point in the decision-making process, it may be necessary to loop back to an early phase (dashed arrows in Fig. 3.3).

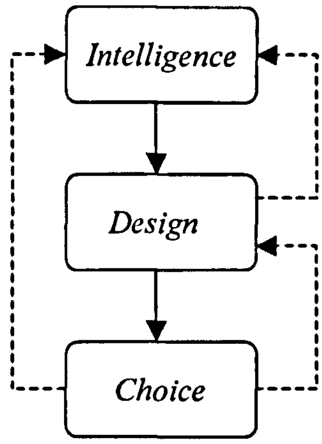

Fig. 3.3: Basic structure of the decision-making process.

3.3 FRAMEWORK FOR SPATIAL MULTICRITERIA DECISION ANALYSIS

Decision-making is a process that involves a sequence of activities that begins with decision problem recognition and ends with recommendations. There are numerous alternative ways to organize the sequence of activities in the decision-making process (Raiffa, 1968; Brown *et al.*, 1974; Rietveld, 1980; Burrough, 1990; Goodwin and Wright, 1992; Kleindorfer *et al.*, 1993) and the quality of the decision can depend on the sequence in which the activities are undertaken. This study is based on an approach built up by the GISAP group at the Institute of Aquaculture, Stirling, which has been researching GIS for aquaculture support for some years (http://www.stir.ac.uk/departments/naturalsciences/aquaculture/GISAP/Pubs/Full_List.htm for a comprehensive list). It is based on the analytical hierarchy process and the pairwise comparison method developed by Saaty (1977) and which has also been recommended by other authors (Pereira and Duckstein, 1993; Lowry *et al.*, 1995; Barredo, 1996; Malczewski, 1999).

What follows is a brief discussion of the multicriteria decision making (MCDM) framework for this study, which is organized based on the sequence of activities involved in the spatial multicriteria decision analysis. The framework, shown in Fig. 3.4, integrates the phase model of decision-making already identified in Fig. 3.3 and the major elements of MCDM.

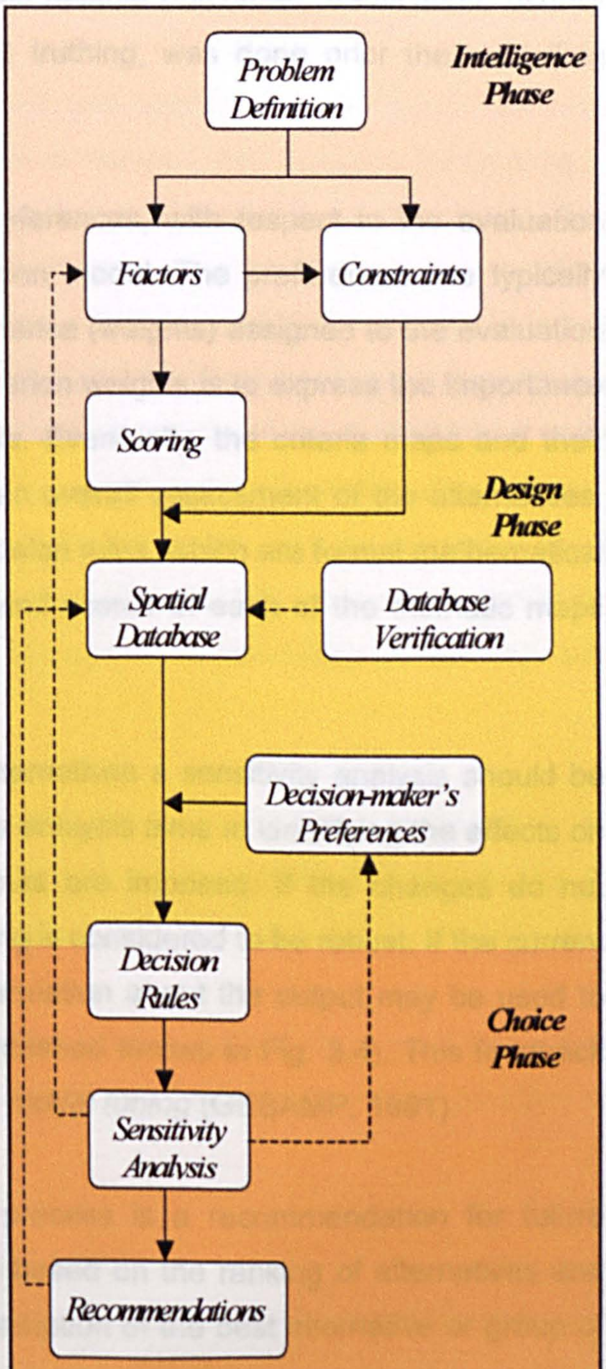

Fig. 3.4: Framework for spatial multicriteria decision analysis followed in this study.

Any decision-making process begins with the recognition and definition of the decision problem. Once the decision problem is identified, the spatial multicriteria analysis focuses on specifying and creating a comprehensive set of evaluation criteria (also know as production functions) that reflects all the concerns relevant to the decision problem. These evaluation criteria can be of two types, factors and constraints. A factor can be defined as a criterion which enhances or detracts from the suitability of a specific alternative for the activity under consideration. On the other hand, a constraint is a criterion which serves to limit the alternatives under consideration. Integration of the factors and constraints into the GIS builds up the spatial database. Given the variety of scales on which all criterion can be measured, multicriteria decision analysis requires that the values contained in the various criterion map layers be transformable to comparable units. This step is known as standardization or scoring. Database verification, also referred to as error analysis (Malczewski, 1999), is an important aspect of the modelling process because of the need to control the quality of data used to obtain reliable outcomes. Verification, usually conducted by field sampling or ground truthing, was done prior the modelling stage.

At this stage, the decision maker's preferences, with respect to the evaluation criteria, are incorporated into the decision model. The preferences are typically expressed in terms of the relative importance (weights) assigned to the evaluation under consideration. The purpose of criterion weights is to express the importance of each criterion relative to other criteria. Eventually, the criteria maps and their weights must be integrated to provide an overall assessment of the alternatives. This is accomplished by appropriate decision rules, which are formal mathematical expressions that combine the weights and scores of each of the thematic maps used.

Subsequently, to obtain a ranking of alternatives a sensitivity analysis should be performed to determine robustness. This analysis aims at identifying the effects on the outputs when variations in the inputs are imposed. If the changes do not significantly affect the outputs, the ranking is considered to be robust. If the current result is found to be unsatisfactory, information about the output may be used to return to the problem formulation step (dashed arrows in Fig. 3.4). This feedback from the sensitivity analysis is known as *model tuning* (GESAMP, 1991).

The end result of a decision-making process is a recommendation for future action. The recommendation should be based on the ranking of alternatives and sensitivity analysis. It may include a description of the best alternative or group of alternatives considered as candidates for implementation.

3.4 CRITERIA CONTROLLING CAGE CULTURE IN TENERIFE

The first step of this study was to identify all the possible criteria (production functions) that may influence the development of marine fish-cage culture in Tenerife. A criterion is defined as any factor that controls the development of an economic activity (Meaden and Kapetsky, 1991).

No universal technique is available for determining a set of criteria. It is obvious that the set of criteria depends on the particular system being analysed, thus making the set of production functions problem specific. Massam (1993) pointed out that the type and amount of information required and available for tackling a particular decision problem is related to the decision situation's complexity. The complexity is, in turn, a function of the number of alternatives and evaluation criteria under consideration, as well as the number of decision makers (interest groups) involved in the decision-making process. However, irrespective of the nature of the decision problem, the procedure for identifying a set of criteria should be a multi-step iteration process which may result in the elimination of redundant criteria, the combination of two or more production criteria, or the decomposition of a criterion into a number of attributes. The set of evaluation criteria for a particular decision problem may be developed through an examination of the relevant literature, analytical study, and opinions.

Selection of the criteria in this study was done by extensive examination of relevant case studies and survey of opinion by a group of experts (by means of questionnaires, see section 5.3.1).

It is not always possible to examine all the criteria defined for a project in great detail, however, there is a need to endeavour to at least review each function in the following terms:

- the degree of influence of each of the criteria,
- the cause and degree of its fluctuation (temporal as well as spatial), and

- the degree of possible manipulation of the criteria to satisfy the necessary requirements.

Criteria were initially subdivided into two major groups, factors and constraints. A factor can be defined as a production function which enhances or detracts from the suitability of a specific alternative for the activity under consideration (Eastman, 1993). An example of a factor could be the water temperature. This factor may increase the growth of fish if values meet the physiological needs of the species or it may reduce its growth if the temperature is out of the acceptable range for the species. On the other hand, a constraint is a production function which serves to limit the alternatives under consideration (Eastman, 1993). Constraints were developed as Boolean images (containing either one or zero). For example, military areas and natural reserves are constraints. It does not matter how suitable those areas may be, they cannot be used.

Factors were further subdivided into natural groupings, such as water quality factors, infrastructure factors and so on. The factors and constraints identified in this study are listed in Table 3.1.

Table 3.1: Groups of factors and constraints relevant to marine cage aquaculture development in Tenerife.

1	BEACHES 1.1 Length 1.2 Width 1.3 Composition 1.4 Rate of occupation 1.5 Rate of urbanisation
2	FISHERIES 2.1 Fingerling accumulation 2.2 Pelagic fisheries 2.3 Rocky platforms ("rasas")
3	INFRASTRUCTURE 3.1 Harbours (fishing refuges and piers) 3.2 Freezing Industry

4	**MARINE ENVIRONMENT** 4.1 Bathymetry 4.2 Bathymetry Slope 4.3 Currents 4.4 Waves short term 4.5 Waves long term

5	**NAUTICAL SPORTS** 5.1 Scuba-diving sites 5.2 Scuba-diving in particular marine habitats 5.3 Shipwrecked boats sites 5.4 Spearfishing 5.5 Windsurfing sites 5.6 Near-shore sailing sites

6	**WATER QUALITY** 6.1 Sewage discharges 6.2 Temperature 6.3 Suspended solids

7	**VIEWSHED** 7.1 Viewshed from tourist resources 7.2 Viewshed from beaches

8	**CONSTRAINTS** 8.1 Seagrass meadows 8.2 Sewage pipes 8.3 Harbours (inside and entrance) 8.4 Windsurfing in El Medano beach 8.5 Proximity to industrial areas

3.5 DATA INPUT

Data input refers to the process of identifying the data sources for those criteria previously identified, gathering the required data, and finally entering this data into the GIS system.

Successful decision-making depends on the quality and quantity of information available to decision makers, and data quality is an important consideration in creating a GIS database. Quality is a function of accuracy, precision and uncertainty. Accuracy is defined as closeness to the truth and the less error, the more accurate are the data. Precision is the ability to repeat a measurement coming to the same answer each time. High precision does not guarantee high accuracy, and vice versa. Uncertainty can be defined as the indeterminacy in spatial/temporal location or attribute classification (Malczewski, 1999). Although it is virtually impossible to eliminate all spatial data errors, all errors must be recognized and dealt with properly to improve the quality of the data.

The data required for this study were available in the form of paper maps, tables, charts, satellite images and surveys. An advantage gained from using GIS is the efficiency of integrating such a wide range of data and information sources into a compatible format. The additional methods used in this study for data capture were very varied, including keyboard entry (for nonspatial attributes and occasionally locational data), manual locating devices (e.g., table digitiser and on-screen digitising), automated devices (e.g., scanning), or by the importation of existing data files (direct conversion from other digital sources)

3.5.1 Digitising

Digitising process involves encoding analog data (hard-copy maps or graphics) into digital using a digitising table and a puck with a cursor to trace and record points, lines and polygons. The digitising in this study was done using a CalComp Drawingboard III digitising table in conjunction with the digitising software CARTALINX v. 1.2 (Clark Labs, USA).

The problem with this method of data input is that most maps are generated for the purpose of displaying information to the user and may not always depict the spatial location of objects exactly (Jones, 1997). Most digitising errors can be attributed to poor map bases and scale. Human error is also a concern and can cause significant errors, depending on a number of factors that influence the ability to trace lines on a consistent basis for long periods of time (Jones, 1997). The Root Mean Square (RMS) error is a measure of the variability of measurements about their true values, and is used to estimate the errors introduced in the digitising process.

3.5.1.1 Estimating the Root Mean Square (RMS)

The RMS error is estimated by taking a sample of measurements and comparing them to their true values. These differences are then squared and summed. The sum is then divided by the number of measurements to achieve a mean square deviation. The square root of the mean square deviation is then taken to produce a characteristic error measure in the same units as the original measurements. The RMS error is directly comparable to the concept of a standard deviation.

The total RMS error of the input data will result from the combined errors of several components. Error estimates from varying components can be combined by taking the square root of the sum of squared RMS's from the contributing element (Eq. 3.1).

$$RMS_{Total} = \sqrt{\sum RMS^2_{contributing}} \qquad \text{Eq. 3.1}$$

3.5.1.2 RMS Error When Digitising a Map Source

When digitised map data are acquired, there are two major sources of error that need to be accommodated, positional errors of the map and errors introduced by the digitising process. Both are themselves combinations of several elements. Errors in maps are introduced by control survey errors, detail survey errors, compilation errors, map production errors, and errors resulting from distortions of the map itself. Digitising errors are introduced by errors related to the tablet registration process, operator errors in the digitising of map positions and non-linearity in the output of the tablet itself. In practice, these are usually estimated as two collective components (Eq. 3.2), the *RMS of the map component* and the *RMS of the digitising component*

$$RMS_{Total} = \sqrt{\sum RMS^2_{contributing}} = \sqrt{RMS^2_{map} + RMS^2_{digitizing}} \qquad \text{Eq. 3.2}$$

The RMS of the Map Component

Most national mapping agencies set a national map accuracy standard that is applied to national map products (such as topographic maps). The most widely quoted standard is the 1947 revision of the United States National Map Accuracy Standards. Similar standards are in use by many mapping agencies, and the general logic of the procedure can be applied to any similar statement.

According to the 1947 revision of the United States National Map Accuracy Standards, maps should have no more than 10 percent of tested points in error by more than 1/30 inch (0.85 mm) for 1:20,000 scale maps or smaller, and no more than 1/50 inch (0.5 mm) for maps greater than 1:20,000. This is commonly known as the circular map accuracy standard since it describes a circle about the true position in which we would expect to find 90% of all representations. If the positional errors are assumed to follow a circular normal distribution about the true position, the statement above describes the distance over which 90% of mapped points would be expected to fall with respect to their true position. In terms of the shape of a two-dimensional normal distribution, this would correspond to a distance of 1.64 RMS errors. Thus the contributing RMS of map positions can be estimated as:

$$RMS_{map} = \frac{\text{stated accuracy for 90\% of positions}}{1.64} * \text{scale denominator} \qquad \text{Eq. 3.3}$$

For example, for a 1:20,000 scale map that has a stated accuracy of 0.00085 m for 90% of points, the RMS may be estimated as:

$$RMS_{map} = (0.00085 / 1.64) * 20000 = 10.36 \text{ m}$$

The RMS of the Digitising Component

The error introduced by the digitising process itself can be reasonably estimated (if there are adequate control points) from the RMS reported by the tablet registration process. This will include errors attributable to the digitising capabilities of the operator and non-linearities in the output of the tablet. To provide an accurate estimation of the combined effects of all elements in the digitising component (including paper distortion), it is important that an adequate number of control points be digitised with as even a distribution as possible over the surface of the map. If this is done, then the RMS reported in the tablet registration procedure can be used as a fair estimate of this component.

3.5.2 Scanning

A Hewlett-Packard flatbed scanner model ScanJet 3c was used in conjunction with the Deskscan II v. 2.8 software to input map information. The quality of this information is related to the quality of the scanner and the quality of the base map being used. Errors may occur during the scanning process due to the resolution, documentation source, and the geographical feature being interpreted (Aronoff, 1989; DeMers, 1997).

3.5.3 Remote Sensing

Remote sensing is one of the main sources of data for a GIS. It can be defined as a process of gathering data about the surface of the earth and the environment from a distance, usually from aircraft or space sensors. A remote-sensing image is in raster format which consists of cells (pixels), each containing a value recorded by the sensor. Since the raw remote-sensing images contain radiometric and geometrical errors, they have to be processed prior to their incorporation into GIS. This study made use of NOAA-AVHRR images for retrieval of sea surface temperature. These images were individually radiometrically and geographically corrected (section 4.6.3).

3.5.4 Global Position Systems (GPS)

GPS is a geographical information technology that operates through a constellation of satellites orbiting above the Earth and is used to determinate precise coordinate locations. Although the system was originally developed by the

U.S. Department of Defence as a navigation aid, its use has evolved far beyond its military origins over the last decade or so.

The basic idea behind GPS technology is simple. Each satellite broadcasts a constant stream of timing information from highly accurate atomic clocks. The satellites transmit signals that can be decoded by specially designed receivers to determine positions with varying accuracy. The GPS receiver measures a signal's time and range data and converts them to navigation and position data. In essence, the receiver "reads" the timing information from GPS satellites and compares the signals with its own clock to calculate the distance to each satellite. The receiver then calculates its location by triangulation. Consequently, there must be at least three satellites available at any time to provide an accurate location fix. A fourth satellite in view makes possible the determination of altitude. The U.S.A previously employed a technique called Selective Availability (SA) to globally degrade the civilian GPS signal. This was disabled in May 2000.

In this study a hand held global positioning system GARMIN GPS III was used for data collection during the two field trips to the study area. The typical normal accuracy is of about 10 m horizontal and 13 m vertical.

3.5.5 Data Sharing and Interchange

One way to avoid the difficulties and time constraints imposed in gathering and input data is to use data already generated by a third party. This study made use of some information resources available on the Internet as well as digital data available on CD-ROM (CD-Map, 1999).

3.6 DATA-BASE GENERATION, MANIPULATIONS AND SCORING

Having established the criteria for evaluating alternative decisions and their data sources, criteria need to be represented as thematic maps in the GIS database. Thematic maps were created by georeferencing each criterion map to a common reference system, and by applying further general manipulations to the input data in some cases such as reclassification, overlay, scalar and distances. Subsequent manipulations focused on scoring (or standardising) the thematic maps. The need for data standardization arises as a consequence of the need to integrate the source data which will have been measured in different units and also on different scales of measurement (Pereira and Duckstein, 1993)

3.6.1 Georeferencing

The concept of position as defined by coordinate systems is essential, both to the performance of spatial analysis of geographical information and to the process of map-making. Therefore, it is necessary to define the position of points on the features with respect to a common frame of reference, or coordinate system.

The Earth is a very irregular and complex shape. If the position of particular features is to be known or mapped, it is necessary to make a simple model of the basic shape of the earth on which the coordinate systems can be based. There are two basic shapes of the earth which can be used, the *geoid* and the *ellipsoid* (DeMers, 1997). The geoid can be thought of as mean sea level or where mean sea level would be if the oceans could flow under the continents. More technically, the geoid is an equipotential surface of gravity defining all points in which the force of gravity is equivalent to that at sea level (Campbell, 1996). Because of uneven distribution of mass, the geoid is not a perfectly smooth, oblate spheroid, but is somewhat irregular (a fact that introduces ambiguities into distance measurements and the exact determination of relative location). An ellipsoid is a mathematical surface defined by revolving an ellipse around its minor (polar) axis and which approximates the surface of the earth without its topographic undulations. This gives an abstract and perfectly smooth reference surface commonly used by modern geodetic surveys (Campbell, 1996). Selecting a specific reference ellipsoid to use for a specific area, and orientating it to the landscape, defines what is known in Geodesy as a *datum*. A geodetic datum is a smooth mathematical surface that closely fits the mean sea-level surface throughout the area of interest. It is defined by a spheroid and the position and orientation relationship of the spheroid to a reference mathematical model of the earth (Cracknell, 1997). The georeferenced coordinates are unique only if qualified by a datum. Most datums only attempt to describe a limited portion of the earth (usually a national or continental scale), however, there are some which cover the entire globe.

The following logical step is to define a map projection system, which is a system designed to present the surface of a sphere or spheroid (such as the earth) on a plane. Since it is physically impossible to flatten a globe without distortion, scale will vary across the projection surface with consequent distortions in distance, area, and angular relationships. Therefore, each map projection system compromises accuracy between conservation of distances, angles or area (Jones, 1997). Finally, a grid reference system (coordinate system) can be assigned. A grid referencing system can be thought of very simply as a systematic way in which the plane coordinates of the map sheet can be related back to the geodetic coordinates of measured earth positions.

All the processes previously described constitute what is known as *georeferencing*. Georeferencing refers to the manner in which locations of an image or vector files are related to earth surface locations. In this study, all thematic maps (raster and vector) were georeferenced using the WGS 85 Ellipsoid, REGCAN-95 datum and UTM projection (UTM-28N) (Fig. 3.5).

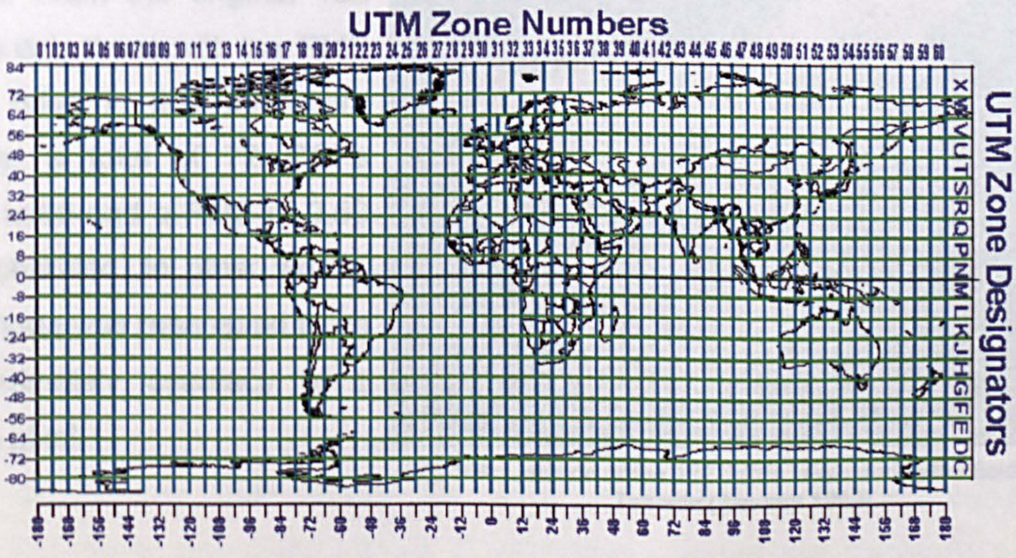

Fig. 3.5: Universal Transverse Mercator (UTM) system.

The common approach for georeferencing an image involves assuming that there is some mathematical transformation relating the coordinates of a pixel in the original raw data array (X, Y) and the geographical coordinates. The coefficients in the transformation are determined by using a number of control points (or ground control points, GCPs). A GCP is a point or fixed feature that can be recognised both on a map with a known reference system and in the raw image that one is trying to rectify. The chosen GCPs are used to determine the coefficients in the chosen transformation. Having found the coefficients, they can be used with any pixel from the original un-rectified image to determine the geometrical coordinates of the centre of that pixel. The accuracy of the rectification of a scene using the transformation can be estimated from the standard deviation of the best fit result.

IDRISI32 has two modules for georeferencing images. In cases where the input image has no reference system (such as scanned images or satellite images), the RESAMPLE module, together with GCPs, were used. In cases where the input reference system was known, the PROJECT module was used to transform the image to a new reference system.

Fig. 3.6 shows the 132 GCPs selected during a field trip in January 1999. The location of these points was confirmed using the GARMIN GPS III. The module RESAMPLE was used within IDRISI32 to resample the image. From the original 132 GCPs only those with low RMS were used in this operation. Finally, a total of 72 GCPs were used and a RMS of 0.53 was obtained. In other words, the image was resampled to an approximately accuracy of ± half a pixel.

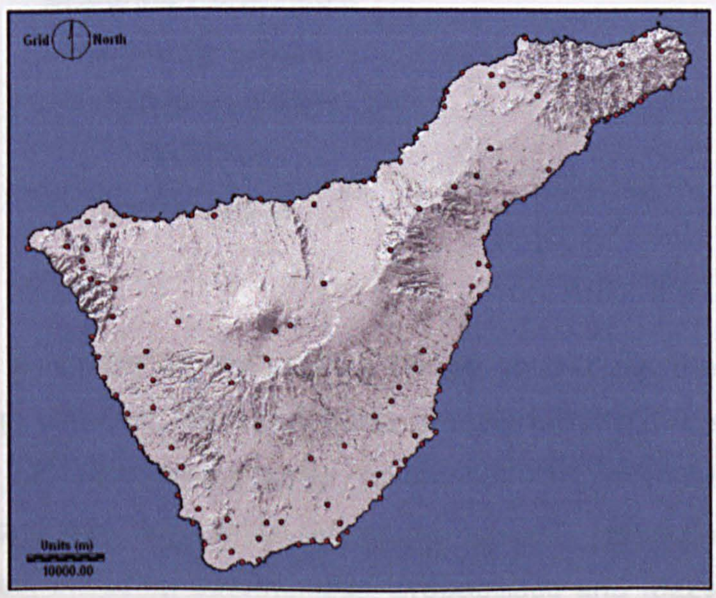

Fig. 3.6: Location of the 132 GCPs taken during the field trip to Tenerife (January 1999).

3.6.2 Scoring

Given the variety of scales on which attributes can be measured, multicriteria decision analysis requires that the values contained in the various criterion map layers be transformed to comparable units. In other words, if various thematic maps are to be combined, the scales must be commensurate. Consequently, raw data must be converted into standardized criterion scores, referred as suitability scores in this study. In this study a scoring system of 1 to 8 was chosen and applied to all data layers, 8 being the most suitable and 1 the least for developing aquaculture (Table 3.2). Similar studies have used standardized criterion scores of 1 to 4 and 1 to 16 (Aguilar-Manjarrez, 1996; Salam, 2001), but it was found that the former scoring system gave poor results while the latter was too complicated to use.

Table 3.2: Score system used.

Score	Denomination
1	Totally unsuitable
2	Unsuitable
3	Marginally-unsuitable
4	Moderately-unsuitable
5	Marginally-suitable
6	Moderately-suitable
7	Suitable
8	Very-suitable

When scoring a thematic layer, a number of approaches can be used to set the threshold values for each scoring category. These methods broadly fall into three categories, (1) mathematical, (2) interviews, group consensus or personal knowledge of the study area and the purpose of the study, and (3) literature review. Mathematical approaches, including deterministic, probabilistic and fuzzy methods (Barredo, 1996; Malczewski, 1999), are useful when the decision-maker does not have any other source of information to set the threshold values.

Because these methods are mathematically based, they may not provide a set of threshold limits which are representative of the problem on hand. In other words, they are not task-oriented, and therefore, for a particular thematic map they will always provide the same threshold values, which is not appropriate for all study cases.

For example, if one of these mathematical methods was used to set the threshold limits for the sea temperature in this study, it will provide a certain fixed number of standardized criterion scores as shown in Fig. 3.7. This will always be the same, independent of the application for which this map was used. Fig. 3.8 shows the same sea temperature map, but this time using standardized criterion scores based on expert knowledge of the activity at hand, aquaculture site selection in Tenerife, and knowledge of the study area.

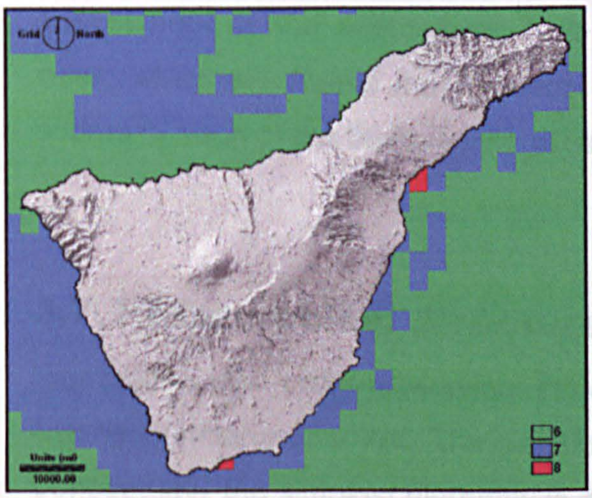

Fig. 3.7: Example of the sea temperature map scored using a mathematical threshold method.

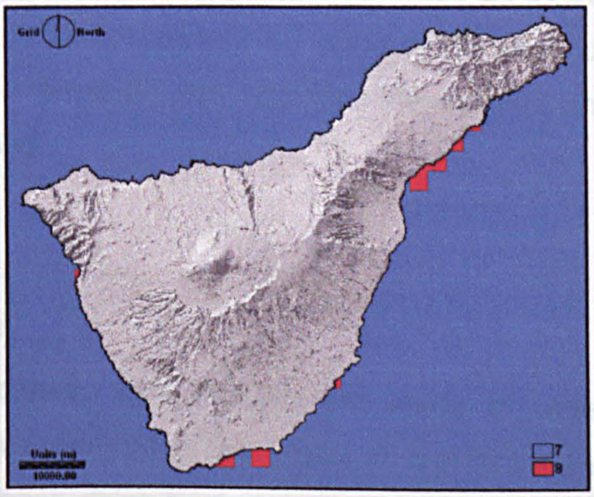

Fig. 3.8: Example of the sea temperature map scored using knowledge of the fish temperature sensitivity and the study area.

Clearly, whenever possible, it is best to use threshold values proposed by experts with knowledge of the task at hand as well as the particular study area. Literature sources can be very useful on their own or in combination with experts assessment. When none of these are available, the mathematical approach is the only alternative.

Threshold values for this study were set based on the combination of the personal opinion of the author, guidance from an expert panel of professionals in aquaculture, fish physiology and environment at the Institute of Aquaculture, opinions by means of questionnaires from a range of professionals familiar with aquaculture in the study area and by use of relevant literature.

3.7 GIS MODELS

The model structure for selecting the best sites for marine fish cage aquaculture in Tenerife was built based on *hierarchical structures.* Hierarchical structures break down all criteria into smaller groups (or submodels). Once structured, the decision maker's preferences with respect to the evaluation criteria can be incorporated into the decision model. The preferences were expressed in terms of the weights of relative importance assigned to the evaluation under consideration. Finally, the standardized criteria maps and their weights were integrated to provide an overall assessment of the alternatives. This is accomplished by appropriate decision rules, which are formal mathematical expression that combine the weights and scores of each of the thematic maps used.

3.7.1 Hierarchical Structure

Hierarchies are order-preserving structures. They involve the study of order among partitions of a set. The partitions are called the levels of the hierarchy. Conceptually the simplest hierarchy is linear, rising from one level to the next. The complexity of the arrangements of the elements in each level may be the same or it may increase from level to level. This also applies to the depth of analytical detail. The structure of each level may take the form of a general network representing the appropriate connections among its elements (Triantaphyllou and Mann, 1995)

Up to this point, the idea of hierarchy has only been presented as a tool for modelling the real world. However, hierarchical structures can also be used to break down all the criteria into large groupings or clusters, and further divide them into smaller clusters and so on. The objective would then be to obtain the priorities of all elements by means of clustering. This is by far a more efficient process than treating all the elements together (Malczewski, 1999) and is an approach developed for aquaculture projects by the GIS group at the Institute of Aquaculture (GISAP).

To break down a hierarchy into clusters, first it must be decided which elements to group together in each cluster. This is done according to the proximity or similarity of the elements with respect to the function they perform or property they share (Saaty, 1988). Fig. 3.9 represents the suitability analysis for marine fish cage site selection in Tenerife as a hierarchical structure. The top or first level in the hierarchy represents the ultimate goal of the multi-criteria decision-making analysis process. The intermediate or second hierarchy level lists the relevant evaluation criteria. Each of these clusters can be considered as a submodel. The lowest level in the hierarchy contains the evaluation objects. These are all the criteria identified as influencing the goal of the study and may represent primary data or be the result of some preliminary data manipulation or model.

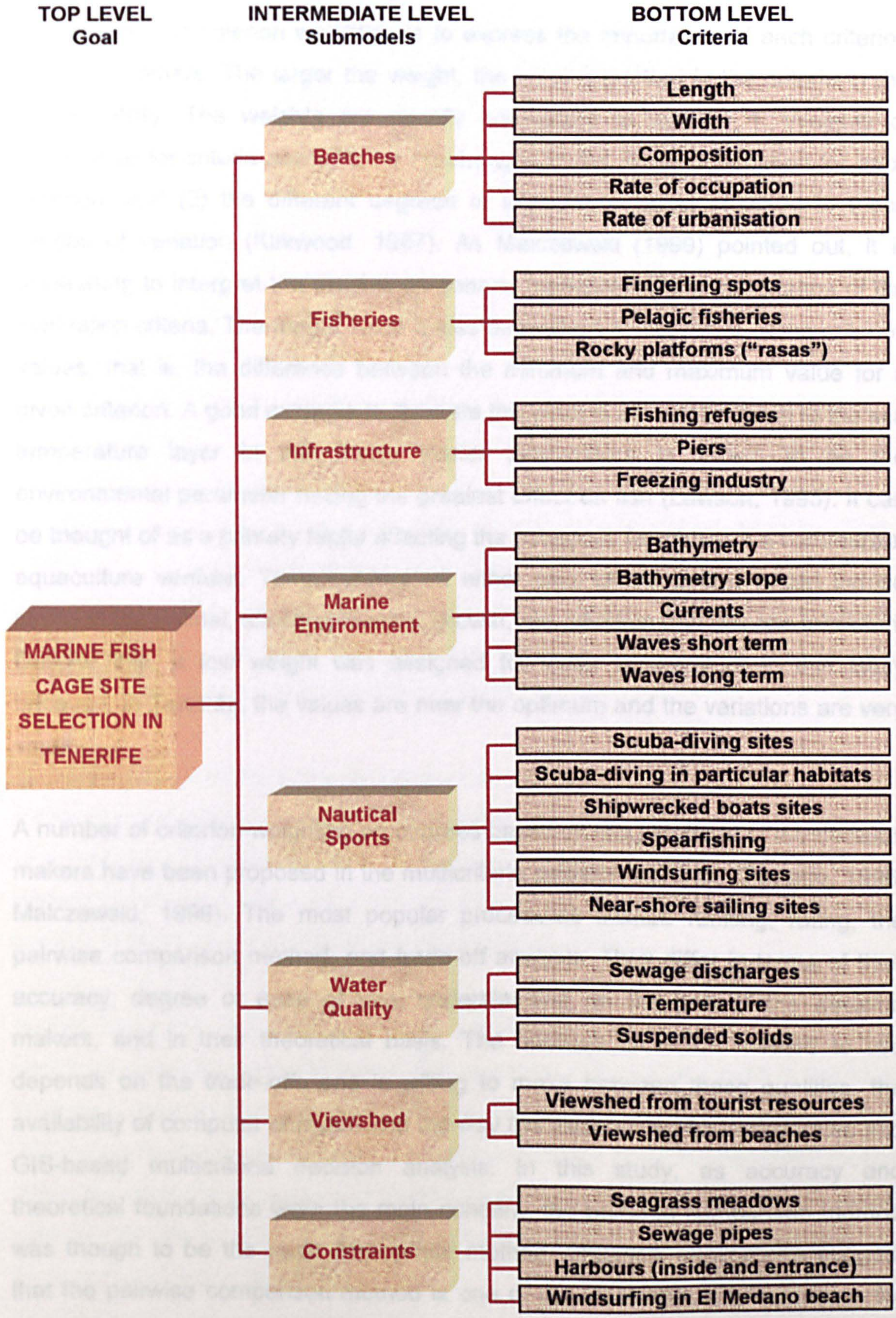

Fig. 3.9: Conceptual structure of the suitability analysis for Tenerife the marine fish cage site selection as a hierarchical structure.

3.7.2 Criterion Weighting

The purpose of criterion weighting is to express the importance of each criterion relative to others. The larger the weight, the more important is the criteria in the overall utility. The weights are usually normalized to sum to 1. Weights of importance for criteria accounts for (1) changes in the range of variation for each criterion, and (2) the different degrees of importance being attached to these ranges of variation (Kirkwood, 1997). As Malczewski (1999) pointed out, it is misleading to interpret the weights as general measures of the importance of the evaluation criteria. The weight value is also dependent on the range of the criterion values, that is, the difference between the minimum and maximum value for a given criterion. A good example to illustrate this point is the weight given to the sea temperature layer in this study. Water temperature is known to be the environmental parameter having the greatest effect on fish (Lawson, 1995). It can be thought of as a primary factor affecting the economic feasibility of a commercial aquaculture venture. Temperatures on either side of the optimum can induce stress in the animal, affecting feeding, growth, reproduction and disease inhibition. Despite this, a low weight was assigned for water temperature in this study because, in Tenerife, the values are near the optimum and the variations are very small.

A number of criterion-weighting procedures based on the judgment of the decision makers have been proposed in the multicriteria decision literature (Barredo, 1996; Malczewski, 1999). The most popular procedures include ranking, rating, the pairwise comparison method, and trade-off analysis. They differ in terms of their accuracy, degree or ease of use, understanding on the part of the decision makers, and in their theoretical basis. The decision on which method to use depends on the trade-offs one is willing to make between these qualities, the availability of computer software and the way the method can be incorporated into GIS-based multicriteria decision analysis. In this study, as accuracy and theoretical foundations were the main concern, the pairwise comparison method was though to be the most appropriate method. Empirical applications suggest that the pairwise comparison method is one of the most effective techniques for spatial decision-making (Eastman *et al.*, 1993; Malczewski *et al.*, 1997).

The pairwise comparison method can be implemented by specific designed software, such as the popular EXPERT CHOICE or spreadsheet environments, and the calculated weights may later be incorporated into the GIS environment. Some GIS software, such as IDRISI32 used in this study, has already incorporated this method into its GIS-based decision making procedures. IDRISI32 offers a built-in decision support module, called WEIGHT, for calculating weights of relative importance using the pairwise comparison method.

3.7.1.1 Pairwise Comparison Method

The pairwise comparison method (PCM), developed by Saaty (1977) in the context of the analytic hierarchy process, is employed to determine the priority weight of criteria. The PCM is a theory of measurement concerned with deriving dominance priorities (or weights) from paired comparisons of homogeneous or clustered heterogeneous elements with respect to a common attribute (Saaty 1994). The procedure consists of three major steps: generation of the pairwise comparison matrix, computation of the criteria weights, and estimation of the consistency ratio. Each of these three steps are described briefly here, and a more detailed explanation can be found in Saaty (1977; 1980)

1. Development of the pairwise comparison matrix·

Pairwise comparisons are quantified by using a special scale which is a one-to-one mapping between the set of discrete linguistic choices available to the decision maker and a discrete set of numbers which represents the importance, or weight, of these choices (Triantaphyllou and Mann, 1995).

In this study, the 1-9 scale proposed by Saaty (1997) is used, 1 being least important and 9 the most important. The proposed scale of nine units is based on findings in experimental psychology (Miller, 1956). The nine levels can be labelled with numbers (the numerical mode) or with preference phrases (the verbal mode). When the verbal mode is used, a conversion table is applied to translate the verbal preferences into numbers. The scale of intensity of importance is from 1 to 9 and its verbal meaning is shown in Fig. 3.4.

Table 3.3: Scale of relative Importance (according to Saaty, 1977).

Intensity of Importance	Definition	Explanation
1	Equal importance	Two activities contribute equally to the objective
3	Weak importance of one over another	Experience and judgment slightly favour one activity over another
5	Essential or strong importance	Experience and judgment strongly favour one activity over another
7	Demonstrated importance	An activity is strongly favoured and its dominance demonstrated in practice
9	Absolute importance	The evidence favouring one activity over another is of the highest possible order of affirmation
2, 4, 6, 8	Intermediate values between the two adjacent judgments	When compromise is needed
Reciprocals of above non-zero	If activity *i* has one of the above non-zero numbers assigned to it when compared with activity *j*, then *j* has the reciprocal value when compared with *i*.	

This method allows decision makers to make the pairwise comparisons verbally or numerically. In verbal comparisons decision makers select one phrase from a list of nine that best represents their opinion (for example, "moderately preferred" or "extremely preferred"). Numerical comparisons reflect directly the extent to which a decision maker prefers alternative A to B (for example three times) and all judgements are finally converted into numbers.

While verbal statements are intuitively attractive for determining preference, there is overwhelming evidence that people have very different numerical interpretations of the same verbal expressions. The numerical values assigned to the same verbal expression display large ranges (Stone and Johnson, 1959; Lichtenstein and Newman, 1967; Budescu and Wallsten, 1985; Clarke *et al.*, 1992). The conversion table of the PCM overestimates the preference differences of decision makers. For example, Huizingh and Vrolijk (1997) found that although the expression "moderately preferred" is assigned a score of 3, most decision makers assign this statement a lower value of 2. Therefore, the use of the verbal mode without knowing how people interpret the preference phrases leads to a small loss of decision quality (Budescu *et al.*, 1988; Erev and Cohen, 1990; Huizingh and Vrolijk, 1997). On the other hand, numerical judgments have a number of distinct advantages compared to verbal judgments. Numerical judgments are more precise, they permit communication to be less ambiguous and they can be used in calculations (Hamm, 1991; Huizingh and Vrolijk, 1997).

Given the well-known preference of people for verbal instead of numerical judgments (Zimmer, 1983; Budescu and Walls-ten, 1985; Hamm, 1991), the optimal solution would be to include a personal conversion table for each decision maker. Although optimal, it may not be a practical solution. Therefore, if accuracy is not very important, the ease and comfort of verbal expressions may be worth the small loss in decision quality (Hamm, 1991; Huizingh and Vrolijk, 1997). However, as Dyer and Forman (1991) pointed out, verbal judgments may be used for one set of judgments and numerical judgments for another, but one should not mix the verbal and numerical modes for any set of judgments. In this study, because precision was of utmost concern, only the numerical mode was used.

If too many criteria are being compared, the method may get very large and complicated for the decision makers. With n criteria, $n(n-1)/2$ comparisons are involved. For example, a decision problem with 10 evaluation criteria would require 45 pairwise comparisons. Some authors have suggested breaking down the criteria into smaller submodels, which are easier and more intuitive to deal with (Aguilar-Manjarrez, 1996; Ross, 1998; Salam, 2001), and this approach is used in this study.

2. Computation of the criterion weights.

Based on the comparisons between different criteria using the intensity scale of importance, the weights of criterion levels are calculated. This step involves the following operations: (a) summing the values in each column of the pairwise comparison matrix, (b) dividing each element in the matrix by its column total (the resulting matrix is referred to as the *normalized pairwise comparison matrix;* Saaty, 1977), and (c) computing the average of the elements in each row of the normalized matrix, that is, dividing the sum of normalized scores for each row by the number of criteria. These averages provide an estimate of the relative weights of the criteria being compare. Using this method, the weights are interpreted as the average of all possible ways of comparing the criteria.

3. Estimation of the consistency ratio.

The consistency ratio (CR) indicates the probability that the matrix ratings were randomly generated. In other words, this step determines the consistency of the comparisons made by the decision-maker, providing a measure of departure from consistency. This, in turn, will help the decision-maker express his interpretation of the importance and relation of each criterion with all the other criteria.

Saaty (1977, 1988, 1994) indicated that matrices with CR ratings smaller than 0.10 have a good consistency, while CR values greater than 0.10 suggests a departure from consistency. In such cases, the decision-maker should reconsider and revise the original values in the pairwise comparison matrix.

3.7.3 Decision Rules

Up to this point, the main elements of spatial multicriteria decision analysis, evaluation criteria (factors and constraints) and decision-makers preferences (weights), have been determined. The ultimate aim of the analysis is to combine these elements using multicriteria decision rules, also referred to as multi-criteria evaluation (MCE). The decision rules provide the basis for ordering the decision alternatives and for choosing the most preferred alternative

There are numerous decision rules that can be used. For a comprehensive review of MCE methodology refer to Keeney and Raiffa (1976), Keeney (1980), Pitz and McKillip (1984), Kirkwood (1997), and Goodwin and Wright (1998). This section focuses only on the method used in this study.

The *weighted linear combination* (WLC), also referred to *as simple additive weighting method* or *scoring methods*, was the chosen method. This technique is most often used for tackling spatial multicriteria decision-making. It is based on the concept of weighted average. The decision maker assigns weights of relative importance to each attribute (as seen in section 3.6.2). A weighted average is then obtained for each criterion by multiplying the weight assigned by the scaled value for that criterion, and summing the products over all criteria as shown in Eq. 3.4.

$$A_i = \Sigma_j w_j x_{ij} \qquad \text{Eq. 3.4}$$

where x_{ij} is the score of the i^{th} alternative with respect to the j^{th} attribute, and the weight w_j is the normalized weight, so that $\Sigma w_j = 1$. Fig. 3.10 illustrates the use of the weighted linear combination method. IDRISI32 offers a built-in decision support module, called MCE, for multi-criteria evaluation calculations by using the weighted linear combination method.

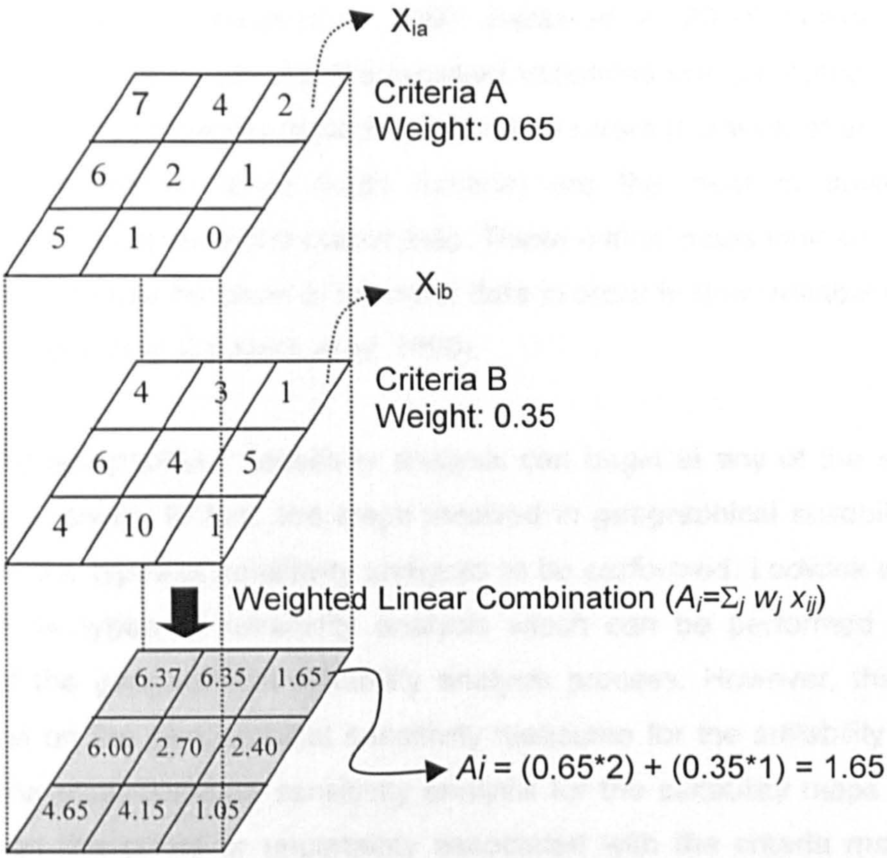

Fig. 3.10: Example of the weighted linear combination method (redrawn from Barredo, 1996).

3.8 SENSITIVITY ANALYSIS

The strategies and techniques for tackling the spatial multicriteria decision problem of siting fish cages in Tenerife initially assume that complete information is available. However, in real-world situations, the information available to the decision maker is often uncertain and imprecise due to measurement and conceptual errors. (Fisher *et al.*, 1997; Arbia *et al.*, 1998; Malczewski, 1999; Li *et al.*, 2000; Woodcock and Gopal, 2000)

Typically, only limited information may be available on actual errors associated with a particular geographical analysis. Such information is, more often than not, difficult and costly to obtain in most situations. However, much knowledge can still be gained about a geographical analysis and the quality of its results through sensitivity analysis (Lodwick *et al.*, 1990; Saltelli *et al.*, 2000), in which variations are imposed on the inputs and the resultant variations are computed even in total absence of any information regarding the actual errors (Lodwick *et al.*, 1990). This analysis can indicate what maps (criteria) are the most or least critical in determining the values of the output map. These critical maps indicate where most or least care should be taken in the input data in order to draw reliable conclusions from the output map (Lodwick *et al.* 1990).

A study of geographical sensitivity analysis can begin at any of the stage of the suitability analysis. In fact, the steps involved in geographical suitability analysis determine the types of sensitivity analyses to be performed. Lodwick *et al.* (1990) identified 14 types of sensitivity analysis which can be performed at different stages of the geographical suitability analysis process. However, this study will only focus on the geographical sensitivity measures for the suitability maps as a whole. The most common sensitivity analysis for the suitability maps as a whole focuses on the errors or uncertainty associated with the criteria maps and the decision maker's preferences (weights) (Malczewski, 1999).

3.8.1 Sensitivity of Criterion Values

The thematic map errors are referred to as the uncertainty associated with GIS data sets on the basis of which the map was created (Fisher *et al.*, 1997). The GIS database errors can be classified into *measurement* or *conceptual*, the former being associated with imprecision in the measurement of criterion values (Arbia *et al.*, 1998), and the latter being attributed to the process of translating real-world entities into map objects (Van Rompaey *et al.*, 1999; Li *et al.*, 2000). In other words, it studies the discrepancy that might arise between the GIS data model and the nature of the reality that it is seeking to capture (Altman, 1994)

The simplest and most widely used representation of sensitivity analysis is to show the percentage change in a variable and its output graphically. This is achieved by systematically changing one variable, and observing the output (Fisher *et al.*, 1997). It is, however, considered to be limited, since it only demonstrates the sensitivity to variations in one variable at a time and synergistic or antagonistic interactions can not be quantified (Saltelli *et al.*, 2000).

With large number of attributes, this analysis involves a number of iterations, and the results may not be easy to interpret. In practice, values associated with criteria having high weights are the most likely candidates for sensitivity analysis. Since the weights of the attributes are high, even slight changes in estimated values may result in a change in the ranking of the alternatives. Also, attribute values that involve a high degree of uncertainty and subjectivity in estimation should be considered in sensitivity analysis to investigate the effect of their variation on the ranking of alternatives. Therefore, the candidate criteria selected in this study for sensitivity analysis were based on these two principles (section 6.3).

3.8.2 Sensitivity of Weights

In addition to the GIS data-set-errors, there is uncertainty involved in the specification of preferences by decision-makers. Of these, sensitivity to attribute weights is perhaps more important (Malczewski, 1999). This is associated with the fact that judgment plays a key role in spatial multicriteria decision-making. In other words, criteria weighting is a subjective appreciation of the problem at hand, and does vary among different decision-makers. In some situations decision makers are not able to provide precise judgements with respect to the relative importance of evaluation criteria due to limited or imprecise information and knowledge, or general inconsistency (Saaty, 1980)

A sensitivity analysis of weights consists of investigating the sensitivity of the alternatives to small changes in the value of attributed weights. If the rankings remain unaffected as the weights are varied, errors in the estimation of attributed weights can be considered insignificant. This study incorporated sensitivity analysis of the weights based on the opinion of three different groups of experts, (using questionnaires, see section 5.2), rather than changing the weights by means of any probabilistic, mathematical or random techniques.

3.9 DATABASE FIELD VERIFICATION

3.9.1 Selection of the Sampling Criteria

Some database verification was conducted to check the reliability of sources and to help ensure reliable outcomes. It would be preferable to sample all criteria, however this was not possible from a practical or economical point of view. Therefore, a selection of sampling criteria was made based on; (a) the relative importance of a factor in relation to the other factors, (b) the need to verify the database of that factor (e.g. spatial or temporal variability), and (c) the time and effort required. The criteria selected for field verification were, (1) rate of beach occupation, (2) rate of beach urbanization, (3) beach composition, (4) land use, (5) land cover and (6) soil texture. Land use, land cover and soil texture were variables used for the suspended solid estimation.

3.9.2 Sampling Design

Choosing the right sampling approach is a vital part of any survey. The primary determinant of a sampling design should be the aims and objectives of the project. However, factors such as time and resources available for a study, the type of habitat, accessibility, and proposed methods of data analysis and representation must be also considered (Kent and Coker, 1996).

The selection of the field sampling points for beach occupation, beach urbanization and beach composition criteria was done by random sampling. Strict application of random sampling means that every point within the survey area should have an equal chance of being chosen on each sampling occasion. Random points were selected by using the module RANDOM within the GIS software IDRISI32. Selection of the field sampling points for land use/land cover and soils was initially done by random sampling. However, the exact locations of those points in the field proved difficult to find, if not impossible in some cases, due to rough terrain or woodland. Therefore, all randomly selected points were slightly modified to coincide with accessibility and known locations on a map, such as road intersections or well define structures.

Fig. 3.11 shows the location of 12 sampling points for the beach database, while Fig. 3.12 shows the location of 32 sampling points for land use/land cover and soil databases for the field trip carried out during April 2001.

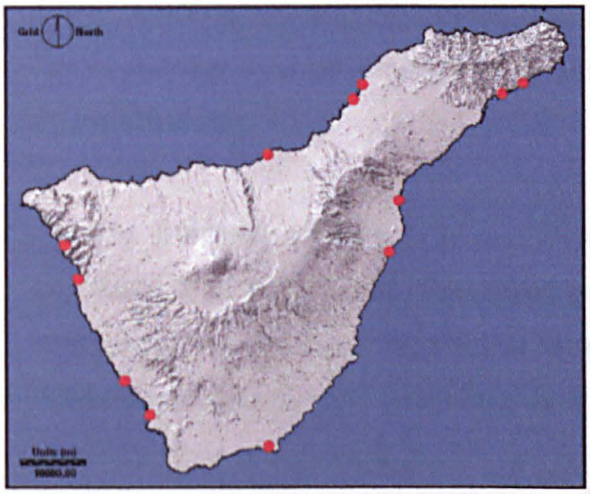

Fig. 3.11: Beach sampling stations assessed during the April 2001 field trip.

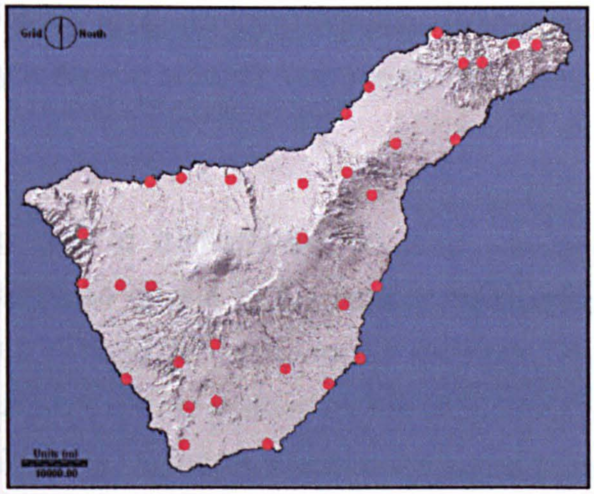

Fig. 3.12: Land use/land cover and soil sampling stations assessed during the April 2001 field trip.

3.9.3 Beach Criteria (occupation, urbanization and composition)

Beach composition, rate of occupation (how much the beach is being used by people for recreation purposes) and rate of urbanisation (degree of infrastructure around the beach site) were visually assessed using the criteria and scoring shown in Table 3.4.

Table 3.4: Field sampling values used for beach criterion.

	4	3	2	1
Composition	Small stones	Sand+ Gravel +Small stones	Sand+Gravel	Sand
Rate of Occupation	Low	Medium		High
Rate of urbanisation	Virgin	Rustic	Semi-urban	Urban

3.9.4 Land Use/Land Cover Determination

Although there are several vegetation description methods (see Kent and Coker, 1996 for a comprehensive review and description), they broadly fall into two categories; physiognomic or structural methods and floristic methods. Physiognomic methods describe flora species based on external morphology, life-form, stratification and size of the species present. Floristic methods, on the other hand, identify species present in a study area and records their presence/absence or abundance.

As the purpose of this field sampling was to gather data on land use and percentage of vegetation, this study made use of one of the floristic methods of estimating abundance (qualitative data). Among the abundance methods, the *cover estimated by eye* technique was used. Cover is defined as the proportion of ground within a quadrant (10x10 m) which is occupied by the above-ground parts of each species when viewed from above, and is estimated visually as a percentage. Since estimation is done by eye, there is an inherent degree of error associated in recording. In an attempt to decrease this bias in the sampling, the estimation of vegetation cover was done by consensus between two field observer.

3.9.5 Soil Texture Determination

Soil texture indicates the relative content of particles of various sizes, such as sand, silt and clay in the soil. Soil texture influences the amount of water and air it holds, and can provide an indication of the rate at which water enters and move through soil (Coche, 1985).

3.9.5.1 Soil Sample Preparation And Extraction

Sample preparation, although often taken for granted, has frequently been shown to significantly affect analytical results (Olson, 1981; Soil Survey Division Staff, 1993). It is therefore critical that standardized sample handling and texture determination procedures are used.

As only texture determination was of concern, soil drying was not necessary. However, crushing and mixing of soil samples were needed for loosening and homogenizing the samples, after which no segregation of the samples by aggregate size should be apparent. Fig. 3.13 shows an example of a soil sample before and after the homogenisation process. Subsamples (triplicates) were obtained by dipping into the centre of the mixed sample for analysis.

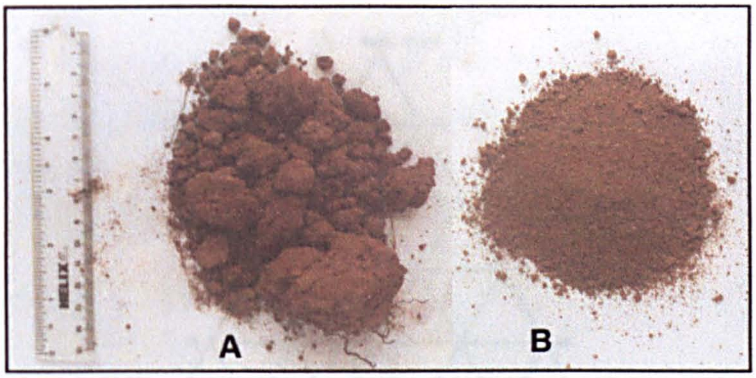

Fig. 3.13: Soil sample before (A) and after (B) after crushing and mixing.

3.9.5.2 Soil Textural Classes and Field Tests for Their Determination

There are several soil texture classification systems and they are generally based on particle size or on some additional soil priorities such as plasticity and compressibility. Soil classification based on the particle-size characteristic is widely used, especially for preliminary or general description. In the field, there are several ways to classify soils into textural classes. The field estimation of soil texture is known as *apparent soil texture*. This term refers to soils that do not disperse completely in the standard particle size analysis during laboratory analysis (Soil Survey Division Staff, 1993). Among these, Coche (1985) reviewed a range of simple and comprehensive methods, from which two were selected for this study. The first method is the so called *manipulative test* and the second the *bottle test*. The manipulative test runs a series of manual manipulations with the soil to assess its texture. The bottle test, which involves simple decantation, provides a general idea of the proportion of sand, silt and clay in the soil. These two tests were selected for their simplicity and because they are sufficiently different to provide an independent sets of results that can be compared. The manipulative test is more a qualitative test, while the bottle test is quantitative.

Soil samples were collected and analysed (triplicates) using the manipulative and bottle test. The mean values of the triplicates (percentage of sad, silt and clay) were used to estimate the soil texture using a soil texture classification diagram (Fig. 3.14).

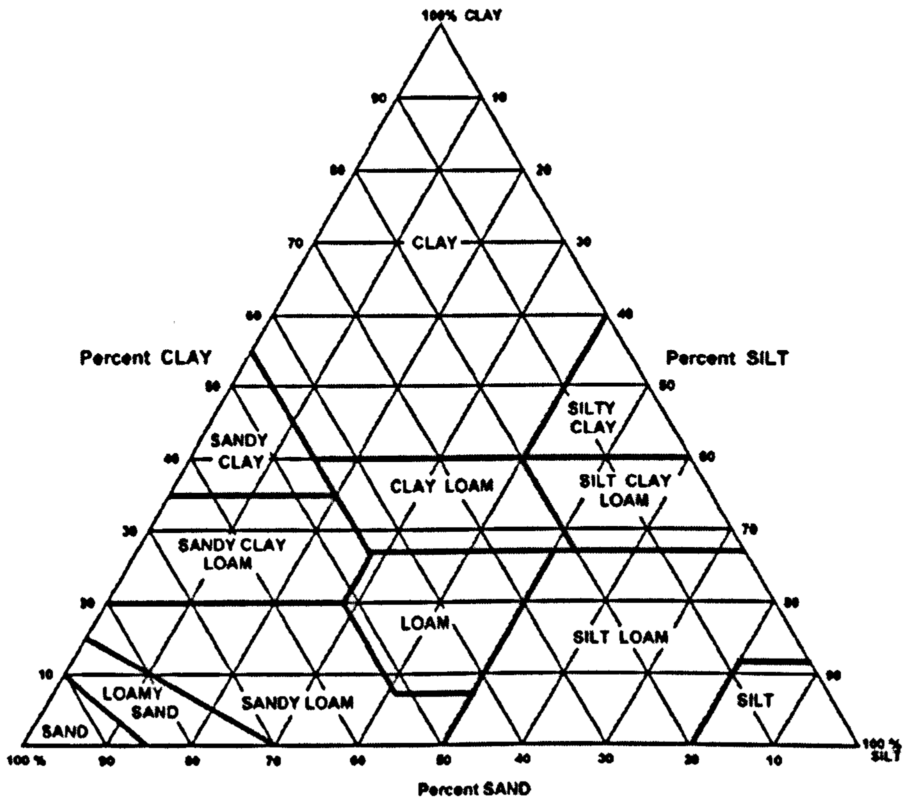

Fig. 3.14: Soil texture classification diagram (from Coche, 1985).

The manipulative test

The manipulative test provides a better idea of soil texture than other similar tests (Coche, 1985). For accurate results this test must be performed in the exact sequence as described below, as each progressive step indicates more silt and clay present in the sample.

1. Take a handful of soil and wet it (Fig. 3.15, A) so that it begins to stick together, but not sticking to your hands;

2. Roll the soil sample into a ball about 3 cm in diameter (Fig. 3.15, B);
3. Put the ball down (Fig. 3.15, C) ...
    - If it falls apart, it is sand
    - If it sticks together, go to the next step
4. Roll the ball into a sausage shape, 6-7 cm long (Fig. 3.15, D)...
    - If it does not remain in this form, it is loamy sand;
    - If it remains in this shape, go to the next step.
5. Continue to roll the sausage until it reaches 15-16 cm long (Fig. 3.15, E)...
    - If it does not remain in this shape, it is sandy loam;
    - If it remains in this shape, go to the next step.
6. Try to bend the sausage into half circle (Fig. 3.15, F)...
    - If you can not, it is loam,
    - If you can, go to the next step.
7. Continue to bend the sausage to form, a full circle (Fig. 3.15, G)...
    - If you can not, is heavy loam;
    - If you can, with slightly cracks in the sausage, it is light clay;
    - If you can, with no cracks in the sausage, it is clay.

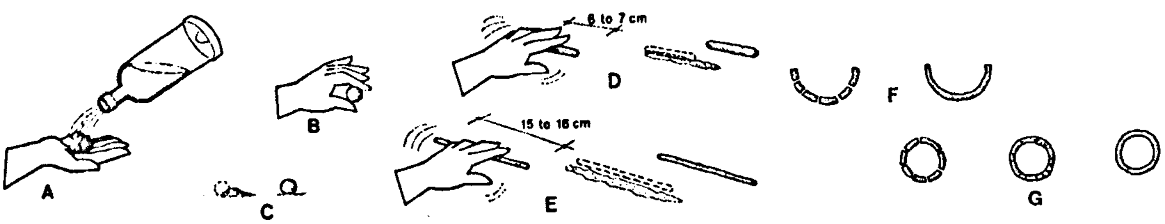

Fig. 3.15: Manipulative test steps sequence (redrawn from FAO, 1985).

The bottle test

This is a simple test which provides a general idea of the proportion of sand, silt and clay in the soil (Coche, 1985).

1. Put 5 cm of soil in a bottle (Fig. 3.16, A) and fill it with water.
2. Stir the water and soil well, leave it to settle for 1 hour (Fig. 3.16, B). At the end of an hour, the water will have cleared and you will see that the larger particles have settled (Fig. 3.16, C).
3. At the bottom, is a layer of sand;

4. In the middle, is a layer of silt;
5. On the top, is a layer of clay. If the water still not clear, it indicates that some of the finest clay is still mixed with the water;
6. On the water surface, there may be bits of floating organic matter (Fig. 3.16, C).
7. Measure the approximate proportion of each layer (Fig. 3.16, D).

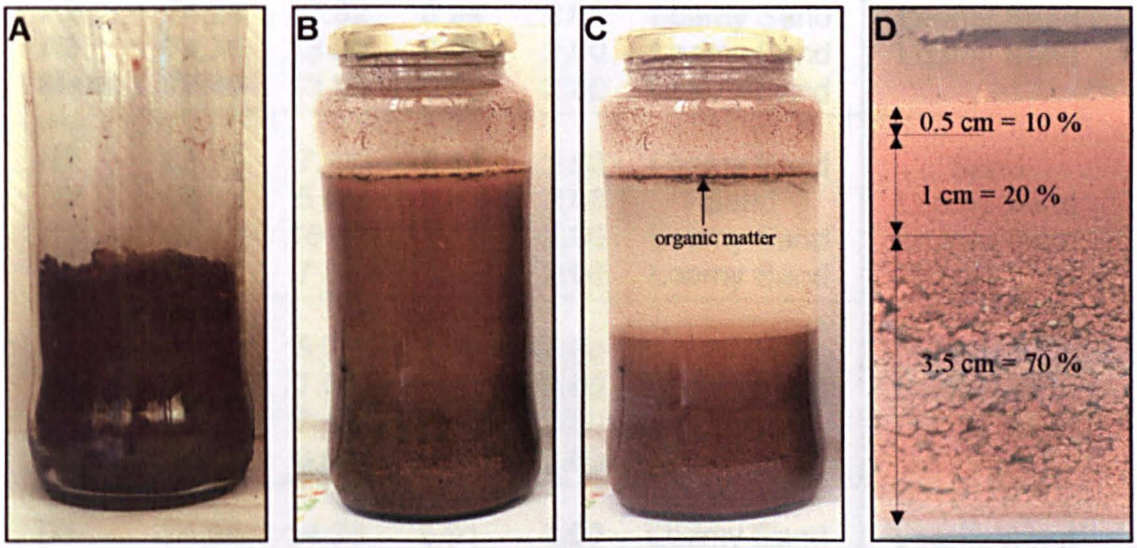

Fig. 3.16: Bottle test steps sequence.

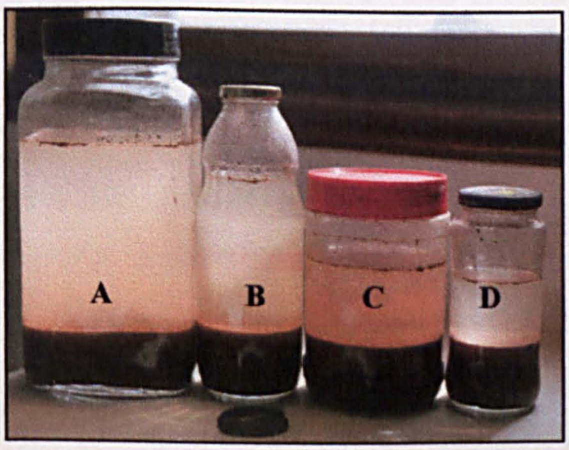

Fig. 3.17: Candidate bottles.

Before using the bottle test, potential variability due to different bottle shapes and volumes was assessed with four candidate bottles (Fig. 3.17). Testing was performed by analysing the same soil sample three times per bottle. The manipulative test was also conducted for comparison. Table 3.5 shows the results of the bottle and manipulative test for each trial. As the composition of the soil sample used was not known, the criteria used for selecting a bottle among the four candidates was based on the consistency of the results. In other words, the bottle providing the most consistent results which also best corresponds with the results from the manipulative test was chosen. Table 3.5 shows that bottle D (refer to Fig. 3.17) tested to be the most constant, and was therefore chosen for use in the bottle test.

Table 3.5: Results of the bottle test and the results form the manipulative test (hand test).

	% Sand	% Silt	% Clay	% O. M.	Texture	Hand Test
A1	85.49	9.38	3.13	2.00	Sand	Loamy Sand
A2	74.24	17.82	5.94	2.00	Loamy Sand	Loamy Sand
A3	74.75	13.29	9.97	2.00	Loamy Sand	Loamy Sand
Mean	77.49	13.96	6.55	2.00	Loamy Sand	
B1	83.75	7.13	7.13	2.00	Loamy Sand	Sand
B2	88.93	5.44	3.63	2.00	Sand	Loamy Sand
B3	83.21	10.17	4.62	2.00	Loamy Sand	Loamy Sand
Mean	85.30	7.56	5.14	2.00	Loamy Sand	
C1	90.31	5.76	1.92	2.00	Sand	Sand
C2	78.78	7.69	11.53	2.00	Loamy Sand	Loamy Sand
C3	86.91	7.40	3.70	2.00	Sand	Loamy Sand
Mean	85.35	6.95	5.69	2.00	Sand	
D1	74.84	14.25	8.91	2.00	Loamy Sand	Loamy Sand
D2	72.52	15.68	9.80	2.00	Loamy Sand	Loamy Sand
D3	73.50	15.75	8.75	2.00	Loamy Sand	Loamy Sand
Mean	73.65	15.22	9.13	2.00	Loamy Sand	

Chapter 4

Database Generation and Manipulation

Database development has been acknowledged as the most challenging and time-consuming task in a GIS project and is likely to account for more than half of the total cost of a GIS project (Lang, 1990; Budić, 1993). Sources of data to be integrated in GIS can be varied and may include existing paper or digital maps, satellite images, field surveys, aerial photographs, statistics, etc. This chapter details the manipulations and processes carried out to generate the GIS database for this study grouped in the 8 submodels described earlier.

4.1 BEACH SUBMODEL

As indicated in Chapter 2, beaches in Tenerife are a rare and fragile resource. The 600,000 local inhabitants of the island together with a constant tourist presence are increasing the usage pressure on the beaches. Aquaculture cages occupy space which can affect local amenities, boat traffic, local currents and sedimentation dynamics and decrease the water quality of nearby beaches. Therefore, cage siting should be planned to avoid interference and conflict for space and water.

Information on beach location, beach length, beach width, beach composition, beach rate of occupation (degree of beach use by people) and beach rate of urbanisation (degree of infrastructure around the beach site) was collected from several sources including archive material (Luengo *et al.*, 1995; Marín and Luengo, 1998) and the Official Spanish Beach Guide web site developed by the Spanish Ministry of Environment (http://www.mma.es/docs/costas/playas/html/0/pg/espanha.htm).

A preliminary screening, from a total of 137 beaches catalogued in Tenerife, was done to identify the important beaches on the island. This classification focused on two criteria; composition and size. All sand beaches were first selected regardless of their size. Secondly, beaches with gravel or a mix of gravel, cobble and sand, longer than 100 m in length and 20 m in wide were also selected. Each of the 79 beaches was on-screen digitised using a 10x10 metres pixel image of Tenerife provided by CD-Map (1999) (Fig. 4.1), a 1:100,000 topographic map and information obtained by Luengo *et al.* (1995), Marín and Luengo (1998) and the Official Spanish Beach Guide web site. Fig. 4.2 shows the location of the 79 beaches identified by this initial screening. The digitised vector was reclassified with the values of length, width, composition, rate of occupation and rate of urbanisation to generate five layers.

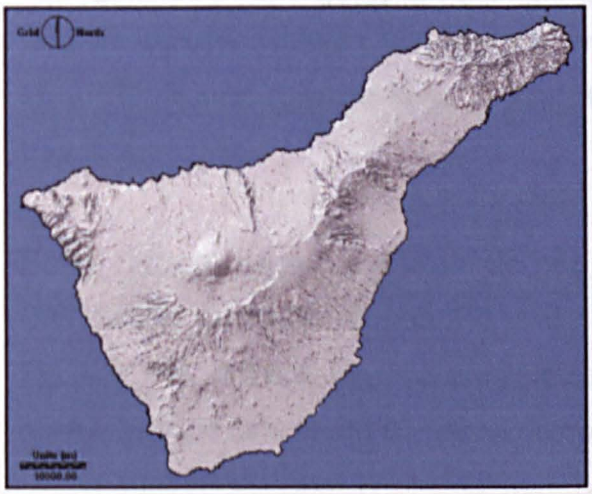

Fig. 4.1: Tenerife 10 x 10 m pixel image.

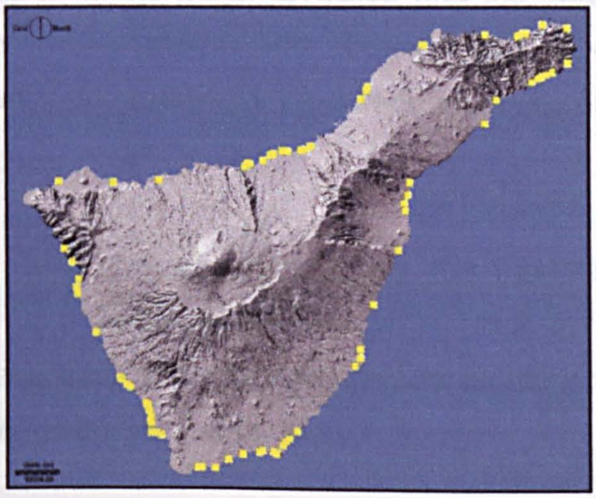

Fig. 4.2: Most important beaches in Tenerife.

The beach database was validated as explained in Section 3.8.3. The data taken from the 12 randomly selected sites correspond 100% with the data used in this submodel, therefore, it was concluded that the beach database was accurate.

4.2 FISHING SUBMODEL

Besides tourism, fishing is also an important economic sector in the overall island's economy. Therefore, it is necessary to identify and map the fisheries if aquaculture practices are to be successfully integrated. Only coastal fisheries are of interest in this study for obvious reasons.

Criteria used for this model were; fingerling accumulation areas, coastal pelagic resource areas and rocky platforms. Fingerlings are important because they are used for live bait for some pelagic fisheries. The coastal pelagic resources include sardine, mackerel, blue jack mackerel, bogue, etc. Rocky platforms are of interest because they are an important source of fish and invertebrates of high economic value.

The fingerling accumulation areas and coastal pelagic resource areas were obtained from Luengo *et al.* (1995) and Marín and Luengo (1998). These maps were scanned and imported to the GIS software as bitmaps. Finally, each map was georeferenced using the module RESAMPLE within IDRISI32 and the data was on-screen digitised. Information on rocky platforms was obtained from CD-Map (1999) and Luengo *et al.* (1995) which was used for on-screen digitising of this layer.

Buffer zones were calculated around each thematic map using the module DISTANCE and later reclassified using the threshold values shown in Table 4.1. Fig. 4.3, Fig. 4.4 and Fig. 4.5 show the suitability maps for fingerling accumulation areas, pelagic fish accumulation and rocky platforms respectively.

Table 4.1: Distance threshold values (m) for each criteria.

Criteria \ Score	8	7	6	5	4	3	2	1
Areas of fingerling accumulation	>1900	1750-1900	1600-1750	1450-1600	1300-1450	1150-1300	1000-1150	<1000
Areas of pelagic fish accumulation	> 0							0
Rocky platforms	>250	225-250	200-225	175-200	150-175	100-150	50-100	<50

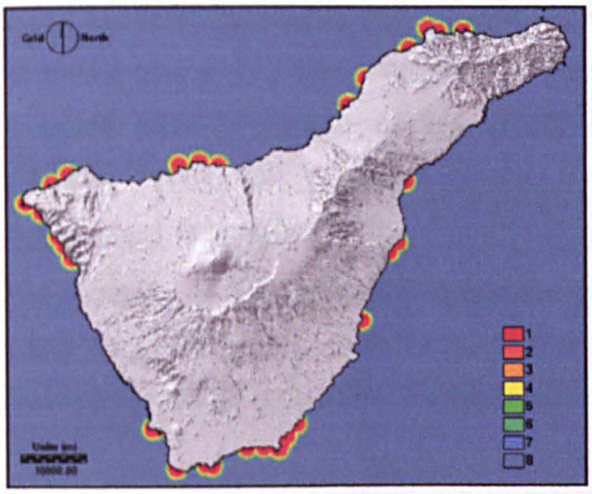

Fig. 4.3: Fingerling accumulation.

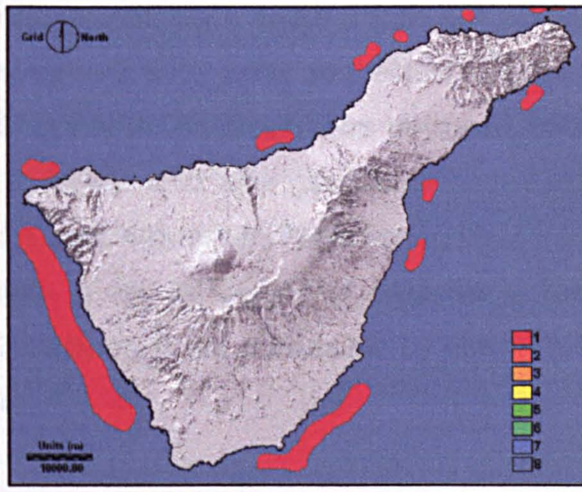

Fig. 4.4: Coastal pelagic resources.

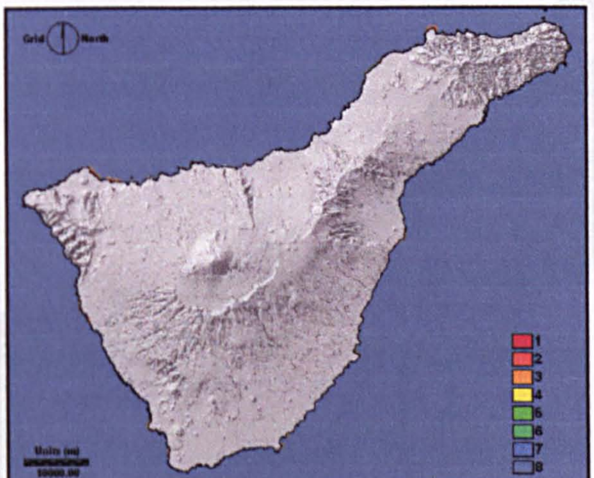

Fig. 4.5: Rocky platforms.

4.3 INFRASTRUCTURE SUBMODEL

Infrastructure refers to the background facilities which are needed for the development of cage culture in Tenerife. The most important factors identified were the presence of nearby ports and the Freezing industry. Information on ports was obtained from Luengo *et al.* (1995), Marín and Luengo (1998) and Morales-Matos and Pérez-González (2000), and information on the Freezing industry was obtained from personal knowledge of the study area. These thematic layers were created by on-screen digitising.

In Tenerife, there are two major categories of ports; *fishing refuges* and *piers*. Fishing refuges are ports which provide access for medium-draught boats and piers are infrastructures that provide access only to small boats (these are mostly old historic ports or the Fishermen's Associations). Only ports connected to a road network were of interest for this study. Information on roads was obtained from CD-Map (1999) which were imported to IDRISI32 and later georeferenced using the module RESAMPLE. Fig. 4.6 shows the road network in Tenerife together with the location of the fishing refuges and piers. It can be seen that only one of the ports (the pier on the northenwest tip of the island) is not accessible by road. This isolated pier was omitted from the analysis.

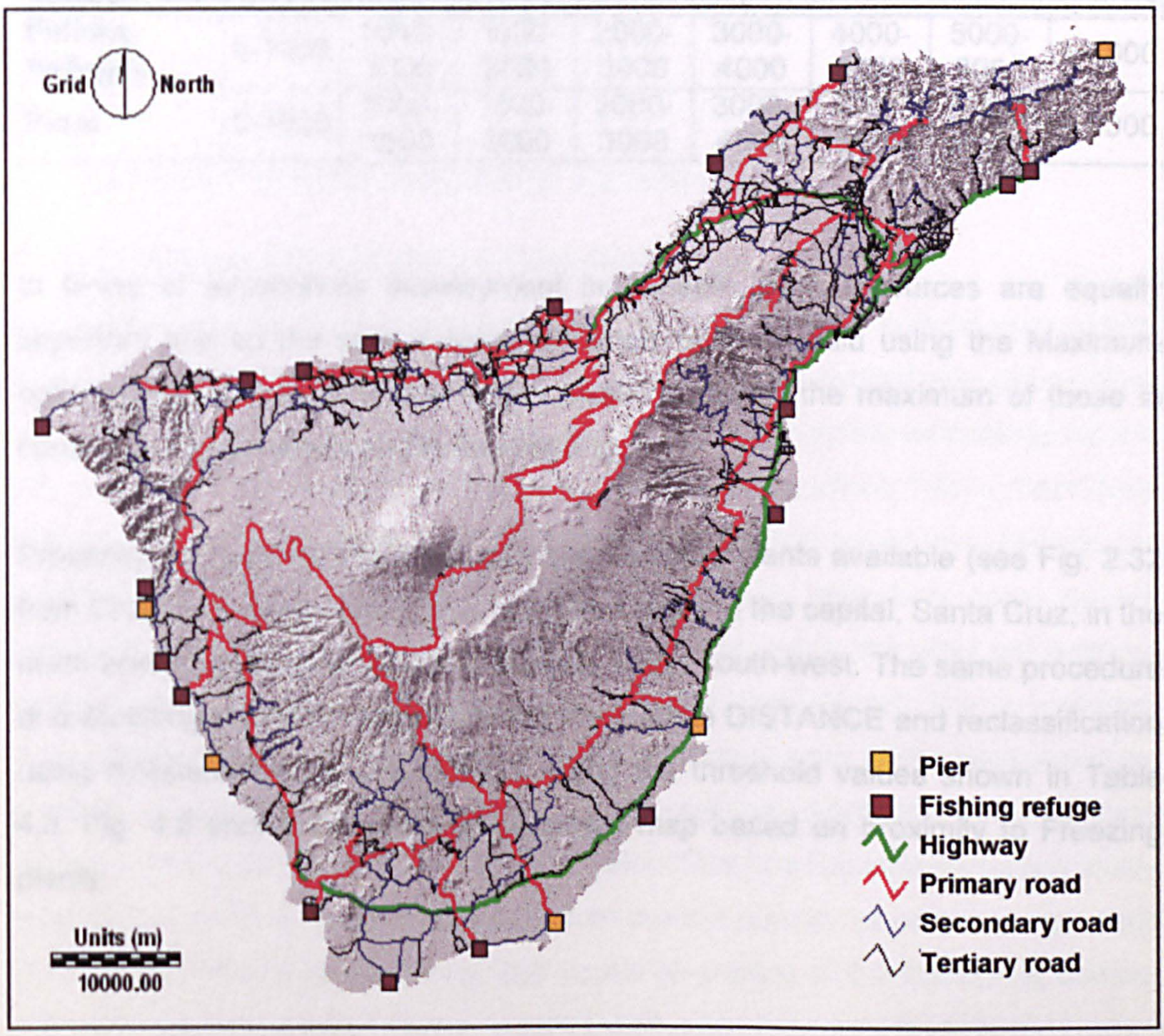

Fig. 4.6: Road network and location of the fishing refuges and piers in Tenerife.

The module DISTANCE was used to estimate proximity ranges from ports. Suitability scores were established by considering the distance that boats will need to travel from a port to a potential fish cage site. The farther away a cage is from a port, the more time and cost is needed to reach the installations, and therefore the less suitable it will be. Table 4.2 shows the distance thresholds used to reclassify each criterion. Threshold values are the same for fishing refuges and for piers as the classification is based on distances from ports, and not on the type of ports.

Table 4.2: Distance threshold values (m) used for each port category.

Score / Criteria	8	7	6	5	4	3	2	1
Fishing Refuges	0-1000	1000-1500	1500-2000	2000-3000	3000-4000	4000-5000	5000-6000	> 6000
Piers	0-1000	1000-1500	1500-2000	2000-3000	3000-4000	4000-5000	5000-6000	> 6000

In terms of aquaculture development in Tenerife, both resources are equally important and so the scored suitability maps were overlaid using the Maximum option within IDRISI32, where output pixels represent the maximum of those in corresponding positions on the images (Fig. 4.7).

Presently, in Tenerife, there are only two Freezing plants available (see Fig. 2.32 from Chapter 2: Study Area). One is located close to the capital, Santa Cruz, in the north-east and the other in Los Cristianos, in the south-west. The same procedure of calculating proximity rages by using the module DISTANCE and reclassification using threshold values was applied, using the threshold values shown in Table 4.3. Fig. 4.8 shows the resulting suitability map based on proximity to Freezing plants.

Table 4.3: Distance threshold values (km) used for Freezing plants.

Score / Criteria	8	7	6	5	4	3	2	1
Freezing Industry	>140	120-140	100-120	80-100	60-80	40-60	20-40	0-20

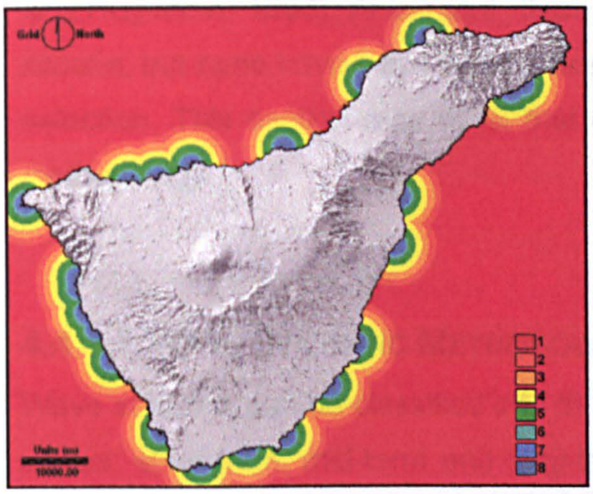

Fig. 4.7: Distance to ports (Fishing refuges + Piers).

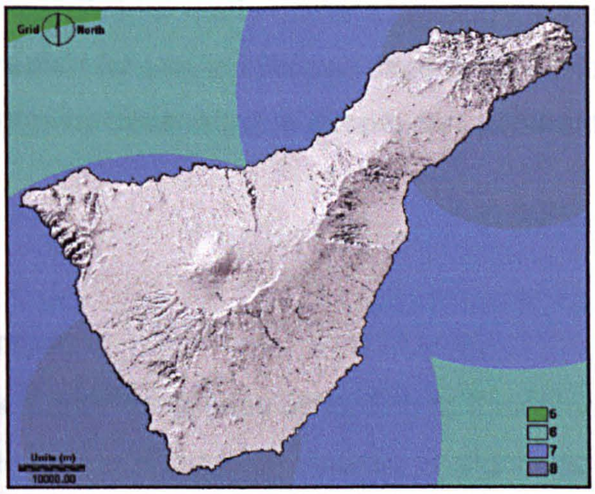

Fig. 4.8: Distance to Freezing Industry.

4.4 MARINE ENVIRONMENT SUBMODEL

4.4.1 Waves (Short and Long-term)

Of all the possible environmental problems with offshore cage culture, wave action is of utmost concern. Knowledge of wave action at a potential site (also called *wave climate*) will help in choosing a proper cage and mooring technology for the site, as well as estimating the risk of failure (Cairns and Linfoot, 1991). Both likely highest waves over a certain period (design wave or return wave) and prevailing or average wave heights are significant measures in assessing cage system structure. The former may cause instant total failure, while the latter will promote gradual failure or what is commonly know as "structural fatigue". This is important for calculating the frequency of replacement of different parts of the cage structure. In addition, greater wave motion increases the relative motion between the water and nets suspended from a slow-moving collar. This has implications for the ability of staff to operate in rough weather. Higher relative motion not only requires much stronger net enclosures, but may also cause de-scaling of the fish during storms, with consequent osmotic trauma, increased disease risks and mortalities (Turner, 1991).

The challenges of siting and operating cage systems in exposed sites fall into two major areas; storm survival and servicing or operating capabilities. Neither areas have a substantial amount of information on which to base decisions (Willinsky and Huguenin, 1996). At present, there are diverse methods for estimating wave climate, but none have been clearly presented for use in offshore cage culture site selection. This section tries to fill that gap by presenting a simple but accurate methodology.

4.4.1.1 Wave Statistic Methodology

Wave statistics can be classified into three main categories according to their time scales; short-term, mid-term and long-term. The short-term statistic or significant height, H_s, is the average height of one-third of the highest values in a continuous series. Goda (1977) found that this was the most stable parameter to characterise ocean waves which are subject to statistical variability due to irregularity of wave profile. The simplest medium-term statistics are monthly, seasonal or annual averages of *sea state* (wave condition described by means of height, period and direction parameters). They are particularly useful in describing wave conditions at a specific locality. The usual way of presenting and analysing this type of data is by means of plots and histograms, which may provide a first indication of trends, if any, and visual comparison between months or years. Another mid-term statistic often analysed is the marginal distribution of wave height in the form of non-exceedance, which is the probability that a wave height (H_i) is smaller than a fixed critical value (H_c). This calculation is needed for the use of the long-term statistic.

For design of coastal structures it is very important to obtain information on wave characteristics over a period of time sufficiently long to cover the lifetime of the structure. Normally, these measurements are either unavailable or are scarce. One way to solve this problem is to represent wave statistics using a probability function which fits the data, and then to obtain the necessary design information from that probability function. Ordinal statistics, which deal with data dispersion around a population mean, are of little value as it is necessary to know the distribution far away from the mean. Study of a phenomenon in its extreme conditions requires the use of statistical methods specifically designed for it.

Short and mid-term statistics are simple and straight forward procedures, requiring no further explanation. On the other hand, the long-term statistic can be a confusing procedure and so a detailed review is presented prior to its use.

LONG-TERM STATISTIC

The reliable estimation of extreme waves is normally based upon the data for the significant wave height, H_s, which is then fitted to one or more probability distributions. This gives the cumulative probability distribution function, $P(H_s)$, for different H_s values. Finally, wave heights for specific return periods are calculated. The main problems involved in calculating extreme wave heights are to obtain sufficiently accurate wave data, and to employ proper statistical techniques in the calculations.

Two different methods are currently employed to prepare extreme statistics of storm waves. The *Total Sample Method*, employs the whole wave data record at regular interval of a few hours, whereas the *Peak Value Method (PVM)*, uses the wave heights from individual storms to construct an extreme wave data set. The data set for the PVM can be either a *partial-duration series* (used in this study) or the *annual maximum series*. The reliability of predicted extremes is directly related to the accuracy of available data and the number of years recorded. As a general rule-of-thumb, heights can be extrapolated to return periods up to 3 times the length of record (Borgman and Resio, 1977). Possible wave data sources are marine buoys, use of recorded visual height from boats and modelled data. Numerical simulation of wave transformation processes have been acknowledged as an extremely rational and efficient method of quantifying wave behaviour (Wei *et al.*, 1990).

The extreme wave calculation methodology used in this study is basically that proposed by Goda (1979), Isaacson, *et al.*, (1981), Goda (1988) and Muir and El-Shaarawi (1986), in which an input array of extreme significant wave heights are fitted to five candidate probability distributions. General assumptions in this approach are: (1) all extreme wave heights come from a single statistical population of storm events, (2) wave height properties for an event are reasonably represented by the significant height, (3) extreme wave heights are not limited by any physical factors such as shallow-water depth, (4) the data must be independent of each other, (5) probability distributions must be constant from storm to storm, (6) the probability distribution $P(H_s)$ is not only constant, but also its functional form is known except for the constants, and (7) data must be stationary and all autocorrelation removed.

Probability Distribution Functions

In extreme data analysis, selection of a distribution function to be fitted to the data is always a difficult task. A large number of probability distributions have been used for the calculation of extreme wave heights and there have been many reasons given for preferring one distribution to another. Some of these reasons contain logical flaws, others rely on mathematical reasoning and others rely on statistical arguments. It should be kept firmly in mind, however, that there is no physical, theoretical or empirical reason for preferring one distribution to another (Muir and El-Shaarawi, 1986). The approach commonly used is to try several candidate distributions with each data set and select the one that fits best. None of the distributions used can be true or false but only good or bad and a distribution function can be selected so long as it provides a good fit to the observed wave data (Goda, 1979). However, the reliability of any estimate will depend directly upon the sample size. If data are limited, then no amount of statistical manipulation will give clear and unambiguous answers.

The five candidate probability distributions used were, Fisher-Tippett Type I (also known as Gumbel) and Weibull with four exponents ranging from 0.75 to 2.0. However, it is important to bear in mind that there are more distributions used by other authors such as Fréchet (Thom, 1973), Gamma (Yamaguchi *et al.*, 1978), etc. These five distributions were selected because they are most commonly used and studied, their use is not complicated and they also provide a wide range of possibilities for best data fit. The most commonly used lognormal distribution was not adopted because its characteristics are quite similar to those of the Weibull distribution with k=2.0 (Gumbel, 1958).

Fisher-Tippett type I (Gumbel) Distribution:

This distribution (Eq. 4.1) was specifically designed for use in calculating extreme values.

$$F(H_S \leq \hat{H}_S) = e^{-e^{-\left(\frac{\hat{H}_S - B}{A}\right)}} \qquad \text{Eq. 4.1}$$

Weibull Distribution:

This distribution (Eq. 4.2) was not initially designed for the study of maximum extreme values, however it has proved useful for this purpose (Martinez-Aranzabal and Martín-Soldevilla, 1990).

$$F(H_S \leq \hat{H}_S) = 1 - e^{-e^{-\left(\frac{\hat{H}_S - B}{A}\right)^k}} \qquad \text{Eq. 4.2}$$

where:

$F(H_s \leq \hat{H}_s)$ = probability of $\hat{H}_s$ not being exceeded
H_s = significant wave height
$\hat{H}_s$ = particular value of significant wave height
B = location parameter
A = scale parameter
k = shape parameter

The shape parameter k in Eq. 4.2 is assigned one of the values k=0.75, 1.00, 1.40 and 2.00 (Goda, 1988). The parameters A and B in Eq. 4.1 and Eq. 4.2 are estimated by computing a least squares fit of the five candidate distribution functions to the data.

Fitting Method

Subsequent manipulations focused on fitting a set of extreme wave data to a chosen distribution function. This is a critical step, because the same data set could forecast different return wave heights (up to 3m) depending on the fitting method used (Cardone, 1986; Muir *et al.*, 1986). There are four methods; the geometric mean slope (also known as the graphical method), the method of moments, the maximum likelihood method and the least squares method. A detailed mathematical description of the methods for various distributions can be found in Martinez-Aranzabal and Martín-Soldevilla (1990) and examples of their use in Martín-Soldevilla and Martinez-Aranzabal (1990).

The graphical method is susceptible to subjective judgement and not recommended except for initial analysis. The moment method requires fewer calculations than the least square method, but cannot deal with the censored data. The maximum likelihood method is theoretically rigorous and favoured by many statisticians, but the calculations are tedious (Goda, 1988). The least squares method is a sophistication of the graphical method. It is simple and clear to calculate and so is the most commonly adopted for the extreme wave data analysis. A detailed description of this method can be found in Goda (1988). However, a drawback of the least square method for extreme data analysis is the necessity to choose a plotting position formula for each distribution function.

The least squares method ranks the input data in descending order of significant height. The probability to be assigned to each ordered set of extreme data depends upon the ordered number and the total data number only and is called the plotting position. For the data of *N* annual maxima or peak values, the probability of non-exceedance is generally assigned by Eq. 4.3.

$$F(H_s \leq H_{sm}) = 1 - \frac{m - \alpha_1}{N_T + \beta_1} \qquad \text{Eq. 4.3}$$

The parameters $\alpha 1$ and $\beta 1$ are given different values depending on the plotting rules used. Goda (1988), Muir and El-Shaarawi (1986), and Petrauskas and Aagaard (1970) suggested the following values for the Gumbel (Eq. 4.4) and Weibull (Eq. 4.5) distributions.

Gumbel $$F(H_s \leq H_{sm}) = 1 - \frac{m - 0.44}{N_T + 0.12} \qquad \text{Eq. 4.4}$$

Weibull $$F(H_s \leq H_{sm}) = 1 - \frac{m - 0.20 - \frac{0.27}{\sqrt{k}}}{N_T + 0.20 + \frac{0.23}{\sqrt{k}}}$$ Eq. 4.5

where:

$F(Hs \leq Hsm)$ = probability of the mth significant height not being exceeded
Hsm = m^{th} value in the ranked significant heights
m = rank of a significant height value = 1,2,...,N
N_T = total number of events during the length of record (which may exceed the number of input significant heights)

Selection of a Distribution Function

As previously mentioned, there is no absolute criterion to choose a particular function among several candidates fitted to an extreme data set. The five distribution functions considered are sufficiently different that only one or two can be expected to provide a good fit to any particular data set. Muir and El-Shaarawi (1986) described several possible approaches, but the use of correlation coefficients together with the residuals is sensitive enough to be useful in distinguishing between different distributions. Plots and the width of confidence intervals also help to judge the fit between data and distribution functions.

The correlation coefficients are the primary selection criterion. The distribution function that gives the highest correlation should be selected. The sum of the squares of residuals is usually smallest for the distribution function with the highest correlation. If a second distribution function fits nearly as well as the best fit (i.e., the correlation is nearly as high and the sum of the squares of residuals is comparable), it would be appropriate to consider extreme heights from both distributions. Extreme heights from the two distribution functions could be averaged together. Alternatively, the higher of the two could be used if a conservative estimate is desired.

Return Period

The chosen fitted distribution is then extrapolated to obtain the design H_s value corresponding to a known magnitude of $P(H_s)$ that in turn is derived from a specified return period. The return period is defined as the average time interval between successive events of an extreme significant wave height being equalled or exceeded. For example, the 50-year significant height can be expected to be equalled or exceeded on average once every 50 years. Depending on the distribution functions fitted to the data, the return wave heights vary and the difference increases as the return period estimate is made longer. The return value or the expected extreme wave height for a given return period (*r*) is then calculated by Eq. 4.6.

$$H_{sr} = Ay_r + B \qquad \text{Eq. 4.6}$$

where:

H_{sr} =significant wave height with return period r

$y_r = -\ln\left[-\ln\left(1-\frac{1}{\lambda T_r}\right)\right]$ Gumbel

$y_r = \left[\ln(\lambda T_r)\right]^{1/k}$ Weibull

λ = average number of events per year = $\frac{N_T}{K}$

T_r = return period (years)

k = length of record (years)

Confidence Intervals

Finally, confidence intervals for the estimated return wave are calculated. Estimation of confidence intervals is an essential part of extreme wave analysis. There is very little use in having an estimate of a return wave unless the confidence intervals are known (Losada-Rodriguez *et al.*, 1992). Typically, the period of record is short, and the level of uncertainty in extreme estimates with long return periods is high. Confidence intervals give a quantitative indicator of the level of uncertainty in estimated extreme wave heights.

It must be emphasised that any estimation of return value is accompanied by statistical variability due to sampling error. In other words, an extreme wave data under analysis is but a sample taken from an unknown population of storm waves. Depending on the characteristics of a particular sample relative to those of a population, the result of extreme data analysis might be an overestimate or an underestimate compared with the population value, which remains unknown. Another set of extreme waves to be obtained in the coming several tens of years will form a sample different from the present sample, even if no long-term climatic changes exist. The two sets of extreme data will yield different distribution functions and the return wave heights will eventually be different (Goda, 1988).

The approach of Gumbel (1958), Lawless (1978) and Goda (1988) for estimating standard deviation of return value when the true distribution is known is used. The formula of normalised standard error presented as Eq. 4.7 would serve as a guide to measure the magnitude of uncertainty.

$$\sigma_{nr} = \frac{1}{\sqrt{N}}\left[1 + a(y_r - c + \varepsilon \ln v)^2\right]^{\frac{1}{2}} \qquad \text{Eq. 4.7}$$

where:

σ_{nr} = normalised standard deviation of significant wave height with return period r
N = number of input significant heights
$a = a_1 \; e^{a_2 N^{-1.3} + k\sqrt{-\ln v}}$
v = censoring parameter = N/N_T
a_1, a_2, c, ε, k = empirical coefficients read from Table 4.4

Table 4.4: Coefficients of empirical standard deviation formula for extreme significant height (Goda, 1988).

Distribution	α_1	α_2	k	c	ε
FT-I	0.64	9.00	0.93	0.00	1.33
Weibull (k=0.75)	1.65	11.4	-0.63	0.00	1.15
Weibull (k=1.0)	1.92	11.4	0.00	0.30	0.90
Weibull (k=1.4)	2.05	11.4	0.69	0.40	0.72
Weibull (k=2.0)	2.24	11.4	1.34	0.50	0.54

The absolute magnitude of the standard deviation of significant wave height is calculated by Eq. 4.8:

$$\sigma_r = \sigma_{nr}\,\sigma_{Hs} \qquad \text{Eq. 4.8}$$

where:

σ_r = standard error of significant wave height with return period r
σ_{nr} = normalised standard deviation of significant wave height with return period r (from Eq. 4.7)
σ_{Hs} = standard deviation of input significant heights

Confidence intervals are calculated by assuming that significant height estimates at any particular return period are normally distributed about the assumed distribution function. Factors by which to multiply the standard error (Eq. 4.8) to get bounds with various levels of confidence are given in Table 4.5. It is important to note that the width of confidence intervals depends on the distribution function, *N*, and *v* but it is not related to how well the data fits the distribution function.

Table 4.5: Confidence interval bounds for extreme significant heights.

Confidence Level (%)	Confidence Interval Bounds Around H_{sr}	Probability of Exceeding Upper Bound (%)
80	$\pm 1.28\ \sigma_r$	10.0
85	$\pm 1.44\ \sigma_r$	7.5
90	$\pm 1.65\ \sigma_r$	5.0

4.4.1.2 DATA

Data screening identified four possible sources of wave data for the study area; visual observations from ships, six land-based wind stations (which could be used to estimate wave heights; US Army Corps of Engineers, 1984), two marine buoys and 15 WANA points (the daily wave forecast output from the fourth generation WAve Model ,WAM (Günther *et al.*, 1991), used by the Spanish Department of Maritime Climate). The WAM-model solves the wave transport equation explicitly without any presumptions on the shape of the wave spectrum. It represents the physics of the wave evolution in accordance with knowledge for the full set of degrees of freedom of a 2D wave spectrum. It has been installed at about 35 institutions world wide and is used for research and also operational application. It is also being applied for interpreting and assimilating satellite wave data. Visual observations from ships and wind data (Fig. 4.9) were not used due to their inaccuracy relative to the other available data sources and also their lack of coverage. Similarly, although marine buoys are the most accurate source of information, the limited spatial coverage afforded by only two buoys (Fig. 4.9) did not provide enough detail for this study. Hence, the 15 WANA points were used as the data source as their coverage (Fig. 4.9) and predicted accuracy (Fanjul *et al.*, 1998) was adequate. The WANA data was provided by The Spanish Department of Maritime Climate. The wave records used cover a period of 5 years with a temporal resolution of 6 hours, from 1995 to 1999, with 6740 values of H_s, T_p and mean wave direction per WANA point.

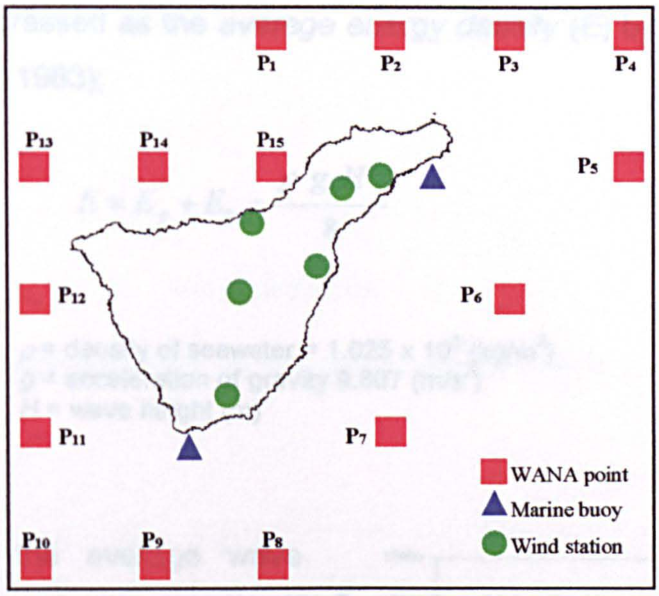

Fig. 4.9: Distribution of the 15 WANA points, marine buoys and wind stations.

4.4.1.3 Calculating and Mapping the Mid-term Statistic

Mid-term statistics was used to characterise the average wave regime in Tenerife (the mean wave height over a certain period of time). The data was individually analysed for each of the 15 WANA points. To provide a first indication of possible data trends, Fig. 4.10 shows the mean H_s and the standard deviation, while Fig. 4.11 shows the maximum H_s for each point.

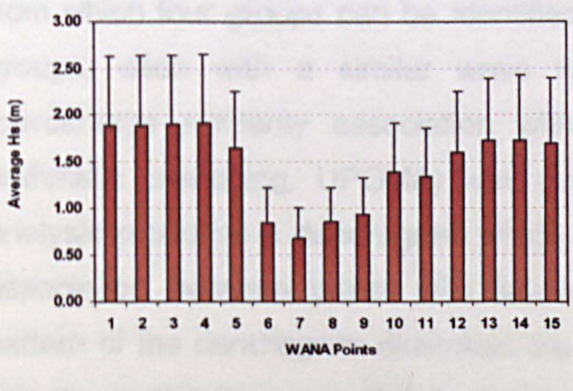

Fig. 4.10: Mean significant wave height (H_s) and error bars (standard deviation) for WANA points in Tenerife.

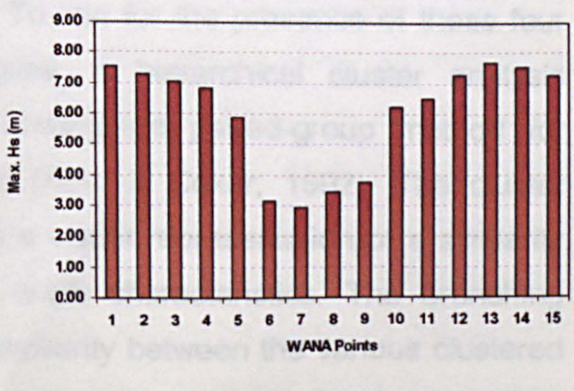

Fig. 4.11: Maximum significant wave height (H_s) for WANA points in Tenerife.

The average wave energy for each location is also an important parameter that provides an indication of the environmental stress which a fish cage will need to withstand. The energy of a sinusoidal wave (per unit area of wave in deep water) can be divided into potential energy (*E_p*) and kinetic energy (*E_k*), and its combined formula can be expressed as the *average energy density* (*E*) by following Eq. 4.9 (Pond and Pickard, 1983);

$$E = E_p + E_k = \frac{\rho\, g\, H^2}{8} \qquad \textbf{Eq. 4.9}$$

where;

ρ = density of seawater = 1.025 x 10^3 (kg/m^3)
g = acceleration of gravity 9.807 (m/s^2)
H = wave height (m)

Fig. 4.12 shows the average wave energy (J m^{-2}) and the standard deviation for the five year data set. A limited version of this approach was used to successfully quantify kelp canopy responses to several wave energy levels over a single peak storm period (Bushing, 1997).

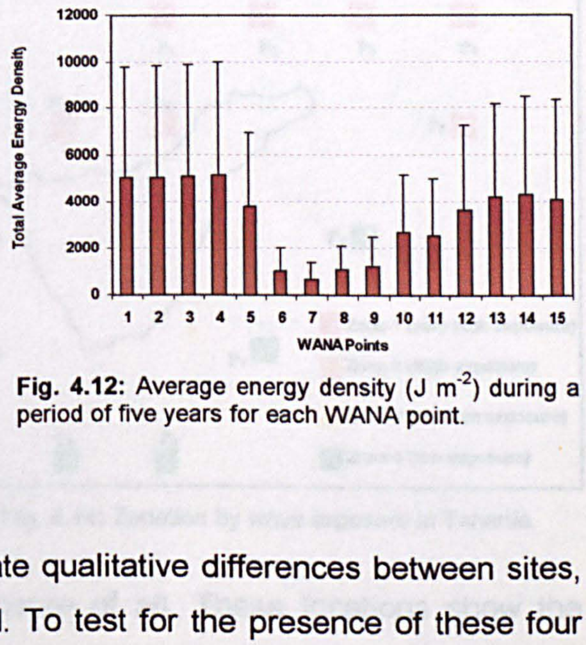

Fig. 4.12: Average energy density (J m^{-2}) during a period of five years for each WANA point.

Fig. 4.10, Fig. 4.11 and Fig. 4.12 illustrate qualitative differences between sites, from which four groups can be identified. To test for the presence of these four groups, each with a similar wave regime, a hierarchical cluster analysis (percentage similarity association with unweighted paired-group method for arithmetic averaging, UPGMA) was used (Kent & Coker, 1992). The cluster analysis produces a dendrogram which is a visual representation of a similarity association between points with similar wave characteristics. The branching pattern of the dendrogram illustrates the similarity between the various clustered objects, in that the more closely they are linked, the more similar they are. Fig. 4.13 shows the dendrogram produced for the data set.

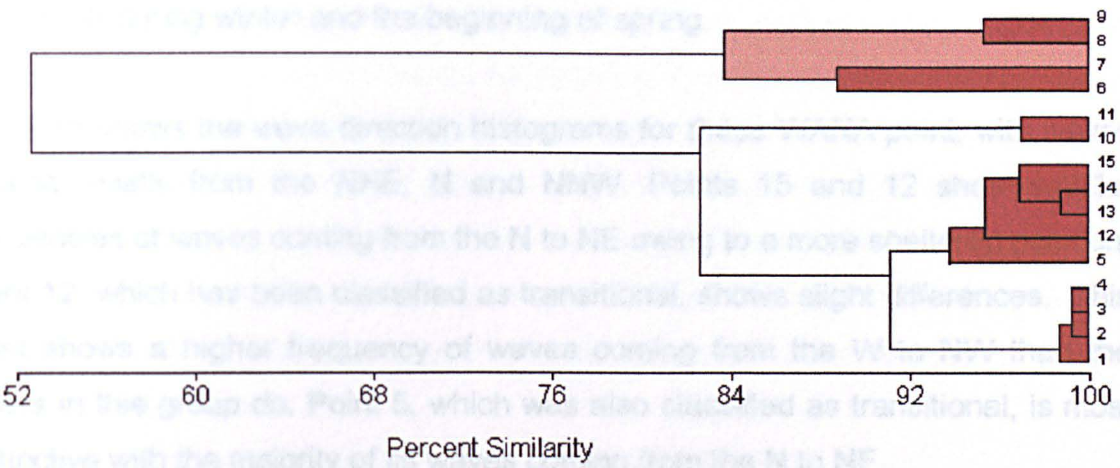

Fig. 4.13: Dendrogram (using UPGMA) showing similarities between wave sites.

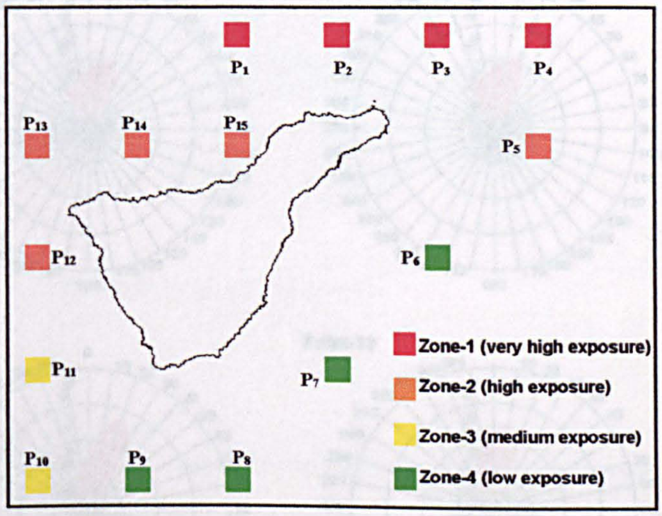

Fig. 4.14: Zonation by wave exposure in Tenerife.

The combined use of the dendrogram (Fig. 4.13), the mean and maximum H_s (Fig. 4.10 and Fig. 4.11), and the average wave energy density (Fig. 4.12) was used to characterise the Tenerife coastline according to wave exposure. Wave characterisation identified four major zones (Fig. 4.14). Points 1, 2 ,3 and 4 form a very homogeneous group (zone-1), characterised by the highest wave exposure of all. These locations show the highest wave heights and the greatest average energy density. They are located in the N and NE, where there is most exposure to wave action. The second zone, composed of points 5, 12, 13, 14 and 15 may be classified as a high exposure area, characterised as having high average energy density, but smaller maximum wave heights than zone-1. This zone may be further subdivided into two sub-zones. One composed of points 5 and 12 and the second by points 13, 14 and 15. The former may also be seen as a "transitional zone" between the N and S wave regimes of the island. Zones-1 and 2 are the most exposed areas of the island due to their opening to the Trade Winds coming from the NNE and the stormy weather from the N during winter and the beginning of spring.

Fig. 4.15 shows the wave direction histograms for these WANA point, with waves coming mostly from the NNE, N and NNW. Points 15 and 12 show smaller frequencies of waves coming from the N to NE owing to a more sheltered position. Point 12, which has been classified as transitional, shows slight differences. This point shows a higher frequency of waves coming from the W to NW than the others in this group do. Point 5, which was also classified as transitional, is most distinctive with the majority of its waves coming from the N to NE.

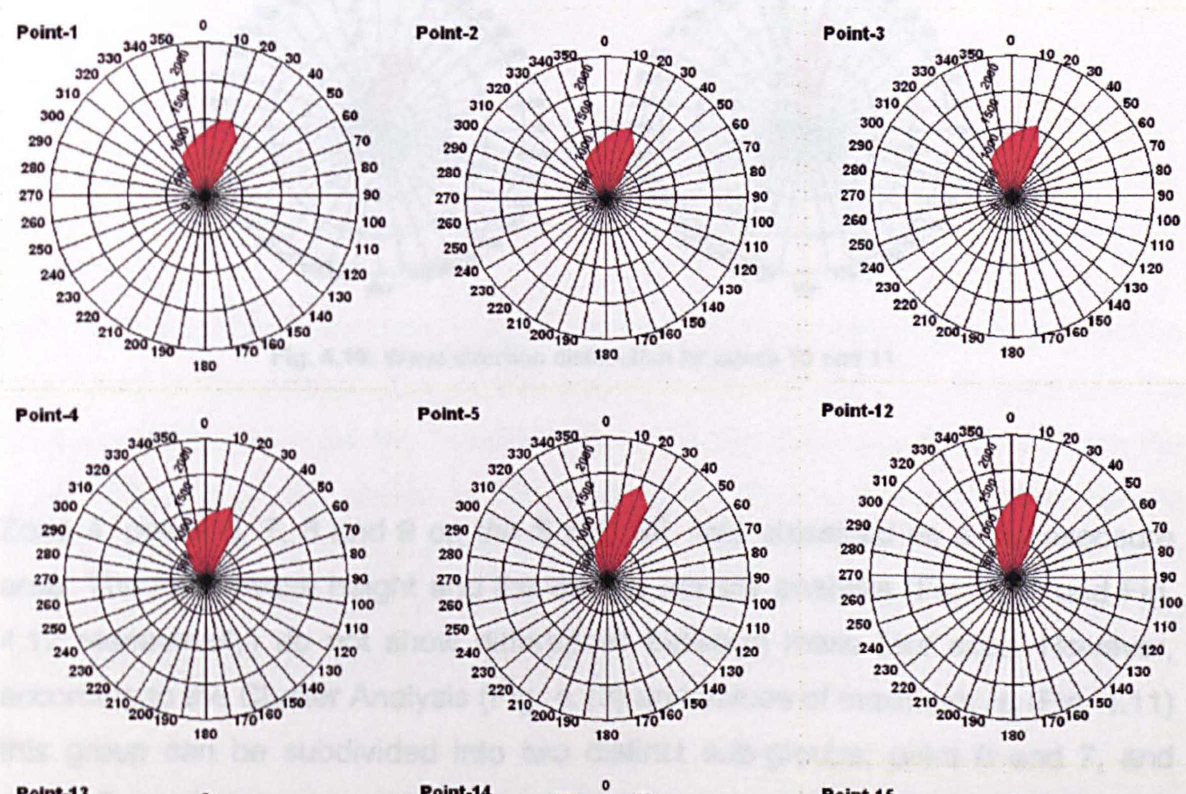

Fig. 4.15: Wave direction distribution for points 1,2,3,4,5,12,13,14 and 15.

The third zone, formed by points 10 and 11, is located in the SE part of the island. This zone is characterised by a medium to low wave regime throughout most of the year. However, some sporadic episodes of high waves occur when stormy weather comes from the SW. Looking at the total energy density, these two points can be classified as medium exposure sites. The wave direction distribution for these two points (Fig. 4.16) shows that most of the waves come from the N and NNE. However, there is a small frequency of waves coming from the NNW to NW. The N to NE wave frequency at point 11 is lower than at point 10 owing to shelter provided by the island.

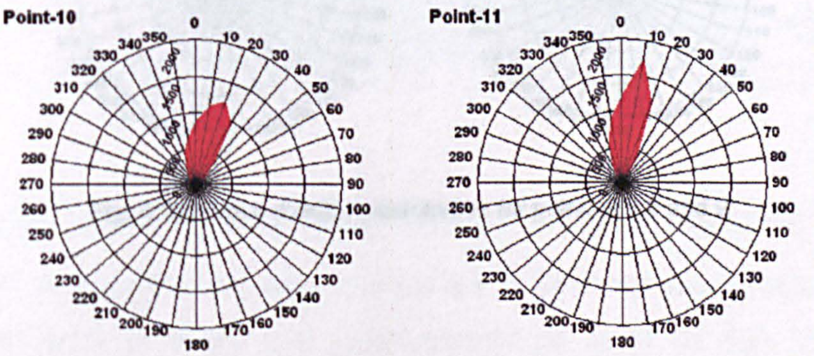

Fig. 4.16: Wave direction distribution for points 10 and 11.

Zone 4, points 6, 7, 8 and 9 on the S and SE, was classified as a low exposure area. The mean wave height and the energy density analysis (Fig. 4.10 and Fig. 4.12 respectively) do not show differences between these four sites. However, according to the Cluster Analysis (Fig. 4.13) and values of maximum H_s (Fig. 4.11) this group can be subdivided into two distinct sub-groups; point 6 and 7, and points 8 and 9, based on differences in highest wave heights which are higher at points 8 and 9, due to their proximity to stormy weather coming from the SW. The wave direction distribution for these points (Fig. 4.17), although apparently similar, also shows some differences between the two sub-groups. The main wave direction for these four points is NE, however, points 8 and 9 have a distinctive NW component

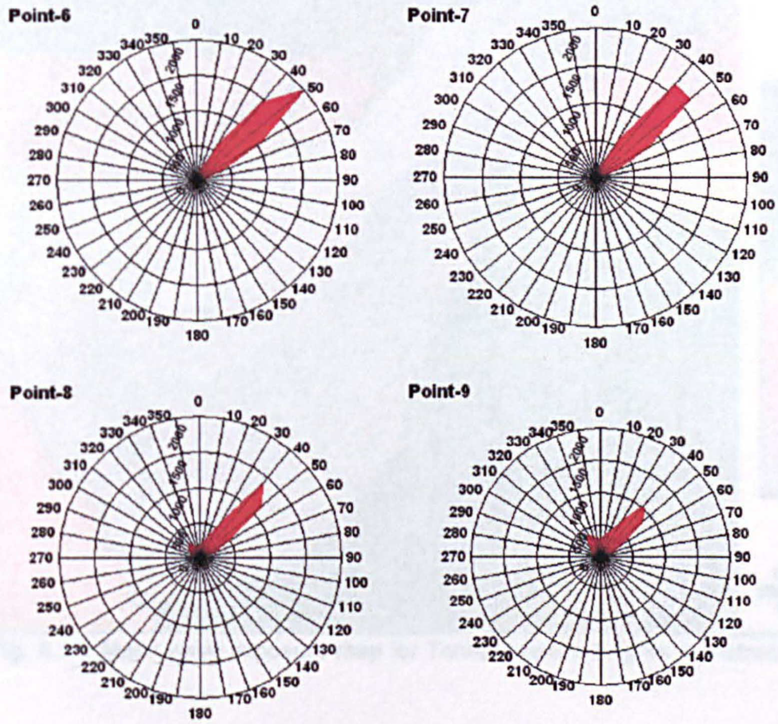

Fig. 4.17: Wave direction distribution for points 6,7,8 and 9.

Information on the mean wave heights together with information on wave direction was used in the spatial data builder software CARTALINX 1.2 to generate the mean wave height layer for Tenerife. The wave direction was extracted from the wave direction graphs shown in Fig. 4.15, Fig. 4.16 and Fig. 4.17. The module COGO was used to estimate the approximate wave direction coming from each WANA point. Finally, this vector file was exported to IDRISI32 to generate the mean wave exposure layer for the coastline in Tenerife (Fig. 4.18).

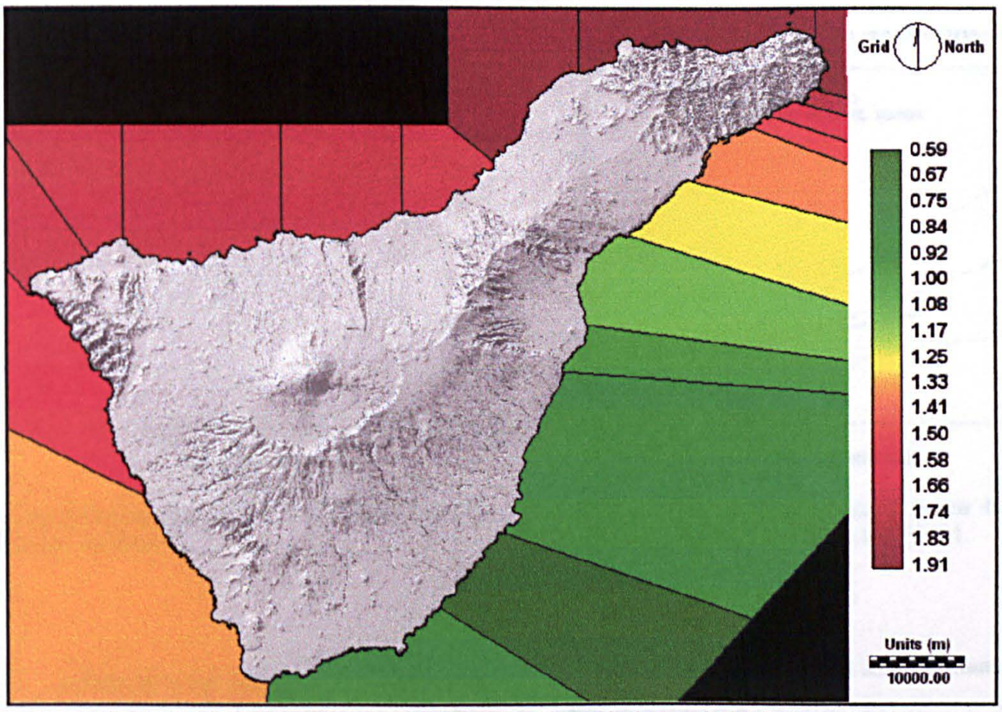

Fig. 4.18: Mean wave exposure map for Tenerife (wave heights in metres).

4.4.1.4 Calculating and Mapping the Long-term Statistic

Barker (1990) suggested that extreme values of environmental factors which are not exceeded once in every 100 years should be used for fish farming siting. However, in waters where the environmental data is well established, *e.g.* the European continental shelf, a 50-year return period may be acceptable. Other authors are less rigorous. Nayak *et al.* (1990) suggested that only 5 to 10 years of wave data was necessary for reasonable prediction of a maximum design wave. It is therefore reasonable to assume that a return period which covers the lifetime of the structure (15 to 20 years) is satisfactory for siting an offshore cage system, although, of course, longer data periods are always desired and recommended.

The monthly maximum wave values of extreme significant wave height for each of the 15 WANA points were analysed using ACES (Automated Coastal Engineering System) version 1.07f software (Leenknecht *et al.*, 1992). An extreme wave height plot for each of the five probability distribution functions was created, and wave return periods extracted. Fig. 4.19, Fig. 4.20, Fig. 4.21, Fig. 4.22 and Fig. 4.23 show an example, of the five plots for WANA Point-1 (refer to Fig. 4.9), and Table 4.6 shows some return wave heights from different return periods extracted from the plots.

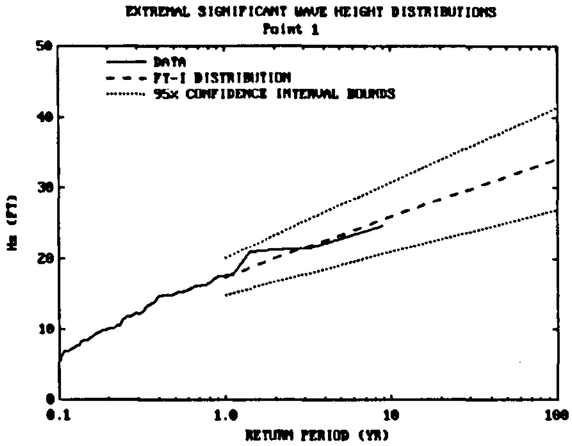

Fig. 4.19: Extremal significant wave height for FT-I distribution in Point-1.

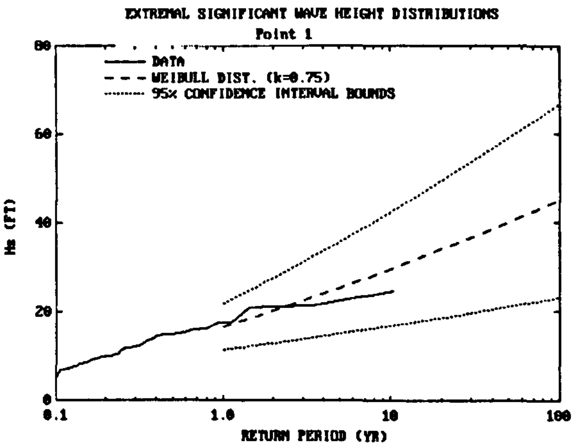

Fig. 4.20: Extremal significant wave height for Weibull distribution (k=0.75) in Point-1.

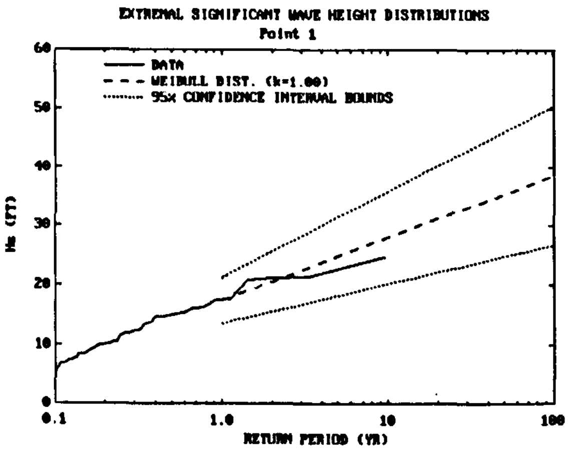

Fig. 4.21: Extremal significant wave height for Weibull distribution (k=1.00) in Point-1.

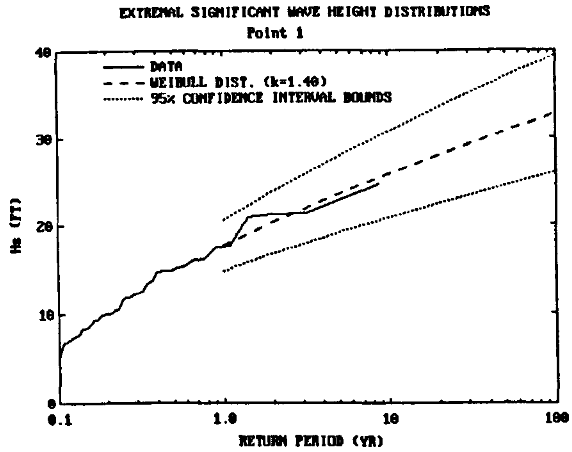

Fig. 4.22: Extremal significant wave height for Weibull distribution (k=1.40) in Point-1.

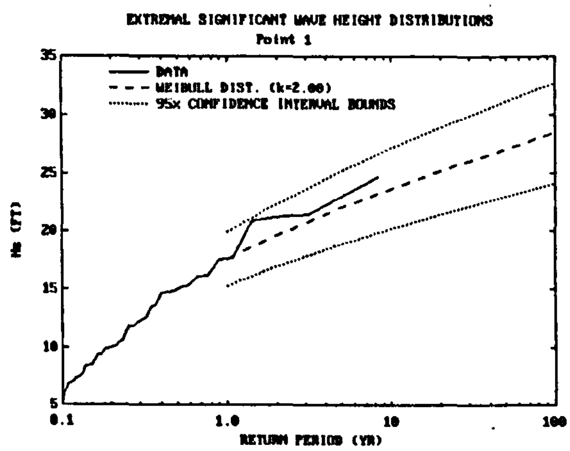

Fig. 4.23: Extremal significant wave height for Weibull distribution (k=2.00) in Point-1.

Table 4.6: Return periods for each of the probability distributions (Point-1).

Return	FT-I	Weibull k = 0.75	Weibull k = 1.00	Weibull k = 1.40	Weibull k = 2.00
Period (Yr.)	Hs (m)	Hs (m)	Hs (m)	Hs (m)	Hs (m)
2	6.11	6.17	6.28	6.20	6.00
5	7.12	7.75	7.57	7.18	6.74
10	7.89	9.03	8.54	7.87	7.24
25	8.89	10.83	9.88	8.74	7.84
50	9.65	12.26	10.80	9.38	8.27
100	10.40	13.74	11.16	9.99	8.67

From the five distribution functions fitted to each WANA point, that with the highest correlation and smallest sum of the square of residuals was chosen as the probability distribution which best fit the data set. Table 4.7 shows an example of the correlation and residual values computed for the data set in Point-1, from which the Weibull distribution (k=1.40) was chosen.

Table 4.7: Correlation and residual values for each of the probability distributions (Point-1).

	FT-I	Weibull k = 0.75	Weibull k = 1.00	Weibull k = 1.40	Weibull k = 2.00
Correlation	0.98	0.95	0.98	**0.99**	0.98
Sum Square of Residuals	0.22	1.58	0.32	**0.09**	0.34

The sequence of steps described above was carried out for each of the 15 points that compose the wave data set for Tenerife. Table 4.8 shows the significant wave height for a 15-year return period calculated for each WANA point and their associated confidence intervals. In this study, return periods higher than 15 years may not be significant as only 5 years of data were available for calculations.

Table 4.8: Extreme significant wave height for a 15 year return period with 95% confidence interval.

	Hs (m)	Lower confidence interval (m)	Upper confidence interval (m)
POINT 1	8.26	6.65	9.87
POINT 2	8.24	6.65	9.83
POINT 3	8.19	6.62	9.76
POINT 4	8.13	6.58	9.67
POINT 5	6.41	5.28	7.54
POINT 6	3.37	2.84	3.90
POINT 7	3.04	2.55	3.53
POINT 8	3.84	3.15	4.53
POINT 9	4.09	3.33	4.84
POINT 10	6.30	4.57	8.04
POINT 11	6.63	4.73	8.52
POINT 12	7.23	5.79	8.67
POINT 13	7.57	6.10	9.05
POINT 14	7.83	6.29	9.37
POINT 15	7.92	6.33	9.51

The information on the 15-year return wave heights together with information on wave direction was used in the spatial data builder software CARTALINX 1.2 to generate the extreme wave height layer for Tenerife. Knowing the exact location of each WANA point and the wave direction (azimuth) of the 20 highest waves recorded in each point, the module COGO was used to estimate the approximate direction for extreme waves coming from each of these WANA point. Alternatively, if a more conservative estimate was required, the values of the upper confidence interval limit could be used to generate this layer Finally, this vector file was exported to IDRISI32 to generate the extreme wave height layer for Tenerife shown in Fig. 4.24.

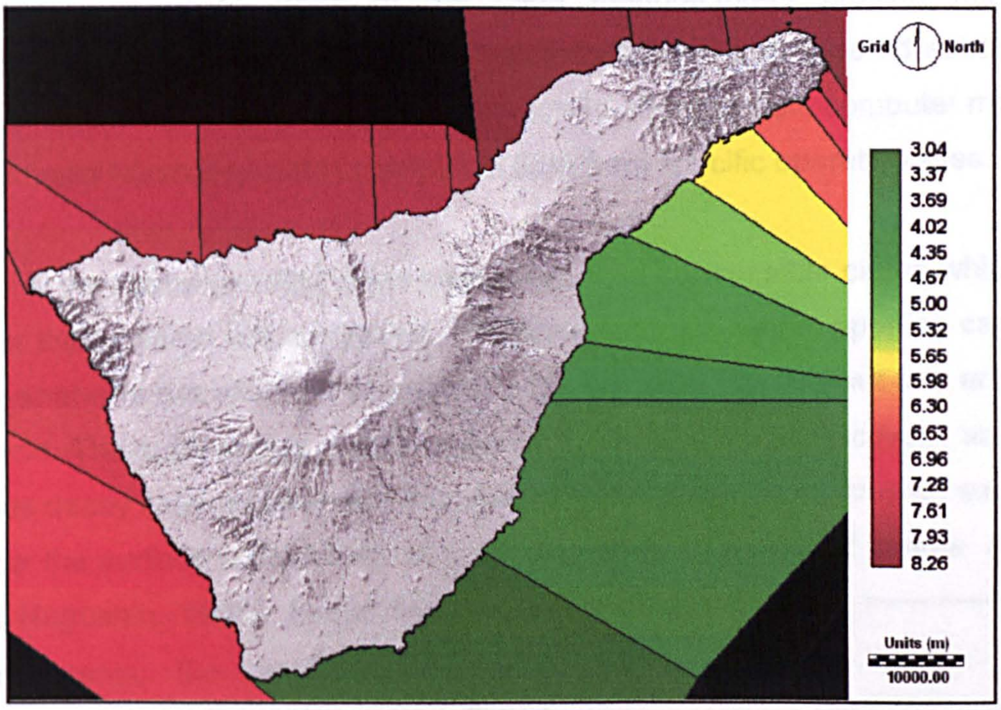

Fig. 4.24: Extreme wave height map for Tenerife (wave heights in metres).

Fig. 4.24 shows that the roughest conditions are mostly located on the northern and western coasts, while along the southern coast there is a regular decrease of wave height from east to west.

4.4.1.5 Selection of Cage Type

Selection of a suitable sea-cage design for a particular offshore location should take into account several factors (Linfoot et *al.*, 1990): (1) economic; capital cost amortisation and routine maintenance (operating cost), (2) biological; maintenance of optimum stock holding conditions including minimisation of exposure to disease, stress and maintenance of water quality levels through adequate water exchange, and (3) engineering; structural integrity, longevity and safety. This study focuses primarily on their capability to withstand certain wave climates.

Tenerife has a broad range of wave climate as seen from Fig. 4.18 and Fig. 4.24, ranging from a mild environment on the southern and south-eastern coasts to a highly exposed environment on the north coast. Three cage systems were selected as suitable for deployment based on their ability to withstand these conditions. However, none of the cage manufacturers provide full written specifications on wave heights for which the cages are considered suitable. The little available information which manufacturers offer are from computer modelling, small scale laboratory tests or empirical data from specific operating sites.

For the very dynamic sites (high exposure), rigid submersible cages which would retain their volume are suggested. Self-tensioned and self-supporting cages hold their shape in the absence of weights but will also do so without any anchor line tension. The submersible systems can avoid storm effects effectively, since wave forces decay exponentially with increase of water depth. Even modest submersion below the surface substantially reduces wave forces from local storms (Willinsky and Huguenin, 1996). Based on these requirements, the SeaStation® cage system was chosen (Fig. 4.25). This cage has at its core a single spar, around which an eight sectioned rim is placed. The nets are strung between the top and bottom of the spar to the rim so that the cage resembles two cones with their bases connected together. The typical dimension of this cage is 25 m by 15 m, with a volume of about 5000 m^3.

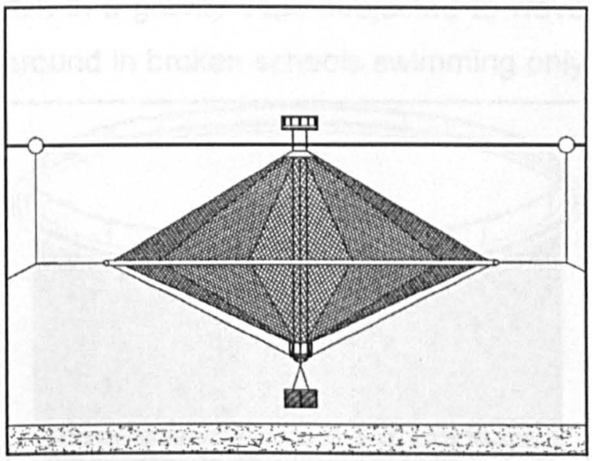

Fig. 4.25: SeaStation® cage system (redrawn from Loverich, 1997).

In the intermediate exposure sites, rigid cages (anchor tensioned) should also be used. Anchor tensioned cages rely on very taut moorings to hold their shape and volume, and they are not dependent on weights for maintenance of net shape. Any external forces applied to the netting enclosure will cause the anchor line tensions to increase which, in turn, resists cage deformation. Fish are therefore able to swim in greater net volumes throughout the whole cage. For these mid exposure sites the Ocean Spar® cage system was chosen (Fig. 426). The typical dimension of this cage is 24x24x9 m, with a volume of about 5000 m^3.

Finally, for the low energy sites, the simplest and cheaper gravity cages could be used. Gravity cages usually consist of surface floats in the form of a circle or polygon, from which a net enclosure is hung. The term 'gravity cage' comes from the fact that the net is prevented from becoming flattened in water currents by weights hung on the bottom of the net enclosure. Even so, gravity cages can lose more than half their volume in the presence of strong currents (Aarsnes and Rudi, 1990). The fish in a gravity cage subjected to wave motion are normally very excited, darting around in broken schools swimming only where the net volume is greatest, effectively reducing the net volume more (Loverich, 1997). Though there are many gravity cage systems to choose from, Corelsa® cages were selected as this system is already being used successfully in Tenerife (Fig. 4.27). The typical dimension of this cage is 20 in diameter and 10 depth, with a volume of about 3000 m^3.

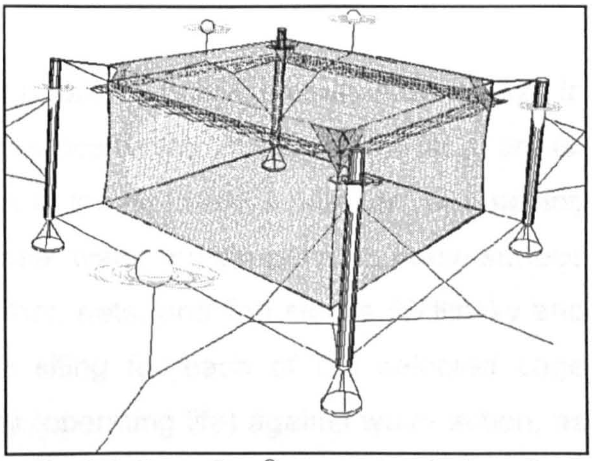

Fig. 426: Ocean Spar® cage system (redrawn from Loverich, 1997).

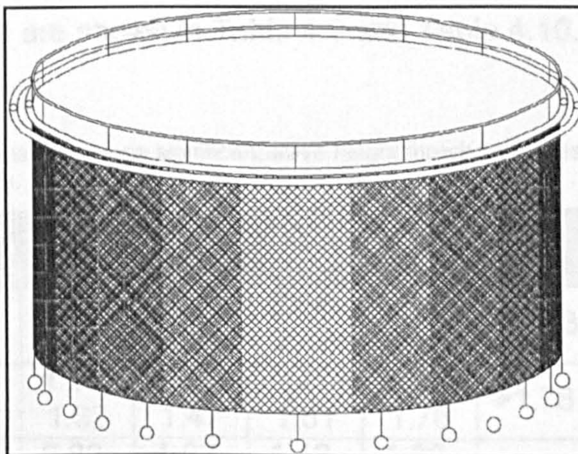

Fig. 4.27: Corelsa® cage system (redrawn from Loverich, 1997).

Bugrova (1996) studied the economical feasibility of different cage systems, including offshore cages. He showed that capital cost is 43% higher for semi-submerged than for floating cages, however this is compensated by lower labour costs, lower feed costs, better survival rate and higher fish quality. He concluded that in "real terms" the unit production costs for floating systems are 3% higher than those for semi-submerged ones. Therefore, operations that use semi-submerged and submerged cages may be most effective.

4.4.1.6 Suitability Maps

Sea cages and the fish within them can only tolerate certain sea states. In moderate to severe wave conditions, cages positioned at the sea surface, or just below, act as breakwaters and are subject to the destructive pressure of breaking waves. Simultaneous exposure to the circular water motion beneath these surface wave fields affects moorings, flotation collars, nets, and fish stocks (Willinsky and Huguenin, 1996). Therefore, appropriate siting for each of the selected cage systems is crucial to ensure their longevity (operating life) against wave action, as well as safety for the operators.

To generate the suitability maps for siting each of the cage systems, the two wave exposure maps (Fig. 4.18 and Fig. 4.24) were reclassified. The threshold values for each score were based on personal interpretation of cage designs obtained from the manufacturers and literature, and are shown in Table 4.9 and Table 4.10.

Table 4.9: Seacage performance reclassification in terms of average significant wave height threshold values (m).

Score / Cage type	8	7	6	5	4	3	2	1
SeaStation®	0-1.47	1.47-1.61	1.61-1.76	1.76-1.90	1.90-2.04	2.04-2.19	2.19-2.33	> 2.33
Ocean Spar®	0-0.89	0.89-1.03	1.03-1.18	1.18-1.32	1.32-1.47	1.47-1.61	1.61-1.76	>1.76
Corelsa®	0-0.6	0.6-0.74	0.74-0.89	0.89-1.03	1.03-1.18	1.18-1.32	1.32-1.47	>1.47

Table 4.10: Seacage performance reclassification in terms of extreme significant wave height threshold values (m).

Score / Cage type	8	7	6	5	4	3	2	1
SeaStation®	0-6	6-7	7-8	8-9	9-10	10-11	11-12	>12
Ocean Spar®	0-4	4-5	5-6	6-7	7-8	8-9	9-10	>10
Corelsa®	0-3	3-3.5	3.5-4	4-4.5	4.5-5	5-5.5	5.5-6	>6

The average and extreme wave height suitability maps for each cage system are shown Fig. 4.28 and Fig. 4.29, Fig. 4.30 and Fig. 4.31, and Fig. 4.32 and Fig. 4.33.

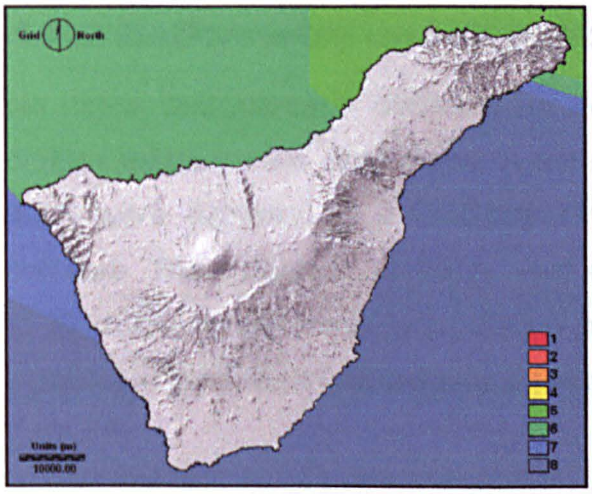

Fig. 4.28: Average wave height suitability map for SeaStation®.

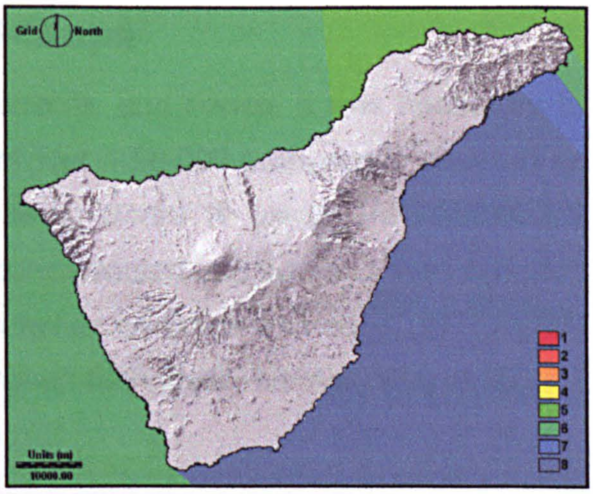

Fig. 4.29: Extreme wave height suitability map for SeaStation®.

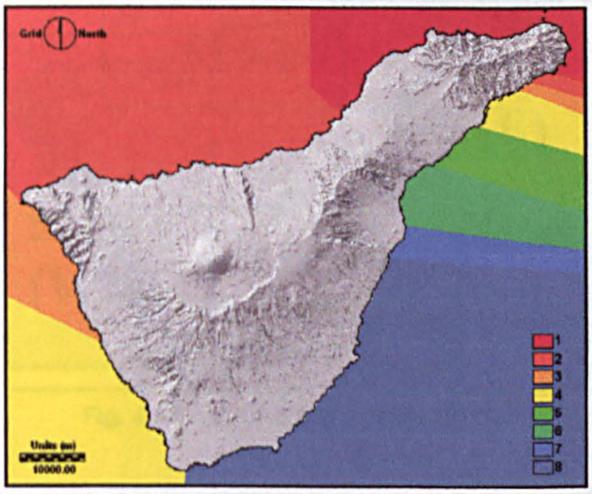

Fig. 4.30: Average wave height suitability map for Ocean Spar®.

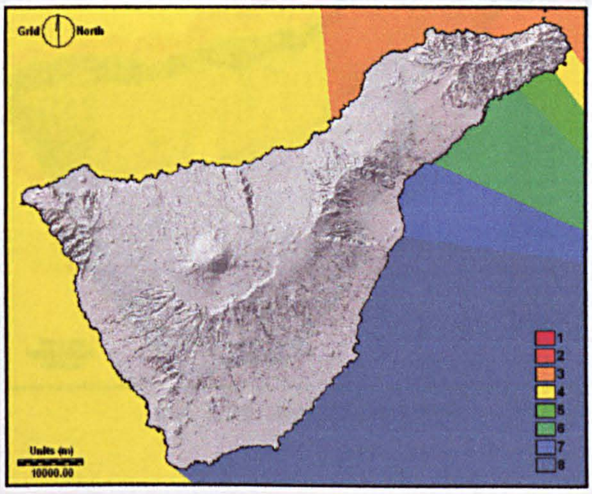

Fig. 4.31: Extreme wave height suitability map for Ocean Spar®.

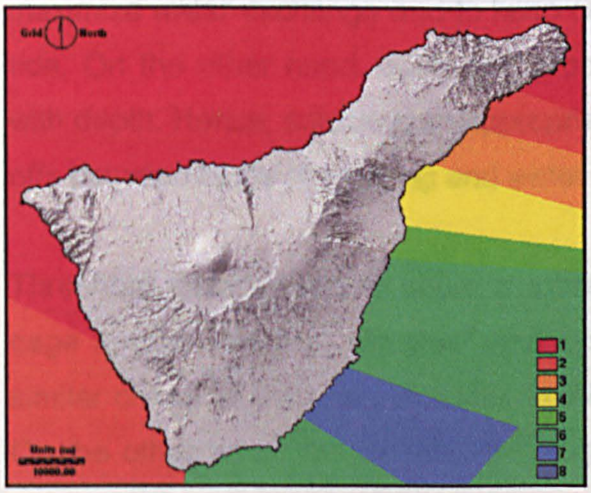

Fig. 4.32: Average wave height suitability map for Corelsa®.

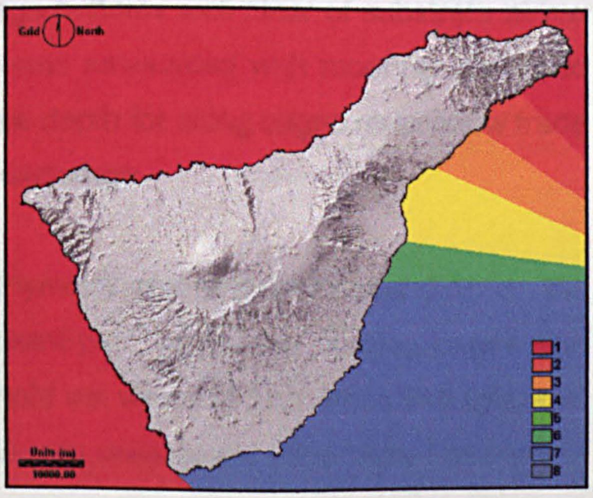

Fig. 4.33: Extreme wave height suitability map for Corelsa®.

4.4.2 Bathymetry and Seabed-Slope

No digital bathymetry is available for Tenerife, and hence, it was necessary to digitise existing hard copy maps. A set of four 1:50,000 bathymetric charts (Fig. 4.34) were digitised on a CalComp Drawing Board III using CARTALINX 1.2 software. The 4 digitised contours were concatenated into one and then exported to IDRISI32 where linear interpolation between contours was used (INTERCON module) to produce a faceted model (complete bathymetry surface) (Fig. 4.35).

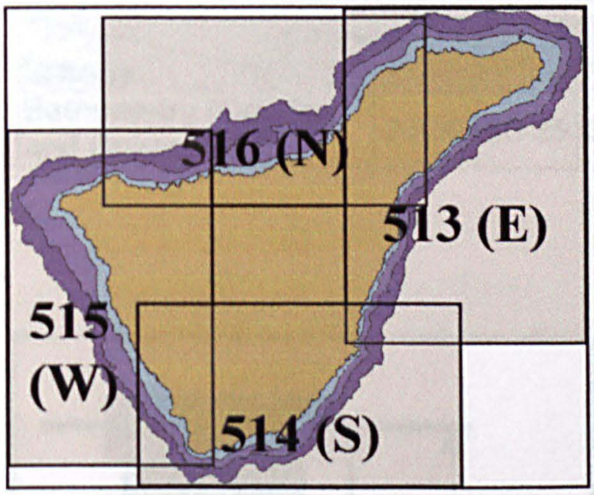

Fig. 4.34: Digitised bathymetric charts.

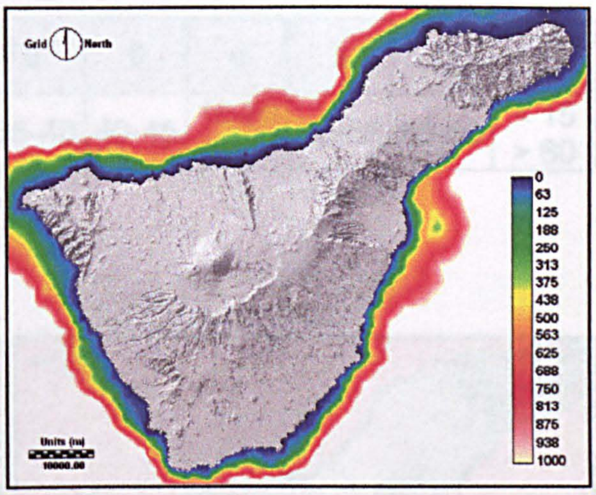

Fig. 4.35: Bathymetry map.

Floating cages should be located at sites where the water depth is sufficient to maximize water exchange and to keep cage bottoms well clear of substrate at low tide. On the other hand, costs and problems associated with mooring increases with depth. Hence, selecting an appropriate depth for siting cages must allow trade offs between costs of mooring and water exchange.

Threshold values used to score the bathymetry are different depending on the cage system selected. Corelsa® and OceanSpar® cages are floating cages with similar characteristics, so, a single threshold set was used for these two systems. On the other hand, the SeaStation® cage was considered separately because of its very different characteristics.

Threshold values for the Corelsa® and OceanSpar® cages are shown in Table 4.11 and were based on the following two assumptions; a minimum distance of at least 5 m between the cage bottom and the seabed for efficient waste dispersion Beveridge (1996), and (2) the cage depth was assumed to be 15 m. Hence, 20 m is the ideal depth for minimal mooring cost and effective waste dispersion for these cage systems (Fig. 4.36). Fig. 4.37 shows the bathymetry suitability map based on these parameters.

Table 4.11: Bathymetry threshold values (in metres) used for Corelsa® and OceanSpar®.

Score / Criteria	8	7	6	5	4	3	2	1
Bathymetry (Corelsa® and OceanSpar®)	20-30	30-35	35-40	40-45	15-20 45-50	50-55	55-60	< 15 > 60

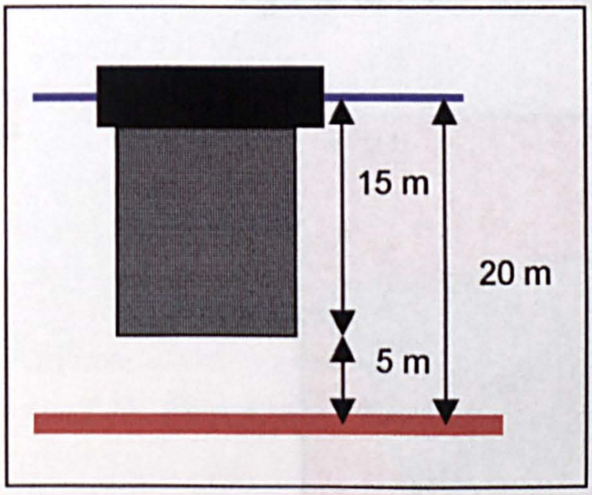

Fig. 4.36: Ideal water depth for Corelsa® and OceanSpar®.

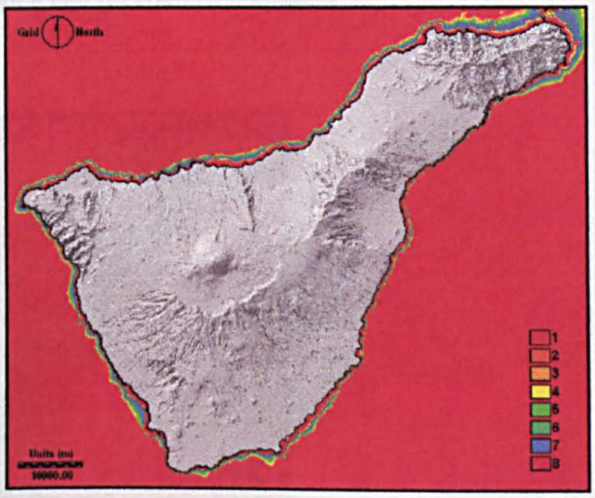

Fig. 4.37: Bathymetry suitability map for Corelsa® and OceanSpar®.

Threshold values for the SeaStation® cages, shown in Table 4.12, were based on the same assumptions. However, the SeaStation® cages' ideal depth is based on the cage dimension (16.2 m) and the required depth for submergence (8.6 m) as seen in Fig. 4.38. Therefore, the ideal depth for this system was estimated to be 30 m (16.2 m of cage + 8.6 m of submergibility + 5 m for waste dispersion = 30 m). Fig. 4.39 shows the bathymetry suitability map for this cage system based in these parameters.

Table 4.12: Bathymetry threshold values (m) used for SeaStation®.

Criteria \ Score	8	7	6	5	4	3	2	1
Bathymetry (SeaStation®)	30-40	40-45	45-50	50-55	55-60 25-30	60-65	65-70	>70 <25

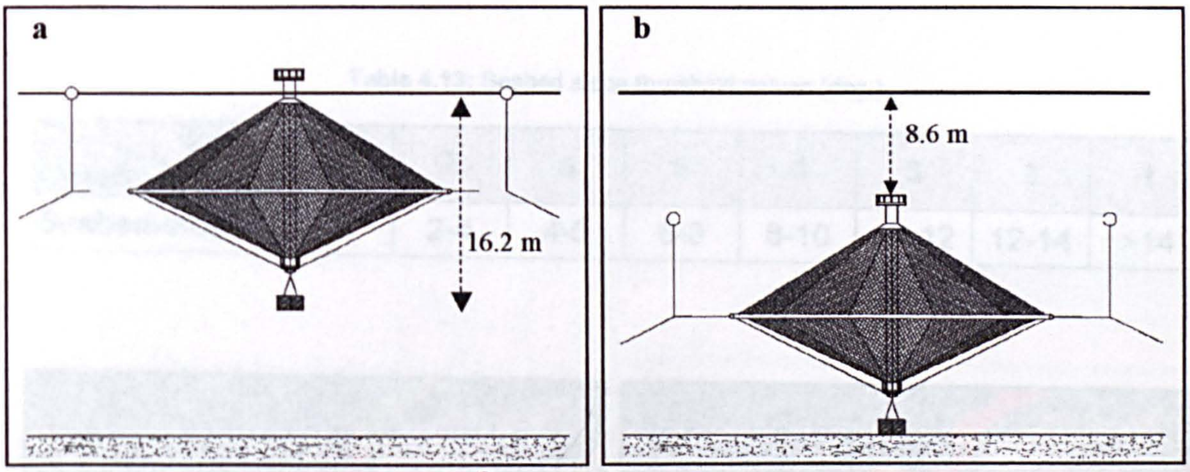

Fig. 4.38: SeaStation® (a) dimension and (b) submergible depth.

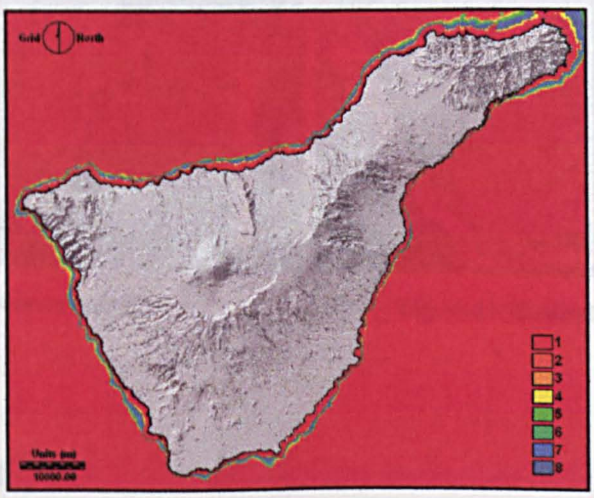

Fig. 4.39: Bathymetry map for SeaStation® cages.

Seabed-slope was not initially included as a criterion in this study. However, feedback from the questionnaires used revealed that some decision-makers from the focus groups considered this criterion to be important (see section 5.3.1), and it was therefore included. Slopes are of importance as the greater the slope the more complicated and expensive is the mooring system required.

Slopes were calculated by using the module SLOPE on the bathymetric map (Fig. 4.40). SLOPE determines the slope for a cell based on the cell resolution and the values of the immediate neighbouring cells to the top, bottom, left and right of the cell in question. Table 4.13 shows the threshold values used, and Fig. 4.41 shows the seabed slope suitability map.

Table 4.13: Seabed slope threshold values (deg.).

Criteria \ Score	8	7	6	5	4	3	2	1
Seabed-slope	<2	2-4	4-6	6-8	8-10	10-12	12-14	>14

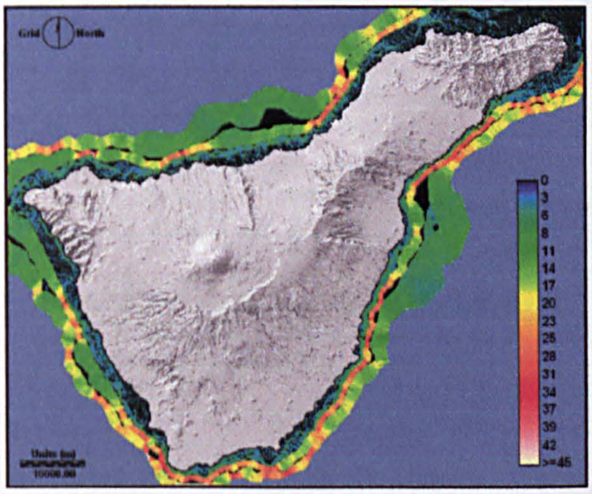

Fig. 4.40: Seabed slope.

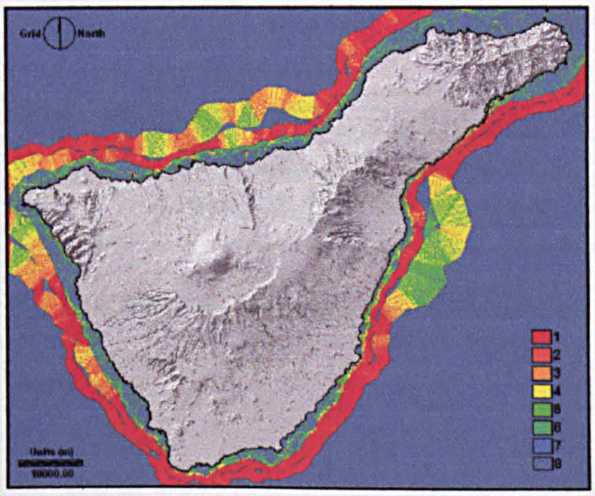

Fig. 4.41: Seabed slope suitability map.

4.4.3 Currents

Currents are very important for cage site selection because they control the water exchange rate, which is essential for replenishment of oxygen and removal of waste metabolites (Beveridge, 1996). Currents influence fish behaviour, affecting social hierarchies, growth and growth disparities among stock (Loverich, 1997). However, excessive currents impose additional dynamic loadings on the cage, supporting structures and moorings, may adversely affect fish behaviour, and contribute towards food losses (Huguenin, 1997).

The floating frame enclosures of some cages, are usually flexible or hinged, so strong currents can deform the waterplane area of these cages (Fig. 4.42) and compound the deformations of the netting enclosing the fish (Slaattelid, 1990). In addition, currents also influence the cage nets which are porous and highly flexible. These properties govern the flow pattern both within and around the fish farming structures, resulting in a deflection of the nets as shown in Fig. 4.43 (Løland, 1993).

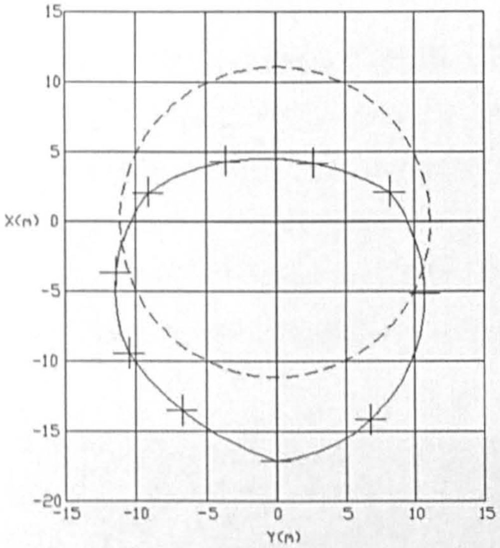

Fig. 4.42: Plot of the float ring (polyethylene tubes, PolarCirckel cages) with net in a 0.577 m/s current (Slaattelid, 1990).

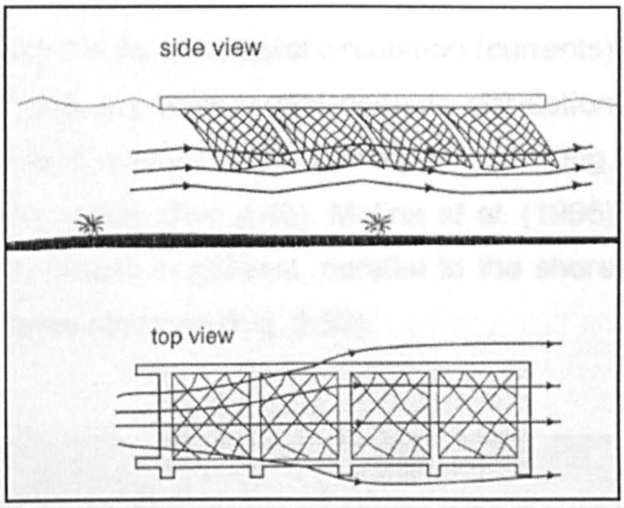

Fig. 4.43: Deflection of the net panels due to current (from Beveridge, 1996).

An important consequence of net deflection is the reduction of cage volume and disturbance of the fish behaviour (Aarsnes and Rudi, 1990). Generally the reduction of the available cage volume due to deflection of the nets in current can be shown to depend on the current velocity, bottom weights, drought of the cage and solidity factor of the nets (Aarsnes and Rudi, 1990). Tests by Aarsnes and Rudi (1990) concluded that up to 80% of the growing volume of a net pen can be lost in currents up to 1 m s^{-1}, even with large amounts of weight on the net bottom, and Table 4.14 shows an example of the reduction of the available cage volume when the freely hanging nets were exposed to current. The reduction of volume represents the averaged value for all six cages (three in each row in the current direction) although the front cage volume reduction will be significantly higher.

Table 4.14: Cage volume reduction under different current velocities and with different bottom weights (from Aarsnes and Rudi, 1990).

Current velocity	Bottom weight	Cage volume*	Reduction in %
0 m s^{-1}	-	12,000 m^3	-
0.25 m s^{-1}	100 kg	7,200 m^3	40
0.5 m s^{-1}	100 kg	3,400 m^3	72
1.0 m s^{-1}	100 kg	1,100 m^3	91
0.5 m s^{-1}	400 kg	6,600 m^3	45
1.0 m s^{-1}	400 kg	2,300 m^3	80

*Initial cage volume = 12,000 m^3

As mentioned earlier few studies have been done on coastal circulation (currents) in Tenerife and most of the available data are from global oceanic circulation studies (Fig. 4.44), from specific mesoscale studies of the Canary Current (Fig. 4.45), or from local studies of the Canary region (Fig. 4.46). Molina *et al.* (1996) suggested that coastal currents in Tenerife are, in general, parallel to the shore and circumnavigate the island in a clockwise direction (Fig. 2.53).

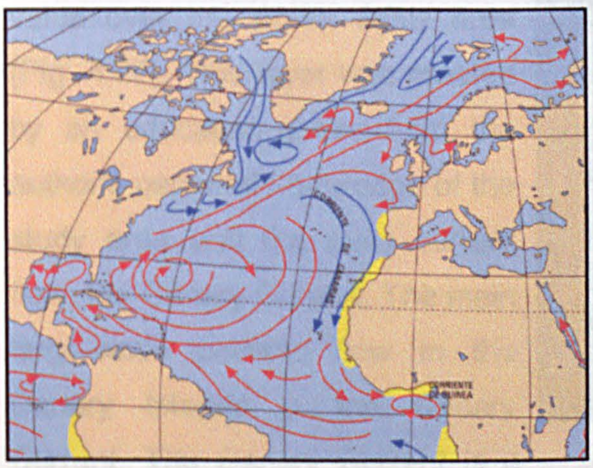

Fig. 4.44: North Atlantic current circulation system (from Morales-Matos and Pérez-González, 2000).

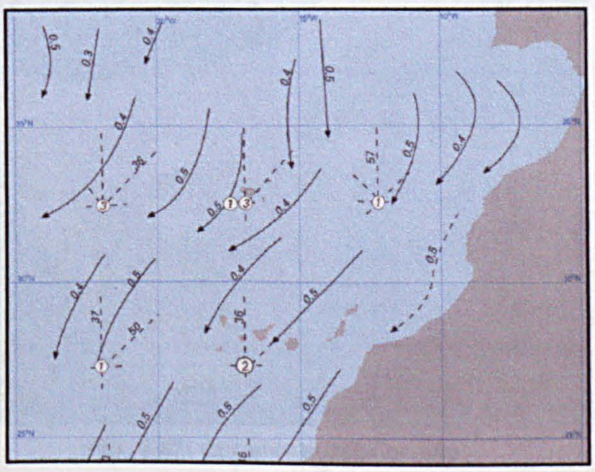

Fig. 4.45: USA Navy Pilot chart showing wind and current data (from Morales-Matos and Pérez-González, 2000).

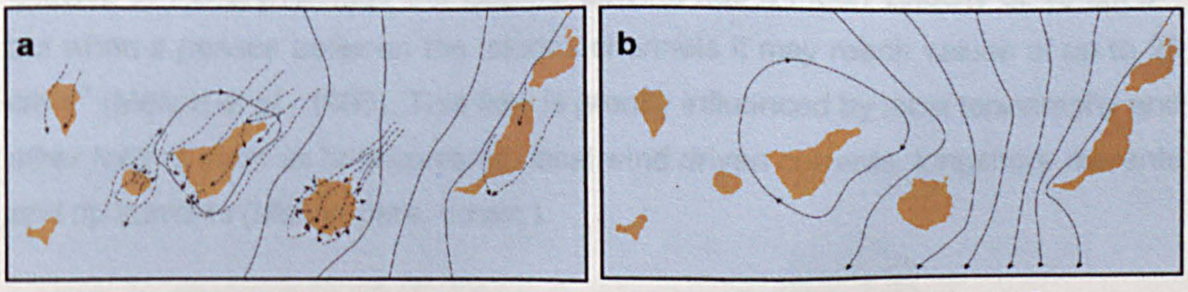

Fig. 4.46: Synthesis of the currents and winds (solid and dashed arrows respectively) in the Canary region during (a) summer and (b) winter (from Morales-Matos and Pérez-González, 2000).

Creating the suitability map for currents in Tenerife was a complicated task, as it is very difficult to recommend specific optimum current velocities for particular species because of the influences on cage design and stocking density. Capital cost of cages and moorings must increase with current velocity. While production can be increased at sites with high current velocities since stock rates can be increased. By contrast, beyond a certain point there will be unacceptable reductions in net volume and fish may have to expend excessive energy to maintain station, adversely affecting production (Aarsnes and Rudi, 1990). As a general rule of thumb, sites where currents exceed 1 m s^{-1} are not generally recommended (Aarsnes and Rudi, 1990; Beveridge, 1996). In addition, data on coastal currents in Tenerife are sparse, both in terms of direction and velocity. Despite this, currents were included in the model due to the great importance that this variable has for proper cage siting.

Currents were included as a variable with a constant suitability value over the whole study area (Fig. 4.47). This layer was created by an educated guess from the author's personal knowledge of the study area and the main current flow, the Canary Current. The main large-scale oceanic flow in the Canary Islands is the Canary Current. The Canary Current is a slightly cold surface current that flows in the SSW direction, and is stronger in the top 200 m (Fiekas *et al.*, 1992). Outside of the archipelago the Canary Current has a mean velocity of 15 cm s^{-1}, but when it passes between the islands channels it may reach values of up to 25 cm s^{-1} (Molina *et al.*, 1996). This flow is greatly influenced by local topography and other factors such as tidal currents, local wind driven currents, longshore currents and rip currents (Molina pers. comm.).

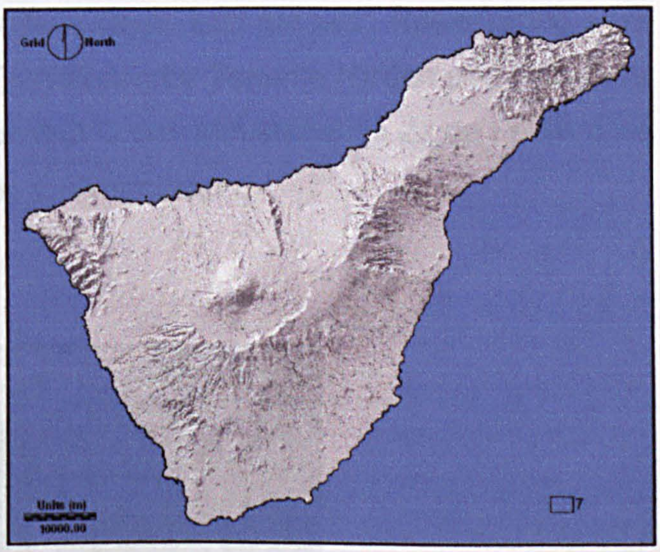

Fig. 4.47: Currents suitability map.

4.5 NAUTICAL SPORTS SUBMODEL

4.5.1 Diving (Scuba-diving and Under-water fishing)

The geographic location and conditions of Tenerife provide its waters with a varied wealth of fauna and flora, with a mix of species from the Mediterranean, the Atlantic and with other of distinctly tropical character. This characteristic along with the variety of sea beds makes Tenerife an ideal place for the practice of scuba-diving and underwater-fishing. Diving is very important attraction for tourism.

Baringo (1999) presented a detailed description of the most distinctive scuba-dive sites on Tenerife. The author used aerial photographs to show the precise location of the diving sites (Fig. 4.48). To incorporate this information into the GIS database, each photograph was scanned and georeferenced. Additional diving sites as proposed by Marín and Luengo (1998) were shipwrecked boats and sites catalogued as "*particular marine habitats, caves and tunnels*". Spearfishing sites were those delimited by the Spanish legislation for Tenerife (Orden de 30 Octubre de 1996; Direccion General de Pesca and Orden Ministerial de 22 de Febrero de 1988; Ministerio de Agricultura, Pesca y Alimentacion)

Fig. 4.48: Example of an aerial photograph used for diving sites location (from Baringo, 1999). The red and white flag shows the diving location.

A buffer zone was calculated around each diving sites and later reclassified using the threshold values shown in Table 4.15. Resulting suitability maps for each criteria are shown in Fig. 4.49, Fig. 4.50, Fig. 4.51 and Fig. 4.52.

Table 4.15: Distance threshold values (m) used for the four diving criteria.

Score / Criteria	8	7	6	5	4	3	2	1
Scuba-diving sites	>1400	1300-1400	1200-1300	1100-1200	1000-1100	750-1000	500-750	500
Particular habitats	>600	500-600	400-500	300-400	200-300	100-200	>0-100	0
Shipwrecked boats	>1400	1300-1400	1200-1300	1100-1200	1000-1100	750-1000	500-750	500
Spearfishing	>600	500-600	400-500	300-400	200-300	100-200	>0-100	0

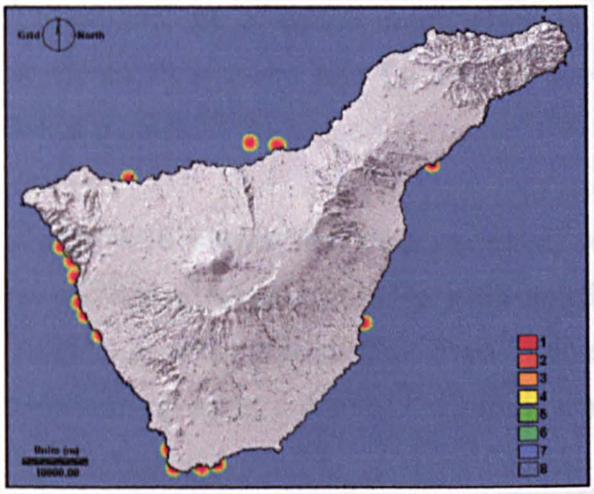

Fig. 4.49: Scuba-diving suitability map.

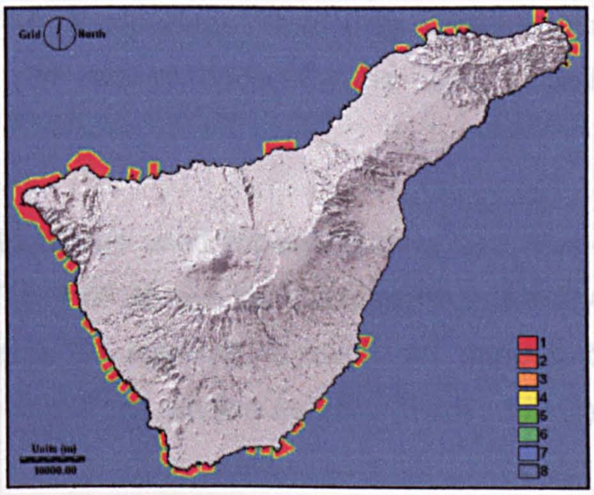

Fig. 4.50: Particular marine habitats, caves and tunnels suitability map.

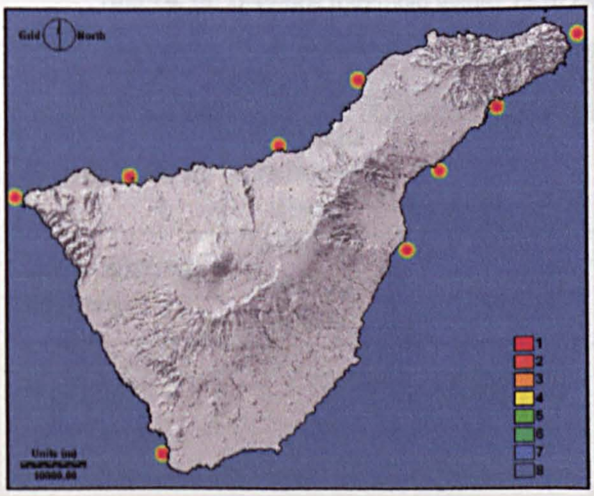

Fig. 4.51: Shipwrecked boats suitability map.

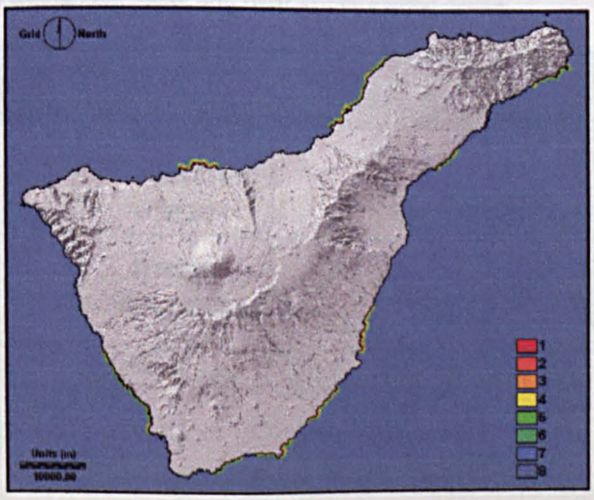

Fig. 4.52: Spearfishing suitability map.

4.5.2 Sailing (Windsurfing and Near-shore sailing)

The weather and the geographical location of Tenerife are ideal for sailing. The trade winds blow at a constant speed ranging from moderate to strong from the N-NE. The strongest winds are in the summer months as a result of a drop in temperature over the Sahara region. Sailing is a popular sport in Tenerife, practised by both locals and tourists and it is important for the tourism industry. Many tourists come to the island for its ideal sailing conditions. The most popular and important types of sailing are windsurfing and near-shore sailing.

El Medano is the most outstanding spot for windsurfing in Tenerife. In 1991, 92 and 93, it was the setting for the waves, slalom and course racing Grand Slam categories, all of which count towards the Windsurfing World Cup. Other spots such as El Cabezo and La Jaquita are also recommended for the highly skilled wind surfers.

Table 4.16 shows the distance threshold values used for windsurfing and near-shore sailing sites, while Fig. 4.53 and Fig. 4.54 shows their respective suitability maps. In the windsurfing map, because El Medano is such an important windsurfing spot, it was considered as a constraint, shown as zero (black colour) in the map.

Table 4.16: Distance threshold values used for windsurfing sites and near-shore sailing areas.

Score / Criteria	8	7	6	5	4	3	2	1
Windsurfing	Outside windsurfing areas				Inside Windsurfing areas			
Near-shore sailing	outside sailing areas				Inside sailing areas			

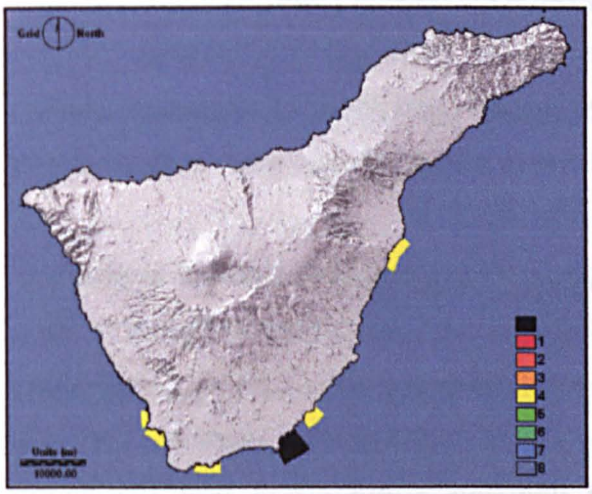

Fig. 4.53: Windsurfing suitability map.

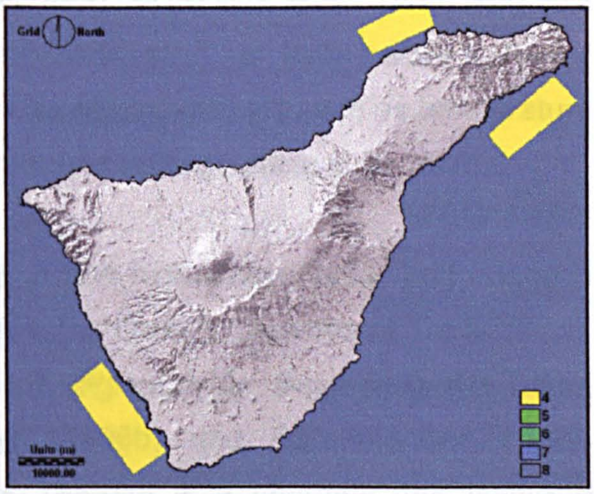

Fig. 4.54: Near-shore sailing suitability map.

4.6 WATER QUALITY SUBMODEL

Any material discharged into the sea inevitably causes some change in the environment. Such change may be great or small, long lasting or transient, wide spread or extremely localised. If the change can be detected and is regarded as damaging, it constitutes pollution (Clark, 1998). GESAMP (1991) defined marine pollution as "*the introduction by man, directly or indirectly, of substances or energy into the marine environment resulting in such deleterious effects as harm to living resources, hazards to human health, hindrance to marine activities including fishing, impairment of quality for use of sea water and reduction of amenities*". Cage culture requires good water quality, thus water properties strongly affect the choice of an aquaculture site. Pollution of various types can be responsible for high fish mortality in cage farming operations (Beveridge, 1996). Therefore, cages should be located in areas uncontaminated by industrial, municipal and agricultural pollutants. Water quality parameters, such as temperature, pH, nitrogenous compounds, dissolved oxygen, etc. should be within the ranges that provide life support and growth for the cultured species.

Among all possible aquaculture water quality parameters (Lawson, 1995), only the most significant parameters that influences cage culture development in Tenerife were reviewed. Due to the conservative and oligotrophic nature of the marine environment, water quality variables such as dissolved oxygen, total alkalinity, total hardness, pH, nitrogenous compounds, hydrogen sulphide are of no concern.

Salinity, which remains almost constant at 36-37 ‰ (Molina *et al.*, 1996) also was not considered. On the other hand, pollutants such as hydrocarbons, heavy metals, sewage and pesticides, and water quality parameters such as temperature and turbidity, were considered for their influence on cage siting in Tenerife.

Tenerife is located in a geographical region with high tanker traffic, and hence is subject to hydrocarbon pollution. In addition, the Canary Current and Trade Winds could bring in this pollutant even when it originates far away from the island coasts. However, Peña-Mendez *et al.* (1996b) and Peña-Mendez (1999) concluded that hydrocarbon pollution in Tenerife is a sporadic and localised phenomenon, and hence, it is not a potential threat to cage culture.

Despite the great concern regarding the effects of heavy metals on aquatic life and organisms higher in the food chain, there have been very few studies on heavy metals in the coastal areas around Tenerife. Díaz *et al.* (1990) conducted a study in the coastal waters around Santa Cruz de Tenerife city, which is considered to be the most polluted area of the island due to the presence of a major harbour, a refining plant and high sewage discharges. Trace metal concentrations are presented in Table 4.17. The authors concluded that, although the presence of heavy metals in this area might be the highest in the island, the waters were not polluted in their opinion.

Table 4.17: Statistical parameters for the concentration (ppb) of several heavy metals for overall samples (480) of 15 sampling stations in Santa Cruz de Tenerife coast (from Díaz *et al.* 1990)

	Hg	Pb	Cd	Fe	Ni	Cu	Zn
Mean	2.88	3.70	0.17	52.29	2.85	7.46	10.69
Min.	0.10	0.20	0.07	4.54	0.50	0.40	0.40
Max.	90.00	116.88	1.60	506.25	13.67	173.35	110.90

Many of the insecticides and herbicides routinely used on agronomic crops are toxic to fish (Lawson, 1995; Beveridge, 1996). Polychlorinated biphenyls (PCBs) compounds can be taken up by fish via the water and bioaccumulate through the food chain. Peña-Mendez *et al.* (1996a) determined the content of seven individual PCB congeners in specimens of a marine winkle (*Ossilinus atratus*) and of limpets (*Patella ullisiponensis aspera*) in Tenerife. The seven congeners determined were chosen because they serve as an indicator of PCB contamination, and their quantification can be used to determine whether PCB levels in food products and environmental samples comply with the maximum levels permitted by legislation. The authors concluded that in the coastal areas of Tenerife the seven PCB congeners were present at low levels and most were undetectable. No significant differences where found between sampling sites along the coast. Therefore, it can be concluded that PCB contamination in Tenerife coastal environments is not currently a problem. This conclusion was corroborated by Diaz-Diaz *et al.* (1998), who noted that because farm land slopes are shallow and the infiltration rates are high in Tenerife, pesticides do not runoff, but will leach into the groundwater instead.

On the other hand, water quality variables identified as major factors influencing cage culture siting in Tenerife are risk of diseases (sewage), suspended solids (runoff and sewage) and temperature.

4.6.1 Sewage

Sewage discharges could be hazardous for cage culture. Domestic outfalls is principally organic but also contains considerable amounts of metals, oils and grease, detergents, and industrial wastes, as well as pathogens. All human sewage contains enteric bacteria, pathogens, viruses, and intestinal parasitic eggs. It was previously believed that pathogenic bacteria and viruses did not survive in seawater. However, it has been shown that bacteria may enter a dormant phase which cannot be detected by routine culture methods and viruses can be very persistent in seawater (Clark, 1998). Seafood organisms that are not filter feeders, such as most crustaceans and fish, do not accumulate pathogens from sewage-contaminated water and do not represent a direct health risk from this source. However, poor environmental conditions (from sewage dumps) may lead to fish stress, causing physiological or metabolic changes in the fish which may increase its sensitivity to the pollutants (Hedrick, 1998). The health of cultured fish, which are already under stress, may be affected by this source of pollution increasing mortalities and reducing profits. The worst cage farm sites from a disease risk point of view are those in which pathogenic or potentially pathogenic organism are endemic prior to the establishment of the farm and sites where disease organisms are likely to thrive following the establishment of a farm. Therefore, as Beveridge (1996) stated that sewage-polluted sites should be avoided completely.

In Tenerife, managers and regulators have tried to apply a "realistic" approach to sewage treatment and disposal by choosing appropriate systems based on the littoral characteristics of the marine environment. These rely on massive dilution using marine sewage pipes, instead of building and running costly installations with capacity for secondary treatment of sewage (secondary treatment is used to reduce the BOD_5, COD and total suspended solids to at least 70%, 75% and 90% respectively). This approach is in concordance with the latest EC guidelines for treatment of sewage waters, which introduced the concept of "*less sensitive areas*" in which sewage discharges will have little impact due to specific environmental characteristics. In Tenerife, the whole coast line has been catalogued as "less sensitive" (CIATFE, 1991). For this type of areas, sewage pipes are considered adequate, and only primary treatment (reduction of the BOD_5 and total suspended solids to at least 20% and 50% respectively) is necessary before discharge the sewage into the sea (CIATFE, 1991).

Despite this, Tenerife's sanitation system still has some deficiencies such as, insufficient sanitation network, inadequate sewage treatment, and insufficient and poorly planed sewage pipelines. Only 56% of the population is connected to a sanitation network (Fig. 4.55), although the legislation clearly specifies that any direct discharge of sewage to the sea is forbidden (CIATFE, 1991). The legislation also specifies that every sewage discharge must be treated (at least with primary treatment) before discharge. Regardless of this, discharges made into the sea are in some cases inadequately treated (CIATFE, 1991). In attempts to resolve this situation, there has been numerous constructions of small scale sewage treatment plants on the island. Fig. 4.56 shows the distribution of these small installations.

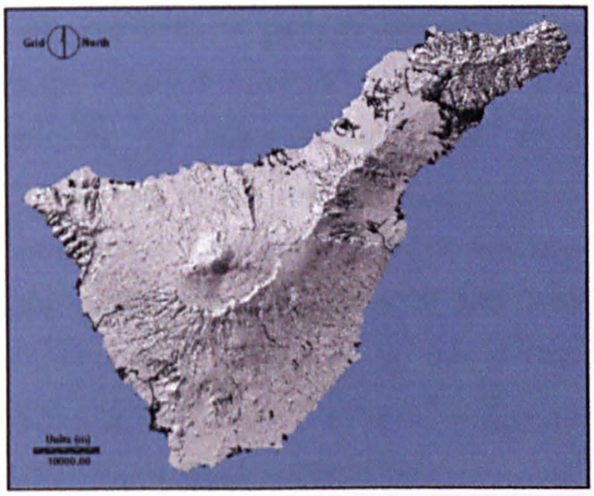

Fig. 4.55: Sanitation network in Tenerife (information obtained from CD-Map, 1999).

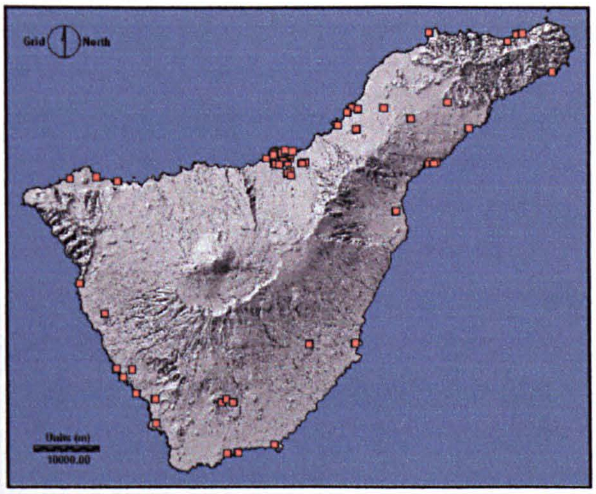

Fig. 4.56: Small scale sewage treatment plants in Tenerife (information obtained from CD-Map, 1999).

CIATFE (1991) reported that sewage pipelines in Tenerife are insufficient. Some pipelines are out of order and others do not meet the minimum requirements established by the legislation. Hence, more units are needed, together with an increase of capacity in many of the existing pipelines. The Spanish legislation for sewage pipes (BOE, 1993) established two important criteria, (1) the minimum distance between the coast line at neap tide and the discharge point must be 500 m and (2), the initial dilution of the outfall must be greater than 100:1. Fig. 4.57 shows the location of the 36 sewage pipes in Tenerife. Only 3 sewage pipelines from the 36 existing meet these requirement in Tenerife (CIATFE, 1991).

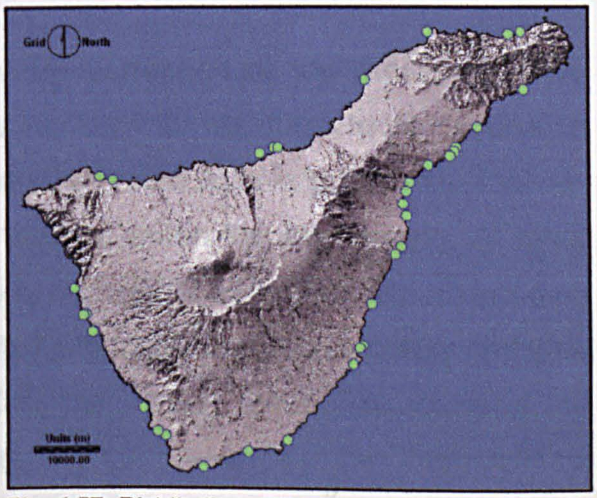

Fig. 4.57: Distribution of the sewage pipes in Tenerife (information obtained from CD-Map, 1999).

Unfortunately, there are no direct measurements of the quantity or quality of sewage discharges in the island. So, to quantify the suitability of cage culture in areas close to sewage discharges, three factors were used to characterise a sewage outfall, they are: (1) the number of people connected to each sewage pipeline system, (2) the presence or absence of any treatment before the sewage is dumped, and (3) the depth of the discharge.

The number of people connected to each pipeline network determines the quantity of sewage that each pipe discharges to the sea and thus (criteria "population" was determined by using a population map for each of the 743 districts (Fig. 4.58) and by the ISTAC (Canary Institute of Statistics) web page (http://www.istac.rcanaria.es/) in conjunction with the sanitation network (Fig. 4.55 and Fig. 4.57).

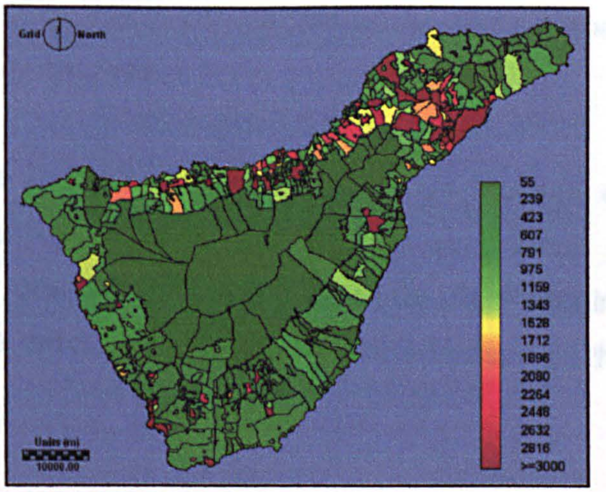

Fig. 4.58: Population map, number of people per district (information obtained from CD-Map, 1996 and ISTAC).

The presence or absence of any treatment prior to discharge, will determine the hazardousness of the discharge. This was determined by using a map that shows the location of the sewage treatment plants (Fig. 4.56) and their connection to the sanitation network (Fig. 4.55 and Fig. 4.57).

The depth of the sewage dump will provide information on the likelihood of the dump to reach surface, and also the time available for the dump to dilute (dilution factor) before it reaches the surface. When the mixed layer is sufficiently shallow, the plumes from the sewer outfalls are trapped within the thermocline. At other times, the mixed layer is sufficiently deep or it does not exist at all and no trapping occurs. Under such conditions, some portions of the plumes undoubtedly find their way to the surface. As highlighted earlier, the marine thermal structure of the superficial layer in Tenerife is characterised by the presence of two thermoclines; the *seasonal thermocline*, which is superficial and variable in its form and magnitude over the year and the *permanent thermocline*, which is more deep and stable. The depth of the seasonal thermocline varies throughout the year, reaching a maximum of about 100 m in mid-summer, and reducing to 15 m during winter and early spring. The permanent thermocline is normally located between 600 and 800 m, however, because it is very weak, it is usually masked by the intrusion of Mediterranean waters (de-Armas pers. comm.). The depth of discharge of each pipe was determined by combination of the sewage-pipe layer

(Fig. 4.57) and the bathymetric map (Fig. 4.35). Discharges above the seasonal thermocline were considered potentially dangerous.

Once the three thematic maps were created, further manipulation focused on dividing the 36 existing sewage pipelines into four groups of importance to determine which sewage pipelines present a higher threat to fish farming development. Each of the three criteria described above were scored based on the thresholds shown in Table 4.18.

Table 4.18: Threshold values used for each criterion.

Criteria \ Score	4	3	2	1
Population (number of people)	< 2,000	2,000-5,000	5,000-10,000	> 10,000
Sewage treatment	Treatment			No treatment
Depth (m)	>40	30-40	20-30	<20

The relative weights of importance were calculated by using the pairwise matrix shown in Table 4.19. It was considered that sewage treatment prior to discharge is the most important variable, followed by the number of people connected to the sewage (population), and finally the depth of the discharge (Telfer pers. comm.). The consistency ratio (CR) was less than 0.1, and therefore, acceptable.

Table 4.19: Pairwise comparisons of criteria in the sewage submodel.

	Population	Treatment	Depth
Population	1		
Treatment	2	1	
Depth	1/2	1/3	1

CR= 0.01

Calculated weights were used in a MCE to combine the 3 criteria as shown in Fig. 4.59. The output from MCE was a classification of the pipelines into 4 categories according to their potential threat for cage aquaculture development. Four sewage pipes were included in category 1 (highest threat), twenty one in category 2, seven in category 3 and four in category 4 (lowest threat).

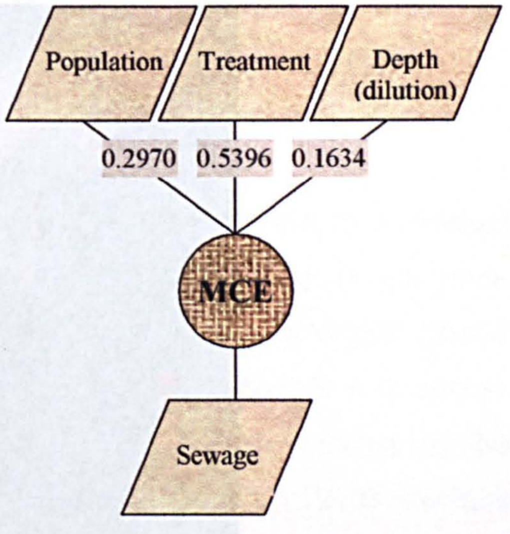

Fig. 4.59: Sewage MCE model showing the criteria used and calculated weights.

Buffer distances from each of the four groups of sewage pipes were calculated (DISTANCE module within IDRISI32), and reclassified (RECLASS module) according to the distance threshold values shown in Table 4.20. Fig. 4.60 shows the sewage suitability map created from this model.

Table 4.20: Sewage distance threshold values (m) used for each sewage category.

Category \ Score	8	7	6	5	4	3	2	1
Distance to Sewage-1	>1700	1500-1700	1300-1500	1100-1300	900-1100	700-900	500-700	<500
Distance to Sewage-2	>1300	1150-1300	1000-1150	850-1000	700-850	550-700	400-550	<400
Distance to Sewage-3	>900	800-900	700-800	600-700	500-600	400-500	300-400	<300
Distance to Sewage-4	>500	450-500	400-450	350-400	300-350	250-300	200-250	<200

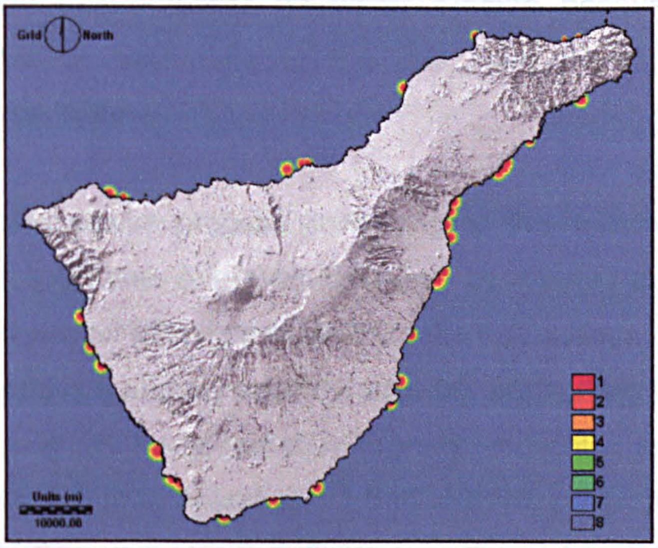

Fig. 4.60: Sewage suitability map.

4.6.2 Suspended Solids (Runoff Sediments)

Turbidity produced by dissolved and suspended substances, such as clay particles, humic substances, silt, plankton, etc. can affect fish (Lawson, 1995). Due to the oligotrophic nature of the waters in Tenerife, the major source of turbidity comes from sporadic runoff episodes. Excessive runoffs from the surrounding watersheds can often cause clay and silt loads to exceed tolerable limits for farmed animals. These particles can clog the gills of small fish and/or stress bigger fish. Turbidity at sufficiently high concentrations can cause gill damage and may trigger diseases as a result of fish stress.

Soil erosion is the process of dislodgement and transportation of soil particles by wind and water. Climate, topography, soil characteristics, vegetation cover, and land use all affect soil erosion (Brooks *et al.*, 1991). The factors controlling soil erosion are the erosivity of the eroding agent, the erodibility of the soil, the slope of the land and the nature of the plant cover (Morgan, 1995). Erodibility defines the resistance of the soil to both detachment and transport. Although a soil's resistance to erosion depends in part on topographic position, slope steepness and the amount of disturbance, the properties of the soil are the most important determinants. Erodibility varies with soil texture, aggregate stability, shear strength, infiltration capacity and organic and chemical content. For a greater and more comprehensive description of these factors and processes, refer to Morgan

(1995). This study only focused on water erosion because it is the main contributing source of sediments to the sea, and therefore influences the development of cage culture.

Soil erosion is a two-phase process consisting of the detachment of individual particles from the soil mass and their transport by erosive agents, in this case runoffs. The dislodgement of soil particles from the soil surface by energy imparted from falling raindrops is a primary agent of erosion, particularly in soils with sparse vegetation cover, such as those found in Tenerife. Individual soil particles can be splashed more than 0.5 m in height and 1.5 m sideways (Morgan, 1995). Surface runoff, or overland flow, is water that flows over the soil surface and occur from areas that are impervious, locally saturated, or areas where the rainfall rate exceeds the infiltration capacity of the soil. The potential runoff erosion depends upon the volume of running water and its velocity. The momentum that can be gained by surface runoff on a slopping area, and consequently, the amount of soil that can be lost from the area depends upon both the inclination and the length of unobstructed slope. As the length of the slope increases, soil loss per unit length is initially accelerated, but it then approaches a constant rate. However soil loss increases with the inclination of the slope. Slope angle and slope length that allow the build-up in momentum of flowing water are major factors in accelerating rill erosion, the steeper and longer the slope the greater the erosion. Once it becomes canalised, uncontrolled surface runoff is capable of creating spectacular gully erosion. Gullies are common features of sparsely vegetated land like the southern region of Tenerife (Rodriguez *et al.*, 1993). In addition, factors such as soils with inherently low permeability and sites where denudation of vegetation is likely, increases the susceptibility to soil loss.

The integration of GIS with hydrological modelling is increasingly facilitating design, calibration, modification and comparison of models. Zhang *et al.* (1990) and Schultz (1993) presented overviews of hydrological modelling with GIS, and De Vantier and Feldman (1993) reviewed GIS applications in hydrological modelling, with particular reference to rainfall-runoff models, flood-plain management and forecasting, erosion prediction and control, water quality prediction and control, and drainage utility implementation. Several procedures have been implemented to integrate databases and geographic information in an effort to characterize the spatial distribution of the risk of soil erosion by water. Although process-based erosion prediction models are being developed to replace empirically based models, the Universal Soil Loss Equation (USLE) is still by far the most widely used method for soil loss prediction (Penning de Vries *et al.*, 1998). The Revised Universal Soil Loss Equation (RUSLE) for rangelands has also been successfully interfaced with GIS.

Of the methods available, the Universal Soil Loss Equation (USLE) is perhaps the most widely applied of the empirical approaches for soil loss estimation in which predictive equations are developed from analyses of source data (Kertész, 1993). The USLE is based on empirical and morphometric data and has the form:

$$A = R * K * (LS) * C * P \qquad \textbf{Eq. 4.10}$$

where;

A = soil loss in tons per unit area

R = a rainfall erosivity factor for a specific area, usually expressed in terms of average erosion index (EI) units

K = a soil erodibility factor for a specific soil horizon

LS = topographic factor, a combined dimensionless factor for slope length and slope gradient, where L is expressed as the ratio of soil loss from a given slope length to soil loss from a 72.6 ft length under the same conditions (it is not the actual slope length), and S is expressed as the ratio of soil loss from a given slope steepness to soil loss from a 9% slope under the same conditions (is not the actual slope steepness).

C = a dimensionless cropping management factor, expressed as a ratio of soil loss from the condition of interest to soil loss from tilled continuous fallow (condition under which K is determined)

P = an erosion control practice factor, expressed as a ratio of the soil loss with the practices (for example, contouring, strip cropping, or terracing) to soil loss with farming up and down the slope.

The basic USLE equation provides an estimate of sheet and rill erosion from rainfall events in upland areas. It does not include erosion from streambanks, snowmelt, or wind, and it does not include eroded sediment that is deposited at the base of slopes and at other reduced-flow locations before runoff reaches the streams or reservoirs.

The cropping management factor (C) and the erosion control practice factor (P) used in the USLE have been replaced by a vegetation management factor (VM) to form the Modified Soil Loss Equation:

$$A = R\,K\,(LS)\,(VM) \qquad \text{Eq. 4.11}$$

Both the USLE and MUSLE require an estimated value for R. R depends upon the rainfall intensity in each rainfall intensity period of the storm. Williams (1975) and Williams and Berndt (1977) modified the USLE by replacing R with a runoff factor. The modification is based on the assumption that the total discharge and peak discharge rate resulting from a storm on the watershed depends upon the duration, amount and intensity of the storm. The equation was developed to estimate sediment yield at the outlet of a watershed directly, rather than soil loss, on a storm by storm basis. The modified equation is:

$$Y_s = 11.8\,(V\,q_p)^{0.56}\,K\,C\,P\,(LS) \qquad \text{Eq. 4.12}$$

where;

Y_s = sediment yield (tons)
V = volume of storm runoff (m^3)
q_p = peak flow rate ($m^3\,s^{-1}$)
$K\,C\,P\,(LS)$ = as defined in the USLE

This equation was developed as a GIS model by creating a thematic map layer for each variable from the MUSLE equation. The detailed establishment of each layer is described below. This made it possible to calculate the soil loss for each individual grid cell. Finally the module DISTANCE was used to measure distances from the stream mouths, and then to reclassify the sediment yields according to their suitability for cage culture development.

4.6.2.1 Storm Runoff (V)

The major runoff discharging points in Tenerife are relatively well known (Fig. 4.61), however, associated inputs from runoffs to the sea are unknown both in space and time. To be able to estimate runoff discharges it is necessary to have a clear knowledge of the surface hydrology of the island, as well the complete hydrologic cycle (precipitation, evapotranspiration, infiltration and runoff) (Brooks *et al.*, 1991). Various processes and pathways determine how excess water becomes stream flow. Excess water represents the portion of total precipitation that runs off the land surface plus that which drains from the soil and thus is neither consumed by evapotranspiration nor leaked into deep groundwater. In this study only surface runoffs were considered to contribute to excess water. This assumption was justified by the special characteristics of Tenerife, a semi-arid region and with very porous rocks. Therefore, it was assumed that all infiltrated water moves downwards to the aquifer (Rodriguez *et al.*, 1993; Díaz-Díaz *et al.*, 1998).

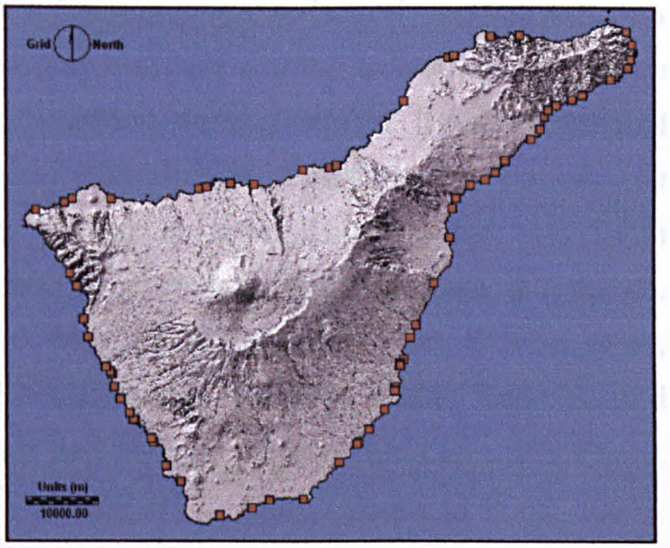

Fig. 4.61: Major runoff-discharging points (information obtained from CD-Map, 1999 and Tenerife's topographic map 1:100,000)

To select the appropriate procedure for estimating runoff, the scope, complexity of the problem and the acceptable level of error must be considered. It is important to bear in mind that runoff is a dependent variable which is a function of rainfall and the catchment characteristics, and the transformation of rainfall into runoff is a complex non-linear process (Kumar and Das, 1998). The Thornthwaite and Mather (1957) hydrological model has been reported as the most accurate method (Heyman and Kjerfve, 1999), and therefore, the most desirable to use. However, the lack of available data for Tenerife constrained its use, and a simplified method, the NRCS Runoff Curve Number method, for estimating direct runoff from storm rainfall was used instead. These procedures are only applicable in small watersheds, as is the case in Tenerife.

NRCS RUNOFF CURVE NUMBER (CN) METHOD

Values for runoff (*V*) came from the NRCS Runoff Curve Number method (USDA-SCS, 1986). A relationship between accumulated rainfall and accumulated runoff was derived from experimental plots for numerous soils and vegetation cover conditions. The equation was developed mainly for small watersheds for which only daily rainfall and watershed data are ordinarily available. It was developed from recorded storm data that included total amount of rainfall in a calendar day (P_{24}) but not its distribution with respect to time. This method has been successfully integrated into GIS-based modelling by many authors (Hill *et al.*, 1987; DeBarry and Carrington, 1990; Muzik and Pomeroy, 1990; Stuebe *et al.*, 1990; DeBarry and Paul, 1991; Sasowsky and Gardner, 1991; Schmidt and Romack, 1991; Muzik, 1992; Warwick and Hanees, 1994; Manguerra and Engel, 1998; Olivera and Maidment, 1998; Theriault *et al.*, 1999; Udouj and Scott, 1999). The NRCS runoff equation is:

$$Q = \frac{(P - 0.2S)^2}{(P + 0.8S)} \qquad \textbf{Eq. 4.13}$$

where:

Q = runoff (inches)
P = rainfall (inches) 24-hour period (P_{24})
S = potential maximum retention after runoff begins (inches)

S is mainly the infiltration occurring after runoff begins. This later infiltration is controlled by the rate of infiltration at the soil surface or by the rate of transmission in the soil profile or by the water-storage capacity of the profile, whichever is the limiting factor. S is related to the soil and cover conditions of the watershed through the CN. CN has a range of 0 to 100, and S is related to CN by Eq. 4.14. When CN and the amount of rainfall have been determined for the watershed, runoff can be determined using Eq. 4.14 and Eq. 4.13.

$$S = \frac{1000}{CN} - 10 \qquad \textbf{Eq. 4.14}$$

The major factors that determine CN are the hydrologic soil group (HSG), cover type, treatment and hydrologic condition. CNs in Appendix I (Tables 1 to 4) represent average previous runoff conditions for urban, cultivated agricultural, other agricultural, and arid and semi-arid rangeland uses.

HYDROLOGIC SOIL GROUPS

Infiltration rates of soils vary widely and are affected by subsurface permeability as well as surface intake rates. USDA-SCS (1986) classified soils into hydrologic soil groups (HSGs) to indicate the minimum rate of infiltration obtained for bare soil after prolonged wetting. The HSGs, A, B, C, and D, and their properties are presented in Table 4.21.

If infiltration rates cannot be directly measured, determination of the HSG can be assessed based on soil texture as indicated in Table 4.21. The approach used for the extrapolation of soil properties over large regional areas depended upon the assumption that soil of similar taxonomy would be similar in their properties. With this assumption in place, average values for a given soil property can be determined for a specific taxonomic category and then applied whenever that category is found in the region of interest (Loague, 1991; 1994). SCS (1972) provides a list of the most common soils and their group classification.

Table 4.21: Hydrologic soil groups classification by properties (from **USDA-SCS, 1986**)

HSG	*Infiltration (cm/hr)*	*Runoff*	*Soil textures*
A	>0.76	low	Sand, loamy sand, or sandy loam
B	0.38 - 0.76	moderate	Silt loam or loam
C	0.13 - 0.38	high	Sandy clay loam
D	0 - 0.13	very high	Clay loam, silty clay loam, sandy clay, silty clay, or clay

Fig. 4.62 shows the soil order map for Tenerife (from Diaz-Diaz *et al.*, 1998). This map was created based on three sources of information; (i) the existing soil map for Tenerife (Fernadez-Caldas *et al.*, 1982), (ii) additional soil information for the island (Departamento de Edafgología y Geología) and (iii) new field data (Diaz-Diaz, 1996). There is presently no more detailed information available on soil

classification, although, for a study of this type it would be desirable to have at least to suborder level (Diaz-Diaz pers. comm.).

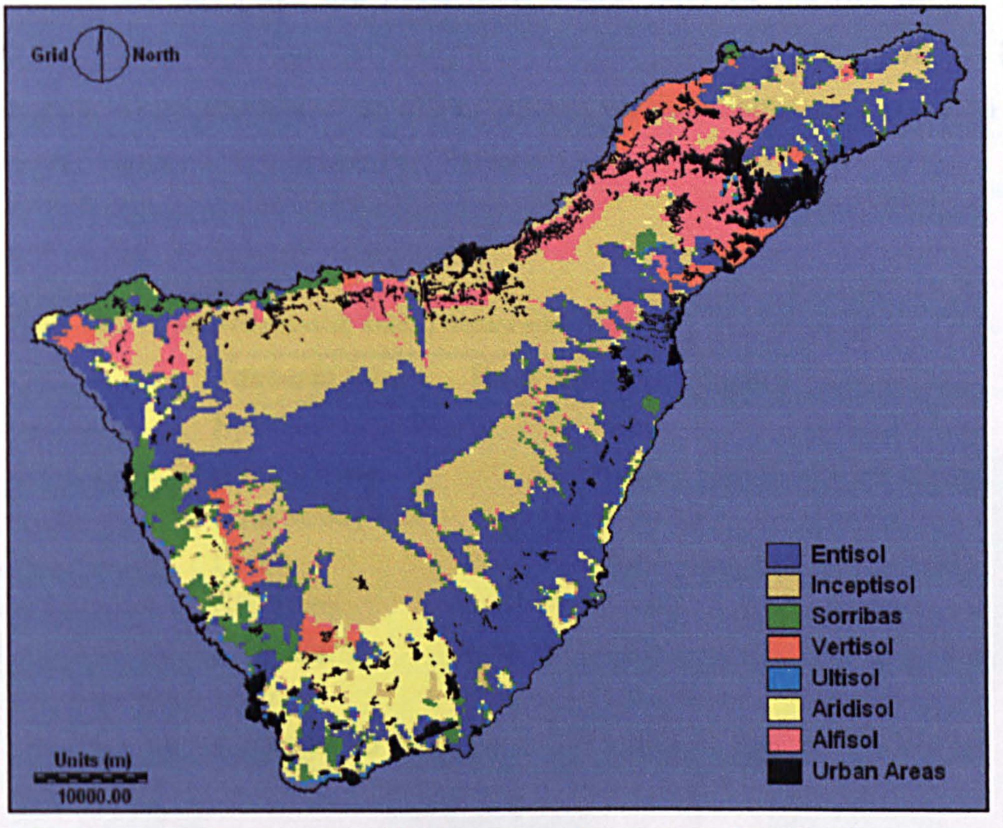

Fig. 4.62: Soil orders; Sorribas are an artificial soil used for agriculture (from Diaz-Diaz *et al.*, 1998).

Because the SCS (1973) soil classification does not take into account the soil orders, the hydrologic soil groups were estimated by using the soil texture. Although Rodriguez *et al.* (1993) presented data on soil texture, it is based on mean samples for the Canary Archipelago and does not cover all soil orders. Consequently, an alternative method of relating bulk density to texture was used to classify Tenerife's soil orders into the hydrological soil groups. Bulk density is the weight of a unit volume of dry soil and is dependent on the spaces (pores) in the sample, how tightly they are packed, and also the composition of the solid material. Normally, a soil sample will have a mixture of sand, silt, clay, and organic material, so its bulk density will depend on the proportion of each of these components in the sample, and how tightly they are packed. Sandy soils have large pore spaces, because sand grains are large. By contrast, silty soils have smaller particles with smaller pore spaces, but there is more total empty space in a silty soil than in a sandy soil. In general, clay soils, are considered to have good soil structure, and have a greater amount of pore spaces due to the small particle sizes. They will most likely have a lower bulk density than sandy or silty soils. Organic soils usually have the most pore space, and as the dry weight of the organic material is less than the weight of mineral particles, they have the lowest bulk density. The Hausenbuiller (1985) general relationship was used to relate bulk density values with soil texture (Table 4.22).

Table 4.22: General relationship among texture and bulk density (from Hausenbuiller, 1985).

Textural Class	Bulk Density (Mg/m^3)
Sand	1.55
Sandy loam	1.40
Fine sandy loam	1.30
Loam	1.20
Silt loam	1.15
Clay loam	1.10
Clay	1.05
Aggregated clay	1.00

The bulk density values for each soil order was obtained from Diaz-Diaz *et al.* (1998) and shown in Table 4.23 from which the soil texture could be classified by reference to Table 4.22. The hydrologic soil groups were then assigned to each texture class by the use of Table 4.21.

Table 4.23: Average bulk density values for soil orders in Tenerife (from Diaz-Diaz *et al.*, 1998), associated textural class and hydrological soil group.

	Soil order						
	Alfisols	**Aridisols**	**Entisols**	**Inceptisols**	**Sorribas**	**Ultisols**	**Vertisols**
Bulk density (Mg m^{-3})	1.125	1.063	0.897	0.688	0.894	0.729	1.210
Texture	Silt loam	Clay loam	Aggregated Clay	Aggregated Clay	Aggregated Clay	Aggregated Clay	Fine sandy loam
HSG	B	D	D	D	D	D	A

Initially, the hydrologic soil groups from Table 4.23 were used for the runoff calculations. However, the database field verification done for soil texture, as explained in Chapter 3 (Section 3.8), suggested the use of bulk density as a proxy data for soil texture in Tenerife was inadequate. Therefore, the soil texture classes for each soil order was estimated as follows.

During the April 2001 field trip 32 soil samples were collected (Fig. 4.63) and analysed in triplicates) using the manipulative and bottle tests (refer to section 3.8.5).

Fig. 4.63: Examples of soil samples from the April 2001 field trip to Tenerife.

Fig. 3.12 shows the spatial distribution of the 32 sampling points taken. The mean values of the triplicates (percentage of sand, silt and clay) were used to estimate the soil texture using a soil texture classification diagram (Fig. 4.64). Table 4.24 shows the estimated percentages of sand, silt clay, organic matter, the textural classes and hydrologic soil groups from the bottle test, and the textural classes and hydrologic soil groups from the manipulative test for each of the 32 soil samples.

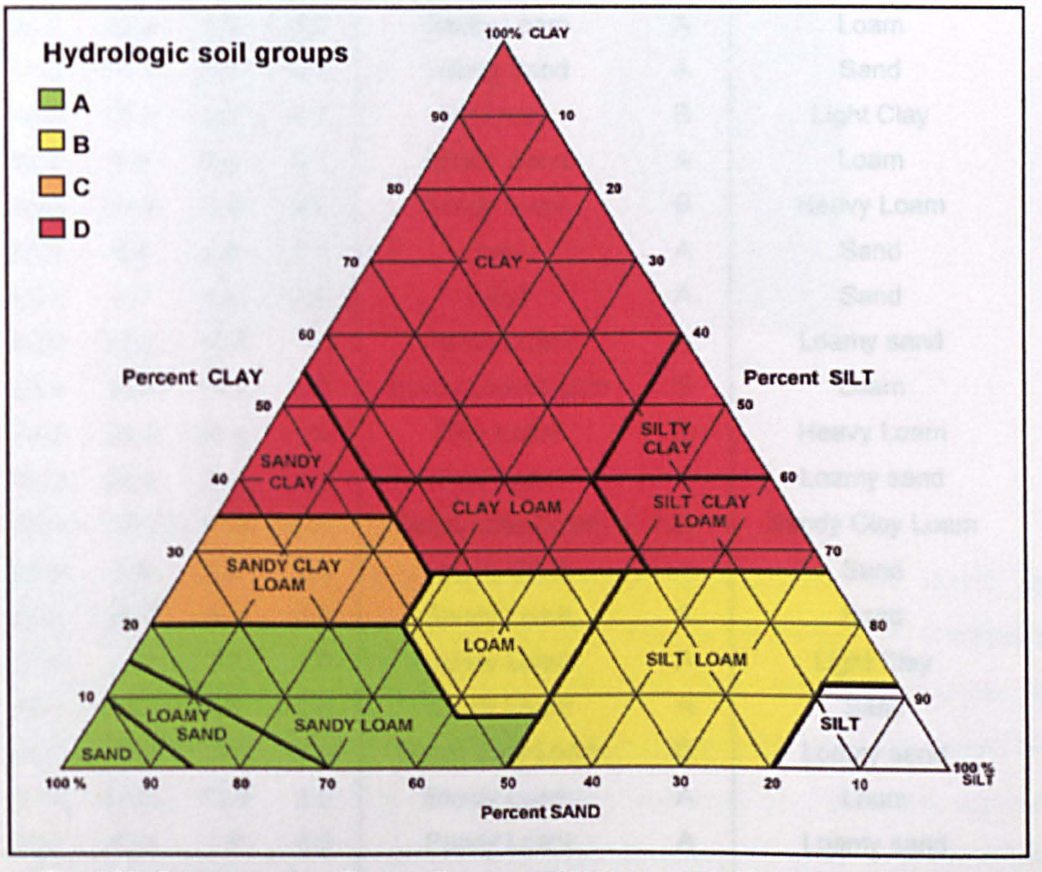

Fig. 4.64: Soil texture classification diagram and their associated hydrologic soil groups.

Table 4.24: Results from the soil sampling test (bottle and manipulative) and their associated hydrological soil groups (HSG).

ID	% Sand	% Silt	% Clay	% O. M.	Texture from bottle test	HSG	Texture from manipulative test	HSG
1	78.6	8.2	4.1	9.0	Sandy Loam	A	Sandy Loam	A
2	35.1	58.2	6.4	0.4	Silt Loam	B	Light Clay	D
3	66.5	30.3	3.0	0.2	Sandy Loam	A	Sandy Loam	A
4	82.3	12.7	5.0	0.0	Loamy Sand	A	Loamy sand	A
5	59.5	18.2	20.3	2.0	Sandy Clay Loam	C	Loamy sand	A
6	64.3	23.7	4.1	8.0	Sandy Loam	A	Sandy Loam	A
7	65.5	22.9	9.1	2.5	Sandy Loam	A	Heavy Loam	A
8	50.6	27.0	22.1	0.2	Sandy Clay Loam	C	Light Clay	C
9	69.5	24.3	6.1	0.1	Sandy Loam	A	Heavy Loam	B
10	55.8	40.2	1.0	3.0	Sandy Loam	A	Loam	B
11	77.3	21.3	1.3	0.1	Loamy Sand	A	Sand	A
12	42.4	55.2	2.3	0.1	Silt Loam	B	Light Clay	B
13	83.8	9.3	6.8	0.1	Loamy Sand	A	Loam	B
14	50.8	36.9	3.3	9.0	Sandy Loam	B	Heavy Loam	B
15	87.6	9.8	2.6	0.1	Sand	A	Sand	A
16	90.7	4.7	1.1	3.5	Sand	A	Sand	A
17	62.6	22.2	13.7	1.5	Sandy Loam	A	Loamy sand	A
18	53.4	30.4	15.2	1.0	Sandy Loam/Loam	B	Loam	B
19	40.9	22.3	33.8	3.0	Clay Loam	D	Heavy Loam	B
20	45.9	24.3	29.7	0.1	Clay Loam	D	Loamy sand	A
21	55.1	27.0	17.8	0.0	Sandy Clay Loam	C	Sandy Clay Loam	C
22	88.8	7.8	1.4	2.0	Loamy Sand	A	Sand	A
23	65.1	28.7	5.2	1.0	Sandy Loam	A	Sand	A
24	67.9	27.4	3.7	1.0	Sandy Loam	A	Light Clay	D
25	64.1	29.1	5.8	1.0	sandy Loam	A	Sand	A
26	48.1	24.4	22.5	5.0	Sandy Clay Loam	C	Loamy sand	A
27	61.6	23.5	12.9	2.0	Sandy Loam	A	Loam	B
28	54.7	43.4	1.9	0.0	Sandy Loam	A	Loamy sand	A
29	67.7	25.4	3.8	3.0	Sandy Loam	A	Loamy sand	A
30	54.2	29.5	13.3	3.0	Sandy Loam	A	Loam	B
31	60.5	34.1	5.4	0.0	Sandy Loam	A	Loamy sand	A
32	62.1	19.5	18.3	0.0	Sandy Loam	A	Loam	B

The final soil classification of soils into hydrologic soil groups is shown in Table 4.25, and the hydrologic soil groups distribution in Tenerife is shown in Fig. 4.65.

Table 4.25: Hydrologic soil groups for soil orders in Tenerife.

	Soil order						
	Alfisols	Aridisols	Entisols	Inceptisols	Sorribas	Ultisols	Vertisols
HSG	B	A	A	A	B	D	A

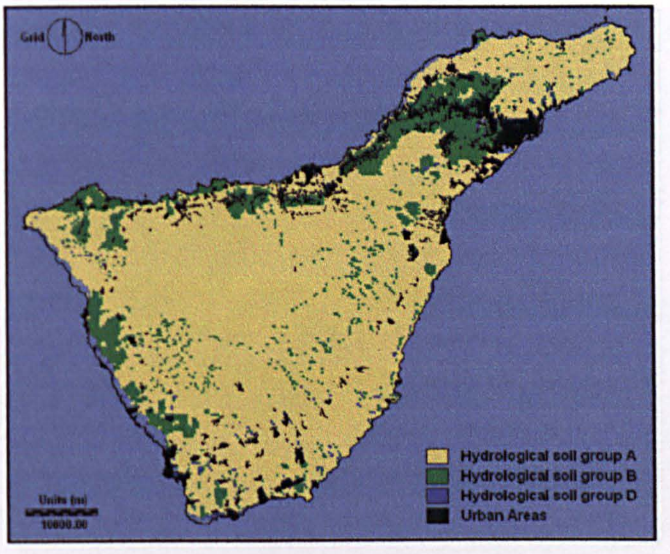

Fig. 4.65: Hydrological soil groups in Tenerife.

COVER TYPE, TREATMENT AND HYDROLOGIC CONDITION

Estimation of runoff curve numbers (Appendix I) is based on cover types, treatment and hydrologic condition. There are a number of methods for determining cover type. The most common are field reconnaissance, aerial photographs, and land use maps. Treatment is a cover type modifier (used only in Table 1 from Appendix 1) to describe the management of cultivated agricultural lands. Hydrologic condition indicates the effects of cover type and treatment on infiltration and runoff and is generally estimated from density of plant and residue cover on sample areas. *Good* hydrologic condition indicates that the soil has a low runoff potential for that specific hydrologic soil group, cover type, and treatment. Some factors to consider in estimating the effect of cover on infiltration and runoff are (a) canopy or density of lawns, crops, or other vegetative areas; (b) amount of year-round cover; (c) amount of grass or close-seeded legumes in rotations; (d) percent of residue cover; and (e) degree of surface roughness.

Fig. 4.66 shows the land use map used for this study (CD-Map, 1999). The percentage of vegetation cover was estimated as described in Section 3.8.4 and using direct personal knowledge of the study area. The estimated runoff curve number for each land use and soil type are shown in Table 4.26.

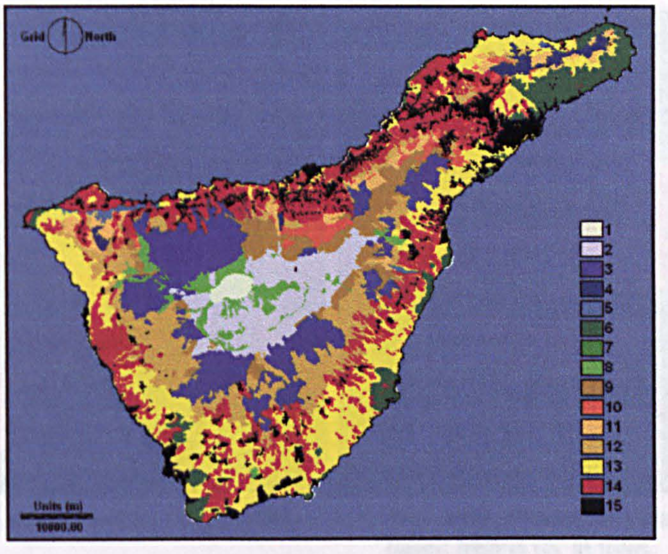

Fig. 4.66: Tenerife's land use map (from 1996) (numbers refer to Table 4.26).

Table 4.26: Curve number for each land use and soil type (from Appendix I).

	A	B	D	Cover type
1	63	77	88	Desert shrub —major plants include saltbush, greasewood, creosotebush, blackbrush, bursage, palo verde, mesquite, and cactus. Poor HC
2	35	56	77	Brush —brush-weed-grass mixture with brush the major element. Fair HC
3	36	60	79	Woods. Fair HC
4	30	58	79	Woods —grass combination (orchard or tree farm). Good HC
5	43	65	82	Woods —grass combination (orchard or tree farm). Fair HC
6	55	72	86	Desert shrub —major plants include saltbush, greasewood, creosotebush, blackbrush, bursage, palo verde, mesquite, and cactus. Fair HC
7	55	72	86	Desert shrub —major plants include saltbush, greasewood, creosotebush, blackbrush, bursage, palo verde, mesquite, and cactus. Fair HC
8	63	80	93	Herbaceous —mixture of grass, weeds, and low-growing brush, with brush the minor element. Poor HC
9	36	60	79	Woods. Fair HC
10	36	60	79	Woods. Fair HC
11	30	55	77	Woods. Good HC
12	49	30	48	Oak-aspen —mountain brush mixture of oak brush, aspen, mountain mahogany, bitter brush, maple, and other brush. Poor HC
13	63	80	93	Herbaceous —mixture of grass, weeds, and low-growing brush, with brush the minor element. Poor HC
14	66	74	82	Crops (Contoured and terraced). Poor HC
15	89	92	95	Urban

The land use map was reclassified for each of the soil hydrological soil groups using the runoff curve numbers values listed in Table 4.26. Fig. 4.67 shows the map of runoff curve numbers, which was used in combination with Eq. 4.14 to create the potential maximum retention after runoff begins (*S*), Fig. 4.68.

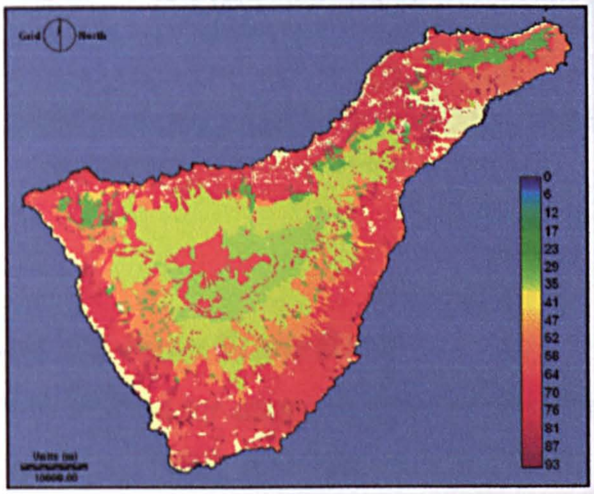

Fig. 4.67: Runoff curve numbers (CN) for Tenerife.

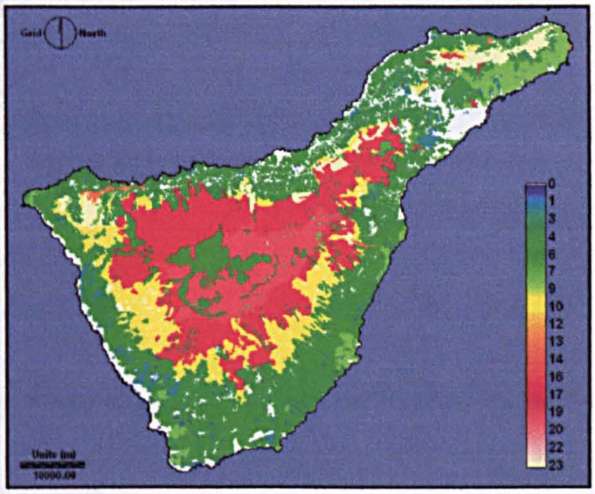

Fig. 4.68: Potential maximum retention after runoff begins (S, in mm).

The thematic map of precipitation (P-24 hours) was created by interpolation of maximum P-24 rain data among 35 stations in Tenerife obtained from the Meteorological Centre in Tenerife. The maximum 24-hour isohyet map (areas of equal rainfall during a given time) in mm is shown in Fig. 4.69. The red dots on the map represent the location of the rain stations used for interpolation. The number of years of data recording is not constant, ranging from a minimum of 7 years to a maximum of 36 years, with an average of 24 years reading. Maximum P-24 values were used instead of average rain values because only the effects of punctual and extreme runoff situations leading to maximum sediment yield washed to sea was of interest. Finally, by using the results from Fig. 4.69 and Fig. 4.68 in Eq. 4.13, the runoff (in inches) was estimated, and later converted to mm as shown in Fig. 4.70.

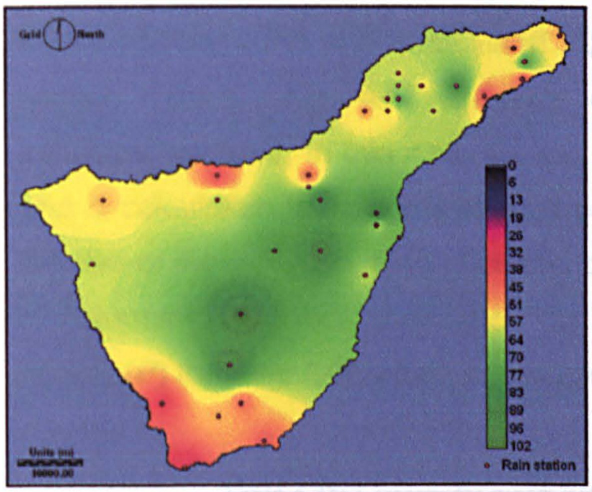

Fig. 4.69: Precipitation (P-24 max in mm).

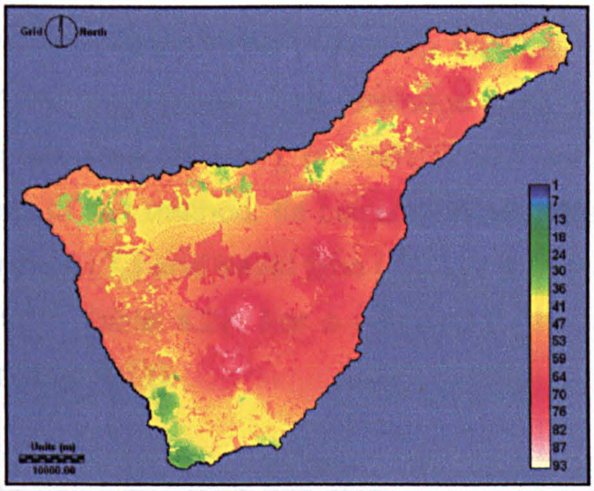

Fig. 4.70: Runoff predictions for Tenerife (mm).

4.6.2.2 PEAK FLOW RATE

The method for approximating peak rates of discharge is based on that proposed by SCS (1973) and USDA-SCS (1986). There are two available methods, the *Graphical Peak Discharge* and the *Tabular Hydrograph* methods. Selection of method is based on the characteristics of the watershed as well as the data. For this study the Tabular Hydrograph method was used, despite the simplicity of the Graphical Peak Discharge method, because the *Tc* (time of concentration) values were too small (under 0.1 h), constraining its use.

Tabular Hydrograph computation

Information required for the Tabular Hydrograph method include (1) 24-hour rainfall (in), (2) appropriate rainfall distribution, (3) curve number (CN), (4) runoff (in), (5) time of concentration (hr), (6) travel time (hr), and (7) drainage area (mi^2). The peak discharge equation used is:

$$q = Q\, A_m\, q_t \qquad \textbf{Eq. 4.15}$$

where:

q = peak discharge (ft^3/s)
Q = runoff (in)
A_m = drainage area of individual subarea (mi^2)
q_t = tabular hydrograph unit discharge (csm/in)

Curve number (*CN)* and total runoff (*Q*) maps were those previously created in section 4.6.2.1, Fig. 4.67 and Fig. 4.70 respectively. The drainage area of individual subarea, in this case for the pixel area (100 m^2), is 3.86102*10^{-5} mi^2. The q_t calculation is the most tedious part of this method. Its calculation requires the use of the I_a/P ratio, time of concentration (T_c) and travel time (T_t). *CN* is used to determine the initial abstraction (I_a) from Table 4.27. For a selected 24-hour rainfall (*P*) the ratio I_a/P is then computed (Fig. 4.71).

Table 4.27: I_a values for runoff curve number (from NRCS-SCS, 1986).

Curve Number	I_a (in)	Curve Number	I_a (in)	Curve Number	I_a (in)
40	3.000	60	1.333	80	0.500
41	2.878	61	1.279	81	0.469
42	2.762	62	1.226	82	0.439
43	2.651	63	1.175	83	0.410
44	2.545	64	1.125	84	0.381
45	2.444	65	1.077	85	0.353
46	2.348	66	1.030	86	0.326
47	2.255	67	0.985	87	0.299
48	2.167	68	0.941	88	0.273
49	2.082	69	0.899	89	0.247
50	2.000	70	0.857	90	0.222
51	1.922	71	0.857	91	0.198
52	1.846	72	0.817	92	0.174
53	1.774	73	0.778	93	0.151
54	1.704	74	0.703	94	0.128
55	1.636	75	0.667	95	0.105
56	1.571	76	0.632	96	0.083
57	1.509	77	0.597	97	0.062
58	1.448	78	0.564	98	0.041
59	1.390	79	0.532		

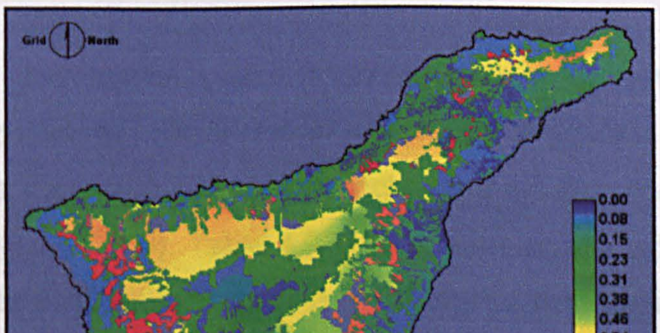

Fig. 4.71: I_a/P values.

Travel time (T_t) is the time it takes for water to travel from one location to another in a watershed. It is a component of time of concentration (T_c), which is the time for runoff to travel from the hydraulically most distant point of the watershed to a point of interest within the watershed. T_c is computed by summing all the travel times for consecutive components of the drainage conveyance system.

$$T_c = T_{t1} + T_{t2} + \ldots Tt_{tm} \qquad \text{Eq. 4.16}$$

where:

T_c =time of concentration (hr)
m =number of flow segments

The travel time (for sheet flow, which is flow over plane surfaces) is calculated as;

$$T_t = \frac{0.007(nL)^{0.8}}{(P)^{0.5} s^{0.4}} \qquad \text{Eq. 4.17}$$

where:

T_t = travel time (hr),
n = Manning 's roughness coefficient (table 3-1)
L = flow length (ft)
P = 24-hour rainfall (in)
s = slope of hydraulic grade line (land slope, ft/ft)

With sheet flow, the friction value (Manning's n) is an effective roughness coefficient that includes the effect of raindrop impact, drag over the plane surface, obstacles such as litter, crop ridges, and rocks, and erosion and transportation of sediment (USDA-SCS, 1986). Table 4.28 gives Manning's n values for sheet flow over various surface conditions and Fig. 4.72 shows the Manning's n map. Fig. 4.73 shows the travel time thematic map created using equation Eq. 4.17.

Table 4.28: Roughness coefficients (Manning 's *n*) for sheet flow. (from NRCS-SCS, 1986).

Surface description	***n*[1]**
Smooth surfaces (concrete, asphalt, gravel, or bare soil)..	0.011
Fallow (no residue)...	0.05
Cultivated soils:	
Residue cover =20%...	0.06
Residue cover >20%...	0.17
Grass:	
Short grass prairie	0.15
Dense grasses[2]	0.24
Bermudagrass	0.41
Range (natural)...	0.13
Woods:[3]	
Light underbrush	0.40
Dense underbrush	0.80

1 The *n* values are a composite of information compiled by Engman (1986).
2 Includes species such as weeping lovegrass, bluegrass, buffalo grass, blue grama grass, and native grass mixtures.
3 When selecting n consider cover to a height of about 0.1 ft. This is the only part of the plant cover that will obstruct sheet flow.

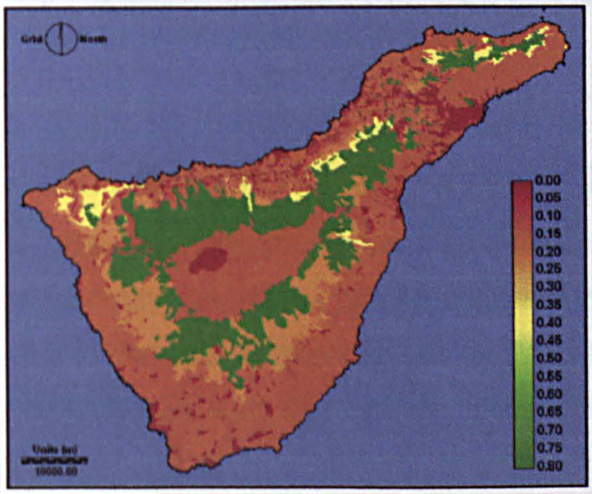

Fig. 4.72: Roughness coefficients (Manning's n).

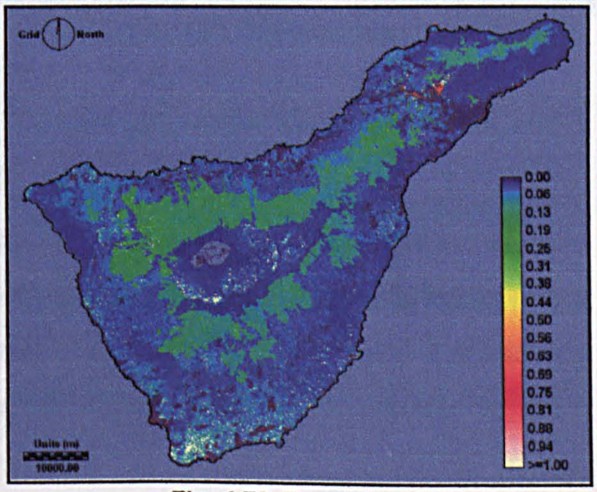

Fig. 4.73: Travel time (hr).

The tabular hydrograph unit discharge (q_t) was calculated using the Tabular Hydrograph tables from USDA-SCS (1986). Tables 5 (5-I, 5-IA, 5-II, and 5-III) from USDA-SCS (1986) shows tabular discharge values for the various rainfall distributions. To be able to use the tables and obtain the peak discharge values, it was first necessary to identify which rainfall distribution fits Tenerife's rain conditions. From the four distributions described by USDA-SCS (1986), Type I was chosen as the most appropriate.

Knowing the rain distribution for Tenerife, the travel time, the time of concentration and the I_a/P ratio, the tabular hydrograph unit discharge can be estimated.

Ultimately, the value for the peak discharge (q) can be calculated by using Eq. 4.15. Fig. 4.74 and Fig. 4.75 show the tabular hydrograph unit discharge and the peak discharge maps respectively.

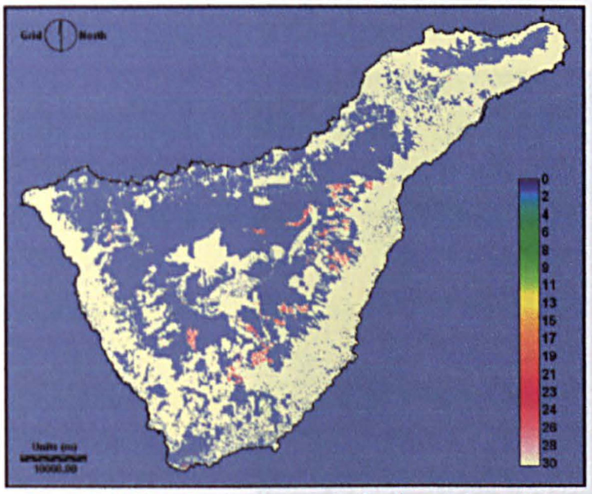

Fig. 4.74: Tabular hydrograph discharge (csm/in).

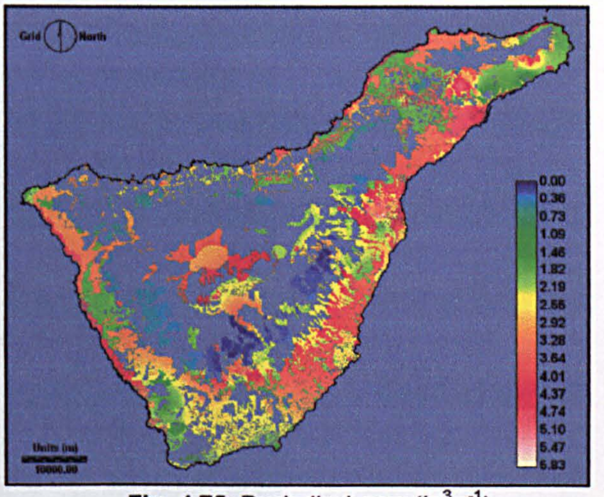

Fig. 4.75: Peak discharge ($in^3 s^{-1}$).

4.6.2.3 Soil Erodibility Factor (*K*)

Wherever possible, *K* should be based on measured values. If no measured data is available, the value can be obtained from the nomograph or calculated from the regression equation presented by Wischmaier *et al.* (1971). However, it should be remembered that this will be an estimated value and hence subject to error (Morgan, 1995).

Despite many published work relating *K* to certain physicochemical and mineralogical parameters of soils, important gaps are apparent with respect to the study of the erodibility of variably charged soils in volcanic regions, such as Tenerife. It is known that *K* calculated according to the method of Wischmaier *et al.* (1971), is not satisfactory for these soil types (Rodriguez *et al.*, 1993). According to the author, soils in Tenerife vary between being considerably resistant (Ultisols, Alfisols, Vertisols, Entisols, Sorribas and Inceptisols) (K= 0.10-0.25) to fairly sensitive (Aridisols) (K= 0.25-0.35). Table 4.29 shows the soil erodibility factor for each soil order in Tenerife, and Fig. 4.76 the reclassified soil map accordingly to these values.

Table 4.29: Soil erodibility factor (K) for the different soils in Tenerife (from Rodriguez *et al.*, 1993).

Soil order						
Alfisols	**Aridisols**	**Entisols**	**Inceptisols**	**Sorribas**	**Ultisols**	**Vertisols**
0.19	0.31	0.20	0.21	0.19	0.18	0.19

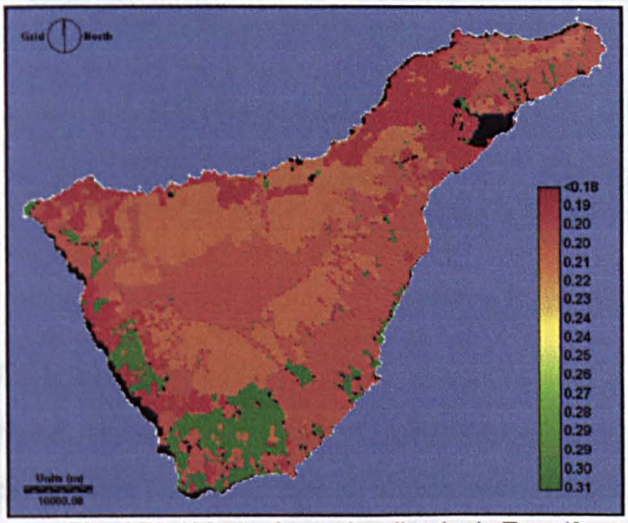

Fig. 4.76: K factor for each soil order in Tenerife.

4.6.1.4 CROP MANAGEMENT FACTOR (C)

The crop management factor (*C*) represents the ratio of soil loss under a given crop to that of bare soil. *C* represents an integration of several factors that affect erosion, including vegetation cover, plant litter, soil surface and land management. Values of *C* range from zero to one. The *C* factor values used are those presented by Zhou (1998) and shown in Table 4.30. The percentage of vegetation cover was estimated as described in Section 3.8.4 and from the author's personal knowledge of the study area. Fig. 4.77 shows the vegetation map reclassified accordingly to those values presented in Table 4.30.

Table 4.30: *C* factor.

Cover (%)	C factor
0 - 30	1.0
31 - 50	0.5
51 - 70	0.3
> 70	0.2

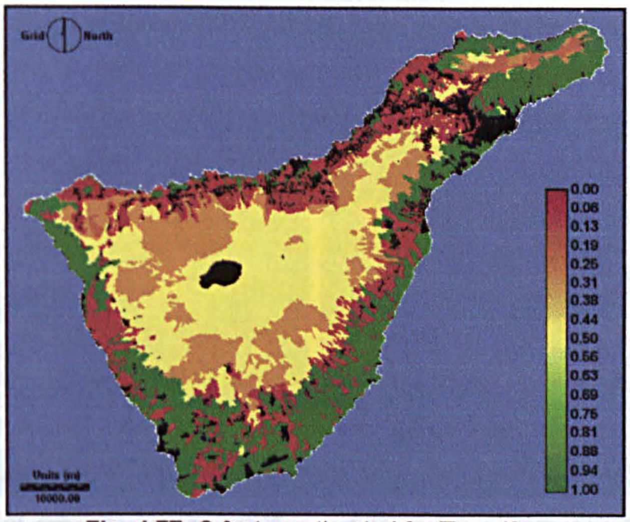

Fig. 4.77: C factor estimated for Tenerife.

4.6.2.5 LS TOPOGRAPHIC FACTOR

Generating the *LS* values poses the largest problem in using the USLE (Hickey *et al.*, 1994). The topographic factors *L* and *S* indicate the effects of slope length and steepness on erosion, respectively. Slope length refers to the overland runoff flow, from its origin to where it reaches a defined channel or where deposition begins. The longer the slope length the greater the amount of cumulative runoff. Also, the steeper the slope of the land the higher the velocity of the runoff contributing to erosion. The *LS* factor was computed using the Wischmeier and Smith (1978) equation Eq. 4.18.

$$LS = \left(\frac{\lambda}{22.1}\right)^m \left(65.41S^2 + 4.565S + 0.065\right) \qquad \textbf{Eq. 4.18}$$

where:

L = slope length (m)
S = slope gradient (%)
$m = 0.6[1-\exp(-35.835\ S)]$

Slope values were calculated by using the module SLOPE on a digital elevation model (DEM). The DEM used in this study came from the digitised contour lines of 209 1:5000 maps (Fig. 4.78) provided by CD-Map (1999). The contour lines, imported into IDRISI32, were interpolated (linear interpolation by the module INTERCON) to produce a faceted model as shown in Fig. 4.79.

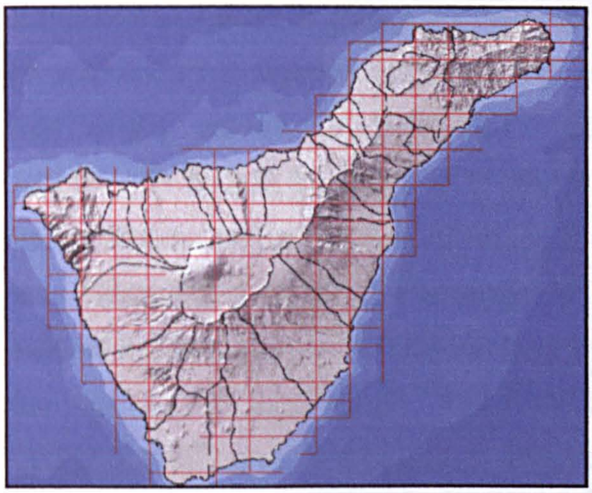

Fig. **4.78**: Distribution of the 209 1:5000 maps used to generate the DEM.

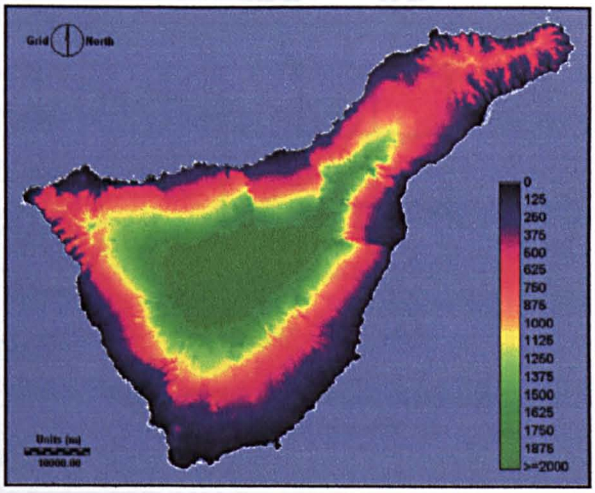

Fig. 4.79: Digital elevation model (DEM) for Tenerife.

The slope map was created by running the module SLOPE (Fig. 4.80). The slope length coverage was produced by developing a flow direction grid. The flow direction grid was developed by first calculating the slopes in the neighbouring cells and then making the highest slope the direction of the runoff using the module ASPECT in IDRISI32. Aspects are output in decimal degrees and use standard azimuth designations, 0°-360°, clockwise from north (Fig. 4.81).

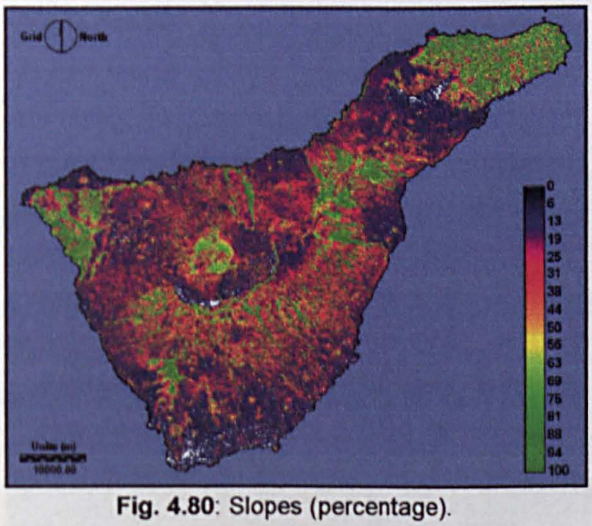

Fig. 4.80: Slopes (percentage).

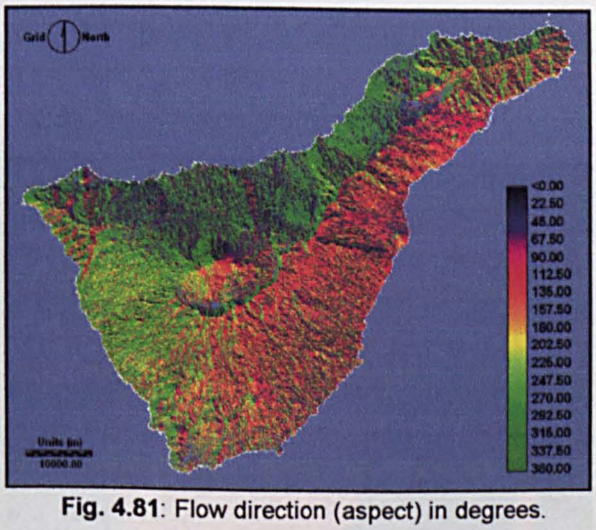

Fig. 4.81: Flow direction (aspect) in degrees.

Each of the values in Fig. 4.81 corresponds to a direction of flow as shown in Fig. 4.82. For angle values of 33.5°-22.5°, 67.5°-112.5°, 157.5°-202.5°, and 247.5°-292.5° the value of the cell for the flow direction length was reclassified equal to the length of one side of the image pixel (10 metres), whereas for values of 22.5°-67.5°, 112.5°-157.5°, 202.5°-247.5°, and 292.5°-337.5° the value of flow direction length was reclassified to the diagonal distance of the pixel (14 meters). The reclassified map with values of 10 or 14 is shown in Fig. 4.84.

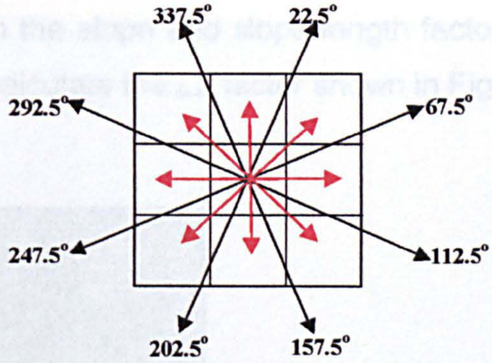

Fig. 4.82: Direction flows corresponding to each angle interval.

To estimate the slope length, the slope must be considered. For the same flow direction length (X), pixels with greater slopes (θ) will have longer slope length (L). A simple trigonometric calculation was used to estimate the L value for a known X and θ (Fig. 4.83). Fig. 4.85 shows the slope length map created.

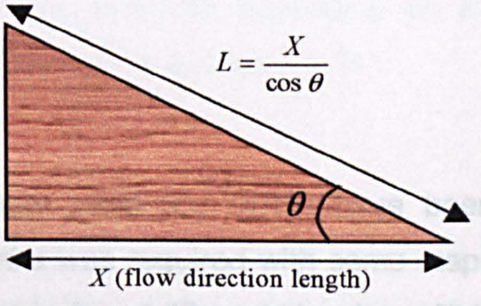

Fig. 4.83: Slope length calculation.

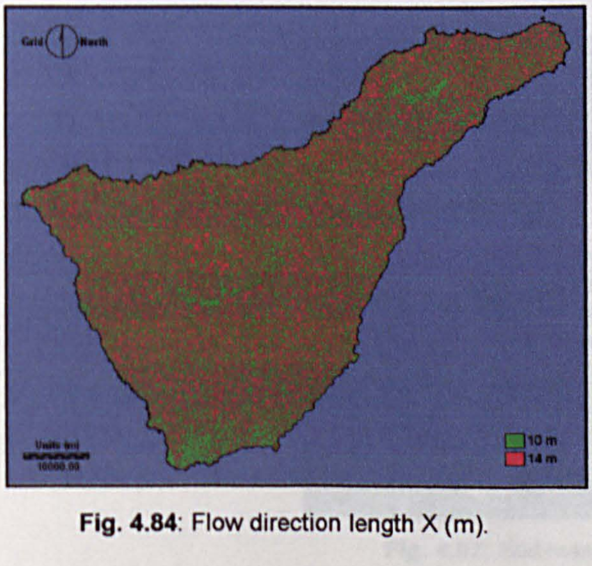

Fig. 4.84: Flow direction length X (m).

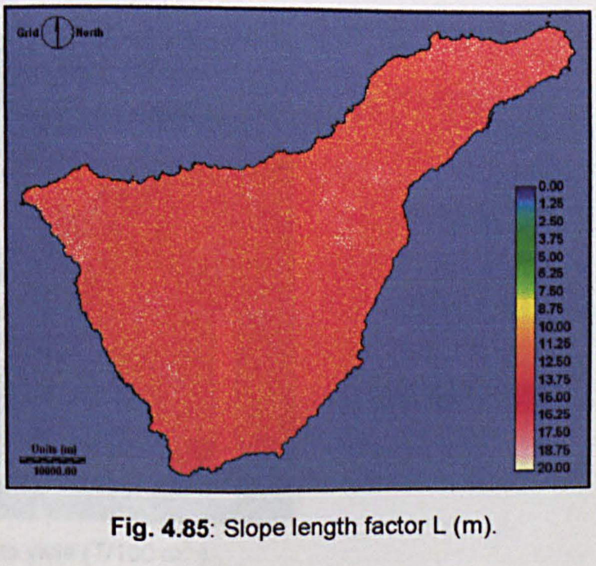

Fig. 4.85: Slope length factor L (m).

Finally, Eq. 4.18 was used in combination with the slope and slope length factor maps (Fig. 4.80 and Fig. 4.85 respectively) to calculate the *LS* factor shown in Fig. 4.86.

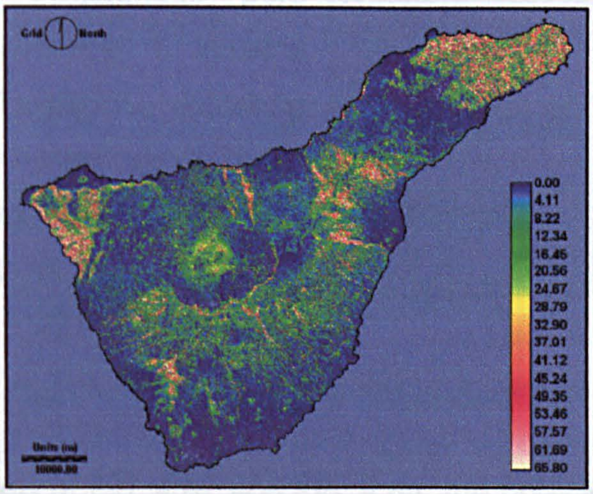

Fig. 4.86: *LS* factor.

4.6.1.6 SEDIMENT YIELD CALCULATION

All variables required to estimate the sediment yield (Eq. 4.12) have been computed previously. However, a change of units was required with some maps before computing the sediment yield map shown in Fig. 4.87 could be done. This map shows the sediment yield per pixel estimated for the maximum or extreme rain event recorded. In other words, this map addresses the worse runoff case scenario.

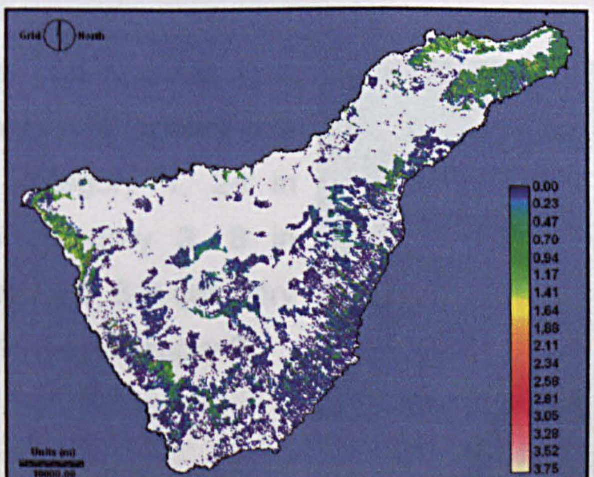

Fig. 4.87: Sediments yield (T/100 m^2).

To estimate the sediment discharge quantity and discharge points, the watershed distribution and extension must be known. Watersheds were extracted from the DEM (Fig. 4.79) using the module WATERSHED following correction to remove depressions (pits). This "depressionless" DEM is known as a hydrologically corrected DEM. Fig. 4.88 shows the 221 watersheds identified.

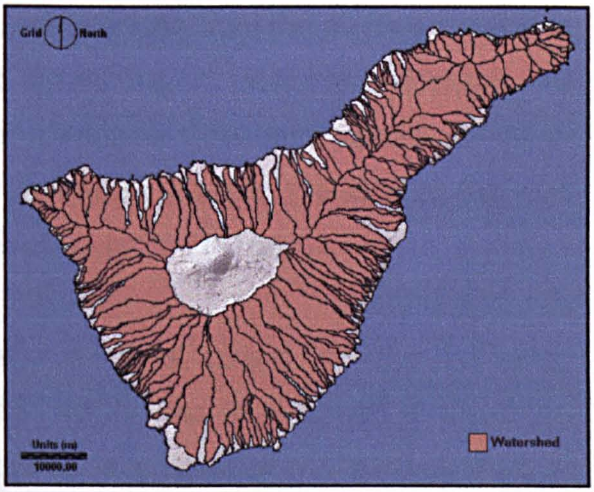

Fig. 4.88: Watersheds.

By the combined use of Fig. 4.87 and Fig. 4.88, the potential sediment yield for each watershed was estimated and scores were assigned depending on the amount of sediment that each watershed carried into the sea (Table 4.31).

Table 4.31: Thresholds values for sediments carried to the sea (tons of sediment/watershed per maximum runoff event).

Criterion \ Score	8	7	6	5	4	3	2	1
Sediments	0-5000	5000-10000	10000-15000	15000-20000	20000-25000	25000-30000	30000-40000	>40000

Fig. 4.89 shows the reclassified watershed map, where 152 watersheds were classified in category 1, 24 in category 2, 20 in category 3, 8 in category 4, 3 in category 5, 6 in category 6, 4 in category 7 and 4 in category 8.

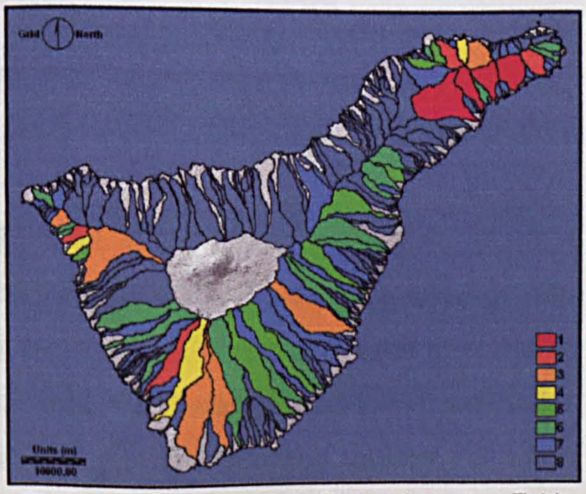

Fig. 4.89: Watershed classification based on Table 4.31.

A further manipulation was made to measure distances from the stream mouths in each of the 8 groups and reclassified according to suitable distances for development of cage culture in Tenerife. Distance threshold values for each watershed group were set following the proposed by Lawson (1995) that fish can withstand short exposure to sediment loads of up to 20,000 mg/l.

Calculations to estimate distance thresholds were based on the following assumptions. A sediment plume discharged into the sea is assumed to distribute as shown in Fig. 4.90a. Horizontal distribution is greater at the surface than in deeper water. It was assumed that sediments will not sink below the thermocline depth, set at 30 m. It is also known that any plume discharged into the sea will be dispersed following the dominant current direction (Clark, 1998). Unfortunately, information on currents was not available, therefore, as a conservative measure, sediments discharged into the sea are assumed to disperse equally in all directions (Fig. 4.90b)

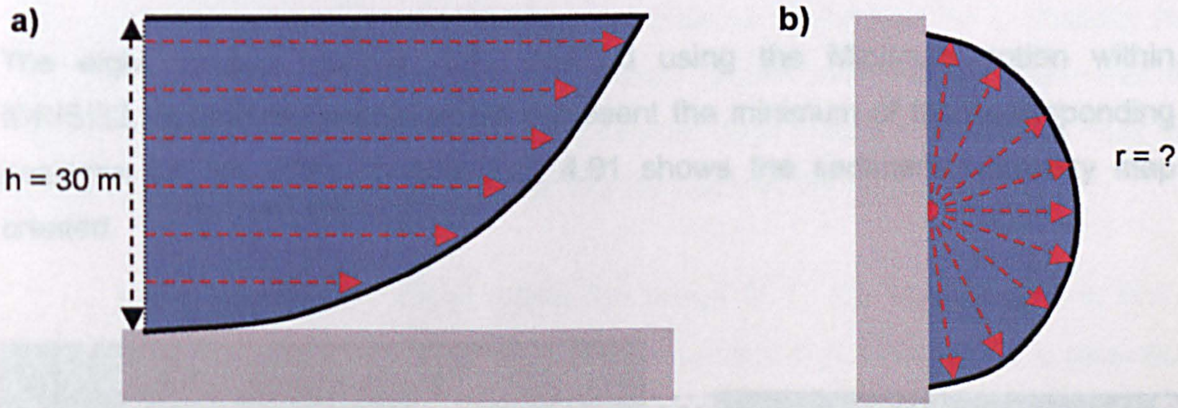

Fig. 4.90: Assumed vertical (a) and horizontal (b) sediment dispersion profiles.

Eq. 4.19 (volume of half sphere section) was used to estimate the distance thresholds, or *r* values, for each watershed category. For each watershed group, values of *r* were iteratively assigned to each score threshold until the mean sediment yield discharged by each group of watershed was diluted to values under 20,000 mg/l. Table 4.32 shows the derived distance threshold values for each watershed group.

$$V=[\pi*h^2*(r-h/3)]/2 \qquad \text{Eq. 4.19}$$

Table 4.32: Watershed distance threshold values (m).

Criteria \ Score	8	7	6	5	4	3	2	1
Distance Watershed-1	>3150	2875-3150	2600-2875	2325-2600	2050-2325	1775-2050	1500-1775	0-1500
Distance Watershed-2	>2550	2325-2550	2100-2325	1875-2100	1650-1875	1425-1650	1200-1425	0-1200
Distance Watershed-3	>1950	1775-1950	1600-1775	1425-1600	1250-1425	1075-1250	900-1075	0-900
Distance Watershed-4	>1700	1550-1700	1400-1550	1250-1400	1100-1250	950-1100	800-950	0-800
Distance Watershed-5	>1350	1225-1350	1100-1225	975-1100	850-975	725-850	600-725	0-600
Distance Watershed-6	>1000	900-1000	800-900	700-800	600-700	500-600	400-500	0-400
Distance Watershed-7	>550	500-550	450-500	400-450	350-400	300-350	250-300	0-250
Distance Watershed-8	>120	110-120	100-110	90-100	80-90	70-80	60-70	0-60

The eight images created were overlaid using the Minimum option within IDRISI32, so that the output pixels represent the minimum of the corresponding positions on the other images. Fig. 4.91 shows the sediment suitability map created.

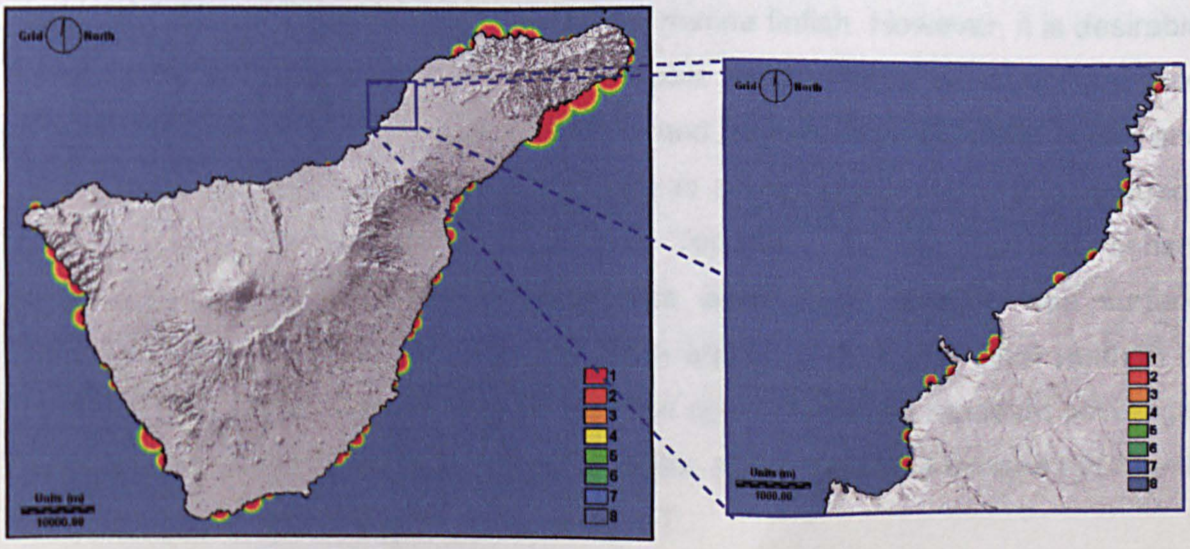

Fig. 4.91: Suspended solids (runoff sediments) suitability map.

4.6.3 Temperature

Fish are poikilothermic, meaning that they essentially have the same body temperature as their surroundings and that temperature is governed by external influences. Each species has a characteristic growth curve and an optimum growth range that is dependent on with temperature and fish size. Every species also has an upper and lower temperature limit beyond which it cannot survive. Fish have a very low tolerance for sudden changes in temperature and, often rapid changes of as little as 5 °C will stress or kill them (Lawson, 1995). In addition, the fish's ability to ward off diseases is best near the optimum growth temperature (Iwana *et al.*, 1997). Optimum temperature ranges differ for different species of fish. The optimum temperature is that which fish would select for itself, given the choice.

Water temperature is the environmental parameter having the greatest effect on fish (Hoar *et al.*, 1979). It can be thought of as a primary environmental factor affecting the economic feasibility of a commercial aquaculture venture. Temperatures on either side of the optimum can induce stress in the animal, affecting feeding, growth, reproduction and disease inhibition. The probability for culture success is greatest near the optimum growth temperature. Temperature control is impractical with cage culture, therefore cage culture of a species must be conducted in geographical regions having the appropriate temperature.

Sea temperature in Tenerife is within the range of 17-25 °C, hence, it is not a constraint for the culture of warm temperate marine finfish. However, it is desirable to identify those areas with the most favourable temperatures, which will enhance growth of the targeted culture species, and reduce the growing cycle and production costs. It was impractical to take *in situ* simultaneous and continuous sea temperature measurements around Tenerife, and so AVHRR sensor measurements from the NOAA-14 satellite were used. Satellite sea surface temperature (SST) measurements are more attractive than any other method of measurements available because of their low cost, global and repeated coverage. A set of 135 NOAA14-AVHRR satellite images, approximately 4 images per month during 3 years, were used for retrieval of SST.

The accuracy of satellite data for sea surface temperature is critically dependent upon the ability of satellite radiometers to view the sea surface unobstructed by cloud. Hence, images were processed for cloud detection and elimination. The determination of SST from cloud-free satellite images was performed by means of multi-channel algorithms using thermal channels 4 and 5 of AVHRR. The SST algorithm was applied to each of the cloud-free images, creating a set of 135 SST images. The final processing step was the georeferencing of these images. All sea surface temperature images were combined to generate a composite map which was used to obtain average sea surface temperatures. This image was reclassified according to suitability scores.

4.6.3.1 NOAA-AVHRR Introduction

Since 1981, the NOAA series of polar-orbiting spacecraft have been carrying the Advanced Very High Resolution Radiometer (AVHRR), an instrument with three infrared (IR) channels suitable for estimating SST (Victorov, 1996). These channels are located within the wavelengths 3.5μm to 4μm and 10μm to 12.5μm. The history of SST computation from AVHRR radiances is discussed at length by McClain *et al.*, (1985). Briefly, radiative transfer theory is used to correct for the effects of the atmosphere on the observations by utilising "windows" of the electromagnetic spectrum where little or no atmospheric absorption occurs. Channel radiances are transformed (with the use of the Planck function) to units of temperature, then compared to *a-priori* temperatures measured at the surface. This comparison yields coefficients which, when applied to the AVHRR data, give estimates of surface temperature (Cracknell, 1997).

Remote sensing data acquisition is limited to the non-blocked spectral regions, called "*atmospheric windows*" (Fig. 4.92).The radiation emitted or reflected from the targets and backgrounds must pass through the intervening atmosphere before reaching the detection system. The radiation is absorbed and re-emitted by molecular constituents of the atmosphere and scattered into and out of the path by various aerosol components. Combinations of detectors and spectral bandpass filters are selected to define the operating region to conform to a window to maximize performance (Campbell, 1996).

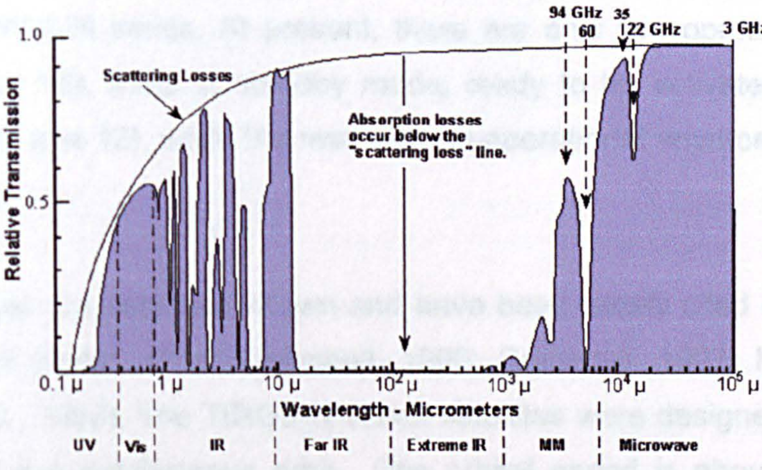

Fig. 4.92: Atmospheric transmission. The atmospheric windows, where the atmosphere blocks energy transmission, are shaded.

At IR wavelengths (Fig. 4.93), the ocean surface emits radiation almost as a blackbody. In principle, without an absorbing and emitting atmosphere between the sea surface and the satellite, it would be possible to estimate SST using a single channel measurement. In reality, surface-leaving infrared radiance is attenuated by the atmosphere before it reaches a satellite sensor (Lillesand and Kiefer, 1994). Therefore, it is necessary to make corrections for atmospheric effects. Water vapour, CO_2, CH_4, NO_2 and aerosols are the major constituents that determine the atmospheric extinction of IR radiance (Minnett, 1990). Among them, absorption due to water vapour accounts for most of the necessary correction (Barton *et al.*, 1989).

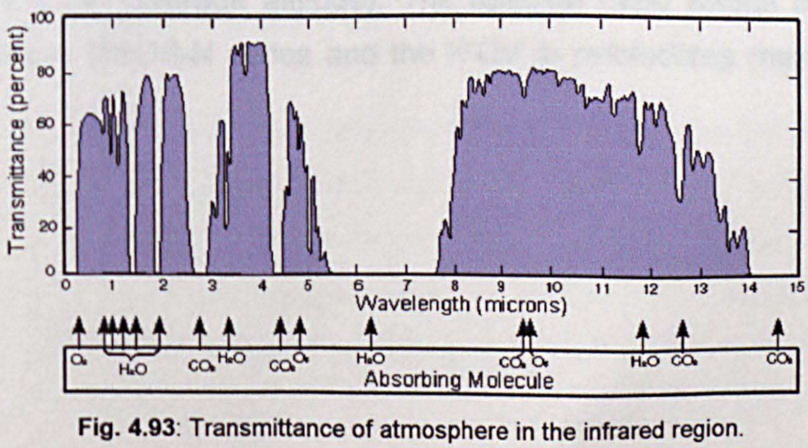

Fig. 4.93: Transmittance of atmosphere in the infrared region.

The NOAA polar orbiting satellites series commenced with the TIROS-N until the latest present day NOAA-15. Despite the fact that only the first satellite was named TIROS and the rest as NOAA, the whole series of these satellites are called the TIROS-N series. At present, there are only two operational satellites (NOAA-14 and 15), three in standby mode, ready to be activated for operation (NOAA-10, 11, and 12), while the rest are non-operational anymore due to failure or breakdown.

These satellites are very well known and have been widely cited in the literature (Lillesand and Kiefer, 1994; Campbell, 1996; Cracknell, 1997; Kindwell, 1998; Vazquez *et al.*, 1998). The TIROS-N series satellites were designed to operate in a near-polar, sun-synchronous orbit. The orbital period is about 102 minutes, producing 14.1 orbits per day, with a distance between orbits estimated to be 25.5°. Because the number of orbits per day is not an integer, the sub-orbital tracks do not repeat on a daily basis, although the local solar time of the satellite's passage is essentially unchanged for any latitude.

A comprehensive and detailed description of the Advanced Very High Resolution Radiometer (AVHRR) on board the TIROS series satellites is presented by Cracknell (1997), but briefly, the AVHRR is a cross-track scanning system with four or five spectral channels. The AVHRR flown aboard TIROS-N, NOAA-6, NOAA-8, and NOAA-10 has four channels, and the AVHRR aboard NOAA-7, NOAA-9, NOAA-11, NOAA-12, NOAA-13 and NOAA-14 has five channels. The Instantaneous Field of View (IFOV) of each channel is approximately 1.4 milliradians leading to a resolution of 1.1 km at the satellite subpoint for a nominal altitude of 833 km (average altitude). The spectral band widths of the AVHRR channels for the TIROS-N series and the IFOV in milliradians (mr) are shown in Table 4.33.

Table 4.33: Spectral band widths (micrometers) and IFOV(milliradians) of the AVHRR.

Channel	TIROS-N	NOAA-6,-8,-10	NOAA-7,-9,-11,-12,-14	NOAA-13	IFOV
1	0.55-0.90	0.58-0.68	0.58-0.68	0.58-0.68	1.39
2	0.725-1.10	0.725-1.10	0.725-1.10	0.725-1.0	1.41
3	3.55-3.93	3.55-3.93	3.55-3.93	3.55-3.93	1.51
4	10.5-11.5	10.5-11.5	10.3-11.3	10.3-11.3	1.41
5	Channel 4 repeated	Channel 4 repeated	11.5-12.5	11.4-12.4	1.30

The scanning rate of the AVHRR is 360 scans per minute. The analogue data output from the sensors is digitised on board the satellite. Each sample step corresponds to an angle of scanner rotation of 0.95 milliradians. At this sampling rate, there are 1362 samples per IFOV. A total of 2048 samples are obtained per channel per Earth scan, which span an angle of +/-55.37 degrees from the nadir (subpoint view). That means a swath width of 2400 km per image at a resolution of 1.1 km at nadir. The IR channels are calibrated in-flight using a view of a stable blackbody and space as reference. No in-flight visible channel calibration is performed (although the space view is available as one reference point).

4.6.3.2 Data Source

The AVHRR images used for this study were provided by CREPAD (Centre for Reception, Processing, Archiving and Dissemination of Earth Observation Data and Products) in the Canary Islands. Gran Canaria (Canary Islands) hosts the Maspalomas satellite ground receiving station, which has a approximate coverage of 3300 km^2 over all Spanish territories, a good part of the South Atlantic Ocean and the North-Western coast of Africa.

The AVHRR images were selected using CREPAD's Internet browser facility (http://www.crepad.rcanaria.es) and a set of approximately 4 NOAA-14 AVHRR images per month with, minimum cloud coverage, was obtained from 1997 to 2000. A total of 135 satellite images, each composed of 5 bands, was provided, already radiometrically corrected by CREPAD.

4.6.3.3 Processing Steps

Preprocessing forms a preparatory phase that, in principle, improves image quality for later analyses that will extract information from the image. It is assumed that the preprocessing changes are beneficial, but it should be borne in mind that preprocessing might create artefacts that are not immediately obvious (Campbell, 1996).

The implementation of the data processing flow is generally a stepwise process that incrementally applies higher order processing in a logical and efficient manner. The sequence of steps followed in this study were;

- Radiometric Calibration
- Cloud Detection
- Atmospheric Correction for Channels 4 and 5
- Geometric Corrections
- Compositing

4.6.3.4 Radiometric Calibration

Although pre-launch calibration procedures have been quite extensive, it is not sufficient to rely on these calibration data alone to achieve the desired accuracy from AVHRR data, therefore, the instrument characteristics may not remain the same in orbit as they were before launch (Kidwell, 1998). Kidwell (1998) suggested that this degradation occurs primarily because the thermal environment varies with the satellite's position in orbit, causing the digital output to vary.

Radiometric calibration was done by CREPAD following standard calibration procedures described by Kidwell (1998). Basically, AVHRR visible data values (Channels 1 and 2) were converted to albedos and AVHRR thermal data values (Channels 3 and 4, and 5) were converted to temperature values. Fig. 4.94 and Fig. 4.95 show an example of channels 1 and 2 while Fig. 4.96 and Fig. 4.97 show an example of channels 4 and 5 respectively, from the same image, that has been radiometrically corrected.

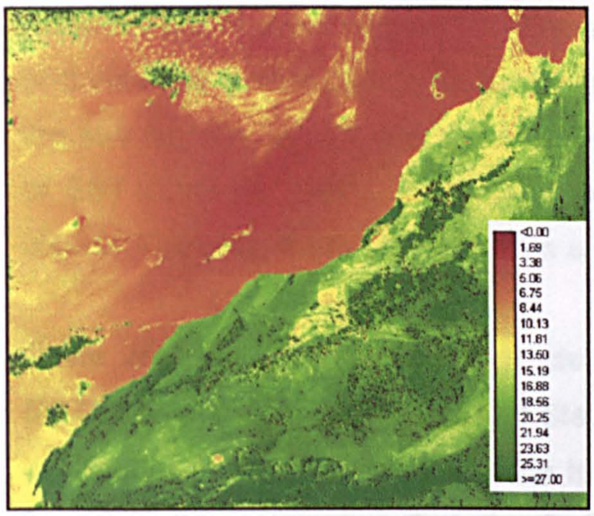

Fig. 4.94: Channel-1 AVHRR-14 image (06-08-1999) radiometrically corrected (percent albedo).

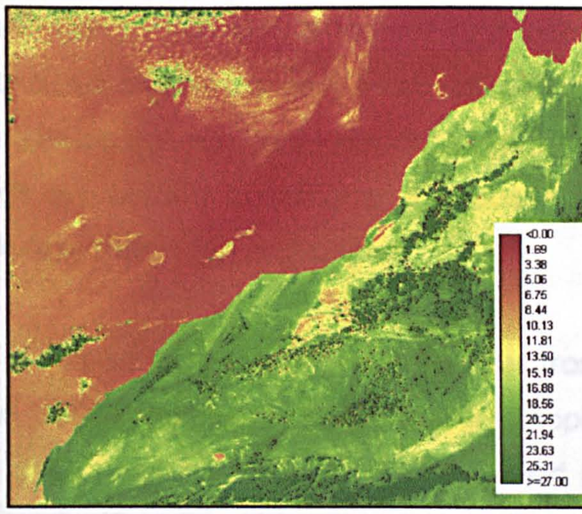

Fig. 4.95: Channel-2 AVHRR-14 image (06-08-1999) radiometrically corrected (percent albedo).

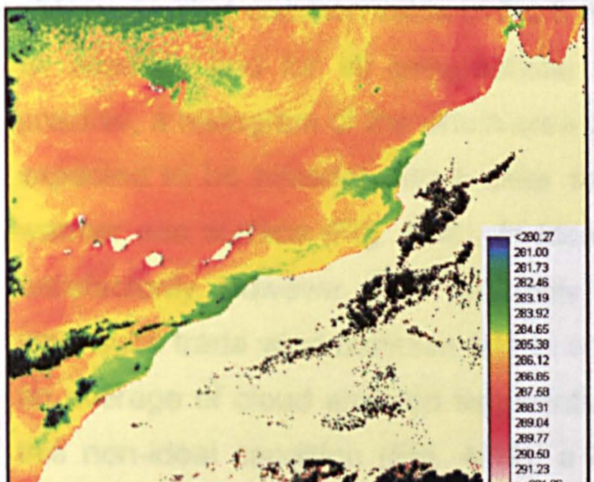

Fig. 4.96: Channel-4 AVHRR-14 image (06-08-1999) radiometrically corrected (Kelvin degrees).

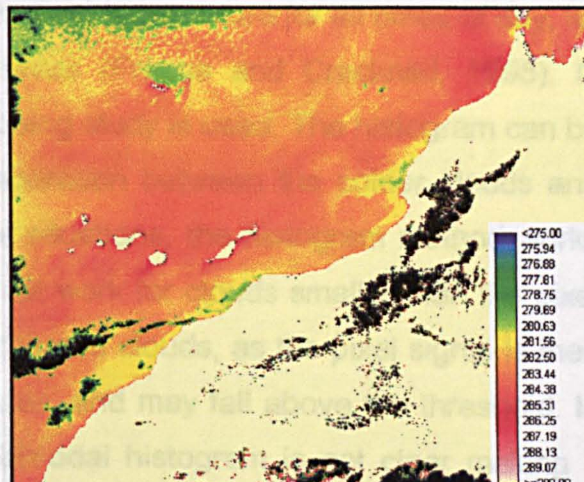

Fig. 4.97: Channel-5 AVHRR-14 image (06-08-1999) radiometrically corrected (Kelvin degrees).

4.6.3.5 CLOUD DETECTION

The accuracy of satellite observations of sea surface temperature is critically dependent upon the ability of satellite radiometers to view the sea surface unobstructed by clouds (Gutman, 1992). The atmosphere introduces errors in satellite measurements of SST through cloud cover, aerosols, water vapour, reflected sky and the presence of other gases, with clouds dominating the errors introduced (Simpson and Humphrey, 1990). Thin clouds and subpixel clouds (clouds smaller than the instrument's field of view, 1.1 km x 1.1 km at nadir for

AVHRR) are of most concern (Cracknell, 1997). Thin clouds include high cirrus and very low stratus clouds. In particular cirrus clouds are very much colder than the sea surface, even a few small cirrus clouds can add large errors to estimates of SST (Stewart, 1985). Subpixel clouds are usually cumulus or thin scattered clouds. Typically, trade wind cumulus are less than 1 km in diameter.

There are several methods which can be used for retrieving cloud cover from NOAA-AVHRR images (Addink and Stein, 1999), but the simplest off all is to apply a constant radiance threshold value to each pixel in the image. This method is based on the assumption that clouds are significantly colder than the surface of the sea, hence, a threshold value is used to distinguish pixels from cloudy and clear areas. However, there is no reason to assume that the best results will be obtained with a common value of the threshold temperature for all times of day, for all seasons and for all geographical areas (França and Cracknell, 1995). In practise, a histogram of the whole area being study is used. The histogram can be expected to be bimodal with a clear separation between the colder clouds and warmer sea surface (Fig. 4.98). In ideal situations, the histogram method works satisfactorily. However, it will generally not work for clouds smaller than the pixel size, such trade wind cumulus or thin scattered clouds, as the pixel signal is then an average of cloud and sea temperatures, and may fall above the threshold. In this non-ideal condition (Fig. 4.99), a bimodal histogram is not clear making it difficult to select a threshold value.

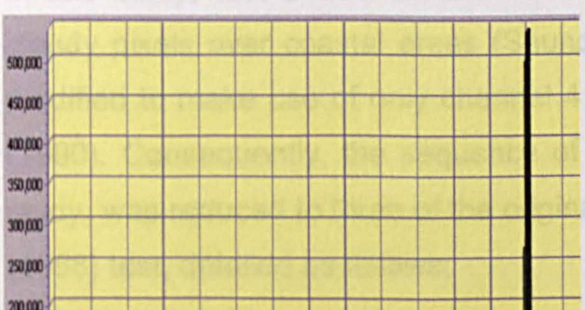

Fig. 4.98: Histogram for Channel-4 AVHRR-14 image (06-08-1999) generated with IDRISI32.

Fig. 4.99: Histogram for Channel-4 AVHRR-14 image (21-12-1999) generated with IDRISI32.

As the clouds in Tenerife were expected to be smaller than the AVHRR pixel size (1.1 km at nadir) due to the constant present of the Trade winds, this method was not adopted in this study.

An alternative is to use the cloud-detection algorithms method of Saunders and Kriebel (1988). Cracknell (1997) considered this method as the best technique for cloud detection and elimination among other methods that have also proven useful (Gutman, 1992; Simpson and Humphrey, 1990). It is based on using five day-time or five night-time tests applied to each individual pixel to determine whether that pixel is cloud-free or not. The five tests are;

1. thermal infrared threshold test (used on channel 5)
2. local uniformity or spatial coherence test (used on channel 4)
3. dynamic reflectance threshold test (used on channel 1 or 2)
4. channel 2/channel 1 ratio test (used on channels 1 and 2)
5. channel 4-channel 5 brightness temperature test (used on Channels 4 and 5)

A pixel is only identified as cloud-free if it passes all five tests. Using the five tests in this way does lead to the possibility that some test will incorrectly identify some cloud-free pixels as cloud-contaminated, but this is the best way to ensure that no cloud-contaminated pixels escape detection. For a detailed explanation of this method refer to Saunders (1986) and Saunders and Kriebel (1988).

In this study, test 2 was omitted because of its poor performance in detecting cloudy pixels over coastal areas (Saunders, 1986; Cracknell, 1997). Test 5 was modified to make use of only channel 4 as proposed by Simpson and Humphrey (1990). Consequently, the sequence of steps to identify cloud-free pixels in this study was reduced to three of the original and one modified Saunders and Kriebel (1988) test, detailed as follows;

Test I; *Thermal infrared threshold test.*

This test, applied to channel 5, is a gross cloud check which rejects all pixels with brightness temperatures less than the threshold value of 10 °C as cloudy pixels

Test II; *Dynamic reflectance threshold test.*

A large albedo on channel 2 can indicate the presence of clouds. If the albedo of a pixel exceeds 8% during the day, then the pixel is flagged as cloud contaminated. Channel 2 was used instead of channel 1 because channel 1's spectral response is unable to detect cirrus clouds (NOAA, 1985).

Test III; *Channel 2/Channel 1 ratio test.*

This test makes use of the ratio between the reflectance in the near-infrared reflectances (channel 2) and visible reflectances (channel 1).

$$Q = \frac{R_2}{R_1} \qquad \text{Eq. 4.20}$$

The *Q* values from cloudy pixels are close to unity due to quite similar scattering effects of the reflectance for both channels. Over the sea R_1 is much greater then R_2. The threshold chosen for over the sea is Q>0.75 for cloud-contaminated pixels.

Test IV; *Minimum Channel 4 Temperature*.

If the channel 4 temperature is too low, it is assumed that cloud-top temperatures are been detected. Pixels with temperatures below 10 °C are flagged as cloud contaminated.

Each pixel must satisfy all the above criteria (pass all test) to be judged as cloud-free. The cloud detection model was written in ERDAS modelling language (Fig. 4.100). This model was executed for each of the AVHRR images. The final output for each image was a Boolean image (cloud mask) with cloud-contaminated pixels and land areas flagged with a value of zero and cloud-free pixels flagged with a value of one (Fig. 4.101.).

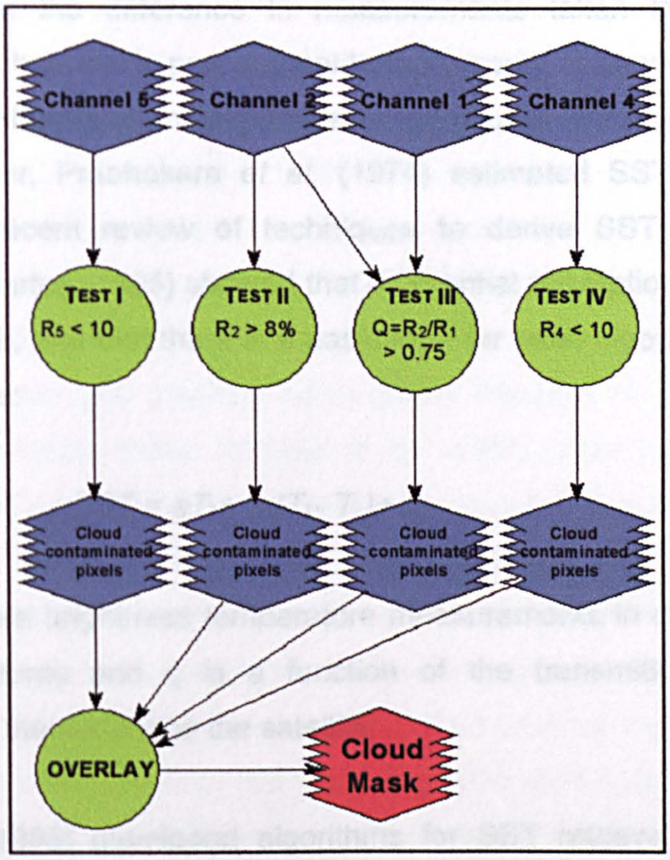

Fig. 4.100: Outline of the algorithm applied to AVHRR image to detect cloud contaminated pixels (model developed in ERDAS).

Fig. 4.101: Example of a cloud mask for an AVHRR-14 image (06-08-1999).

4.6.3.6 Atmospheric Correction for Channels 4-5

Various techniques have been proposed to correct for the atmospheric absorption of surface IR radiance, to produce accurate retrievals of SST. Anding and Kauth

(1970) found that the difference in measurements taken from two properly selected infrared channels is proportional to the amount of atmospheric correction required. Using differences in brightness temperatures, measured with an early satellite radiometer, Prabhakara *et al.* (1974) estimated SST with reasonable accuracy. In a recent review of techniques to derive SST from satellite IR measurements, Barton (1995) showed that differential absorption is exploited in all IR SST algorithms, and that there is a basic form for most algorithms, called *split-window algorithms*:

$$SST = aT_i + g\,(T_i - T_j) + c \qquad \text{Eq. 4.21}$$

where T_i and T_j are brightness temperature measurements in channels i and j, a and c are constants and g is a function of the transmittance through the atmosphere from the surface to the satellite.

McClain *et al.* (1985) developed algorithms for SST retrieval based on linear differences in brightness temperatures among AVHRR channels. This so-called multi-channel sea surface temperature (MCSST) algorithm assumed a constant g. The MCSST algorithm was NOAA's operational procedure for several years, and is written as:

$$SST = \alpha_1 + \alpha_2 T_4 + \gamma\,(T_4 - T_5) \qquad \text{Eq. 4.22}$$

where α_1 and α_2 are constants determined through a least-squares fit to in-situ data. T_4 and T_5, are brightness temperatures as derived from channels 4 and 5 and γ is a weighting factor based on the knowledge of known absorption coefficients (Emery *et al.*, 1994). In this form, the linear model has no correction for water vapour attenuation. At present, there are more than 500 linear algorithms in use by NOAA, ESA and other organisations (CREPAD pers. comm.).

Subsequent improvements incorporated a correction for increased path lengths at larger satellite zenith angles (Cornillon *et al.*, 1987). Other improvements in the atmospheric correction involved non-linear (NLSST) formulations, in which g was proportional to the brightness temperatures, as in the CPSST cross-product SST (CPSST) algorithm described by Walton (1988) and Walton *et al.* (1990). At present, work is currently underway to determine the accuracy of the data using NLSST algorithm (Vazquez *et al.*, 1998). This algorithm is still in experimental stages, and further validation needs to be done to use them in practical work.

SST Algorithm for Canary Islands

SST algorithms have been determined at global (McClain *et al.,* 1985), regional (Shenoi, 1999) or local scales (Arbelo *et al.*, 2000), each having specific use depending on the size of the study area. The main challenge in developing a global SST algorithm is to achieve relatively uniform performance throughout a wide range of atmospheric and oceanic conditions. However, when conditions deviate from the so called "typical" atmosphere and ocean conditions, errors arise in SST retrievals (Shenoi, 1999). Deviations from implicit conditions are, thus, more likely in a global algorithm than in a regionally-tuned algorithms (Arbelo *et al.*, 1996). Emery and Yu (1997) demonstrated that the large-scale (>100 km) SST patterns remained the same irrespective of SST algorithm, while the absolute temperature magnitudes do not. In terms of absolute SST magnitude, the different algorithms can produce an error of 5 °C or more depending on the SST algorithm used (Llewellyn-Jones *et al.*, 1984; Emery and Yu, 1997). Thus, it is not recommended to use global algorithms in regional studies that require absolute knowledge of the SST because a certain degradation of the results is expected (Cracknell, 1997).

In areas such as the Canary Islands, use of global coefficients has been reported to be inadequate and inaccurate (Arbelo *et al.,* 1996;). Moreover, when an algorithm has been designed to be used with data from the AVHRR instrument on board a specific NOAA satellite, if applied to data from another AVHRR sensor, the error can be as large as 2.3 °K (Czajkowski *et al.*, 1998). This is because filter functions for AVHRR channels 4 and 5 change between sensors, in both spectral band width and sensitivity. Consequently, for accurate SST retrieval in this study, a local algorithm for the Canary Island was used. In addition, as AVHRR images on board NOAA-14 satellite were used, it was desirable to apply an algorithm specifically derived for this satellite.

There have been several algorithms developed for the Canary area. The firsts algorithms developed were simple split-window linear algorithms with the coefficients optimised using radiosounding profiles of air temperature and humidity carried out on site. The latest algorithms of this kind were developed by Ariz *et al.* (1998) and CREPAD (pers. comm.). The former made use of vertical profiles of several atmospheric parameters (such as humidity, temperature, ozone, carbon dioxide, etc.) measured by 30 atmospheric sensors launched from Tenerife. This information was used to estimate the values of the coefficient in the SST algorithm (Eq. 4.23) with a standard error of 0.2 °K.

$$SST = 0.033 + T_4 + 1.804\ (T_4 - T_5) \qquad \text{Eq. 4.23}$$

The split-window algorithm used by CREPAD was as presented by McClain (1985). The coefficients were tested and validated by the Canary Marine Sciences Institute (ICCM) in 1997-1998 with *in situ* readings from 4 marine buoys (Sounobouy Sized Databouys) equipped with sea temperature sensors at 1 m depth, atmospheric pressure and temperature. The algorithm was shown to perform well for the Canary area, therefore, it was used in its original form (CREPAD and ICCM pers. comm.):

$$SST = -283.21 + 1.0346T_4 + 2.5779\ (T_4 - T_5) \qquad \text{Eq. 4.24}$$

Arbelo *et al.* (1996) presented an alternative approach to current algorithms, obtaining better results than previous algorithms. The new split-window method combined the information supplied by the TOVS (Tiros Operational Vertical Sounder) and AVHRR sensors onboard NOAA satellites. The coefficients *A* and *B* were determined as a function of the water vapour content (*W*), which is calculated using the TOVS sensor. The T_4 and T_5 temperatures were supplied by the AVHRR system (Fig. 4.102). Combination of both sensors avoids the necessity of making radiosoundings and their associated problems. However, a drawback of this method is its complexity for use in multiple image processing due to the integration of information from two different sensors.

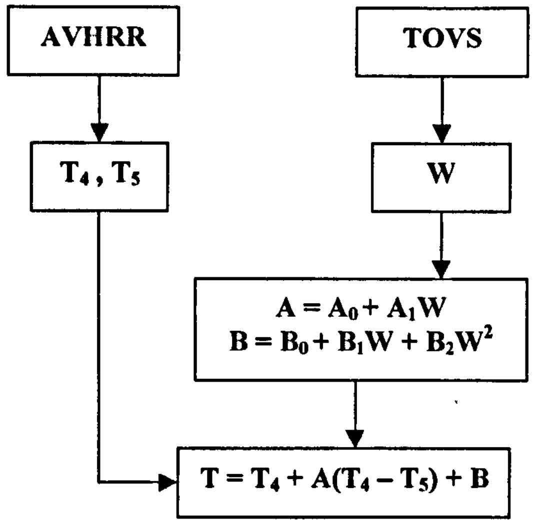

Fig. 4.102: Summary of the proposed method which combines TOVS and AVHRR data (redrawn from Arbelo *et al.*, 1996). The coefficients A and B of split-windows were calculated from results obtained by Coll and Caselles (1994). A_0=1.95, A_1=0.33, B_0=-0.21+0.4091 secθ, B_1=-0.0364+0.0888 secθ, B_2=-0.2219+0.0748 secθ

The latest state of the art SST algorithm for the Canary Islands region (used in this study) was developed by Arbelo *et al.* (2000). This algorithm, developed for AVHRR-NOAA14 images, takes into account not only the water vapour content as the linear algorithms, but a whole range of atmospheric gases (H_2O, CO_2, O_3, CO, CH_4, N_2O, NO, NO_2, NH_3, O_2 and SO_2) and aerosols, as well as the satellite scan angle (θ). This algorithm has been validated with field data, and its standard deviation is 0.4 °K (Arbelo pers. comm.). The split-window equation is:

$$SST= 1.0186\, T_4 + 1.2348\, (T_4 - T_5) + 1.3178\, (T_4 - T_5)\, (\sec\theta - 1) - 4.4616 \qquad \textbf{Eq. 4.25}$$

where:

SST = Sea Surface Temperature
T_4 = brightness temperature in channel 4
T_5 = brightness temperature in channel 5
θ = satellite scan angle

The satellite scan angle (θ) was incorporated in the SST algorithm (Eq. 4.25) as a layer. This layer was created as follows (Arbelo pers. comm.). An AVHRR image is composed of 2046 pixels per line. The maximum scan angle for the AVHRR sensor is 55.37° to each side (Fig. 4.103), therefore, the scan angle per pixel can be estimated by dividing the total scan angle (55.37°) by the number of pixels in half the scan line (1024), resulting in an angle increment of 0.054072265° per pixel. In other words, the first pixel starting from the left hand side of the image will have an angle of 55.37°, the following pixel will have a value of 55.37° - 0.054072265° = 55.31592773° and so on. At the nadir position, the angle will be zero degrees. From nadir position to the right hand side of the image, the angle will increase in the same way as explained before until it reaches the last pixel on the right, having a value of 55.37°. Fig. 4.104 shows the satellite scan angle layer created. This image is composed of 2048 columns and 1440 lines. However, the computation of sea surface temperature was restricted to a 45° scan angle on either side of the nadir so as to avoid pixels near the edges of the scan which are viewed highly obliquely. These pixels correspond to areas whereby the radiation travels through a very long atmospheric path to reach the satellite, and contamination by water vapour present in its field of view increases considerably with an increase in path length (Sasamal, 1999). Therefore, scan angles greater than 45° were masked (Fig. 4.105).

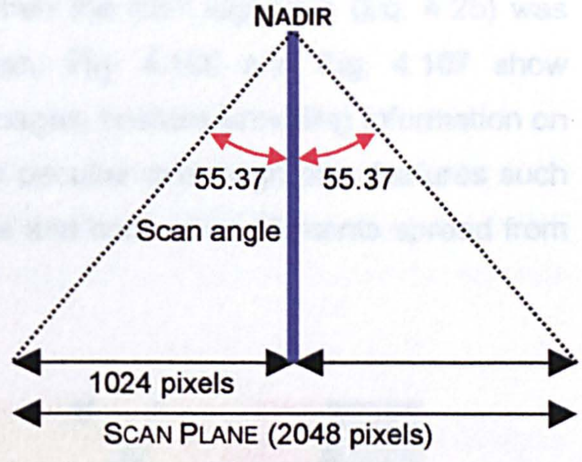

Fig. 4.103: Scan angle.

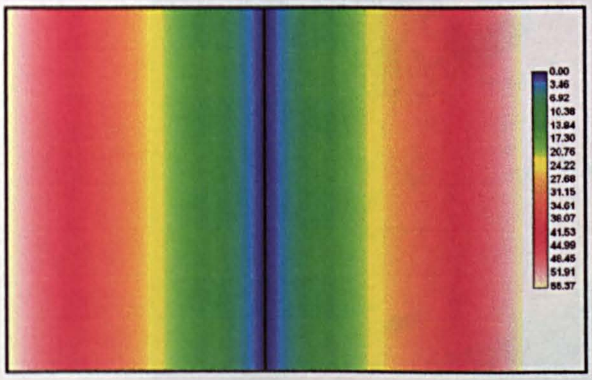

Fig. 4.104: Satellite scan angle.

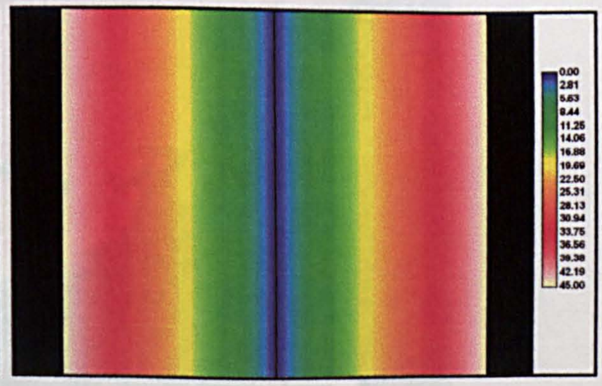

Fig. 4.105: Modified satellite scan angle layer used in the SST algorithm (Eq. 4.25). Scan angle greater than 45° were masked

A set of 135 SST images was created when the SST algorithm (Eq. 4.25) was applied to each of the cloud-free images. Fig. 4.106 and Fig. 4.107 show examples of two of these images. These images, besides providing information on sea surface temperature, also show some peculiar oceanographic features such as island-induced eddies, warm water tails and cold water filaments spread from the African coastal upwelling.

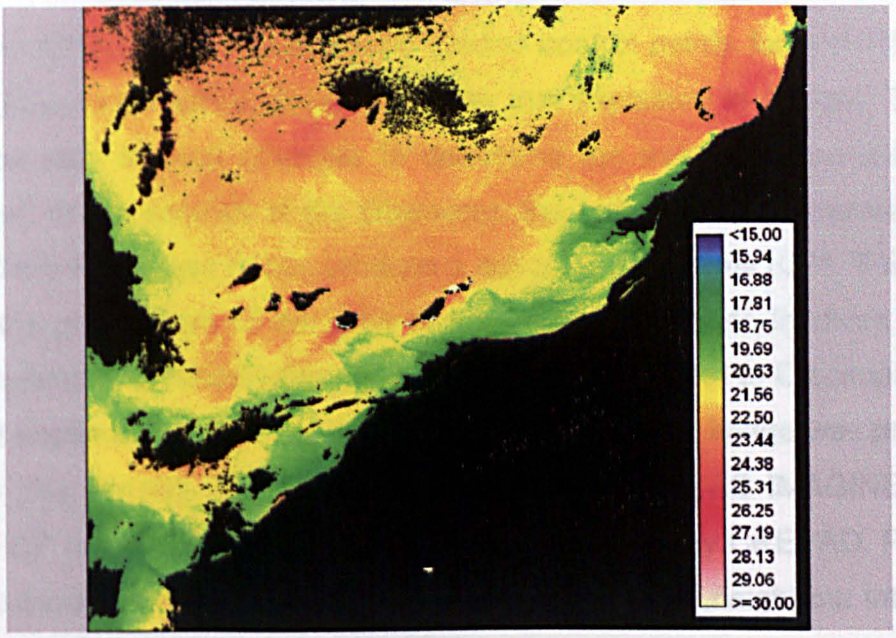

Fig. 4.106: Example of SST image (06-08-1999) derived from AVHRR-NOAA 14.

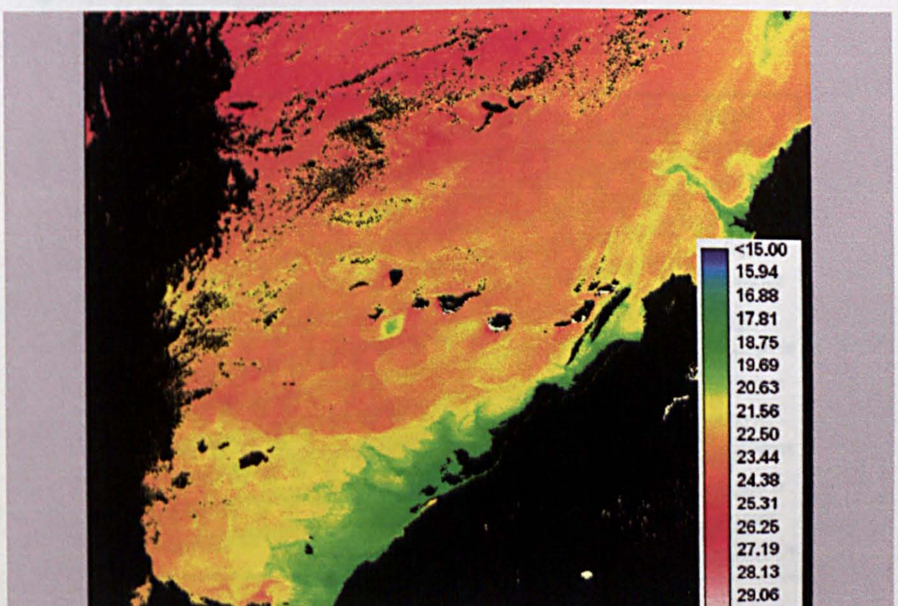

Fig. 4.107: Example of SST image (23-08-1999) derived from AVHRR-NOAA14.

4.6.3.7 Geometric Corrections (Referencing And Resampling)

The final processing step was the georeferencing of all images. Georeferencing involves precise transformation of the image from the sensor-based raw data to an earth surface-based projection. This is done by matching ground and image-based control points, then transforming and resampling the data to a map projection coordinate system (Campbell, 1996). Images were georeferenced to latitude-longitude.

Due to the difficulty of obtaining good ground control points for AVHRR images, the georeferencing method used differ from that explained in Chapter 3 (Section 3.5.2). The new method attempts to determine the exact position and attitude (orientation) of the satellite at the time when the radiation was received from the surface of the Earth, and hence produce a set of control points (CP). This involves knowing the parameters of the orbit of the satellite and also involves using the quite complicated spherical trigonometry of the system (refer to Cracknel, 1997 for a detailed explanation). A set of 280 CPs for each AVHRR image was provided by CREPAD (Fig. 4.108). Georeferencing was done in ERDAS IMAGINE software using the CP and following the methodology established by CREPAD. Polynomial geometric mode transformation (sixth order) using nearest neighbour interpolation methods to estimate the image intensity in each new pixel was applied to each image (CREPAD pers. comm.). Fig. 4.109 shows an example of a georeferenced AVHRR image (cloud free).

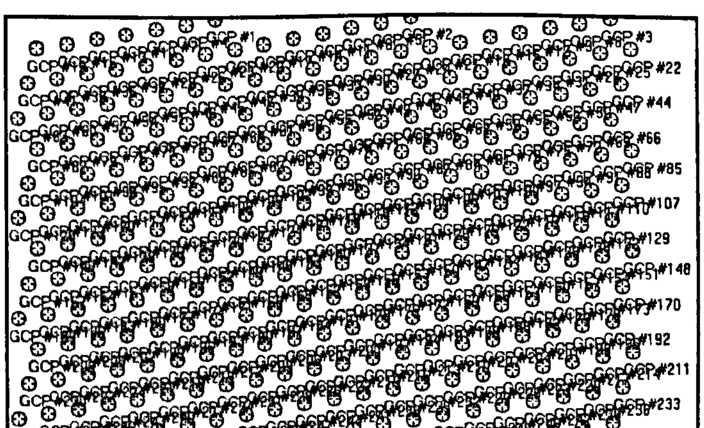

Fig. 4.108: Example of a set of 280 CPs used for georeferencing AVHRR images.

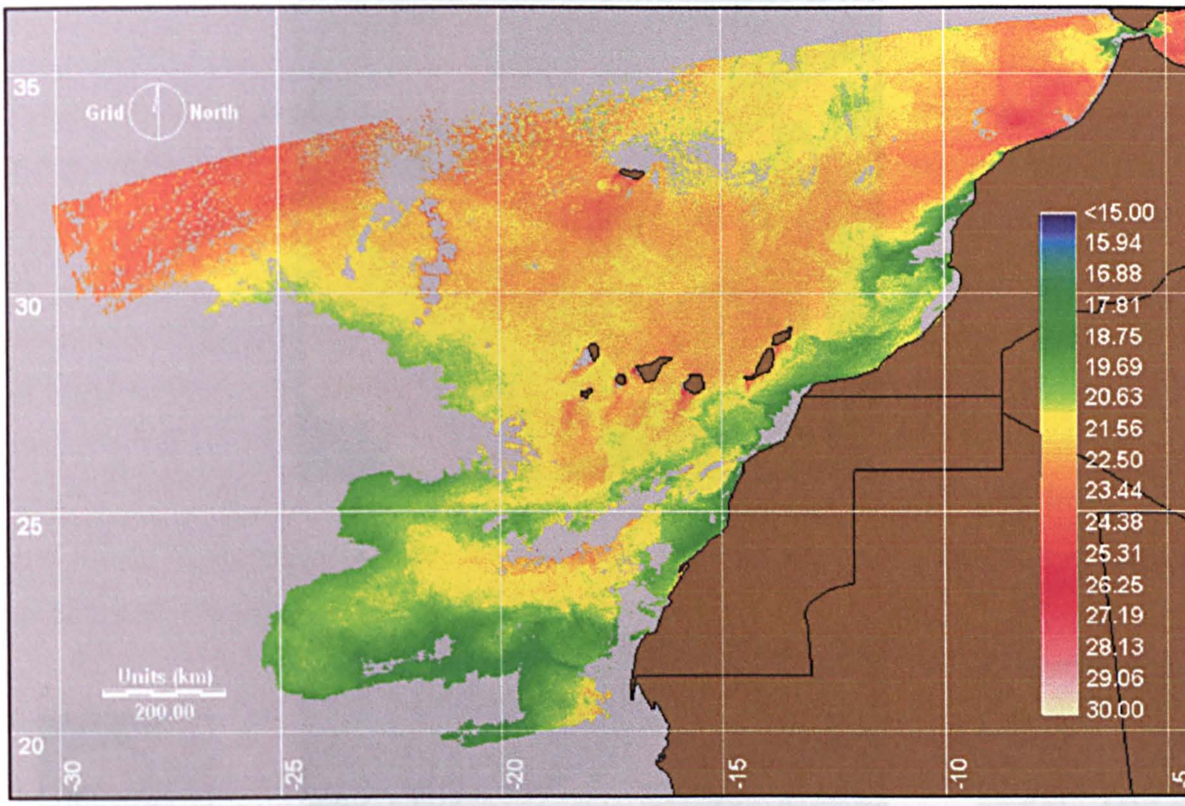

Fig. 4.109: Example of a georeferenced SST image, 16-07-1999 (values are in °C).

4.6.3.8 Compositing and Scoring

All images were combined to generate a single composite map, which was then used to obtain average values of sea surface temperature (Fig. 4.110). This image was reclassified for aquaculture using the suitability scores shown in Table 4.34. Fig. 4.111 shows the average SST suitability map created.

Table 4.34: Suitability scores of SST for aquaculture (values are in °C).

Criterion \ Score	8	7	6	5	4	3	2	1
SST	24-26	24-22 26-27	22-20 27-28	20-18 28-29	18-16 30-31	16-14 31-32	14-12 32-33	<12 >33

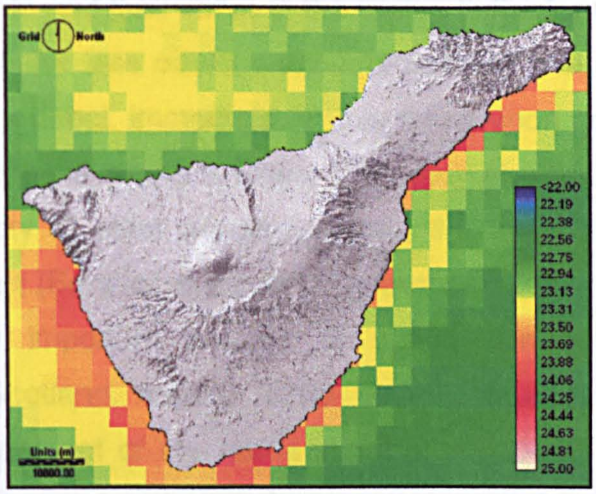

Fig. 4.110: Average SST (values are in °C).

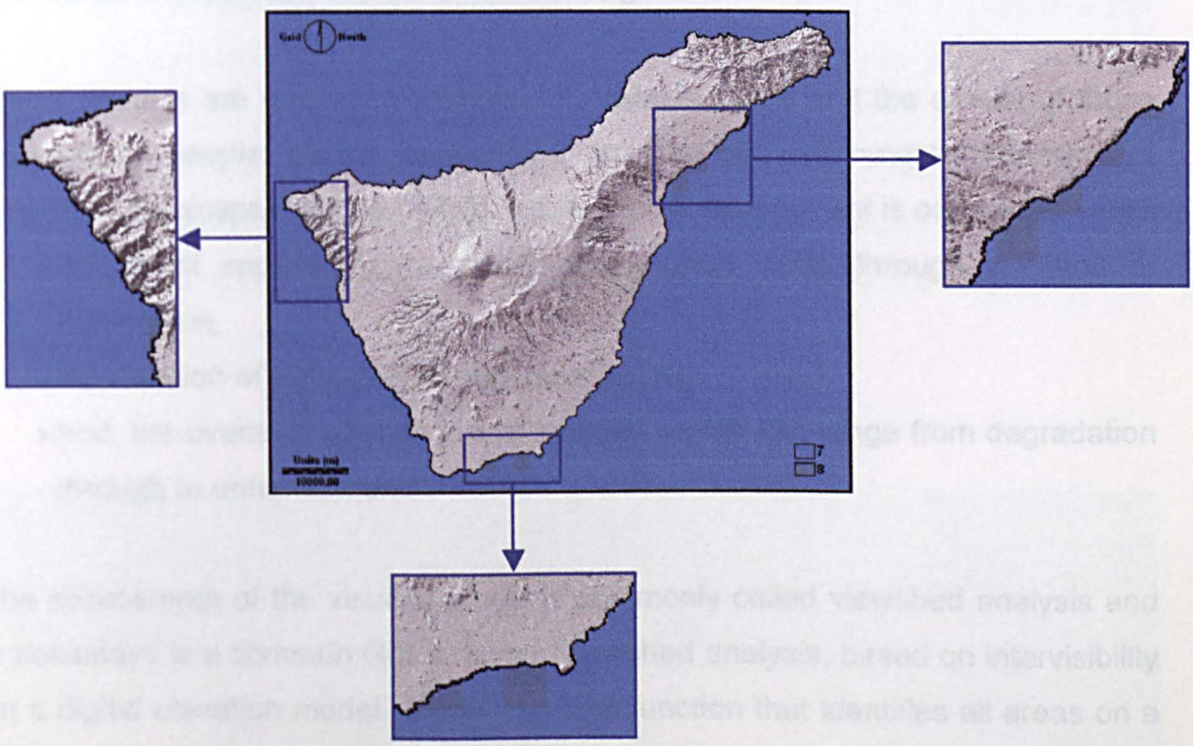

Fig. 4.111: SST suitability map.

4.7 VIEWSHED SUBMODEL

Visual impacts have a high aesthetic component which can be culturally biased, but they also derive from poor design, inattention, and large-scale physical alterations to land (Institute of Environmental Assessment and The Landscape Institute, 1995). Scenic landscapes and other natural attractions provide the basis for tourism in Tenerife and their value in the region to the tourism industry must be fully appreciated. Unlike less obvious impacts such as changes in water quality, visual impact have a direct, immediate, visible effect upon people's surroundings, and therefore may arouse strong feelings. They may also be used by the public as a focus for a variety of other concerns about the impact of marine fish cage farming development (Beveridge, 1996). The author referred to visual impacts as one of the most important causes of public concern about cage farm developments in Scotland, Ireland, Chile and North America. Therefore, it is essential that assessment of the visual impacts of a proposed fish cage site is carried out in as measured and controlled a way as possible. This will involve not only careful prediction of the nature and scale of potential changes, but also assessment of the significance of those changes.

Visual impacts are related to changes in available views and the effects of those changes on people. Hence, according to Institute of Environmental Assessment and The Landscape Institute (1995), visual impact assessment is concerned with;

- the direct impacts of the development upon views through intrusion or obstruction,
- the reaction of viewers who may be affected,
- and, the overall impact on visual amenity, which can range from degradation through to enhancement.

The assessment of the visual impacts is commonly called viewshed analysis and is nowadays is a common GIS function. Viewshed analysis, based on intervisibility on a digital elevation model (DEM), is a GIS function that identifies all areas on a terrain surface that are visible from a pre-defined observation point (Lee and Stucky, 1998). The result of a classical viewshed operation within a raster GIS is a Boolean visibility map, a cell is either classified as visible or invisible (Nackaerts *et al.*, 1999).

A wide variety of applications using visibility information have been described in literature. These include civil engineering, orientation, navigation (Nagy, 1994), visual impacts analysis (Kent, 1986; Hadrian *et al.*, 1988), siting optimisation (de Floriani *et al.*, 1994) and other intervisibility studies (Wheathly, 1995).

The viewshed analysis in IDRISI32 was made by using the module VIEWSHED. This module calculates all cells directly in view of a set of target cells specified on a separate image. To do so, VIEWSHED extends visual rays in all directions and traces lines of sight to the height of cells to determine whether or not they are in view. The two criteria used for estimating visibility of potential fish farm sites, and hence their suitability, were; (1) visibility from important tourist resources, and (2) visibility from beaches.

The visibility from tourist resources (buildings) was calculated as follows. First, the most important tourist resources were identified (Fig. 4.112). For these 15 sites, building distribution was obtained from Fig. 4.113. The module VIEWSHED was then used in combination with the DEM for Tenerife (Fig. 4.79) to calculate the visibility of potential farm sites in the vicinity of these tourist resources. This module takes into account the altitude at which every building is placed. The building distribution, obtained as a vector file from CD-Map (1999), was imported into IDRISI32 and later georeferenced using the module RESAMPLE (Fig. 4.113). The visibility distance was set to 2 kilometres because cages are flat, small and not very visible structures.

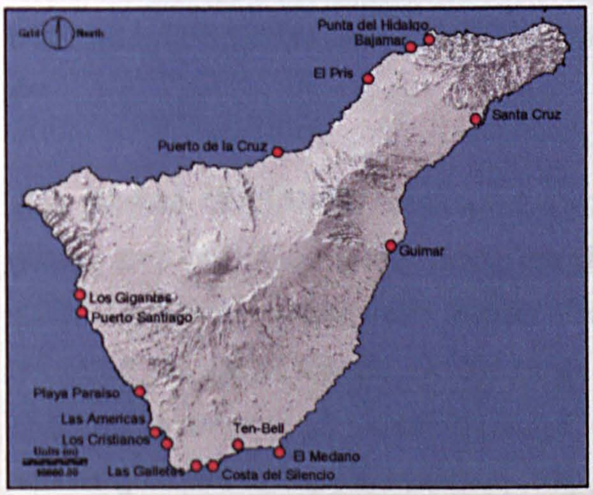

Fig. 4.112: Main tourism resources in Tenerife.

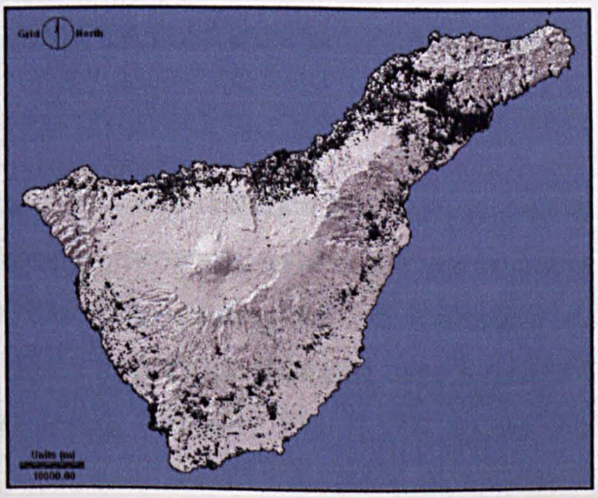

Fig. 4.113: Building distribution in Tenerife.

Fig. 4.114 shows the visibility map from tourist resources created and Fig. 4.115 the visibility from tourist resources suitability map. Suitability scores assigned were a value of one (totally-unsuitable) for visible areas, and eight (very-suitable) for not visible areas.

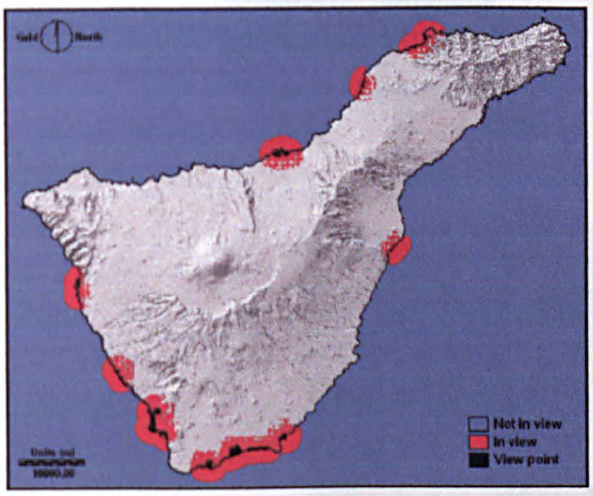

Fig. 4.114: Visibility from tourist resources model.

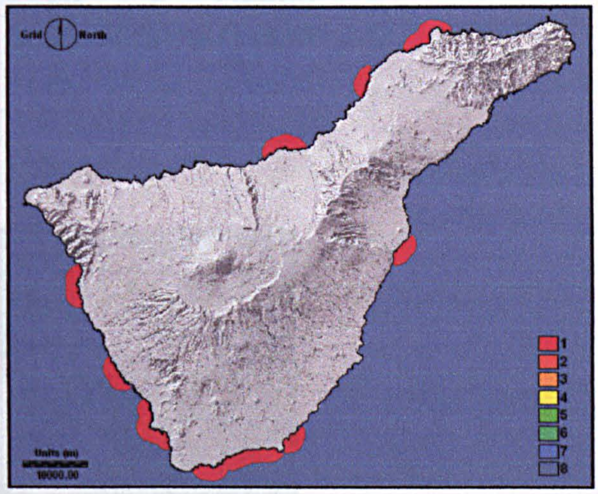

Fig. 4.115: Visibility from tourist resources suitability map

Visibility from beaches was calculated by setting distance threshold values at sea level to designate if a cage would be visible from a beach (scored to value 1; totally-unsuitable) or is not visible (scored to value 8; very-suitable). Values were different for beaches classified as important and for those classified as not important. The beach importance classification followed is as proposed in section 4.1.

The module DISTANCE was used to calculate the distance from each beach group, and later reclassified using the distance threshold values shown in Table 4.35. Threshold values are bigger for beaches catalogued as important to minimise the visual impact. On the other hand, threshold values for less important beaches is smaller as visual impact is of lesser concern. Fig. 4.116 shows the resulting beach viewshed suitability map.

Table 4.35: Distance threshold values (m) used for each beach group.

Criteria \ Score	1	8
Distance Beach-1	2500	> 2500
Distance Beach-2	2000	> 2000
Distance Beach-3	1500	> 1500
Distance Beach-4	1000	> 1000

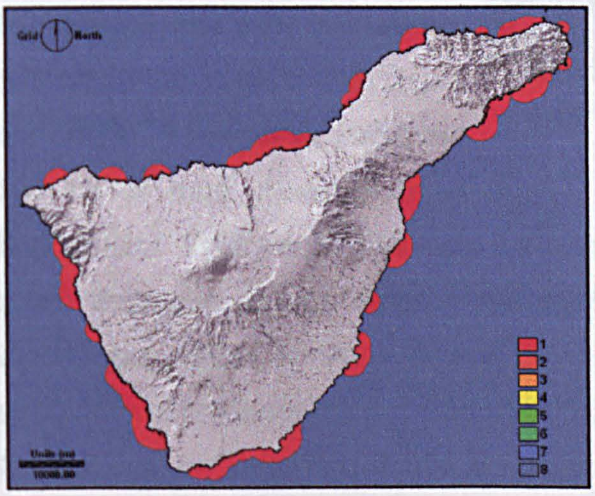

Fig. 4.116: Beach viewshed suitability map.

4.8 CONSTRAINTS SUBMODEL

Constraints are criteria which serve to limit the alternatives under consideration (Eastman, 1993), and are represented as Boolean map (images containing either one or zero). Five constrains were identified in this study: (1) seagrass meadows, (2) sewage pipes, (3) ports (inside and proximity), (4) windsurfing in El Medano, and (5) proximity to industrial areas.

4.8.1 Seagrass Meadows

Seagrasses are key ecosystems because they are important contributors to biological productivity. They provide habitats for many marine organisms, while acting as traps for sediment, and as buffers against wave action (Reyes *et al.*, 1995). Seagrasses (Fig. 4.117) differ from seaweeds in being vascular flowering plants and possessing a system of roots (Larkum *et al.*, 1989). They occur in shallow waters over soft sediments worldwide, from cool temperate climates to the tropics. The distance to which seagrasses extend out from the shoreline is normally determined by the slope of the seafloor. If suitable sediment is present, the seagrasses will extend to the depth at which the annual light flux is just sufficient to support a positive balance of photosynthesis over respiration. However, various conditions may interact with depth in governing light penetration. If the water becomes turbid with suspended silt or mud, possibly as a result of a construction project, light penetration will be reduced and the depth range of seagrasses will decrease. If high nutrient conditions, such as may be caused by sewage discharges, cause a heavy growth of epiphytic algae on the seagrasses or a dense bloom of phytoplankton in the water column, the amount of light reaching the leaves will be reduced. If silt or phytoplankton settles on seagrass leaves, the amount of light reaching the leaves will be further reduced (Mann, 2000).

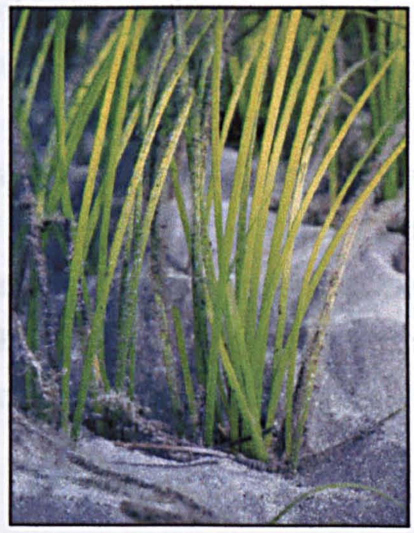

Fig. 4.117: Seagrass (*Cymodocea nodosa*).

The most common and abundant seagrass species in Tenerife is *Cymodocea nodosa* (Alfonso-Carrillo and Gil-Rodriguez, 1980) which forms monospecific submarine meadows or populations mixed with the green alga *Caulerpa prolifera*. *Cymodocea nodosa* is generally established in shallow areas of reduced water activity to about 35 m depth. The northern coast of the island is influenced by the Trade Winds coming from the northeast, leading to high water activity, with strong currents and frequent swell period. These high hydrodynamics, as well as the rocky nature of the shallow bottom, prevent the establishment of *Cymodocea nodosa* meadows. On the other hand, the southern coast is partially protected from the action of the predominant winds and their shallow submarine bottom shows extensive areas with sandy-muddy substrate that permit the development of these meadows (Reyes *et al.*, 1995).

Seagrasses are very sensitive to anthropogenic disturbances and have a very low recovery capacity. Decline of seagrass due to anthropogenic activities have been repeatedly documented (Ardizzone and Pelusi, 1984; Sánchez-Lizaso *et al.*, 1990) and thus is now a major concern in the conservation and management of marine coastal ecosystems (Mann, 2000). Although most of this loss has been attributed to human activities, such as industrial and domestic effluents and shore-line constructions (Shepherd *et al.*, 1989; Short *et al.*, 1995), effluents from cage fish farming might also have a negative effect on seagrasses meadows (Delgado *et al.*, 1997).

Fish farming induces high organic and nutrient loading into the surroundings (Beveridge, 1996). A significant fraction of the organic input (uneaten feed and faeces) accumulates in the sediment under and near by the cages, therefore degrading the benthic macrophyte communities, especially seagrass meadows (Casabianca *et al.*, 1997; Mendez *et al.*, 1997). Moreover, seagrass degradation have been reported long after fish farming activity was interrupted (Delgado *et al.*, 1999). Although organic enrichment seems to be the immediate cause of seagrass decline (Terrados *et al.*, 1999), the mechanisms involved in this decline appear to be relatively complex (Delgado *et al.*, 1999). Part of the organic matter derived from the cages becomes mineralised in the water, and thereby releases nutrients. These nutrients enhance phytoplankton, epiphyte and macroalgal growth which in turn reduces the light available to seagrass (Arzul *et al.*, 1996). A decrease in shoot density and biomass has been reported as a common response of seagrass to natural or artificial light reduction (Dennison and Alberts, 1982; Bulthuis, 1983). A significant fraction of the organic matter input is also incorporated into the sediment, and mineralised there. Under these conditions, anoxia prevails and sulphide compounds are formed due to the anaerobic oxidation of the organic material. Accumulation of reduced compounds have toxic effects on seagrasses (Carlson *et al.*, 1994). Another effect of sediment hypoxia is that all the oxygen requirements of the below-ground organisms have to be met by oxygen transport from the leaves (Smith *et al.*, 1984). Oxygen deficit increases the periods of root hypoxia, which can interfere with N metabolism (Romero *et al.*, 1998), and hence with seagrass growth and vitality. In light of these considerations, extreme caution in management decisions are needed if seagrass ecosystems are to be conserved.

The location of the seagrass areas in Tenerife was obtained from Marín and Luengo (1998). This map was scanned and imported to the GIS software as bitmap. Finally, the map was georeferenced using the module RESAMPLE within IDRISI32 and the data was on-screen digitised. The seagrass meadows layer was reclassified as a constraint (value of zero) where no fish farm can be sited. In addition, as wastes from fish cages are dispersed in adjacent areas (Perez *et al.*, 2002), a 300 metre buffer zone from seagrass meadows was established, and also classified as constraint. Fig. 4.118 shows the seagrass constraint layer created, illustrating the distribution of the meadows and the 300 metres buffer zone.

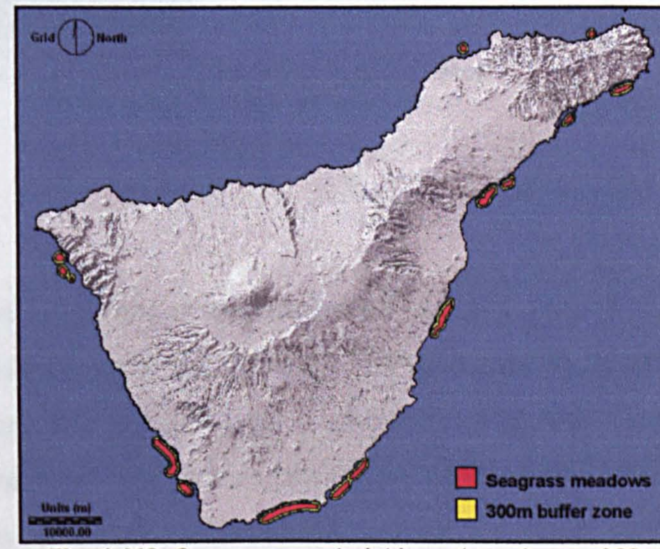

Fig. 4.118: Seagrass constraint layer (meadows + 300m buffer zone).

4.8.2 Sewage Pipes

Sewage pipes are a constraint because they make use of the same seabed space that cages need for mooring. In addition, because the anchor chain of a mooring system is a moving component (and sometimes the anchor itself) a 200 metres security buffer zone was set up to avoid damage to the sewage pipes. The location (Fig. 4.57), length and orientation of all sewage pipelines are known. The module DISTANCE was used to calculate distances from each pipe, which were later reclassified (RECLASS module) to establish a 200 metre buffer zone. Fig. 4.119 shows the sewage pipe constraint layer created.

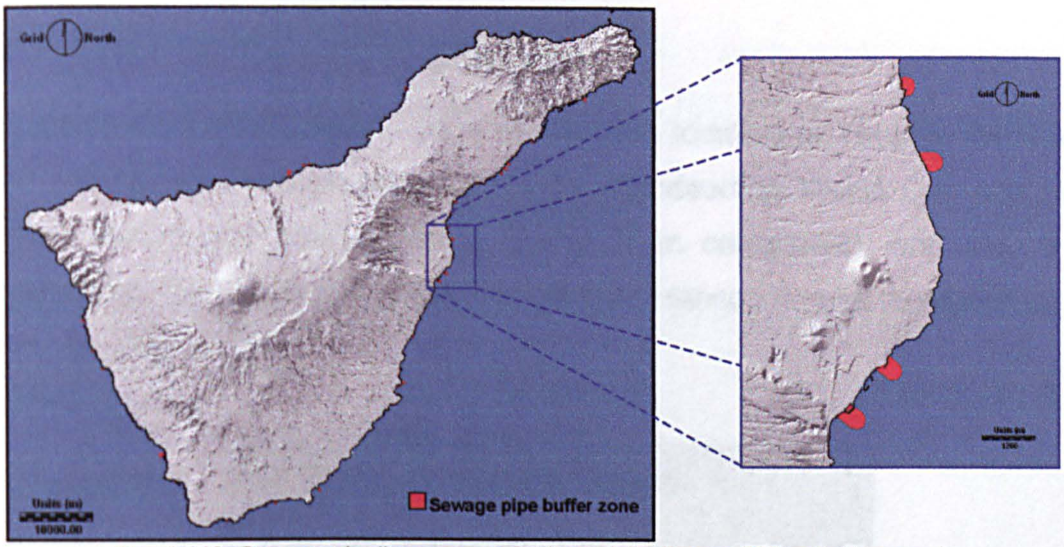

Fig. 4.119: Sewage pipelines constraint layer (pipelines + 200 m buffer zone).

4.8.3 Ports

The port constraint layer takes into account the enclosed areas of ports as well as a buffer zone outside the port, which can not be used for siting cages to avoid interference with navigation. The location of each port is shown in Fig. 4.6. The module DISTANCE was used to measure distances from ports, which were later reclassified (RECLASS module) using distance threshold values for each port category (fishing refuges and piers; section 4.3). Buffer zones for fishing refuges (400 m) were greater than for piers (200 m) because the former have higher boat traffic, both in terms of numbers and sizes of boats. Fig. 4.120 shows the port constraint layer created.

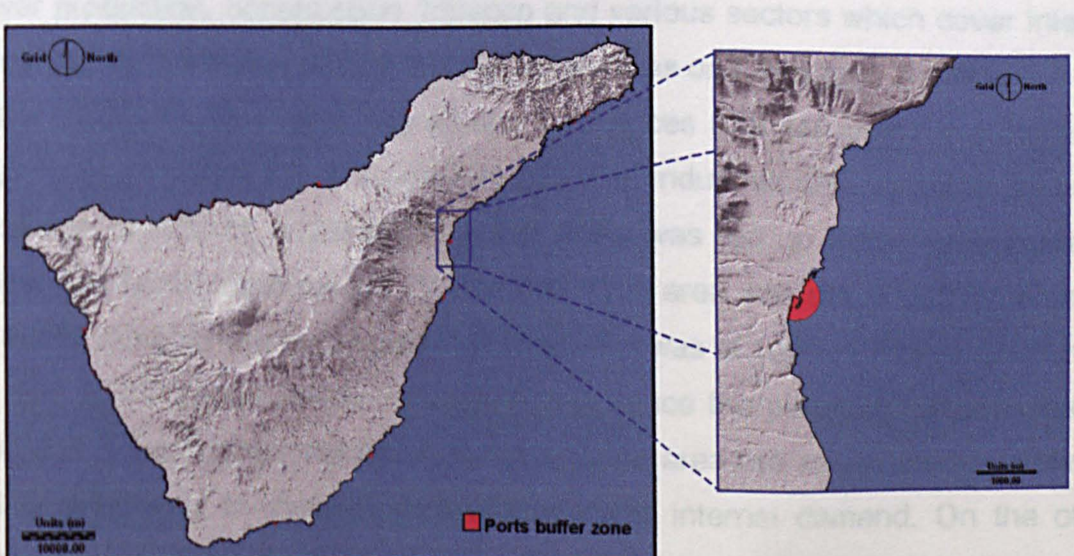

Fig. 4.120: Ports constraint layer.

4.8.4 Windsurfing in El Medano

The importance of El Medano as a windsurfing location in Tenerife has already been highlighted. This area is part of the Windsurfing World Cup competition (waves, slalom and course racing Grand Slam categories), and also a very popular spot for tourists visiting the island. Hence, it was considered as a constraint (Fig. 4.121).

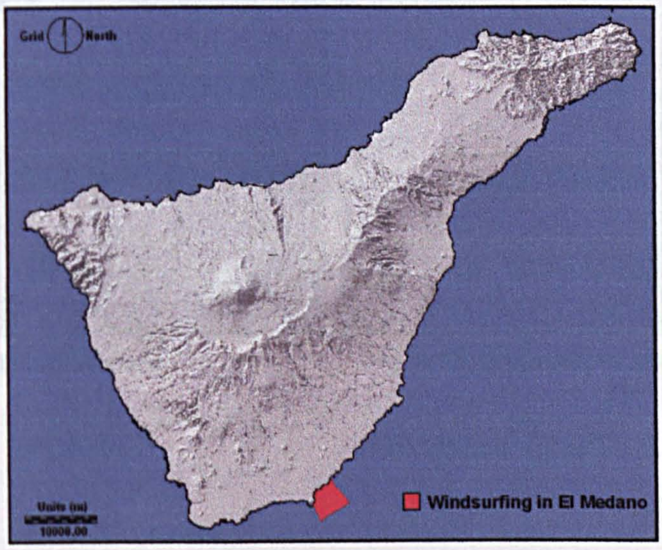

Fig. 4.121: Windsurfing in El Medano constraint layer.

4.8.5 Proximity to Industrial Areas

The most important industrial sectors in Tenerife are the food industry, electric power production, construction, tobacco and various sectors which cover internal demand. Fig. 4.122 shows the two industrial areas on the island. At present, none of the industries discharge any known substances that can present a threat for cage culture. Nevertheless, to prevent potential industrial developments that may discharge pollutants, a constraint buffer zone was set up from these industrial areas. The buffer zone for the Guimar industrial area was set to 500 m, whereas the buffer zone for the Granadilla industrial area was of 1000 m. These differences are due to the nature of the industries, and hence the potential hazardousness, allocated to each area. Industries in the Guimar area are small sized operations, mainly orientated to various sectors that cover internal demand. On the other hand, the industries located on Granadilla are bigger in size and dedicated to construction and electrical power production. This area also has higher boat traffic which supplies some of the industries. Fig. 4.123 shows the constraint layer created.

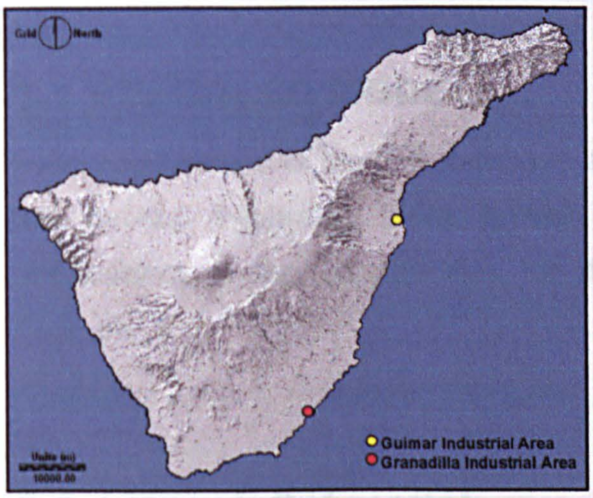

Fig. 4.122: Industrial areas.

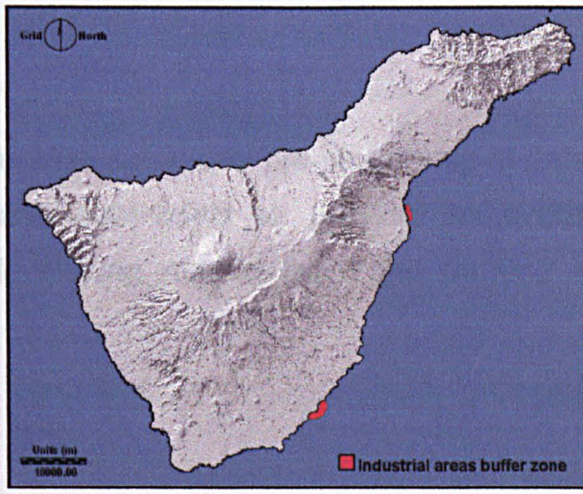

Fig. 4.123: Proximity to industrial areas constraint layer.

Chapter 5

GIS Modelling

5.1 GIS-BASED MODELS

Following creation of the GIS database and the necessary pre-processing of data, this section integrates these layers and submodels to provide an overall assessment of the opportunities for developing marine fish cage farming in Tenerife.

5.1.1 Beach Submodel

Once the most important beaches were identified (section 4.1), a subsequent classification focused on grouping these 79 beaches into four groups of importance, by using Multi-Criteria Evaluation (MCE). This submodel was designed to determine how important each beach is, and therefore, how suitable it will be to develop cage aquaculture in its proximity. For each beach, five criteria were selected to assess its importance; beach length, beach width, beach composition, rate of occupation (how much the beach is used by people) and rate of urbanisation (degree of infrastructure around the beach site). Table 5.1 shows the threshold values used for assigning the standardized criterion scores for each criteria. Basically, beaches that were short in length and width, with a low rate of occupation and urbanisation, and composition other than sand, scored as least important, and therefore, more suitable for aquaculture development in their proximities.

Table 5.1: Threshold values used for classification of beaches.

	Beach-4	Beach-3	Beach-2	Beach-1
Length	< 300 m	300-600 m	601-900 m	> 900 m
Width	< 15 m	15-30 m	31-45 m	> 45 m
Composition	Others	Sand+ gravel + cobble	Sand+ gravel	Sand
Rate of Occupation	Low	Medium		High
Rate of urbanisation	Virgin	Rustic	Semi-urban	Urban

The five criteria were scored and then their relative weights were calculated using the pairwise matrix shown in Table 5.2. The consistency ratio (CR) was less than 0.1, and hence, acceptable.

Table 5.2: Pairwise comparisons matrix used in classification of beaches.

	Length	Width	Composition	Occupation	Urbanisation
Length	1				
Width	1/2	1			
Composition	5	5	1		
Occupation	7	9	5	1	
Urbanisation	7	9	5	1	1

CR=0.06

Calculated weights were used in a MCE to combine the 5 criteria (Fig. 5.1). The output from this operation was a map with beaches classified from 1 (very important) to 4 (least important) depending on their degree of importance.

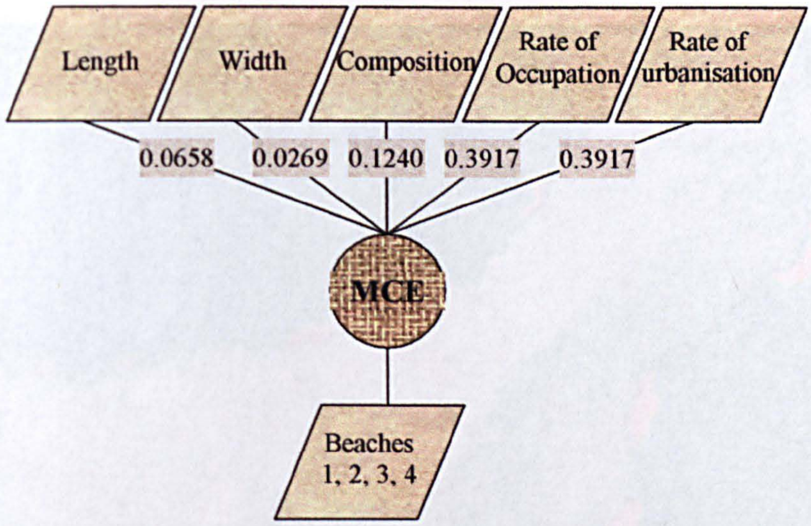

Fig. 5.1: Beaches MCE model showing the criteria used and calculated weights.

In a further manipulation, distances were measured from each of the four groups of beaches (DISTANCE module), and were reclassified (RECLASS) according to the distance threshold values shown in Table 5.3. Distances from beaches tagged as "very important" are greater than for those tagged as "least important".

Table 5.3: Distance threshold values (m) used for each beach group.

Suitability Scores	1	2	3	4	5	6	7	8
Distance Beach-1	<500	500-1000	1000-1500	1500-1750	1750-2000	2000-2250	2250-2500	>2500
Distance Beach-2	<500	500-750	750-1000	1000-1150	1100-1300	1300-1450	1450-1600	>1600
Distance Beach-3	<300	300-450	450-600	600-750	750-900	900-1150	1150-1300	>1300
Distance Beach-4	<300	300-400	400-500	500-600	600-700	700-800	800-900	>900

These four images were overlaid using the Minimum option, where the output pixels represent the minimum of those in corresponding positions on the other images. Fig. 5.2 shows the beach submodel suitability map, where areas close to beaches were scored low (less suitable for developing cage culture) and areas away from beaches scored high (most suitable for developing cage culture).

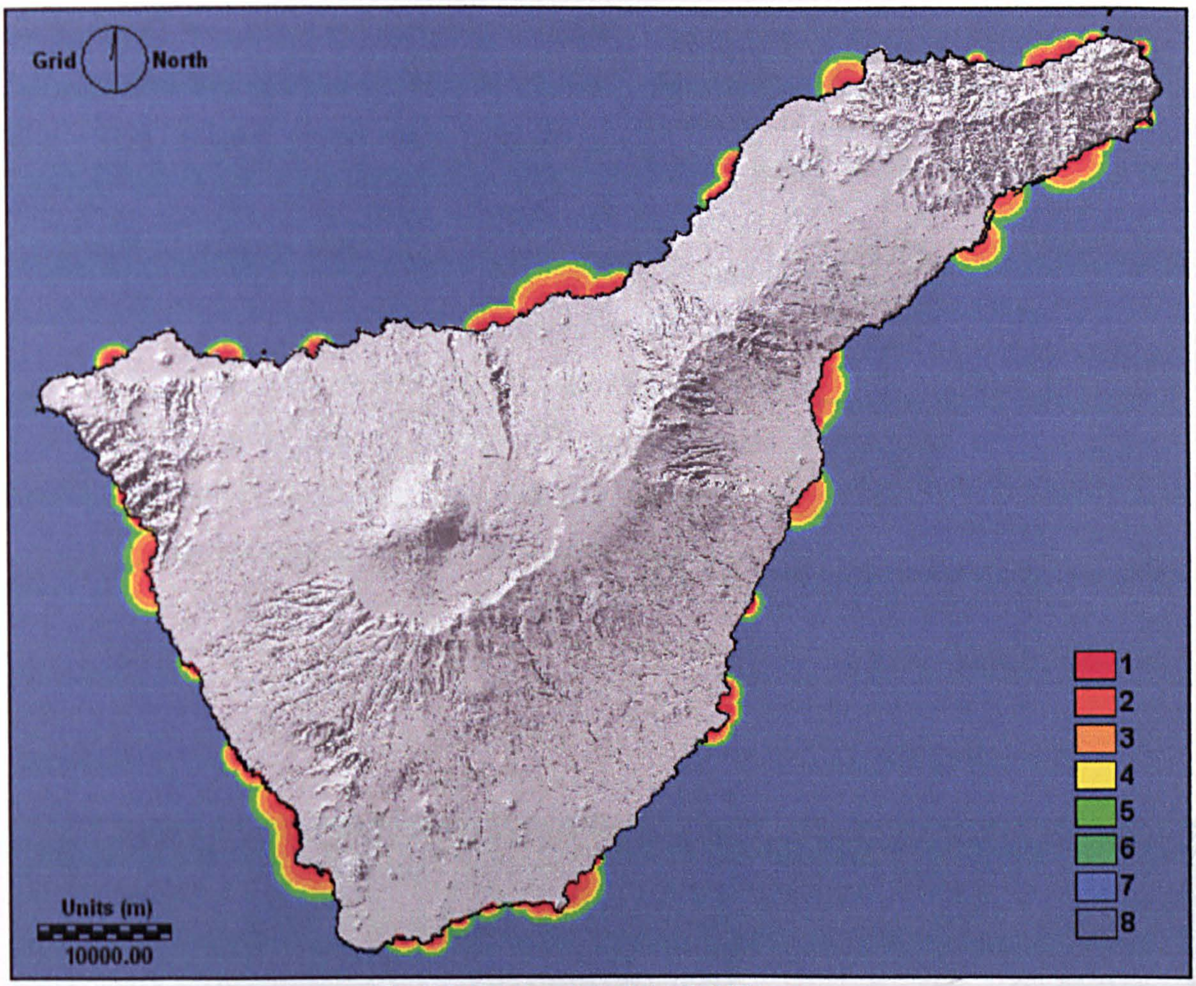

Fig. 5.2: Beach submodel suitability map.

5.1.2 Fishing Submodel

Weights of importance for each of the three criteria forming this submodel, fingerling accumulation (Fig. 4.3), pelagic fish accumulation (Fig. 4.4) and rocky platforms (Fig. 4.5), were calculated using the pairwise matrix shown in Table 5.4. The consistency ratio (CR) was less than 0.1, therefore, acceptable.

Table 5.4: Pairwise comparisons matrix for fishing submodel.

	Fingerling accumulation	Pelagic accumulation	Rocky platforms
Fingerling accumulation	1		
Pelagic accumulation	1/2	1	
Rocky platforms	1/9	1/6	1

CR=0.01

Calculated weights were used in a MCE to combine the criteria as shown in Fig. 5.3. The output from this operation, shown in Fig. 5.4, was the fishing submodel suitability map.

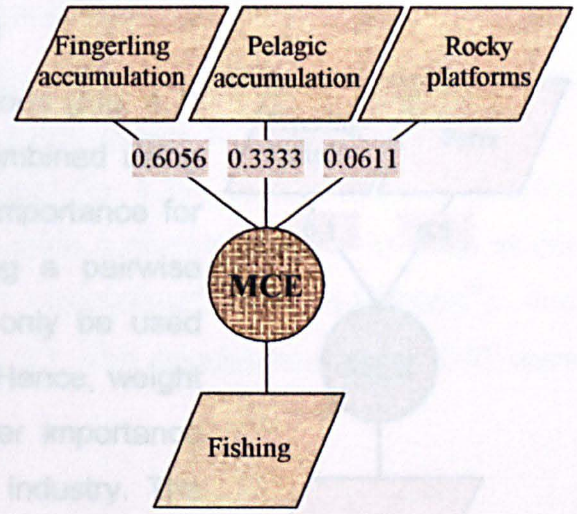

Fig. 5.3: Fishing MCE model showing the criteria used and calculated weights.

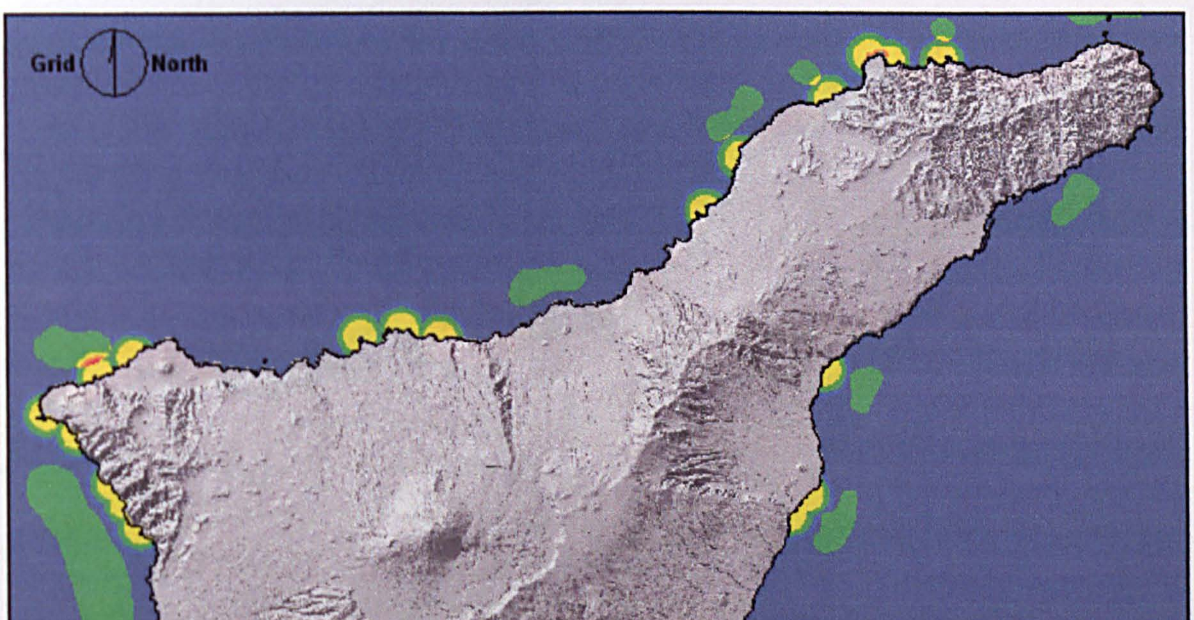

Fig. 5.4: Fishing submodel suitability map.

5.1.3 Infrastructure Submodel

The two criteria forming this submodel, ports (Fig. 4.7) and freezing Industry (Fig. 4.8), were combined using MCE as shown in Fig. 5.5. Weights of importance for these criteria were not calculated using a pairwise comparison matrix as this method can only be used when there are more than three criteria. Hence, weight values were estimated as shown. Greater importance was given to ports than to the freezing industry. The infrastructure submodel suitability map is shown in Fig. 5.6.

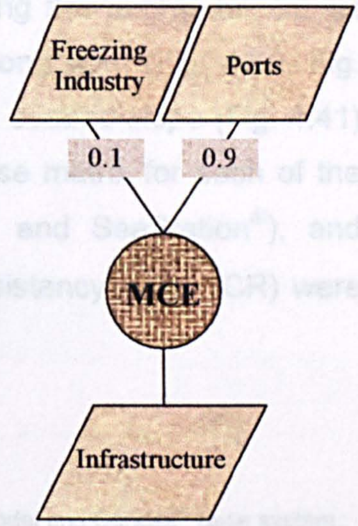

Fig. 5.5: Infrastructure MCE model showing the criteria used and estimated weights.

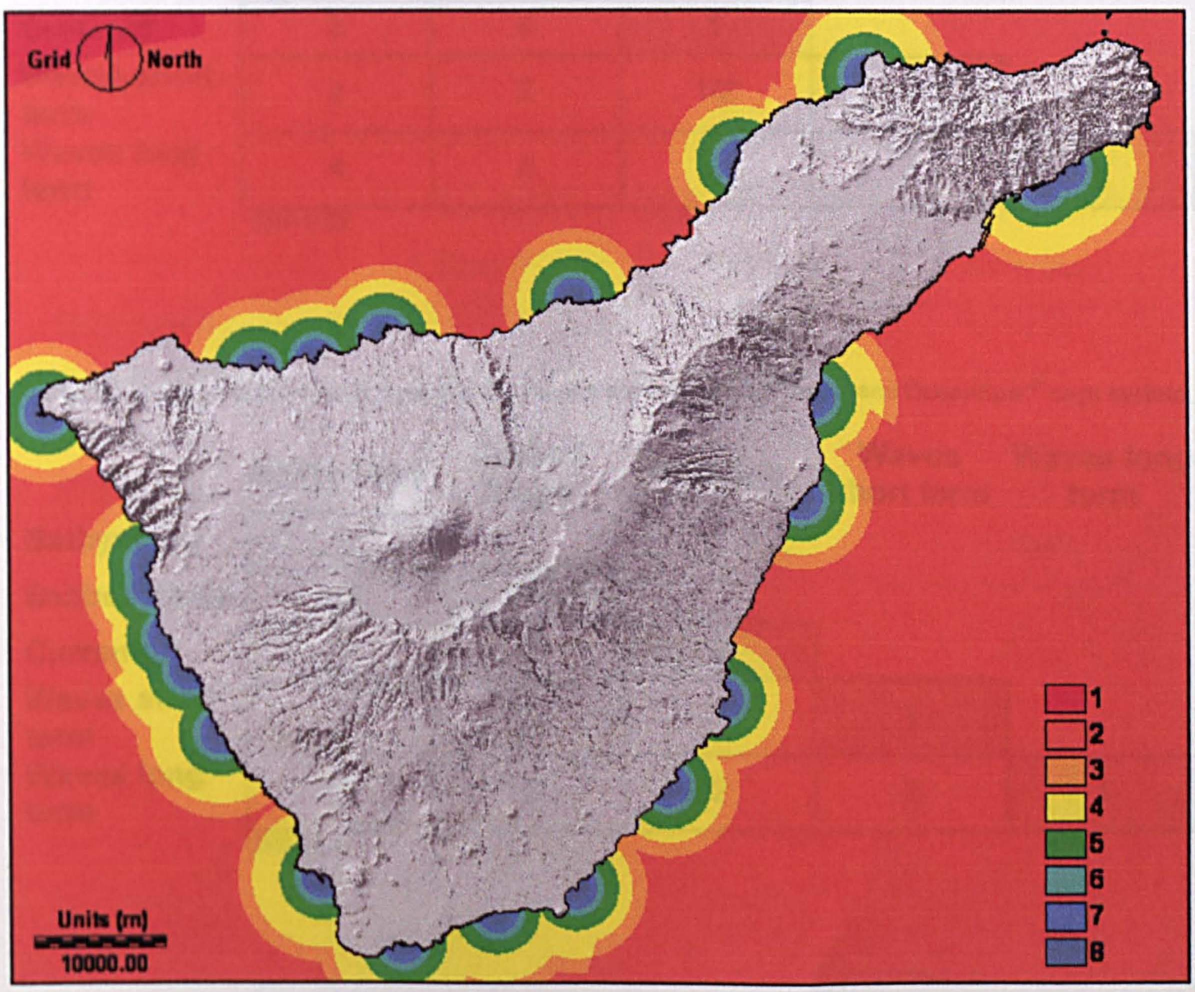

Fig. 5.6: Infrastructure submodel suitability map.

5.1.4 Marine Environment Submodel

Weights of importance for each of the five criteria forming this submodel, waves short term (Fig. 4.28, Fig. 4.30 and Fig. 4.32), waves long term (Fig. 4.29, Fig. 4.31 and Fig. 4.33), bathymetry (Fig. 4.37 and Fig. 4.39), seabed slope (Fig. 4.41) and currents (Fig. 4.47), were calculated using a pairwise matrix for each of the three cage systems selected (Corelsa®, OceanSpar® and SeaStation®), and shown in Table 5.5, Table 5.6 and Table 5.7. The consistency ratios (CR) were smaller than 0.1, therefore, acceptable.

Table 5.5: Pairwise comparisons matrix for the marine environment submodel and Corelsa® cage system.

	Bathymetry	Seabed Slope	Currents	Waves short term	Waves long term
Bathymetry	**1**				
Seabed Slope	1/2	**1**			
Currents	3	4	**1**		
Waves short term	2	2	1/2	**1**	
Waves long term	4	4	2	2	**1**

CR= 0.02

Table 5.6: Pairwise comparisons matrix for the marine environment submodel and OceanSpar® cage system.

	Bathymetry	Seabed Slope	Currents	Waves short term	Waves long term
Bathymetry	**1**				
Seabed Slope	1/2	**1**			
Currents	2	2	**1**		
Waves short term	2	2	1/2	**1**	
Waves long term	3	3	2	2	**1**

CR=0.03

Table 5.7: Pairwise comparisons matrix for the marine environment submodel and SeaStation® cage system.

	Bathymetry	Seabed Slope	Currents	Waves short term	Waves long term
Bathymetry	**1**				
Seabed Slope	1/2	**1**			
Currents	2	2	**1**		
Waves short term	2	2	1	**1**	
Waves long term	2	2	1	1	**1**

CR=0.01

Calculated weights for each cage system (Table 5.8) were used in a MCE to combine the criteria. The output from this operation was the marine environment suitability map for each cage system, and shown in Fig. 5.7, Fig. 5.8 and Fig. 5.9.

Table 5.8: Calculated criteria weights for each cage system.

	Corelsa® Weights	Ocean Spar® Weights	SeaStation® Weights
Bathymetry	0.1017	0.1257	0.1458
Seabed Slope	0.0729	0.0949	0.1097
Currents	0.2739	0.2376	0.2482
Waves short term	0.1659	0.1795	0.2482
Waves long term	0.3855	0.3623	0.2482

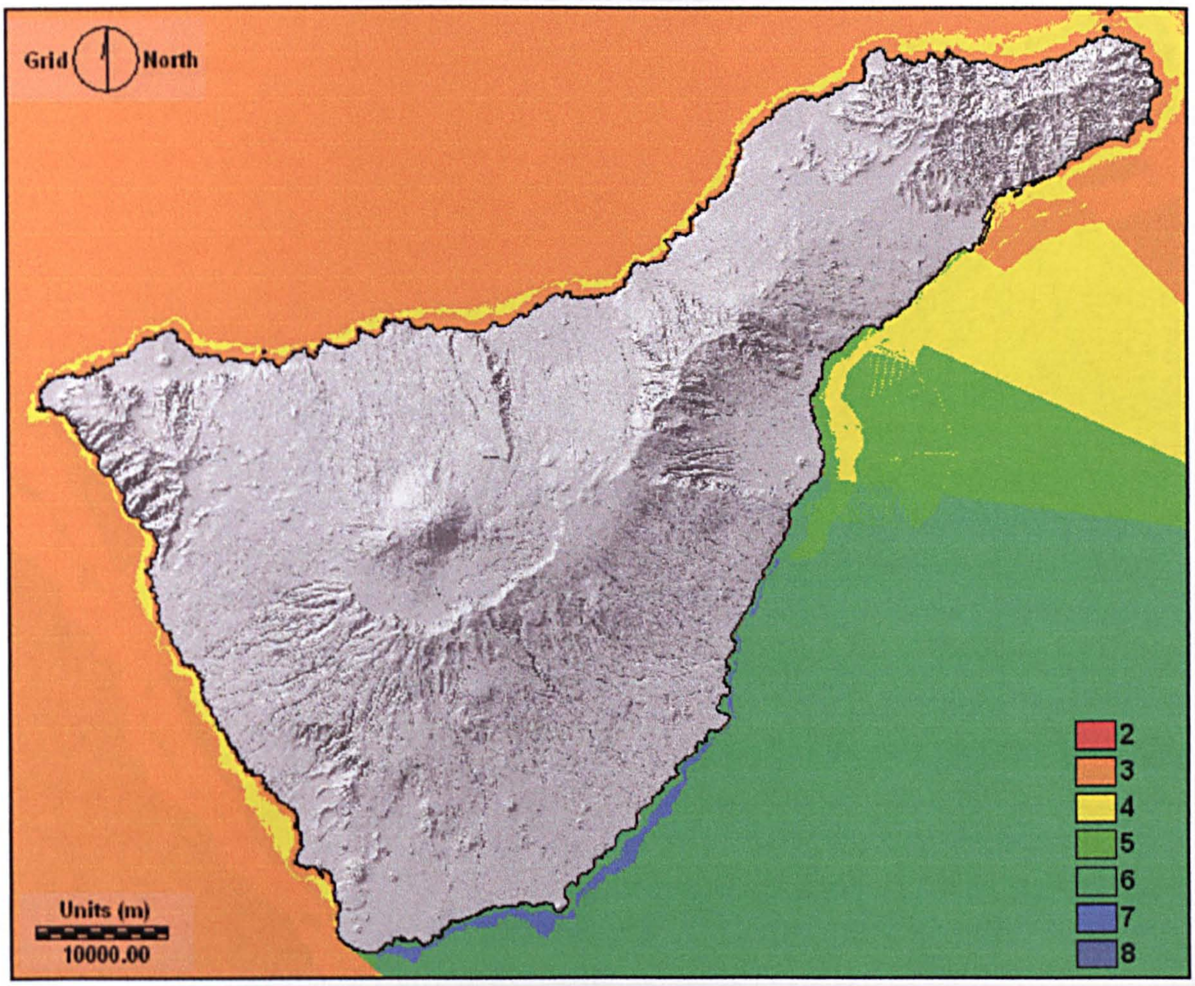

Fig. 5.7: Marine environment submodel for Corelsa® cage system.

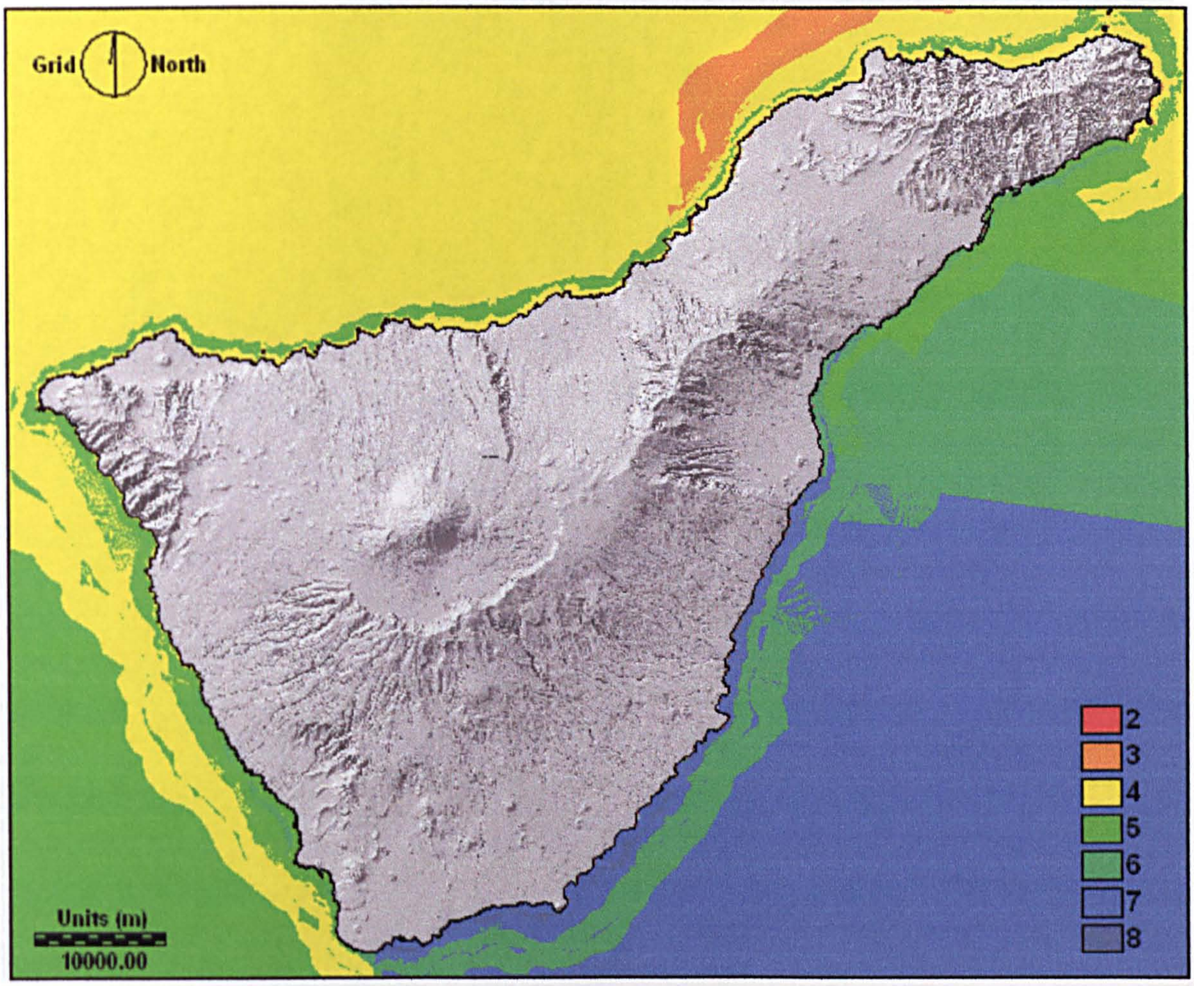

Fig. 5.8: Marine environment submodel for OceanSpar® cage system.

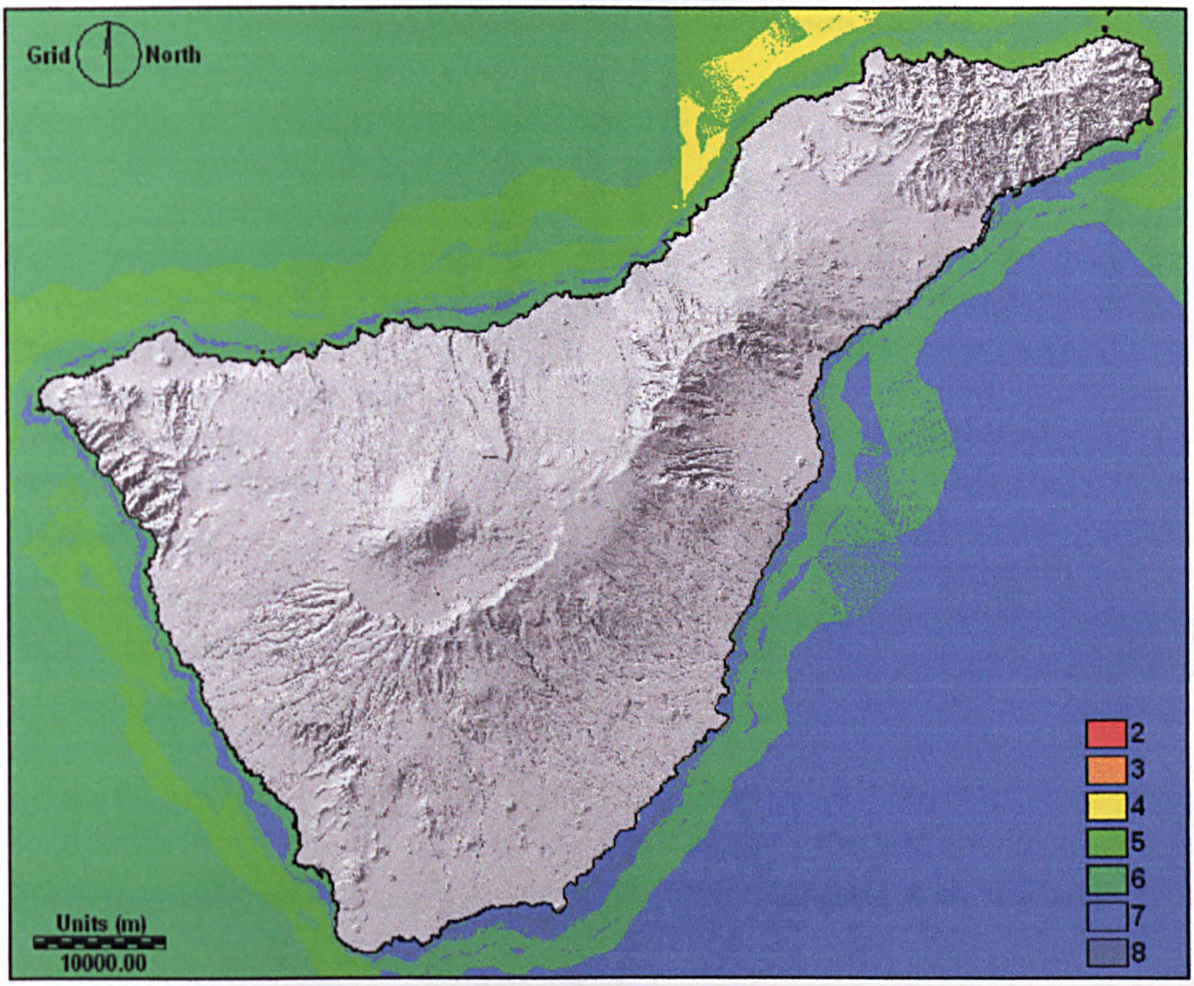

Fig. 5.9: Marine environment submodel for SeaStation® cage system.

5.1.5 Nautical Sports Submodel

Weights of importance for each of the six criteria forming this submodel, scuba-diving (Fig. 4.49), scuba-diving in particular marine habitats (Fig. 4.50), shipwrecked boats (Fig. 4.51), spearfishing (Fig. 4.52), windsurfing (Fig. 4.53) and near-shore sailing (Fig. 4.54), were calculated using the pairwise matrix shown in Table 5.9. The consistency ratio (CR) was smaller than 0.1, therefore, acceptable.

Table 5.9: Pairwise comparisons matrix for nautical sports submodel.

	Scuba-diving	Scuba-diving in particular marine habitats	Shipwrecked boats	Spearfishing	Windsurfing	Near-shore sailing
Scuba-diving	**1**					
Scuba-diving in particular marine habitats	1/3	**1**				
Shipwrecked boats	1/2	1	**1**			
Spearfishing	1/5	1/7	1/6	**1**		
Windsurfing	2	4	3	6	**1**	
Near-shore sailing	1/3	1/2	1/2	3	1/4	**1**

CR= 0.04

Calculated weights were used in a MCE, Fig. 5.10, to combine the 6 criteria. The output from this operation was the nautical-sport suitability map shown in Fig. 5.11.

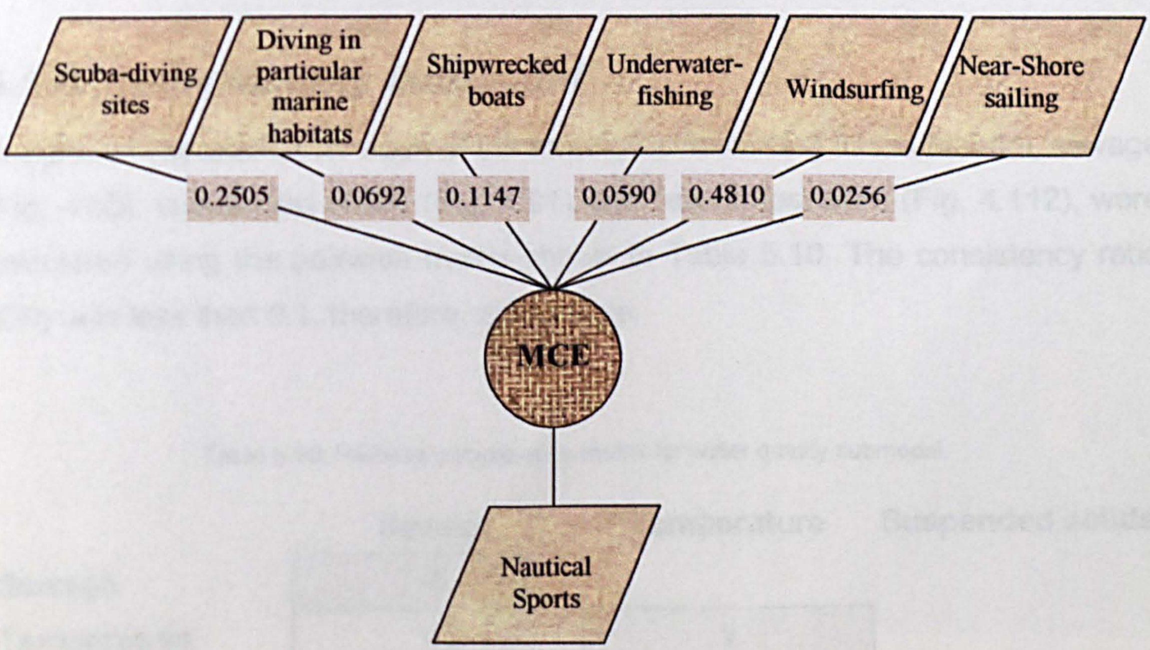

Fig. 5.10: Nautical sports MCE model showing the criteria used and calculated weights.

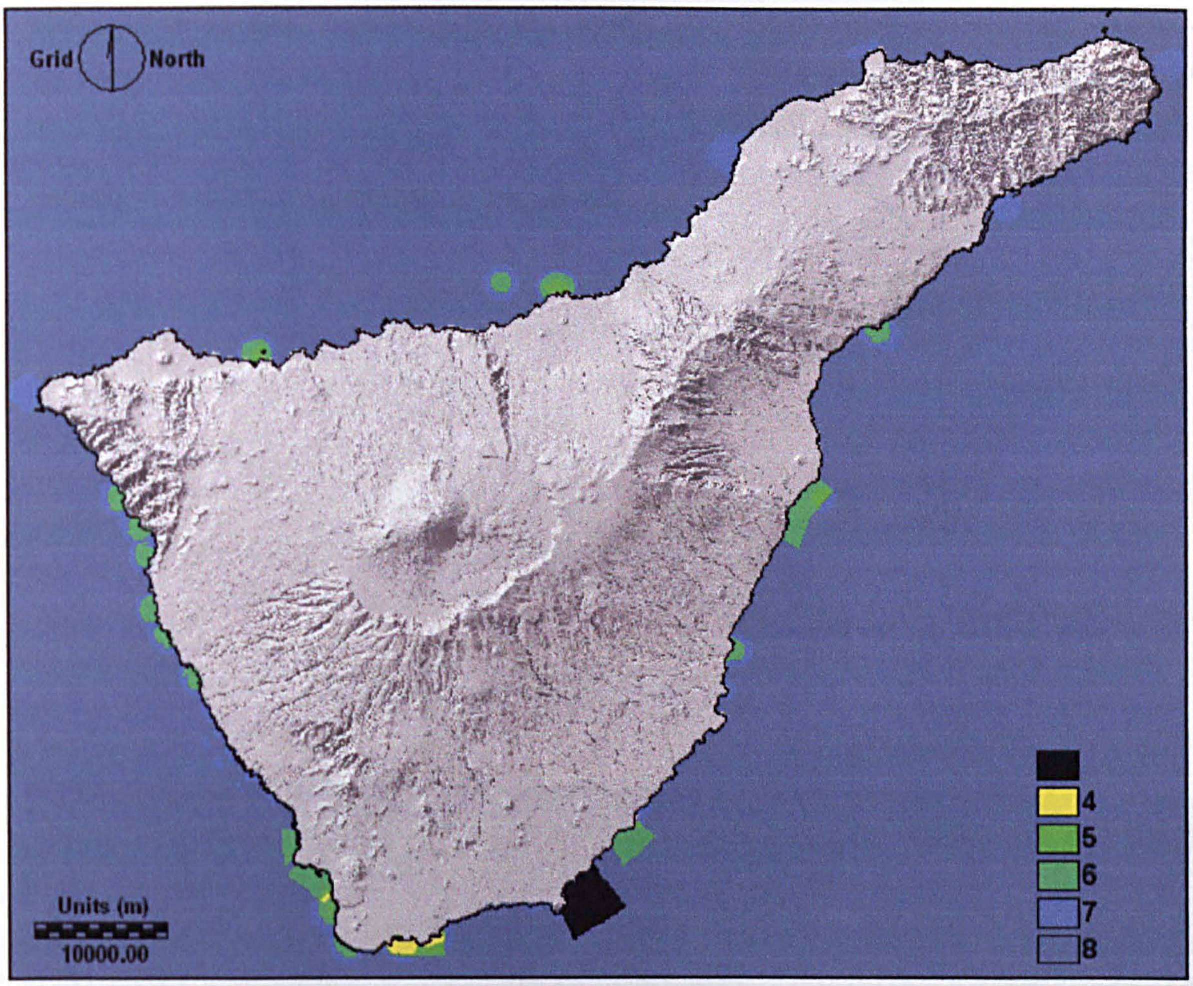

Fig. 5.11: Nautical sport submodel suitability map. Note the black colour in the map (zero value), this area corresponds to the windsurfing spot in El Medano and was set as a constraint because it important for this sport (section 4.5.2).

5.1.6 Water Quality Submodel

Weights of importance for each of the three criteria forming this submodel, sewage (Fig. 4.60), suspended solids (Fig. 4.91) and sea temperature (Fig. 4.112), were calculated using the pairwise matrix shown in Table 5.10. The consistency ratio (CR) was less than 0.1, therefore, acceptable.

Table 5.10: Pairwise comparisons matrix for water quality submodel.

	Sewage	Temperature	Suspended solids
Sewage	**1**		
Temperature	1/2	**1**	
Suspended solids	1/2	1	**1**

CR= 0.00

Calculated weights were used in a MCE to combine the criteria as shown in Fig. 5.12. The output from this operation was the water quality suitability map shown in Fig. 5.13.

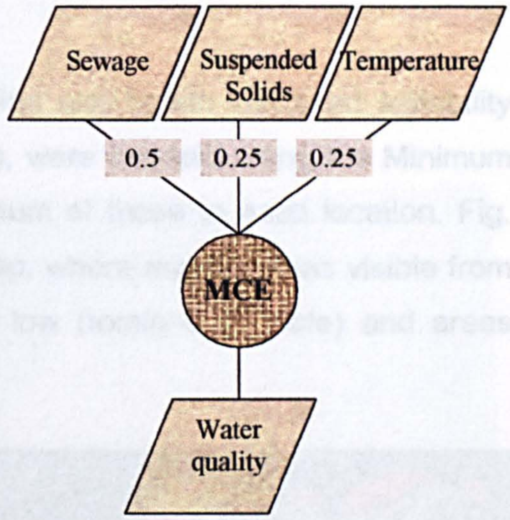

Fig. 5.12: Water quality MCE submodel showing the criteria used and calculated weights.

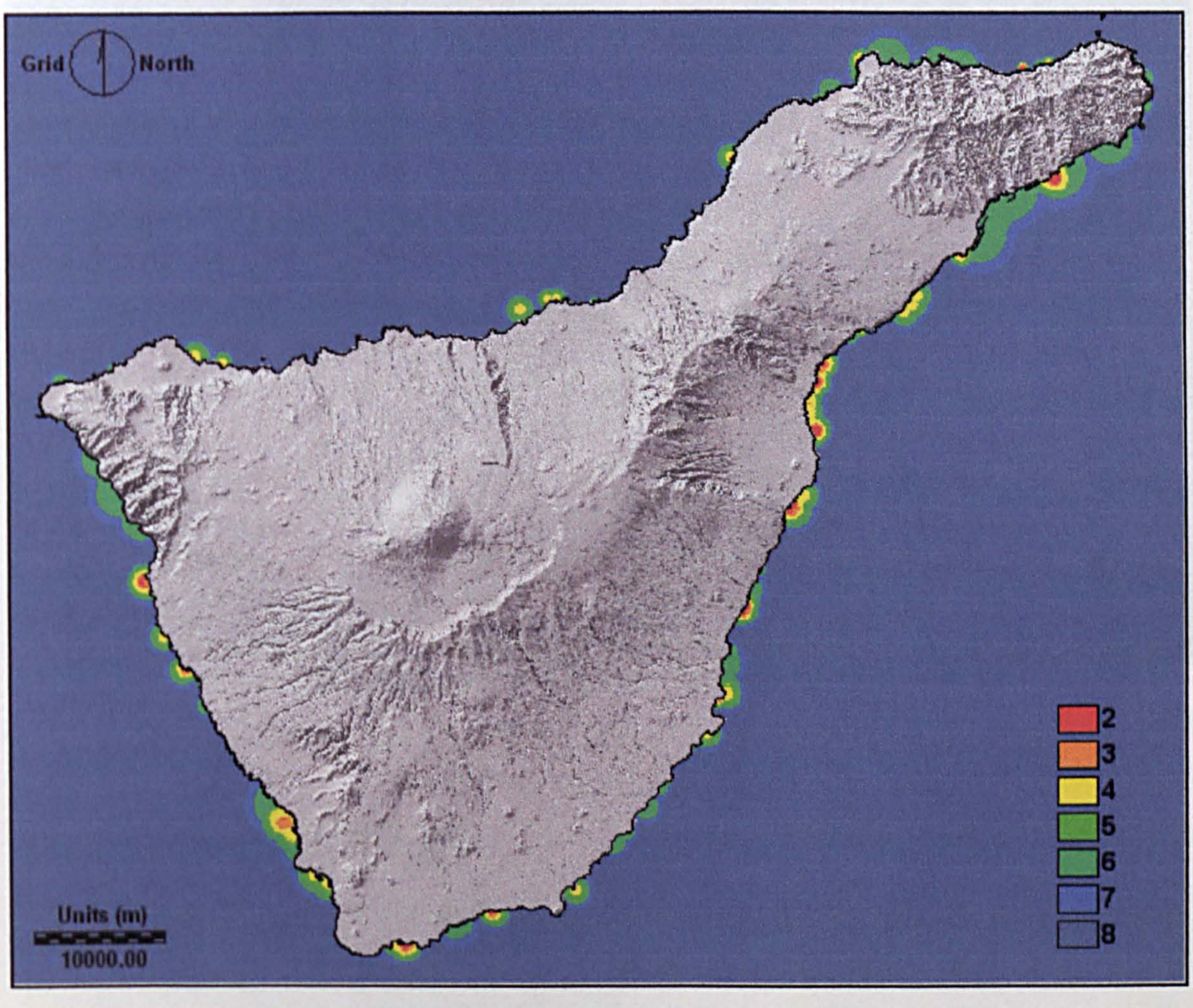

Fig. 5.13: Water quality suitability map.

5.1.7 Viewshed Submodel

The two criteria forming this submodel, building and beach viewshed suitability maps (Fig. 4.116 and Fig. 4.117 respectively), were overlaid using the Minimum option. The output pixels represent the minimum of those in each location. Fig. 5.14 shows the overall viewshed suitability map, where marine areas visible from beaches and tourist resources were scored low (totally-unsuitable) and areas away scored high (very-suitable).

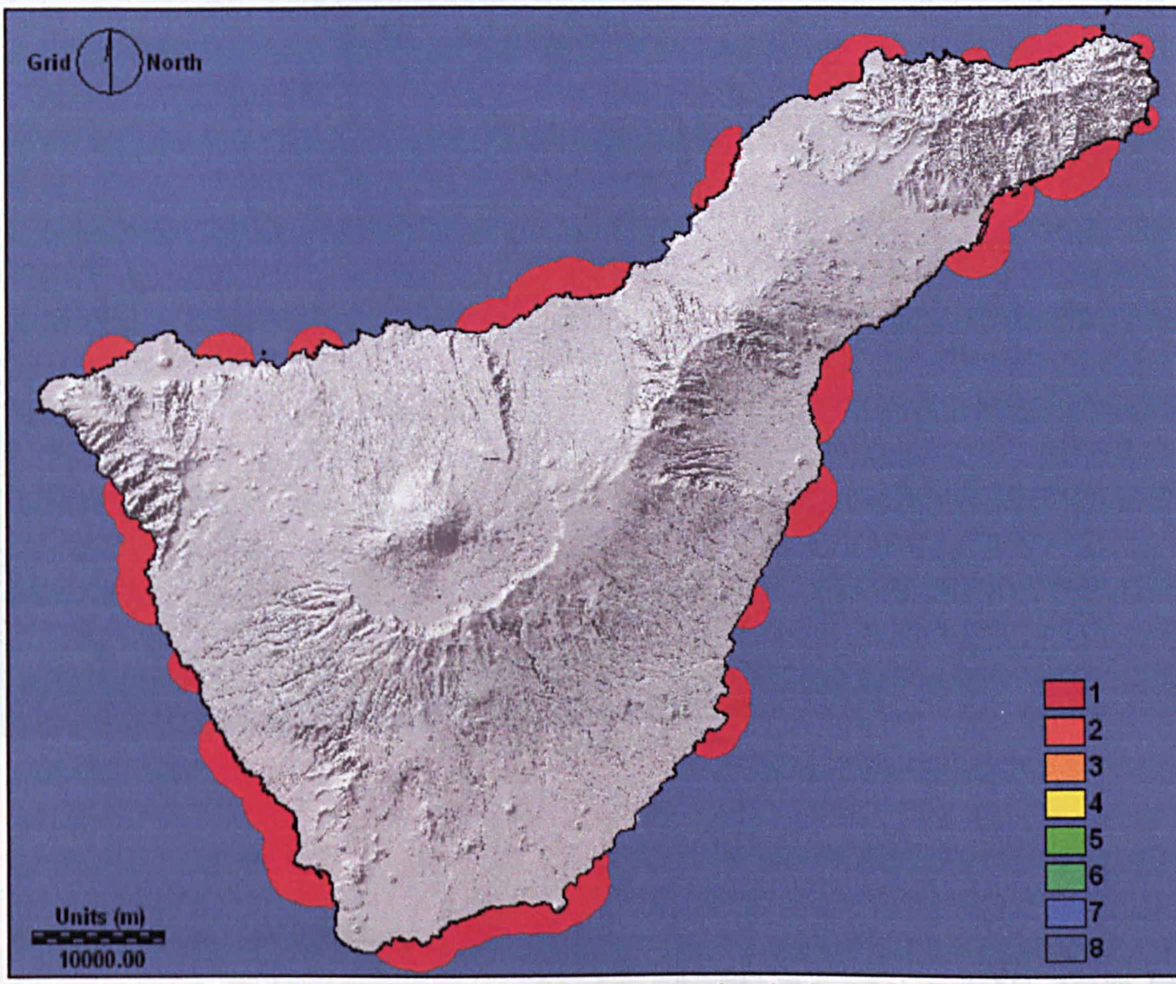

Fig. 5.14: Viewshed model (tourist resources + beaches) suitability map.

5.1.8 Constraint Layer

The five constraint layers created, seagrass meadows (Fig. 4.119), sewage pipes (Fig. 4.120), ports (Fig. 4.121), windsurfing in El Medano (Fig. 4.122) and proximity to industrial areas (Fig. 4.124), were overlaid to generate a single

Boolean constraint layer as shown in Fig. 5.15. The constraints have a value of zero and occupy an area of approximately 78.5 km^2.

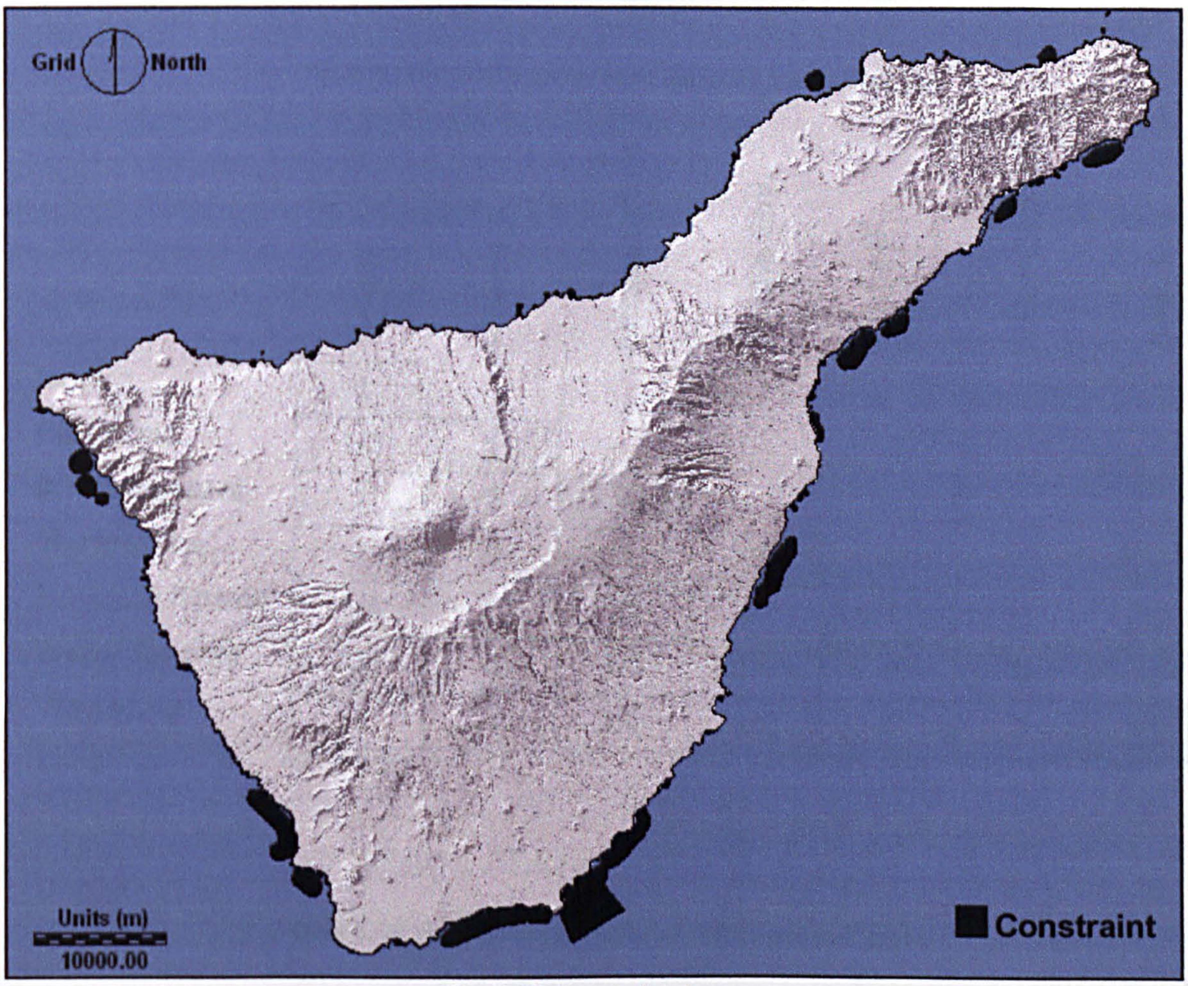

Fig. 5.15: Constraints layer.

5.1.8 Final Output

Finally, the eight submodels assembled to identify the most suitable areas for marine cage culture in Tenerife were combined using a further MCE. Weights of importance for each of the seven criteria submodels, beach (Fig. 5.2), fisheries (Fig. 5.1), infrastructure (Fig. 5.6), marine environment (Fig. 5.7, Fig. 5.8 and Fig. 5.9), nautical sports (Fig. 5.11), water quality (Fig. 5.12) and viewshed (Fig. 5.14), were calculated using a pairwise matrix for each of the three cage systems selected (Corelsa®, OceanSpar® and SeaStation®) as shown in Table 5.11, Table 5.12 and Table 5.13. The consistency ratios (CR) for all the pairwise comparisons were less than 0.1, and therefore, acceptable. The constraint layer was incorporated in the final stage of the MCE.

Table 5.11: Pairwise comparison matrix for Corelsa® cages.

	Beach	Fisheries	Infrastructure	Marine Env.	Nautical Sports	Water Quality	Viewshed
Beach	**1**						
Fisheries	1/3	**1**					
Infrastructure	2	5	**1**				
Marine Env.	3	6	3	**1**			
Nautical Sports	1/4	1	1/6	1/7	**1**		
Water Quality	1/3	3	1/5	1/6	4	**1**	
Viewshed	1	3	1/2	1/2	4	3	**1**

CR = 0.04

Table 5.12: Pairwise comparison matrix for SeaSpar® cages.

	Beach	Fisheries	Infrastructure	Marine Env.	Nautical Sports	Water Quality	Viewshed
Beach	**1**						
Fisheries	1/3	**1**					
Infrastructure	2	4	**1**				
Marine Env.	2	4	2	**1**			
Nautical Sports	1/4	1	1/5	1/4	**1**		
Water Quality	1/3	3	1/4	1/4	4	**1**	
Viewshed	1	3	1/2	1/2	4	3	**1**

CR = 0.04

Table 5.13: Pairwise comparison matrix for SeaStation® cages.

	Beach	Fisheries	Infrastructure	Marine Env.	Nautical Sports	Water Quality	Viewshed
Beach	1						
Fisheries	1/3	1					
Infrastructure	2	3	1				
Marine Env.	2	3	1	1			
Nautical Sports	1/3	3	1/4	1/4	1		
Water Quality	1/3	3	1/3	1/3	3	1	
Viewshed	1	3	1/2	1/2	3	3	1

CR = 0.04

Calculated weights for each cage system (Table 5.14) were used in a MCE to combine the criteria together with the constraint layer (Fig. 5.15). The output from this operation provided an overall suitability map for each cage system, shown in Fig. 5.16, Fig. 5.18 and Fig. 5.20. To focus on the areas of maximum interest for development of cage systems, these images were masked to exclude water depths in excess of 50 m (Fig. 5.17, Fig. 5.19 and Fig. 5.21). This is because mooring systems become very complex to install and manage in deep water (Meyer pers. comm.).

Table 5.14: Ranks and calculated weights for each cage system.

	Corelsa®		OceanSpar®		SeaStation®	
	Rank	Weight*	Rank	Weight*	Rank	Weight*
Beach	4	0.1327	3	0.1541	3	0.1586
Fisheries	6	0.0400	6	0.0476	6	0.0554
Infrastructure	2	0.2249	2	0.2359	1	0.2423
Marine Env.	1	0.3565	1	0.2815	2	0.2423
Nautical Sports	7	0.0339	7	0.0415	7	0.0499
Water Quality	5	0.0712	5	0.0853	5	0.0929
Viewshed	3	0.1408	4	0.1541	4	0.1586

*Based on the pairwise comparisons matrix

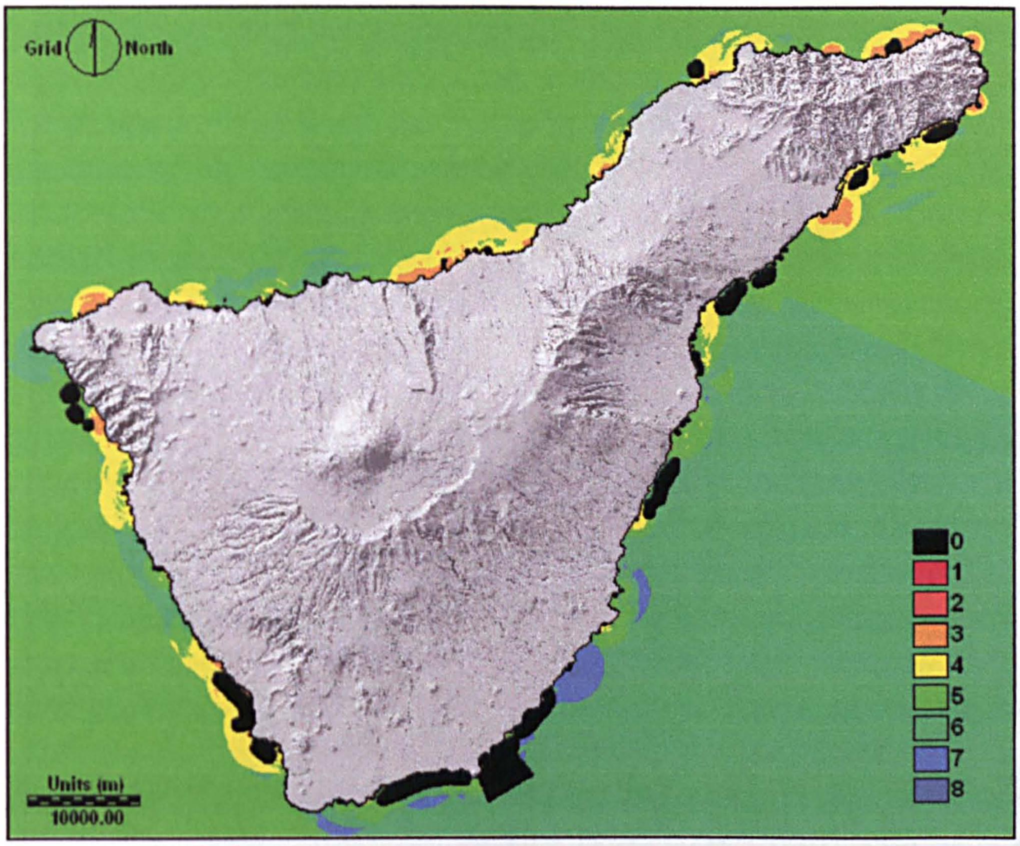

Fig. 5.16: Overall suitability map for siting Corelsa® fish cages in Tenerife.

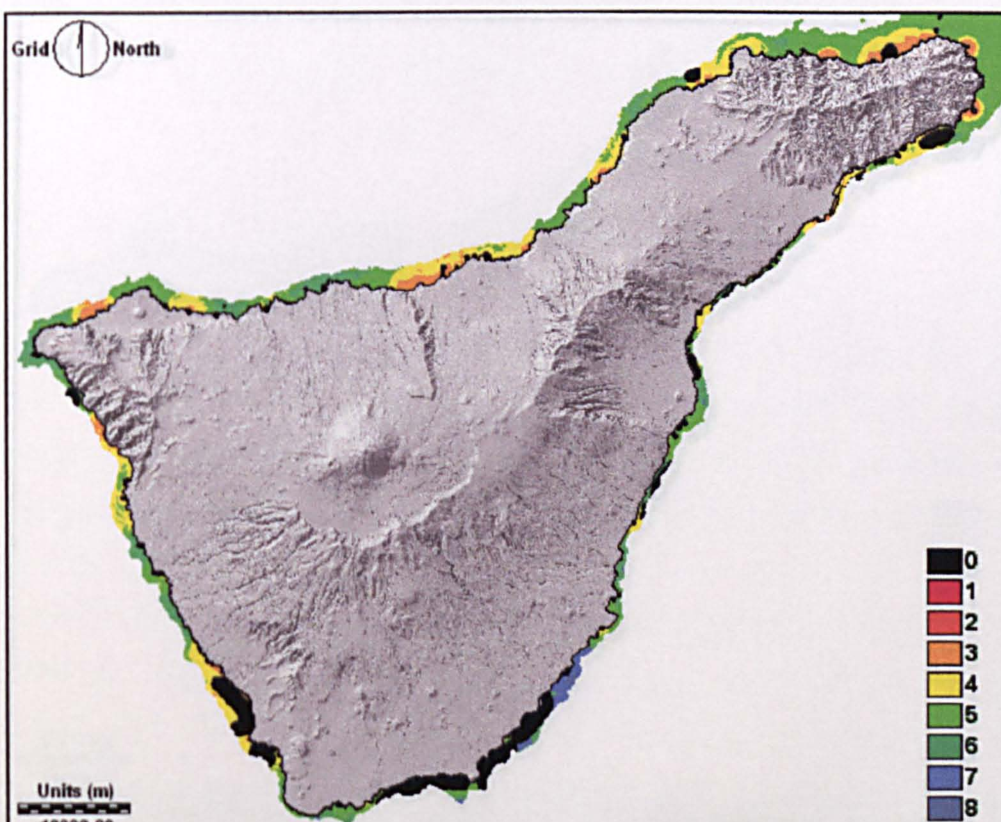

Fig. 5.17: Overall suitability map, masked to depths of 50 m, for siting Corelsa® fish cages in Tenerife.

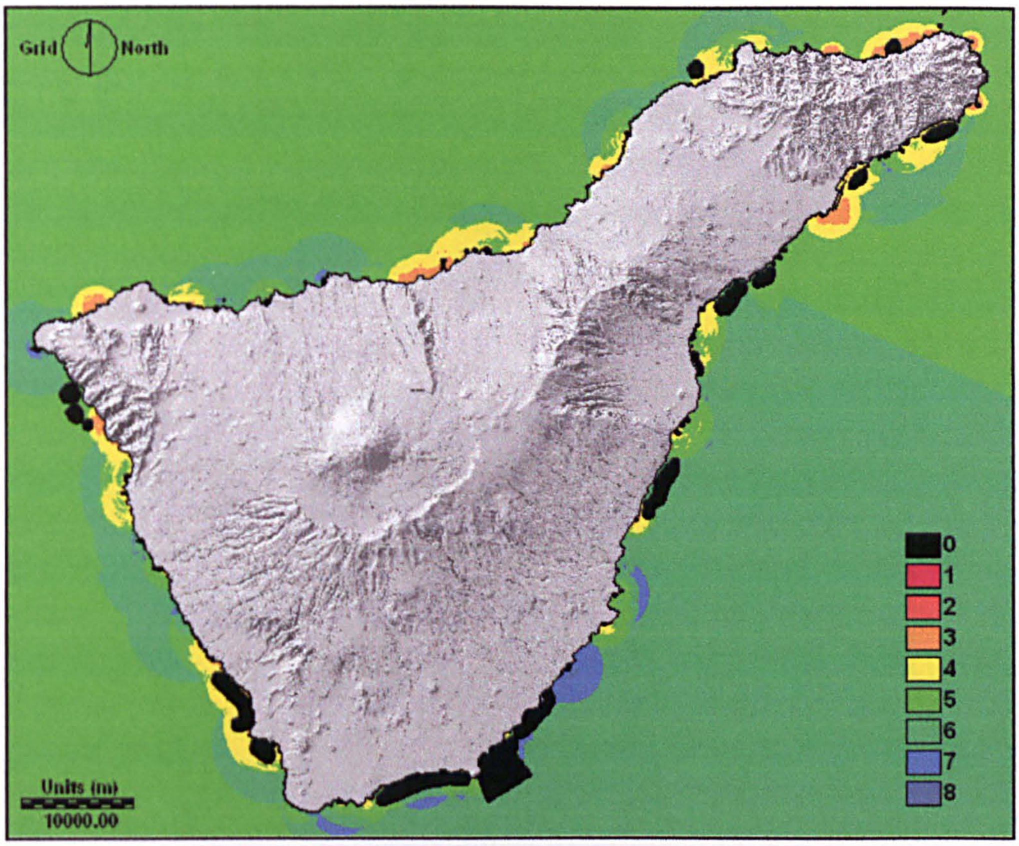

Fig. 5.18: Overall suitability map for siting SeaSpar® fish cages in Tenerife.

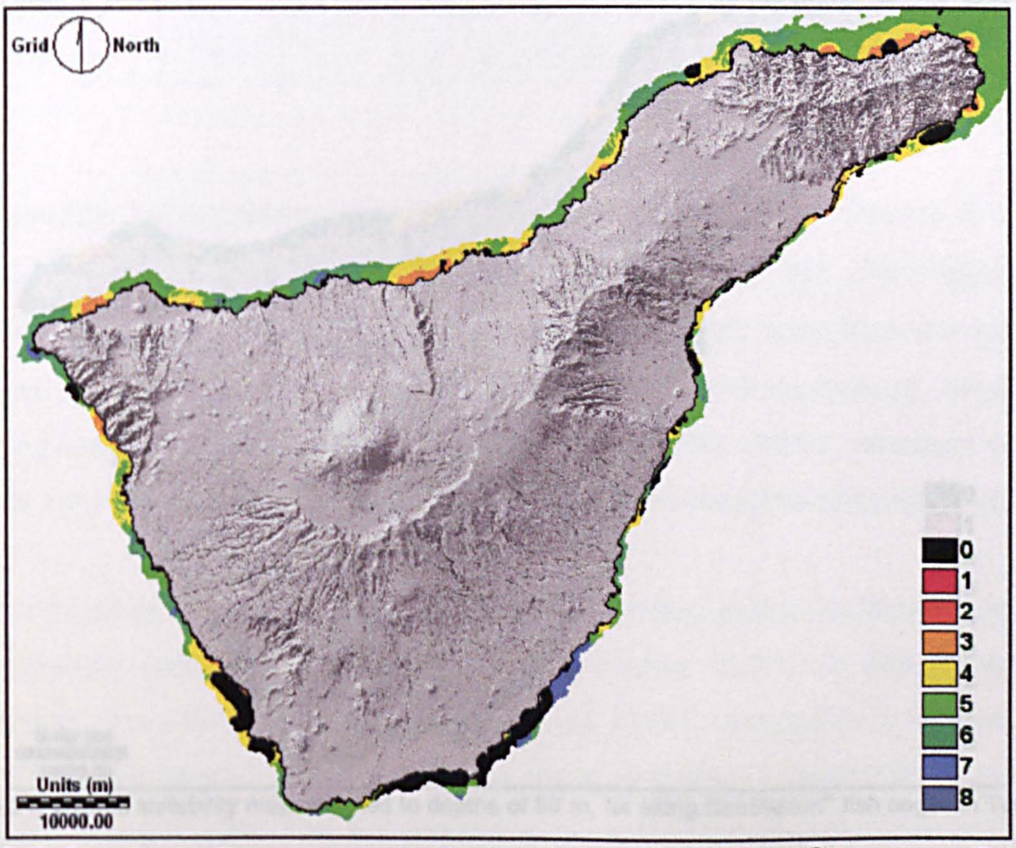

Fig. 5.19: Overall suitability map, masked to depths of 50 m, for siting SeaSpar® fish cages in Tenerife.

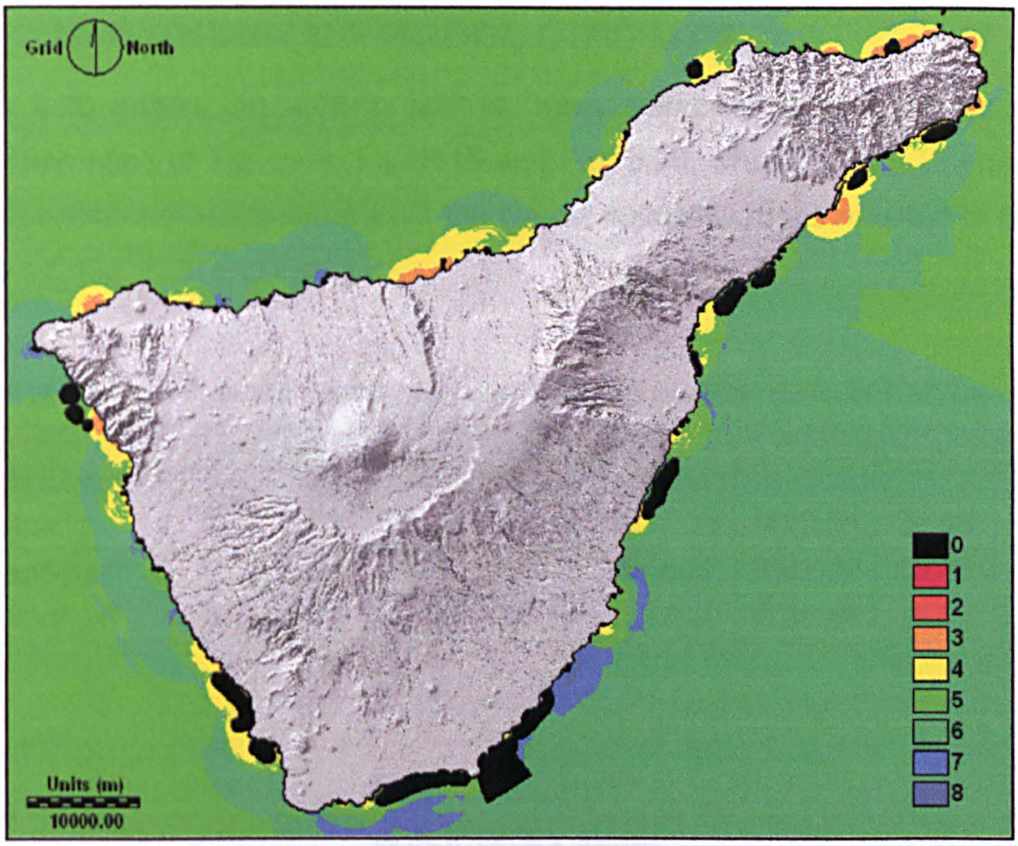

Fig. 5.20: Overall suitability map for siting SeaStation® fish cages in Tenerife.

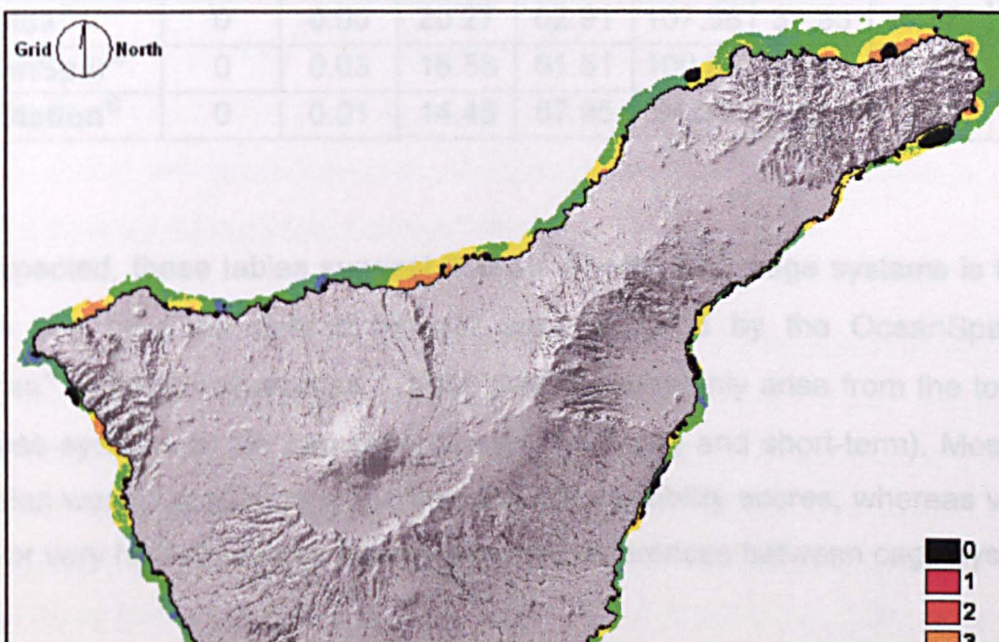

Fig. 5.21: Overall suitability map, masked to depths of 50 m, for siting SeaStation® fish cages in Tenerife.

5.2 COMPARISON OF MODEL OUTPUTS

Table 5.15 shows the area in km^2 for each suitability score from the overall suitability maps of Fig. 5.16, Fig. 5.18 and Fig. 5.20, while Table 5.16 shows the area for each suitability score from the overall suitability maps masked to 50 m of Fig. 5.17, Fig. 5.19 and Fig. 5.21.

Table 5.15: Area, in km^2, for each suitability score from the overall suitability map for each fish cage systems.

Suitability Scores	1	2	3	4	5	6	7	8
Corelsa®	0	0.08	24.44	113.42	2017.13	1429.51	22.48	0.51
OceanSpar®	0	0.03	19.87	103.28	1855.87	1602.33	25.68	0.51
SeaStation®	0	0.01	17.70	89.66	1717.30	1735.86	45.55	1.49

Table 5.16: Area, in km^2, for each suitability score from the overall suitability map, masked to depths of 50 m, for each fish cage systems.

Suitability Scores	1	2	3	4	5	6	7	8
Corelsa®	0	0.08	20.27	62.91	107.58	31.33	5.37	0.51
OceanSpar®	0	0.03	16.53	61.51	100.95	40.51	8.02	0.51
SeaStation®	0	0.01	14.45	57.95	94.31	50.55	9.33	1.45

As expected, these tables suggest that the SeaStation® cage systems is the one which can be used over a broader area, followed by the OceanSpar® and Corelsa® systems respectively. These differences mainly arise from the tolerance of these systems to the sea state (waves, both long and short-term). Most of the variation was located among the intermediate suitability scores, whereas very low (1,2) or very high (8) scores did not show big differences between cage systems.

To quantitatively assess the area difference for siting cages in Tenerife between the different cage systems selected, the Kappa Index of Agreement was calculated. The Kappa index, also know as KHAT, measures the association between two images having exactly the same number of categories. The output from this index ranges from 0.0 indicating no correlation to 1.0 indicating perfect positively correlation, and –1.0 indicating a perfect inverse correlation. This index was calculated for all the possible combinations of the three final output images (Fig. 5.17, Fig. 5.19 and Fig. 5.21). The three possible different combinations and their Kappa values are shown in Table 5.17. The module ERRMAT, which calculates the Kappa index only with cells having non-zero value, was used for this task.

Table 5.17: Kappa index of agreement between the overall suitability maps, masked to depths of 50 m, for each fish cage system.

	Corelsa®	**OceanSpar®**	**Station®**
Corelsa®	**1**		
OceanSpar®	0.82	**1**	
SeaStation®	0.66	0.84	**1**

The calculated Kappa indices confirm the differences between the cage systems which had previously been highlighted. The biggest differences among the selected cage systems are between the Corelsa® and SeaStation® systems, followed by the Corelsa® and OceanSpar® cages, and the least between the OceanSpar® and SeaStation® cages. As pointed out before, these differences are mainly due to the wave tolerance of each system, with the SeaStation® system being with most tolerant and Corelsa® the least.

Table 5.17 gives a quantitative indication of the variation (change in area) between the model outputs for the three cage systems. However, it did not give any indication of the location where the changes occurred. In other words, it does not provide a qualitative indication of the changes. To examine this further, a cross-classification by combination of two images between all the possible combinations of the three final output images (Fig. 5.17, Fig. 5.19 and Fig. 5.21) was used to create a new image that shows the locations of change of all combinations of the categories in the original images as shown in Fig. 5.22, Fig. 5.23 and Fig. 5.24. The legend produced shows these combinations, with the left hand categories referring to the first image and those on the right referring to the second image. The module CROSSTAB was used for this task.

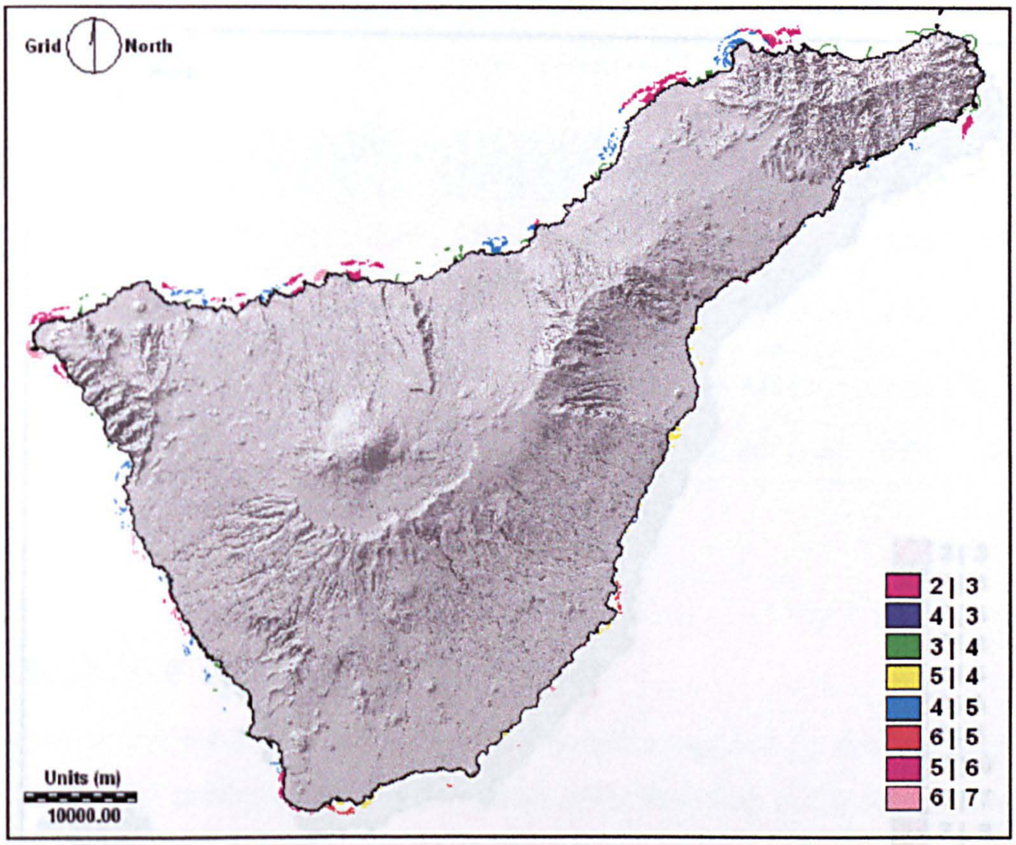

Fig. 5.22: Cross-classification between Corelsa® and OceanSpar® suitability maps, masked to depths of 50 m.

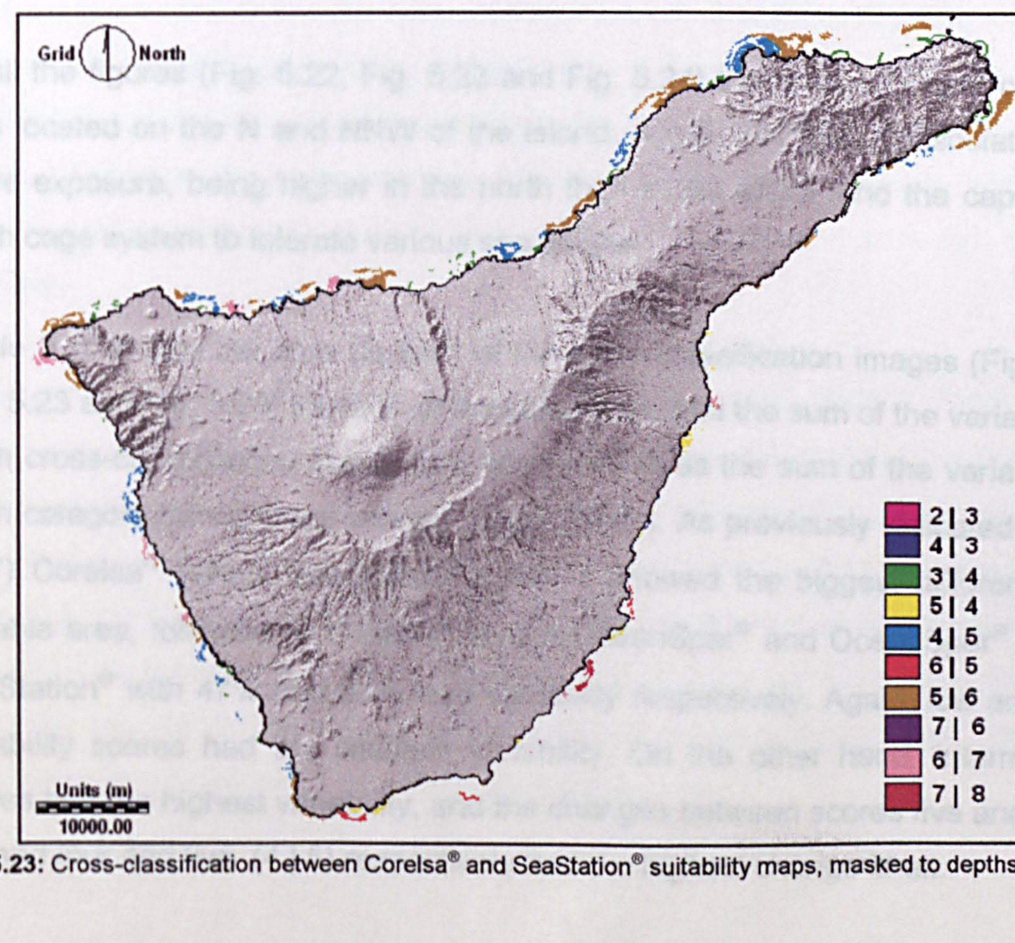

Fig. 5.23: Cross-classification between Corelsa® and SeaStation® suitability maps, masked to depths of 50 m.

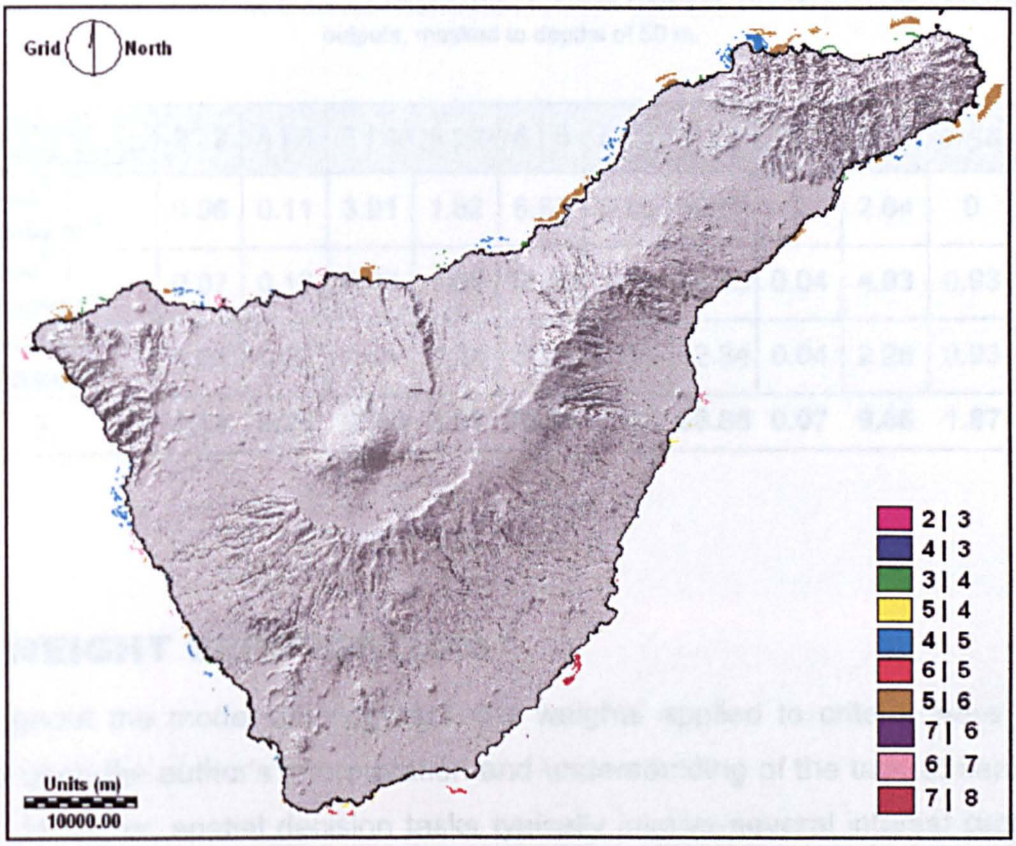

Fig. 5.24: Cross-classification between OceanSpar® and SeaStation® suitability maps, masked to depths of 50 m.

In all the figures (Fig. 5.22, Fig. 5.23 and Fig. 5.24) the area with most changes was located on the N and NNW of the island. Again, this fact is associated with wave exposure, being higher in the north than in the south, and the capacity of each cage system to tolerate various sea stages.

Table 5.18 shows the area (in km^2) of the cross-classification images (Fig. 5.22, Fig. 5.23 and Fig. 5.24) for each of the categories, and the sum of the variation for each cross-classification image (row sum) as well as the sum of the variation for each category for the three images (column sum). As previously indicated (Table 5.17) Corelsa® versus SeaStation® systems showed the biggest differences in suitable area, followed by Corelsa® versus OceanSpar® and OceanSpar® versus SeaStation® with 47% and 53% less variability respectively. Again, low and high suitability scores had the smallest variability. On the other hand, intermediate scores had the highest variability, and the changes between scores five and six (5 | 6) and four and five (4 | 5) respectively had the highest change of all.

Table 5.18: Area, in km^2, for the cross-classification between Corelsa®, OceanSpar® and SeaStation® outputs, masked to depths of 50 m.

CROSS-CLASSIFICATION	2 | 3	4 | 3	3 | 4	5 | 4	4 | 5	6 | 5	5 | 6	7 | 6	6 | 7	7 | 8	Σ
Corelsa® | OceanSpar®	0.06	0.11	3.91	1.62	6.82	0.76	12.59	0	2.64	0	**28.51**
Corelsa® | SeaStation®	0.07	0.13	6.02	1.95	12.80	1.31	25.43	0.04	4.93	0.93	**53.61**
Ocean Spar® | SeaStation®	0.01	0.02	2.11	0.34	5.99	0.55	12.84	0.04	2.28	0.93	**25.12**
Σ	**0.14**	**0.26**	**12.03**	**3.91**	**25.61**	**2.62**	**50.85**	**0.07**	**9.86**	**1.87**	

5.3 WEIGHT VERIFICATION

Throughout the model development, the weights applied to criteria were based solely upon the author's interpretation and understanding of the task at hand (Fig. 5.25). However, spatial decision tasks typically involve several interest groups or decision-makers (Malczewski, 1999). Weights assigned to each criteria by different interest groups reflect different points of view, perceptions and often conflicting interests in the decision-making process. Consequently, the role of the weight verification analysis is to establish a consensus as to the relative importance of various weights associated with the criteria and to consider different points of view to the same problem. The aim of this section was to account for these possible different points of view to the task of siting marine fish cages in Tenerife.

Following established techniques (Aguilar-Manjarrez, 1996; Salam, 2000) several focus groups, all of whom had relevant but different experience in the field, were identified. Specifically developed questionnaires were used to obtain feed-back from these groups. Three focus groups, each comprising of four subjects, were selected; (1) aquaculture researchers form the Department of Aquaculture of the Spanish Oceanographic Centre in Tenerife (COC), (2) marine fish cage farmers in Tenerife, and (3) PhD and MSc students at the Institute of Aquaculture, University of Stirling, with experience in marine aquaculture.

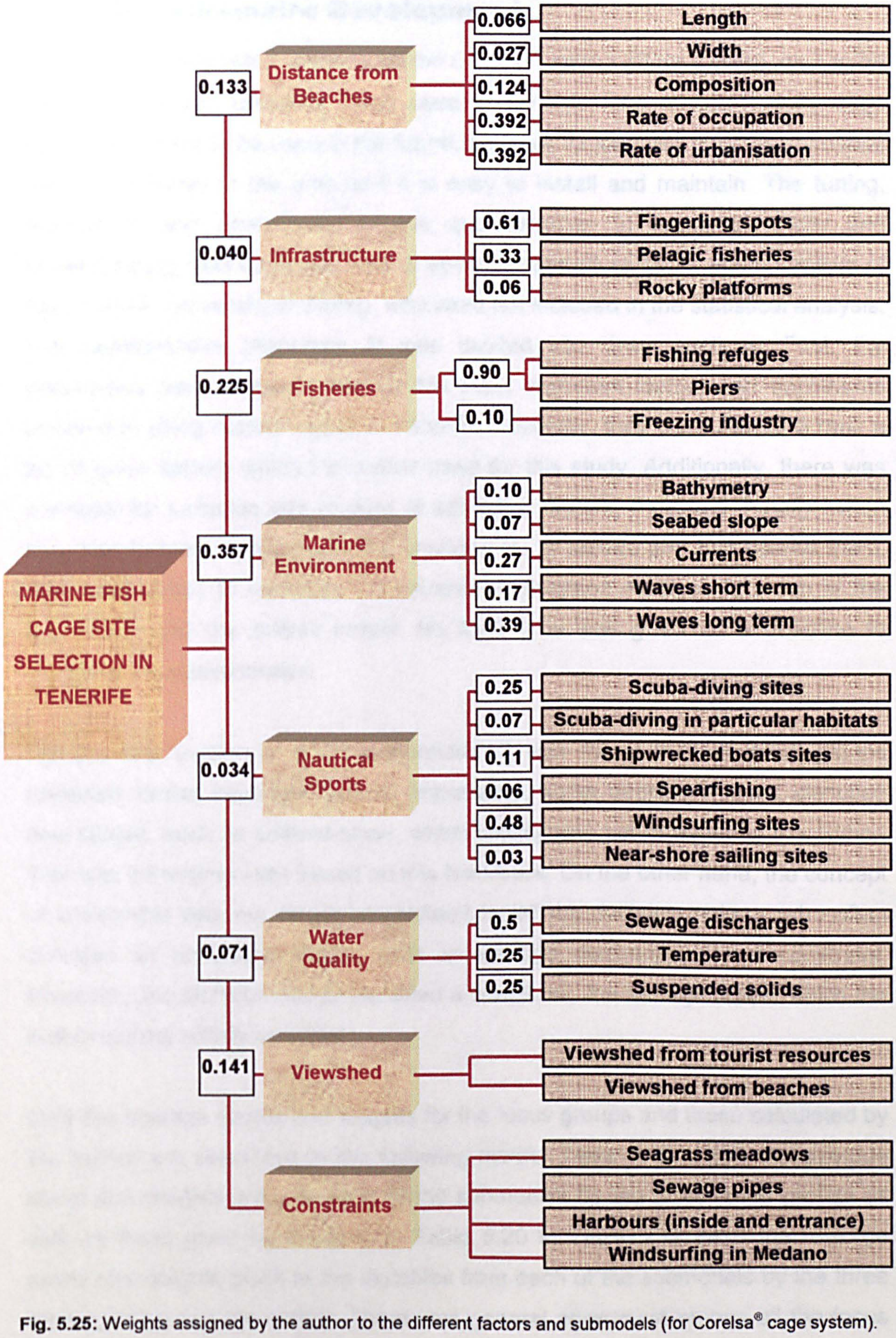

Fig. 5.25: Weights assigned by the author to the different factors and submodels (for Corelsa® cage system).

5.3.1 Questionnaire Development

The questionnaire was targeted with the Corelsa® cage system in mind, as it is the only cage system presently being used in Tenerife, and the most likely cage system of choice to be used in the future, because its low cost, good performance record, familiarity in the area and it is easy to install and maintain. The tuning, adjustment and amendment of the questionnaire, in terms of clarity and understanding, was done with help of several research students at the Institute of Aquaculture, University of Stirling, who were not included in the statistical analysis. The questionnaire (Appendix 2) was divided into three sections. First, the participants were asked to identify the most important factors and constraints involved in siting marine cages in Tenerife. Secondly, they were asked to rank a list of given factors which the author used for this study. Additionally, there was provision for inclusion and ranking of additional factors, if desired. Finally, when they had become familiar with the provided list of factors and had scored them, they were asked to complete the pairwise comparison matrices for each of the submodels and the overall model. No fixed time was given as a deadline to complete the questionnaire.

For the first section of the questionnaire, it was found that all focus groups identified similar important factors. Importantly, some decision-makers identified new factors, such as seabed-slope, which initially was not included by the author. This was introduced later based on this feed-back. On the other hand, the concept of constraints was not clearly understood by all the decision-makers, who often included an unsuitable factor, such as sewage discharges, as a constraint. However, one decision-maker identified a constraint, the sewage pipes, which the author did not initially consider.

Only the average scores and weights for the focus groups and those calculated by the author are presented in the following tables. Table 5.19 shows the average score and weights given to each of the submodels by the three focus groups as well as those given by the author. Table 5.20 to Table 5.25 show the average score and weights given to the variables from each of the submodels by the three focus groups and the author. There was general agreement among all the focus groups that the factors chosen for the evaluation were relevant, and none of them were considered to be unsuitable or rejected by any decision-maker.

Table 5.19: Average scores and weights given to each submodel by the three focus groups and the author.

	Scores					Weights			
	A	B	C	D		A	B	C	D
Beach	**4**	4.8	6.0	4.8		**0.13**	0.12	0.07	0.12
Fisheries	**6**	4.5	3.3	5.5		**0.04**	0.13	0.17	0.09
Infrastructure	**2**	2.5	1.8	3.8		**0.23**	0.20	0.22	0.15
Marine Env.	**1**	1.3	1.8	2.8		**0.36**	0.24	0.22	0.19
Nautical Sports	**7**	6.0	6.3	6.0		**0.03**	0.07	0.06	0.07
Water Quality	**5**	4.3	4.0	1.5		**0.07**	0.13	0.14	0.23
Viewshed	**3**	4.8	5.0	3.8		**0.14**	0.12	0.11	0.15
					Sum	1	1	1	1

A= author, B=COC; C= farmers; D= students

Table 5.20: Average scores and weights given to the beach submodel by the three focus groups and the author.

	Scores					Weights			
	A	B	C	D		A	B	C	D
Length	**4**	4.0	4.3	4.8		**0.07**	0.09	0.12	0.10
Width	**5**	4.5	4.3	4.3		**0.03**	0.09	0.07	0.11
Composition	**3**	3.5	3.0	2.5		**0.12**	0.13	0.19	0.21
Occupation	**1**	1.8	1.8	2.0		**0.39**	0.34	0.33	0.28
Urbanisation	**2**	1.3	1.8	1.5		**0.39**	0.36	0.30	0.30
					Sum	1	1	1	1

A= author; B= COC; C= farmers; D= students

Table 5.21: Average scores and weights given to the fisheries submodel by the three focus groups and the author.

	Scores					Weights			
	A	B	C	D		A	B	C	D
Fingerling accumulation	**1**	1.8	2.3	1.8		**0.61**	0.47	0.33	0.39
Pelagic fish	**2**	1.8	1.8	1.8		**0.33**	0.38	0.39	0.39
Rocky platforms	**3**	2.5	2.0	2.5		**0.06**	0.16	0.29	0.23
					Sum	1	1	1	1

A= author; B= COC; C= farmers; D= students

Table 5.22: Average scores and weights given to the infrastructure submodel by the three focus groups and the author.

	Scores					Weights			
	A	B	C	D		A	B	C	D
Harbours	**1**	1.0	1.0	1.0		**0.9**	0.80	0.78	0.86
Freezing industry	**2**	2.0	2.0	2.0		**0.1**	0.20	0.23	0.14
					Sum	1	1	1	1

A= author; B= COC; C= farmers; D= students

Table 5.23: Average scores and weights given to the marine environment submodel by the three focus groups and the author.

	Scores					Weights			
	A	B	C	D		A	B	C	D
Bathymetry	**4**	2.0	2.3	2.5		**0.10**	0.13	0.15	0.17
Seabed-slope	**5**	3.0	2.8	3.5		**0.07**	0.20	0.18	0.23
Currents	**2**	2.8	2.3	4.0		**0.27**	0.18	0.15	0.27
Waves short term	**3**	3.8	4.0	1.5		**0.17**	0.25	0.27	0.10
Waves long term	**1**	3.5	3.8	3.5		**0.39**	0.23	0.25	0.23
					Sum	1	1	1	1

A= author; B= COC; C= farmers; D= students

Table 5.24: Average scores and weights given to the nautical sports submodel by the author and by the three focus groups.

	Scores					Weights			
	A	B	C	D		A	B	C	D
Scuba-diving	**2**	3.5	4.3	3.0		**0.25**	0.17	0.14	0.16
Scuba-diving in particular habitats	**4**	3.5	3.5	3.0		**0.07**	0.13	0.16	0.16
Shipwrecked boats	**3**	4.3	4.5	5.8		**0.11**	0.13	0.13	0.09
Underwater fishing	**5**	4.8	2.3	4.3		**0.06**	0.10	0.16	0.10
Windsurfing	**1**	2.8	4.0	2.3		**0.48**	0.26	0.19	0.28
Near-shore sailing	**6**	2.3	2.5	2.8		**0.03**	0.23	0.23	0.23
					Sum	1	1	1	1

A= author; B= COC; C= farmers; D= students

Table 5.25: Average scores and weights given to the water quality submodel by the three focus groups and the author.

	Scores					Weights			
	A	B	C	D		A	B	C	D
Sewage	**1**	1.3	1.0	1.3		**0.5**	0.46	0.48	0.51
Temperature	**3**	2.8	3.0	2.5		**0.25**	0.26	0.18	0.21
Suspended solids	**2**	2.0	2.0	2.3		**0.25**	0.28	0.35	0.28
					Sum	1	1	1	1

A= author; B= COC; C= farmers; D= students

Only a few decision-makers completed some of the comparison matrices in such a way that the consistency ratio was less that 0.1. Where difficulty was experienced, the decision-makers were asked to reconsider the pairwise matrix to achieve the desirable CR. Some decision-makers argued that it was easier for them to directly assign weights to the factors without going through the process of completing the pairwise matrix. Moreover, some authors were not satisfied with the weights they obtained when the pairwise matrix technique was used, even though it gave a good CR.

5.3.2 Statistical Analysis of the Questionnaires

Non-parametric correlation analysis was used to assess whether the weights assigned to the factors and submodels given by the author matched those given by the decision-makers. The use of a non-parametric test was justified because the data was not randomly collected, as the questionnaires were given to specific targeted personnel, and secondly, because the data sample size was small. Non-parametric correlation tests operate with the ranks of the measurements for each variable, in other words, they do not use the actual observed data, but the ranks of the data to compute a correlation coefficient. There are several different rank correlation methods commonly used, such as Spearman or Kendall, however, these methods are only used to assess the correlation between two variables. If association between more than two variables is required, the Kendall's coefficient of concordance is used.

The Kendall's coefficient of concordance (*W*) expresses the intensity of agreement among several sets of rankings according to the formula shown in Eq. 5.1. Several equivalent computational formulae for the coefficient of concordance are found in various texts, but Eq. 5.1 was chosen because it is easy to use (Zar, 1996). Kendall's *W* ranges between 0 (no agreement) and 1 (complete agreement)

$$W = \frac{\sum R_i^2 - \frac{\left(\sum R_i\right)^2}{n}}{\frac{M^2\left(n^3 - n\right)}{12}} \qquad \textbf{Eq. 5.1}$$

where:

W = Kendall coefficient of concordance
M = number of variables being correlated
n = number of data per variable
R_i = sums of ranks

When two or more weights have exactly the same value, they are said to be *tied*. The rank assigned to each of the tied ranks is the mean of the ranks that would have been assigned had they not be tied (Zar, 1996). For example, if the third and fourth values had the same weight value, they are each assigned the rank of (3+4)/2=3.5. In this situation, Eq. 5.1 is modified to Eq. 5.2 to account for this tied ranking.

$$W = \frac{\sum R_i^2 - \frac{\left(\sum R_i\right)^2}{n}}{\frac{M^2\left(n^3 - n\right) - M\sum t}{12}} \qquad \sum t = \sum_{i=1}^{m}\left(t_i^3 - t_i\right) \qquad \textbf{Eq. 5.2}$$

where:

W_c = Kendall coefficient of concordance with tied ranks
t_i = number of ties in the *i*th group of ties
m = number of groups of tied ranks
M = number of variables being correlated
n = number of data per variable
R_i = sums of ranks

The significance of the Kendall's coefficient of concordance was also calculated. The significance test is designed to calculate the probability that for a given size, the correlation coefficient could have been derived by chance. The significance test is based upon the hypothesis:

H_0: there is no association among the variables

H_A: there is association among the variables

A simple way to do this involves the relationship between the Kendall coefficient of concordance (W) and the Friedman chi-square (χ_r^2) shown in Eq. 5.3. Therefore, it is possible to convert a calculated W to its equivalent χ_r^2 and then employ the table of critical values of χ_r^2. If the χ_r^2 was larger than predicted χ_r^2, then H_A was accepted, and therefore, was an agreement among the variables tested.

$$\chi_r^2 = M(n-1)W \qquad \text{Eq. 5.3}$$

Initially, to assess the agreement of the proposed weightings from each of the focus groups, the Kendall's coefficient of concordance was calculated between all the decision-makers of each group for all of the submodels and for all of the criteria composing each submodel (Table 5.26). To estimate the degree of agreement between the author's weightings and those proposed from each focus group (mean values among all decision-makers comprising each group), the Kendall's coefficient of concordance was calculated for all possible combinations between the author's opinion, researchers from the Department of Aquaculture of the Spanish Oceanographic Centre in Tenerife (COC), marine fish cage farmers in Tenerife, and PhD and MSc students from the Institute of Aquaculture, University of Stirling, with experience in marine aquaculture (Table 5.27).

Table 5.26: Kendall coefficient of concordance (*W*) and significance of the test for the weights given to the submodels and the criterion within each submodel by decision-makers from each of the three focus groups.

	Kendall Coefficient of Concordance (W)		
	B	C	D
Submodels	0.55*	0.74**	0.53*
Beaches Submodel	0.86**	0.65*	0.95**
Fisheries Submodel	0.32	0.12	0.32
Infrastructure Submodel	1.00*	1.00*	1.00*
Marine Environment Submodel	0.19	0.27	0.40
Nautical Sports Submodel	0.28	0.21	0.42
Water Quality Submodel	0.72*	1.00*	0.44

B= COC; C= farmers; D= students
* Correlation is significant at the .05 level
** Correlation is significant at the .01 level

Table 5.27: Kendall coefficient of concordance (*W*) and significance of the test for the mean weights given to the submodels and the criterion within each submodel by the three focus groups and the author.

	Kendall Coefficient of Concordance (W)					
Submodel	A-B	A-C	A-D	B-C	B-D	C-D
All Submodels (Table 5.19)	0.85	0.83	0.82	0.99	0.82	0.77
Beaches (Table 5.20)	0.97	0.99	0.94	0.94	0.99	0.90
Fisheries (Table 5.21)	1.00	0.75	0.93	0.75	0.93	0.93
Infrastructure (Table 5.22)	1.00	1.00	1.00	1.00	1.00	1.00
Marine Environment (Table 5.23)	0.65	0.60	0.65	0.99	0.32	0.24
Nautical Sports (Table 5.24)	0.70	0.33	0.60	0.77	0.93	0.90
Water Quality (Table 5.25)	0.93	0.93	0.93	1.00	1.00	1.00

A= author; B= COC; C= farmers; D= students

High and significant values of the Kendall's coefficient of concordance were interpreted as an agreement among the different decision-makers applying the same pattern in weighting the factors under study. However, it should be emphasized that high and significant values of the Kendall's coefficient of concordance did not necessarily mean that the weightings observed were "correct". In fact, they may be incorrect if compared to some other focus groups. It can be the case that a group of decision-makers can agree in weighting objects, and therefore have significant *W* values, because they all employ the "wrong" criterion (Aguilar-Manjarrez, 1996).

The results from Table 5.26 suggested that there was variable agreement within each of the focus groups. They all showed moderate agreement in the weightings assigned to the submodels. However, trends were detected based on the degree of agreement to different criteria within some submodels. All the focus groups show good agreement on three of the submodels (beaches, infrastructure and water quality), but on the contrary, they showed very poor agreement to the other three submodels (fishing, marine environment and nautical sports). As expected, models with a higher number of criteria showed more disagreement among decision-makers than those with fewer criteria. Of special significance were the results from the water quality model, in which group D (postgraduate students from the Institute of Aquaculture) showed the highest degree of disagreement compared to any of the other groups. This may be due to the unfamiliarity of the decision-makers from this group to the study area. For example, decision-makers who are familiar with the study area will be aware that the sea temperature in Tenerife, although a very important criterion for the successful development of aquaculture, is always in the optimum range for growing temperate species, and hence, its weight in this particular case is of less importance. The opposite results were true for the marine environment submodels, and it is possible that group D has a greater awareness of the influence of the criteria in composing this model for the development of marine cage culture, such as waves, currents or bathymetry, than the decision-makers from the other groups.

The results from Table 5.27 indicate that, in general, there was moderate agreement between the weights given by the different focus groups and those proposed by the author. The infrastructure model showed complete agreement among all the different focus groups and the author. The models which presented the least agreement were the nautical sports and marine environment. In general, it was found that submodels with a smaller number of factors show better agreement than those with larger numbers. The focus group which differed the most from the author's weights were the farmers (group C) and the postgraduate students from the Institute of Aquaculture, University of Stirling (group D), in that order. The weight given by the farmers to the fisheries and nautical sports submodels showed the least agreement of all with those proposed by the author. This fact may be correlated with the assumption that farmers are not very interested or concerned with the use of coastal space by other users and the influence they have. The reason for the disagreement between the author's weights and by those proposed by the postgraduate students at the Institute of aquaculture could be due to the fact that the latter were not familiar with the peculiarities of the study area. On the other hand, the weights which most correlated with those of the author were given by the research staff from the Department of Aquaculture of the Spanish Oceanographic Centre in Tenerife (COC), focus group B.

The marine environment showed the biggest differences between the focus groups. Groups B and C strongly correlated while group D showed very weak correlation with these two groups. This, again, could be due to the fact that the decision-makers from this group were not familiar with the peculiarities of the study area.

5.3.3 Integrations of Weights From the Questionnaires With the GIS-Based Models

In order to compare the differences between the weights given by the different focus groups and those proposed by the author, the model was re-run with the average weights given by each group. To facilitate the interpretation of the results, these images were masked to depths of 50 m (Fig. 5.26, Fig. 5.27 and Fig. 5.28).

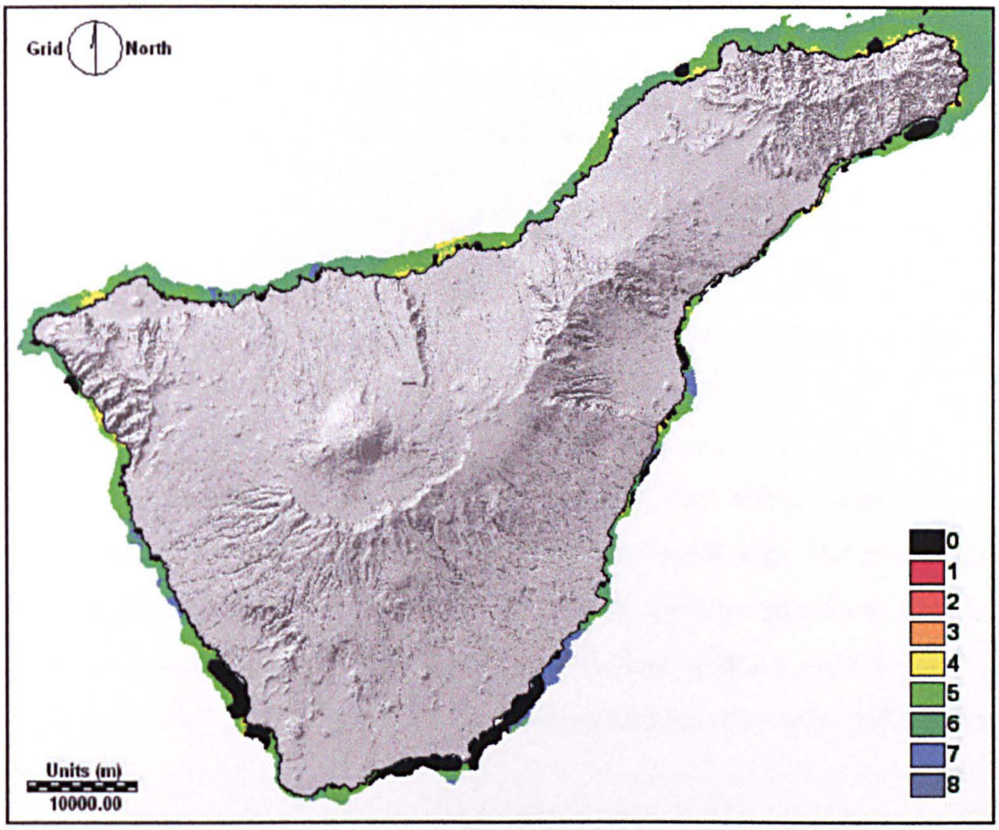

Fig. 5.26: Overall suitability map, masked to depths of 50 m, for siting Corelsa® fish cages in Tenerife using the average weights given by the focus group B (researchers at the COC).

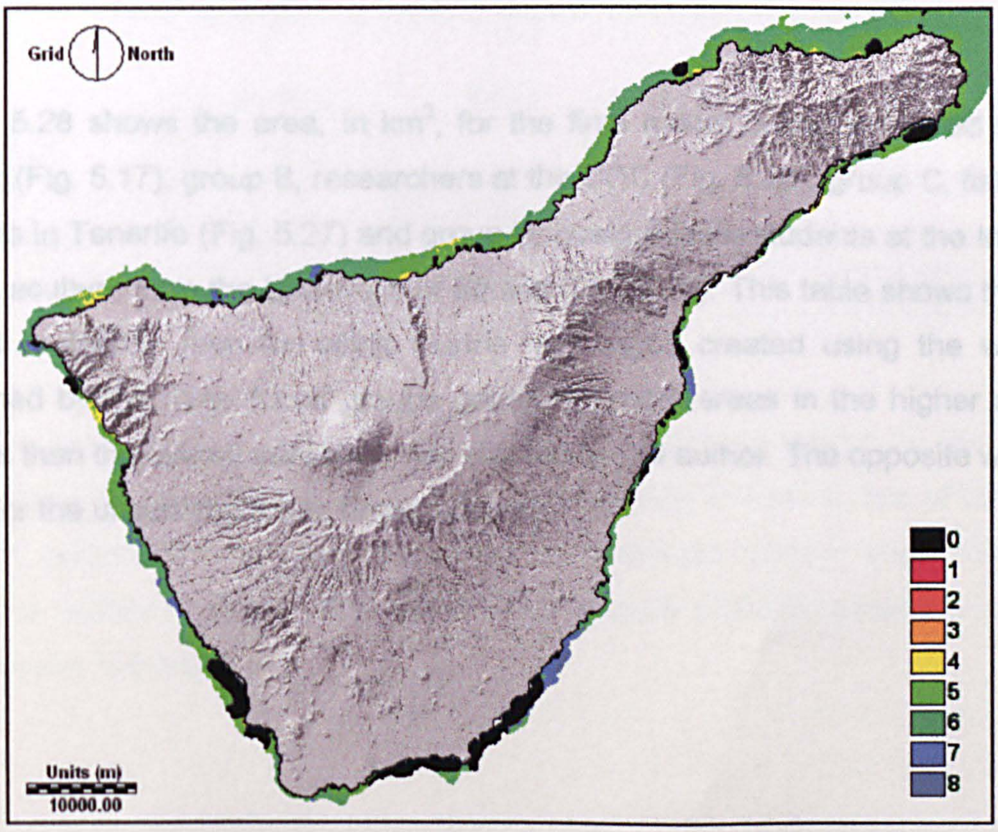

Fig. 5.27: Overall suitability map, masked to depths of 50 m, for siting Corelsa® fish cages in Tenerife using the average weights given by the focus group C (farmers).

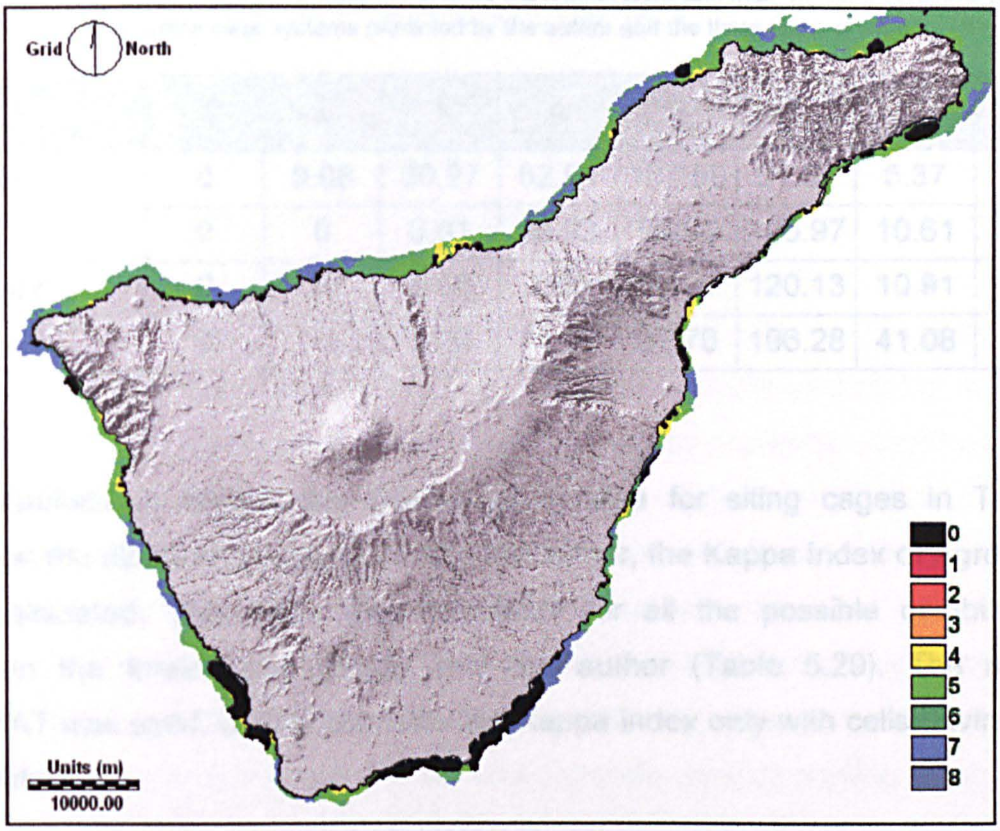

Fig. 5.28: Overall suitability map, masked to depths of 50 m, for siting Corelsa® fish cages in Tenerife using the average weights given by the focus group D (students).

Table 5.28 shows the area, in km^2, for the final model output predicted by the author (Fig. 5.17), group B, researchers at the COC (Fig. 5.26), group C, fish cage farmers in Tenerife (Fig. 5.27) and group D, postgraduate students at the Institute of Aquaculture from the University of Stirling (Fig. 5.28). This table shows that the overall suitability map for siting marine fish cages created using the weights assigned by the three focus groups generated more areas in the higher scores ranges than the overall suitability map created by the author. The opposite was the case for the unsuitable areas (lower scores).

Table 5.28: Area, in km^2, for each suitability score for the overall suitability map, masked to depths of 50 m, for Corelsa cage systems predicted by the author and the three focus groups.

Suitability Scores	1	2	3	4	5	6	7	8
Author	0	0.08	20.27	62.91	107.58	31.33	5.37	0.51
COC	0	0	0.01	15.93	94.56	105.97	10.61	0.97
Farmers	0	0	0.00	7.60	88.51	120.13	10.91	0.90
Students	0	0	0.02	11.92	67.70	106.28	41.08	1.04

To quantitatively assess the differences in area for siting cages in Tenerife between the different focus groups and the author, the Kappa Index of Agreement was calculated. This index was calculated for all the possible combinations between the three focus groups and the author (Table 5.29). The module ERRMAT was used, which calculates the Kappa index only with cells having non-zero value.

Table 5.29: Kappa index of agreement between the overall suitability maps, masked to depths of 50 m, for Corelsa cage systems predicted by the author and the three focus groups.

	Author	COC	Farmers	Students
Author	1			
COC	0.01	1		
Farmers	-0.04	0.73	1	
Students	-0.12	0.45	0.48	1

The calculated Kappa indices indicated that the output predicted by the author differs from those predicted by the three focus groups. Moreover, two of the focus groups, farmers and students, showed a weak inverse relation when compared with the author's output. The three focus groups showed moderate positive correlations between them.

5.4 INTEGRATION OF PARTICULATE WASTE DISTRIBUTION MODELLING WITH THE GIS-BASED MODELS

Areas which have been selected as the most suitable for siting of cages will benefit from a further study to quantify the dispersive nature of a site, and therefore, assist in predicting possible environmental impacts, as well as establishing the maximum desirable production of a site. In this section an improved version of an existing predictive particulate waste distribution model for cage farmed fish, which uses Geographic Information Systems combined with a spreadsheet, is presented (Perez *et al.*, 2002). The model presented uses existing distribution algorithms but also incorporates functions to calculate feed loading for all the cages within a pontoon independently, spreads the input load over the whole cage area and simulates post-depositional distribution of the carbon. The model uses approximate estimates of feed and faecal waste derived from dietary considerations (mass balance model) and separate, unique settling velocities for waste feed and faecal particles. The model incorporates values of current speed and direction recorded over spring and neap tides. Output from the model is in the form of a contour plot of organic carbon (g C m^{-2}), showing distribution of the particulate organic carbon material as deposited on the seabed.

5.4.1 Introduction

The rapid expansion and development of the aquaculture industry has increased environmental concerns and questions about possible ecological impacts. Environmental managers and regulators have pointed out the necessity of minimising environmental impacts if productivity in the aquaculture industry is to be sustainable (e.g. Scottish Executive, 1999). However, a complete reduction to zero of wastes discharged from marine fish cages is not possible for present culture systems, from either a technological or an economical point of view.

There are many forms of wastes produced as a consequence of the transformation of any natural resource into a marketable product, and this is as true for marine fish aquaculture as other forms of resource utilisation. However, of all the possible wastes released by marine fish farming to the environment, particulate organic waste in the form of uneaten feed and faeces are usually the most significant fraction (Beveridge, 1996). This material, which generally settles on the seabed near to the cages, provides a net input of organic carbon and nitrogen to the sediments, thus the accumulation of waste can cause major changes in the benthic community and may exceed the environment's capacity to bioprocess this material (Gowen and Bradbury, 1987; Gowen *et al.*, 1988; Findlay and Watling, 1994; Hargrave, 1994; GESAMP, 1996a). Moreover, environmental deterioration due to high organic matter concentrations in the sediments may affect the health of farmed fishes and hence profitability (Beveridge, 1996; GESAMP, 1991b).

Modelling of input and distribution of wastes and discharges is a cost-effective tool that can assist in the prediction of future impacts and aid decision-makers. Distribution models for organic waste from aquaculture can be used to predict possible impacts on the environment, helping environmental regulators to make informed decisions when licensing new marine fish farm developments and granting consents to discharge waste. Some models have been developed to forecast loading and distribution of particulate waste carbon from fish farms (Gowen *et al.*, 1989; Fox, 1990; Silvert, 1992; Silvert, 1994; Telfer, 1995; Hevia *et al.*, 1996), but only DEPOMOD has undergone some validation (Cromey *et al.*, 2000).

This section describes the development of GIS spatial modelling techniques (Perez *et al.*, 2002) based on a pre-existing particulate distribution model (Walls, 1996; Telfer, 1995; Perez-Martinez, 1997), which is in turn based on distribution equations developed by Gowen *et al.* (1989). The success of GIS for modelling purposes stems from their capacity for fast image generation and manipulation, the flexibility to run alternative scenarios, statistical analysis of the image and generation of sophisticated output which helps visual interpretation of results. The GIS based model was validated using field data and fish production information. See Appendix 3 for more details of the model validation.

5.4.2 Model Development

There are three main stages within this model; quantification of the waste material (uneaten feed and faces) using mass balance techniques, calculation of the distribution of the waste components using Gowen's formula (Gowen *et al.*, 1989), and calculation and generation of the final contour distribution diagrams. The first two submodels are run in a spreadsheet and the third is carried out using the GIS software IDRISI32. The final output from the model is a quantitative contour map showing the distribution of particulate organic carbon deposited on the seabed.

5.4.2.1 Mass Balance

The quantities of waste released to the environment, particulate organic carbon in form of uneaten feed and faecal material, are calculated using a mass balance model (Fig. 5.29). The expected fish production during a set period of time is multiplied by the expected food conversion ratio (FCR) for that period. In the present model, the percentage of water in the feed is assumed to be 8% (Findlay, 1994) while that of carbon in the feed is assumed to be 46% (Penczak *et al.*, 1982). From the feed given to the fish, 90% is consumed and the remaining 10% is lost as uneaten feed (Hargrave, 1994). It is assumed here that 50% of the consumed carbon is respired (Gowen *et al.*, 1988) and that 14% is incorporated into body tissues (Chen, 2000), although it is important to bear in mind that mass balance quantities for organic carbon flux for cage production vary from author to author (e.g. Gowen *et al.*, 1989; Silvert, 1994; Telfer, 1995; Hevia *et al.*, 1996). Carbon in faecal material is calculated as the difference between carbon consumed and carbon used for respiration and growth.

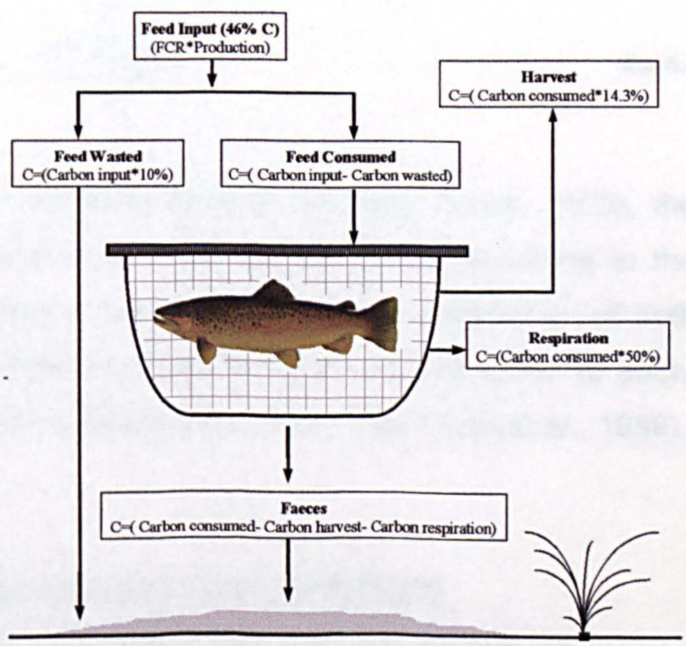

Fig. 5.29: Mass balance used to calculate carbon wasted from uneaten feed and faecal material in fish net-pen culture.

5.4.2.2 DISTRIBUTION EQUATION

For modelling purposes, the farm is located in the middle of a 500 by 500 cell array where each cell representing 1 m^2 and X and Y are their coordinates. The horizontal distribution of a particle (X and Y components for each cage of the farm) is calculated using the equations of Gowen *et al.*, (1989) (see Eq. 5.4 and Eq. 5.5). The depth under the cage (d), the mean current speed (V), current direction (θ), settling velocity (u) and position of each cage (x, y) are site specific measured quantities.

$$X = \frac{d * V\sin\theta}{u} + x \quad \textbf{Eq. 5.4}$$

$$Y = \frac{d * V\cos\theta}{u} + y \quad \textbf{Eq. 5.5}$$

Because wastes fall more or less vertically through the cage (Inoue, 1972), the source of distribution was assumed to be from the depth corresponding to the bottom of cage. The same equation is used to calculate the distribution of both uneaten feed and faeces, but different settling velocities are assigned to each; 0.128 m s^{-1} and 0.04 m s^{-1} respectively (Warrer-Hansen, 1982; Chen *et al.*, 1999).

5.4.2.3 GEOGRAPHICAL INFORMATION SYSTEMS (IDRISI32)

The carbon deposition co-ordinates calculated with Gowen's formula (Gowen *et al.*, 1989) and their associated carbon values are exported to IDRISI32 GIS software. Interpolation between values is then undertaken by the GIS program to generate a complete surface. This technique is a particular strength of using GIS for modelling purposes, in that small or sparse data sets can be used to produce a complete map. However, the nature of the interpolation process means that the carbon quantities are over-estimated and require correction later in the model. The reason for the sparse number of data points used for modelling, and the need to interpolate to smooth the data, is that the current readings, speed (V) and direction (θ), are taken at regular intervals over a defined time period (e.g. 1 hour). During that period (t_0) all the carbon produced is assumed to settle in one location (X_0, Y_0)

and during the subsequent hour (t_1) in another location (X_1, Y_1). In reality, the process of moving from one location to another is done gradually and the carbon is dispersed over all locations, not only at the initial and end locations, as illustrated in Fig. 5.30.

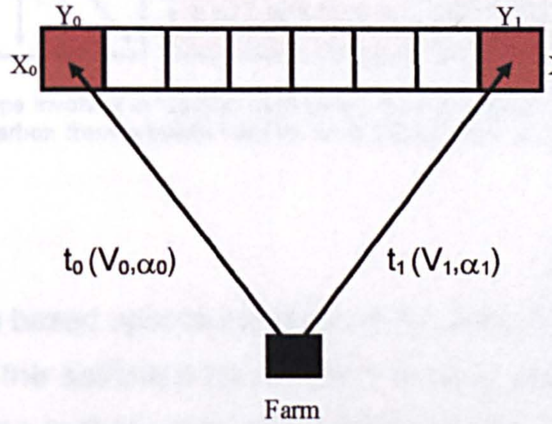

Fig. 5.30: The process of carbon allocation by spreadsheet.

Most models assume a single point as the source of carbon output from a cage (feed and faeces), usually the cage centre. To eliminate this assumption, predicted carbon values allocated on the seabed are spread over an area equal to the cage area by applying a filter within IDRISI32 (Fig. 5.31).

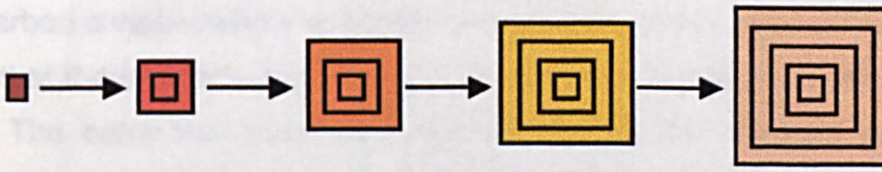

Fig. 5.31: Consecutive filtering technique to spread carbon into an area similar to the cage area.

Variations in initial distribution of waste and post-deposition changes in carbon are considered by using a second filtering technique within IDRISI32, which redistributes the amount of carbon from each cell into the eight surrounding cells by a predetermined percentage, which differs between the relatively dense feed and lighter faeces. Each cell represents $1m^2$, hence the final area affected from each of the initial cells is $9\ m^2$ (Fig. 5.32a, b, c).

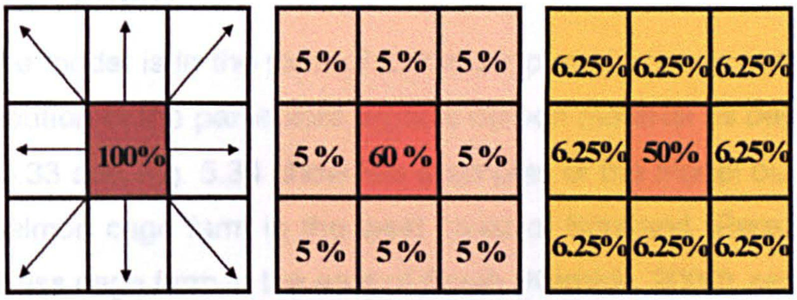

Fig. 5.32: Sequence of steps involved in "carbon spreading". (a) the original cell as predicted from Gowen's equations, (b) spread of carbon from uneaten feed to surrounding cells, (c) spread of faecal carbon to the surrounding cells.

The filter structure is based upon theoretical work (Chen, 2000). Pellets and faecal matter travel along the sediment by saltation (rolling, sliding or hopping) when current speeds attain a critical value, defined here as the velocity that causes 50% of the pellets to move. Distance travelled and number of re-suspended particles are site specific. Although this final GIS filter has minimal impact on modelled carbon distribution, as shown by sensitivity analysis with and without the filter, it is included to give a more realistic picture of the processes involved in the final carbon distribution.

Finally, it is necessary to correct the carbon quantities in the resultant image, which are over-estimated due to the interpolation process. Interpolation generates additional data between a set of known values. However, it does not reduce the original carbon concentrations to compensate for this, which means that the model assumes that there is considerably more carbon entering the sediment than there really is. The correction is achieved by multiplying the resultant output by a correction factor (CF), which is calculated by dividing the total predicted waste carbon from the mass balance (feed and faeces) by the total carbon in the resultant image (Eq. 5. 6).

$$CF = \frac{\text{Total predicted waste carbon (kg)}}{\text{Waste carbon in the image (kg)}} \qquad \textbf{Eq. 5. 6}$$

5.4.2.4 MODEL OUTPUT

Output from the model is in the form of a contour plot of organic carbon (g C m^{-2}), showing distribution of the particulate organic carbon material as deposited on the seabed. Fig. 5.33 and Fig. 5.34 show two examples of the model output run using data from a salmon cage farm in the west coast of Scotland (Perez *et al.*, 2002) and for a seabass cage farm in the east of Spain (Kernick, 2000), respectively.

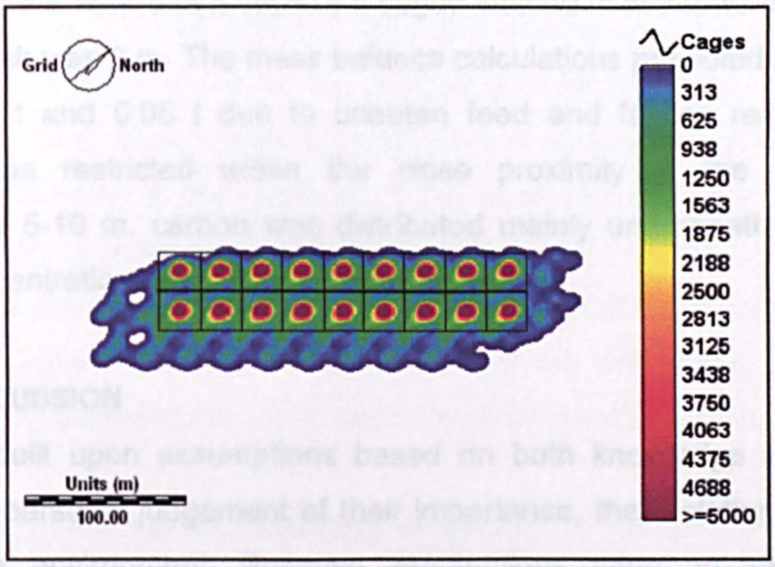

Fig. 5.33: Contour model for a salmon cage farm site on the west coast of Scotland showing distribution of organic waste carbon input (g C/m^2) to the sediment over a 4-month simulation period with a maximum standing biomass of 172.5 t fish and an average FCR over the production period of 1.2.

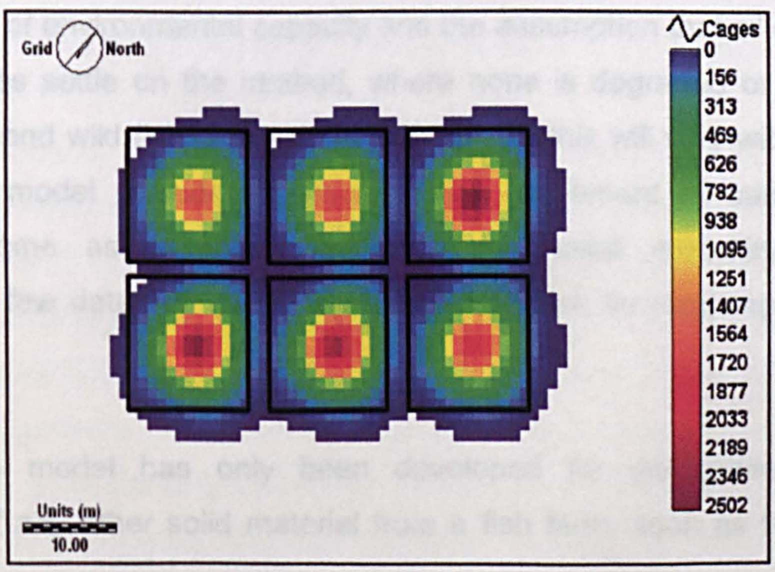

Fig. 5.34: Contour model for a seabass farm site on the east cost of Spain showing distribution of organic waste carbon input (g C/m^2) to the sediment over a 2 month simulation period with a maximum standing biomass of 0.33 t fish and an a feed input of 0.64 t.

The output from Fig. 5.33 shows the distribution of the cages in the farm, which comprised 18 cages located in two rows of 9. The mean depth under the cages was 15 m. From the mass balance calculations 35.4 t of carbon were wasted, 10.3 and 25.0 t due to uneaten feed and faeces respectively. The carbon was distributed mainly in NE and SW directions. The highest concentrations were located under the cage, reaching values of 12 kg C m^{-2}. The concentration of carbon decreased as the distance from the cage increased.

Fig. 5.34 shows a farm distribution of 6 cages located in two rows of 3. In this site the mean depth was 3 m. The mass balance calculations predicted 0.1 t of carbon wasted, 0.06 t and 0.05 t due to uneaten feed and faeces respectively. The dispersion was restricted within the close proximity of the cage system, approximately 5-10 m. carbon was distributed mainly underneath of the cages, reaching concentration as high as 2.5 kg C m^{-2}.

5.4.2.5 Discussion

Models are built upon assumptions based on both knowledge of the process involved and personal judgement of their importance, their relation to each other and with the environment. Because assumptions carry an inherent risk of inaccuracy, it is desirable both to reduce their use to a minimum and to identify their impact on overall predictions in order to understand and interpret model outputs. Possible sources of inaccuracy in the present model are the lack of consideration of environmental capacity and the assumption that all carbon wastes from the cages settle on the seabed, where none is degraded or consumed by invertebrates and wild fish. Although it is likely that this will vary with location, the present GIS model considers post-deposition movement of carbon, and has eliminated some assumptions from previously used modelling techniques. Furthermore, few data are needed to run the model, so reducing costs of field surveys.

Although the model has only been developed for particulate carbon, the distribution of any other solid material from a fish farm, such as N, P or in-feed chemotherapeutants, can also be modelled, providing that accurate data on inputs are available.

5.4.3 Integration of Model

The use of more exposed sites, such as those in Tenerife, although taking advantage of a deeper and more dispersive environment, does not reduce the total waste released into the marine environment. For the same waste output, local effects may be reduced at offshore sites and ecological change affecting farm production is less likely. However, the concept of holding capacity applies to both offshore and inshore sites. Hence it is necessary to match the size of the operation and waste production to the capacity of the ecosystem to assimilate waste, to ensure that there is minimal ecological change and that the long-term production potential of the site can be maintained. Licensing authorities, such as the Spanish Environment Department (Casado *et al.*, 2001), are demanding more stringent standards on the potential effects of these farms on the surrounding environment,

Computerised mathematical modelling is proving to be an invaluable tool in providing the aquaculture industry with a forecast of the expected conditions at the offshore sites and the effect of the proposed farms on the neighbouring ecosystem (Bell and Barr, 1990). However, when using models to predict maritime conditions and the effect on the water environment, it is essential to understand the nature of the problem and the range, application and limitations of the model being used.

Potential applications for the developed particulate waste distribution model are within Environmental Impact Assessment (EIA), design of monitoring programmes, farm management, rapid generation of "*what if?*" scenarios and site selection. An environmental management plan should include an EIA and this often requires the use of predictive models to quantify significant potential impacts and design a monitoring programme (GESAMP, 1996a). Numerical models, such as described here, have the potential to generate quantitative predictions, and are therefore, a useful tool in quantifying impacts of cage aquaculture wastes. Moreover, Jørgensen (1991) suggested that the use of validated models to predict environmental impacts to be the most cost-effective approach. Models can also be used to allocate development areas (zonation) or for comparison of outputs at different sites by modelling the waste deposition pattern at any given production level. Similarly, the maximum desirable production at a site can be established.

Although the developed particulate waste distribution model was not used because there were not available current data to run it, in the context of this study it could be of use for final selection of the most suitable sites. Currentmeters could be deployed in those areas identified as most suitable to quantify the dispersive nature of a site, and therefore, assist in predicting possible environmental impacts on the benthos. Moreover, this model could help regulators to establish the maximum desirable production at a site, and hence, estimate the maximum number of farmed tonnage and number of cages that a site could support for sustainable aquaculture industry development in Tenerife.

5.5 DISCUSSION

In this chapter all variables and submodels were combined to provide an overall model for assessment of the suitability of costal areas in Tenerife for developing marina fish culture in three different cage systems, Corelsa®, OceanSpar® and SeaStation®. A total of 27 factors and 4 constrains, divided into 8 submodels, were included in this study (Fig. 5.25).

The models were built based on hierarchical structures, which break down all criteria into smaller groups (or submodels). Once the models were structured, the decision maker's preferences with respect to the evaluation criteria were incorporated into the decision model. The preferences were expressed in terms of the weights of relative importance assigned to the evaluation under consideration. The larger the weight, the more important was the criteria in the overall utility.

The ultimate aim of the analysis was to combine the main elements of spatial multicriteria decision analysis, evaluation criteria (factors and constrains) and decision-makers preferences (weights), using multicriteria decision rules, also referred to as multi-criteria evaluation (MCE). These are mathematical expressions that combine the weights and scores of each of the thematic maps used. The decision rules provide the basis for ordering the decision alternatives and for choosing the most preferred alternative.

Cage systems that can withstand harsh environments are suitable for use over a broader area of Tenerife's coastline. Thus, the more robust self-tensioned cage (SeaStation®) could be used over a greater area than the weaker gravity cages (Corelsa®). From the 228 km^2 of available area for siting cages in the coastal regions with depth of 50 m, the suitable area (sum of scores 6, 7 and 8) for siting SeaStation® cages was 61 km^2, while the suitable area for SeaStation® and Corelsa® cages was 49 and 37 km^2 respectively. Most of the variation between these three cage systems was found among the intermediate suitability scores (Table 5.16). It was concluded that the biggest differences among cage systems are between Corelsa® and SeaStation® systems, followed by differences between Corelsa® and OceanSpar® cages, and OceanSpar® and SeaStation® respectively. This variability was mostly located on the N and NNW of the island, where the wave regime, both long and short-term, is higher.

The final suitability output from this study was solely based on the weights given by the author, as it was though that the author had a wider knowledge of the study area and the decision-making spatial technique being used. Although the conclusions and recommendations arising from this study are solely based upon the criteria weights assigned by the author's, "real-world" spatial decisions task normally involve several interest groups or decision-makers. These groups could have different points of view, perceptions and often conflicting interest in the decision-making process. Consequently, this study accounted for these different points of view to the task of siting marine fish cages in Tenerife by selecting three focus groups, all of whom had relevant but different experience in the field, and using questionnaires.

The results from the questionnaires proved very useful. General agreement was found among all focus groups that the criteria chosen by the author for the evaluation of marine fish cage site selection in Tenerife were relevant, and none of them were rejected from the evaluation by any of the decision-makers. Moreover, some decision-makers suggested new criteria which initially were not included by the author, such as the seabed slope or the sewage pipes constraint.

It was found that the most difficult part of the questionnaires was the completion of the pairwise matrix to calculate the criteria weights. This finding suggested that it might be necessary to develop a different strategy for future studies if questionnaires are to be used. One possible amendment may be to use of a scale from 1 to 10 which may be more intuitive and easier to use than the proposed 1 to 9, as people are more familiar and confident with that system. Another alternative is to directly assign weights to the factors, thus discarding the need to complete the pairwise matrix, as some decision-makers believe that it would make it easier for them.

The statistical analysis of the questionnaires (weights) was done by using the Kendall coefficient of concordance. This is a non-parametric test that expresses the agreement among independent judges who are rating (ranking) the same stimuli. Variable agreement was found between the weights (ranks) given by the decision-makers within each of the focus groups, making it difficult to conclude that a particular focus groups showed a defined view or set of weights. It was found that, in general, there was moderate agreement between the average weights (ranks) given by the different focus groups and those proposed by the author. The focus group which differed the most from the author weights were the farmers (group C), while the research staff from the Department of Aquaculture of the Spanish Oceanographic Centre in Tenerife (group B) showed the best correlation. In general, it was found that submodels with smaller number of factors showed better agreement that those with larger numbers.

The integration of the criteria and submodel weights given by the different focus groups with the GIS-based models showed that, the overall suitability area for siting marine cages (Corelsa®) is greater than that predicted when the model is run with the weights assigned by the author. In fact, the Kappa indices indicated that the output predicted by the author differed from those predicted by the focus groups.

Finally, a particulate waste distribution model was developed and integrated with the GIS-based models. This waste model, although not directly used in this study due to unavailability of current data, was intended to narrow down the selection of sites already identified as most suitable, by predicting possible environmental impacts on the benthos if aquaculture was to be developed on a specific site. Moreover, this model could help regulators to establish the maximum desirable production at a site, and hence, estimate the maximum number of farmed tons and number of cages that a site could support for a sustainable development of the industry in Tenerife.

Chapter 6

Sensitivity Analysis

6.1 INTRODUCTION

In previous chapters, the strategies and techniques for tackling the spatial multicriteria decision task of siting marine fish cages in Tenerife has been explained and described. The approach assumed implicitly that complete information will be available. However, in "real-world" situations, the information available to the decision-maker is often uncertain and imprecise due to measurement and conceptual errors. In recent years, the issue of error and uncertainty associated with GIS and geographical information in general, has received growing attention from all sectors of the industry, with the realization that there is considerable potential for litigation, loss of personal and agency integrity arising from errors in geographical databases (Epstein *et al.*, 1998).

The model presented in this study is defined by a series of equations, input factors, parameters, and variables aimed at characterising the suitability of siting marine fish cages in Tenerife. Input is subject to many sources of uncertainty including errors of measurements, absence of information and poor or partial understanding of the driving forces and mechanisms (Arbia *et al.*, 1998). This imposes a limit on the confidence in the response or output of the model. Hence, it is necessary to provide an evaluation of the confidence in the model, possibly assessing the uncertainties associated with the modelling process and with the outcome itself. The basic approach to handling uncertainties (error) in multicriteria decision analysis is by sensitivity analysis (SA) (Saltelli *et al.*, 2000). SA in used within this context to increase confidence in the model and its predictions, by studying how the variation in the output of a model can be apportioned to different sources of variation, and how the given model depends upon the information fed into it. Lodwick *et al.* (1990) suggested that a sensitivity analysis of an overlay-based suitability analysis, such as this study, can indicate what maps (criteria) are the most or least critical in determining the values of the output map. These critical maps indicate where most or least care may be taken in the input data in order to draw reliable conclusions from the output map.

Finally, it is necessary to choose a sensitivity analysis technique from the large number of methodologies available. The choice of which SA method to adopt is difficult, as each methodology has its advantages and disadvantages. Such a choice depends on a number of factors: objective of the analysis, the properties of the model under study, the number of input factors involved in the analysis and the computational time needed to evaluate the model. With these factors in mind, local SA was the method chosen in this study as it gives an idea of the inputs (factors) that contribute most to the output variability. Local SA computes partial derivatives of the output functions with respect to the input variables (differential analysis). In order to compute the derivative numerically, the input parameters are varied within a small interval around a nominal value. The interval is not related to degree of knowledge of the variables and is usually the same for all of the variables.

6.2 METHODOLOGY

A study of geographical sensitivity analysis can begin at any step of the suitability analysis. In fact, the steps involved in geographical suitability analysis determine the types of sensitivity analyses. Lodwick *et al.* (1990) identified fourteen types of sensitivity analysis that can be performed at different levels of the suitability analysis process (Table 6.1). Many of these errors can be considered in an integrated manner by focusing on the geographical sensitivity measures for the suitability maps as a whole.

Table 6.1: Types of sensitivity analysis that can be performed at different levels of the suitability analysis process (Lodwick *et al.*, 1990).

SENSITIVITY ANALYSIS	DESCRIPTION
MAP MAKING SENSITIVITIES	Are sensitivities that occur in the process of making a primary map to be used as inputs in geographical analysis.
DELINEATIONAL SENSITIVITIES	Are the variations in the output maps that are due to where lines are placed on a map.
DATA INPUT AND TRANSFER SENSITIVITIES	Are the variations due to transforming primary maps into computer files to be used in a GIS.
REFORMATTING SENSITIVITIES	Are the variations in accuracies that are due to changes in projection or scale of the maps and algorithm associated with a given GIS.
EXTRAPOLATION SENSITIVITIES	Are the variations in the output maps that depend on a variety of contouring or extrapolation techniques used.
ORDER/AGGREGATIONAL SENSITIVITIES	Can occur when a sequence of paired overlays is performed each followed by an aggregation. The order in which the overlay/aggregation occur will make a difference in the resultant map.
TAXONOMIC SENSITIVITIES	Are the variations associated with classifying geographical entities which are used to delineate areas or features on a map.
INTERPRETATIONAL SENSITIVITIES	Are variations in assigning linguistic meaning to geographical data such as the word "low" to a temperature gradient.
VALUE SENSITIVITIES	Are the variations in assigning a quantitative meaning to a geographical entity.
RESOLUTIONAL SENSITIVITIES	Are the variations in the output maps that are due to the level of detail at which the units are mapped and the projection used.
METRIC SENSITIVITIES	Are the variations that arise when different equations are, or could be, employed in the determination of the same analysis.
WEIGHT SENSITIVITIES	Are the variations that occur with respect to perturbations of weights associated with overlay operations to asses suitability.
LAYER SENSITIVITIES	Are the variations in the output map that are due to removing any one or a group of maps in a suitability analysis.
SCALE SENSITIVITIES	Are the variations that arise from different scales ranges used in rating schemes for rank maps.

The two most important elements to consider in a global sensitivity analysis are criterion weights and attribute values. Weight sensitivity analysis is needed because of the uncertainty involved in the specification of a decision-maker's preferences. This is associated with the fact that judgment plays a key role in spatial multicriteria decision-making. In other words, criteria weighting is a subjective appreciation of the problem at hand, and indeed varies between different decision-makers (as seen in Chapter 5). In some situations, decision-makers are not able to provide precise judgements with respect to the relative importance of evaluation criteria due to limited or imprecise information and knowledge. It is also common for inconsistencies to be found while elucidating the decision-maker's preference (Saaty 1980). A sensitivity analysis involving weights consists of investigating the sensitivity of alternatives to small changes in the value of attribute weights. However, this was not performed as sensitivity analysis *per se* in this chapter because it was already addressed in Chapter 5, where the model was run with weights from three different groups and compared with those proposed by the author.

Sensitivity due to errors in estimating the attribute values, or thematic map errors, are referred to as uncertainty associated with GIS data sets on the basis of which the map have been created (Fisher *et al.*, 1997). The thematic map errors can be classified into measurement or conceptual. The former is associated with imprecision in the measurement of criterion values, and the latter attributed to the process of translating real-world entities into map objects (Li *et al.*, 2000). The simplest and most widely used representation of sensitivity analysis is to show the percentage change in the variable and the output. This is achieved by systematically changing one variable, and observing the output. This analysis measures the overall magnitude of change in the attribute values from their "unperturbed" values. In this study interval values of ± 5, 10 and 15% of the reference situation were chosen.

6.3 SENSITIVITY ANALYSIS

A full sensitivity analysis for all thematic maps is a difficult task. With large numbers of attributes, this involves numerous iterations, and the results may not be easy to interpret. In practice, values associated with thematic maps having high importance weights are the most likely candidates for sensitivity analysis. This is because if the weights of the attributes are high, even slight changes in estimated values may result in a change in the ranking of the alternatives. Also, thematic maps involving a high degree of uncertainty and subjectivity in estimation should be considered in sensitivity analysis to investigate the effect of their variation on the ranking of alternatives.

Based on these considerations, five criteria were selected as candidates for sensitivity analysis in this study; short-term waves, long-term waves, sewage discharges (increase in number of people connected to the sewage), sea temperature and suspended solids. To facilitate the interpretation of the results, the sensitivity analysis was only conducted for one of the three cage systems selected in this study, the Corelsa® cages, and was limited to depths less than 50 m. This cage system was chosen because it is the only one presently being used in Tenerife and the most likely future cage system of choice to be used.

During the sensitivity analysis the created maps were not combined with the constraint layer, as was done in Chapter 5 for creating the overall suitability maps, because it was more important to asses the variability of the model rather than the actual suitability area created by each map. Therefore, it was considered that by omitting the constraint layer more coastal area will be available, and consequently, the possible variability of the model to changes could be better understood. As a result, the available area for siting cages increased from 228 km^2 when the constraints are overlaid to 271 km^2 when they are not.

The following sections are each structured in a similar way and show the results of sensitivity analysis for each of the five selected criteria by means of tables and figures. The tables show the area in square kilometres for the suitability scores for the baseline model (referred as "*original*" in the tables) versus the area of each of the suitability score when the variables are changed a certain percentage (± 5, 10 and 15%). There are three tables for each variable: one showing the changes of the variable itself, a second showing the changes in the submodel where the variable is included, and a third presenting the overall changes in the model. Three corresponding figures for each table are presented showing the change in area from the baseline model and the changed variable for each suitability score.

Finally, the absolute sensitivity was calculated for each of the five selected criteria as a measure of their importance on the model overall variability to possible variations.

6.3.1 Short-term waves

Sensitivity analysis indicated that changes in the short-term waves layer had direct impacts on the predicted suitability area as shown in Table 6.2 and Fig. 6.1. The greatest changes were found on the lower suitability scores. Aggregated negative interval values showed the greatest variation in area, up to 370 km^2, while the aggregated positive values showed variations up to 301 km^2.

Table 6.2: Sensitivity analysis for short-term waves. All values in km^2.

Suitability Scores	1	2	3	4	5	6	7	8
original	**186.1**	**30.9**	**2.9**	**5.7**	**4.5**	**30.5**	**10.3**	**0**
+ 15%	217.5	2.9	5.7	4.5	30.6	0	10.3	0
+ 10%	217.5	2.9	5.7	4.5	30.6	0	10.3	0
+ 5%	186.3	31.2	2.9	10.3	30.6	0	10.3	0
- 5%	183.5	2.8	34.1	5.7	4.5	30.6	0	10.3
- 10%	159.9	26.4	31.2	2.9	5.7	35.1	0	10.3
- 15%	112.7	70.8	2.8	34.1	5.7	4.5	30.6	10.3

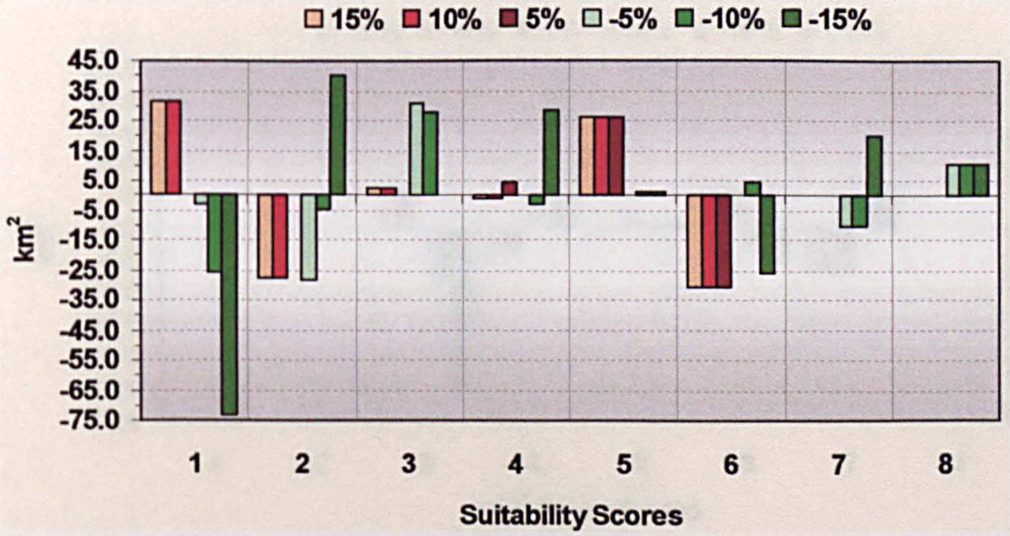

Fig. 6.1: Difference in area for each suitability score between the base line short-term waves layer and the modified percentages.

The sensitivity analysis of the marine environment submodel with the modified short-term wave layers included, found that most of the variation was among the intermediate suitability scores of 3 and 4 and the higher scores of 6 and 7 (Table 6.3 and Fig. 6.2). Generally, changes in area almost doubled for the aggregated negative values (96 km^2) when compared to the aggregated positive values (57 km^2).

Table 6.3: Sensitivity analysis for marine environment submodel when short-term waves values were changed. All values in km^2.

Suitability Scores	1	2	3	4	5	6	7	8
original	**0**	**3.0**	**123.7**	**97.1**	**7.6**	**24.5**	**19.8**	**0**
+ 15%	0	3.0	129.4	92.9	7.2	29.9	13.3	0
+ 10%	0	3.0	129.4	92.9	7.2	29.9	13.3	0
+ 5%	0	3.0	123.7	97.1	8.6	30.0	13.3	0
- 5%	0	3.0	120.4	100.1	7.6	21.7	22.9	0
- 10%	0	3.0	115.5	104.2	7.9	22.1	22.9	0
- 15%	0	3.0	98.2	121.0	8.5	18.7	26.4	0

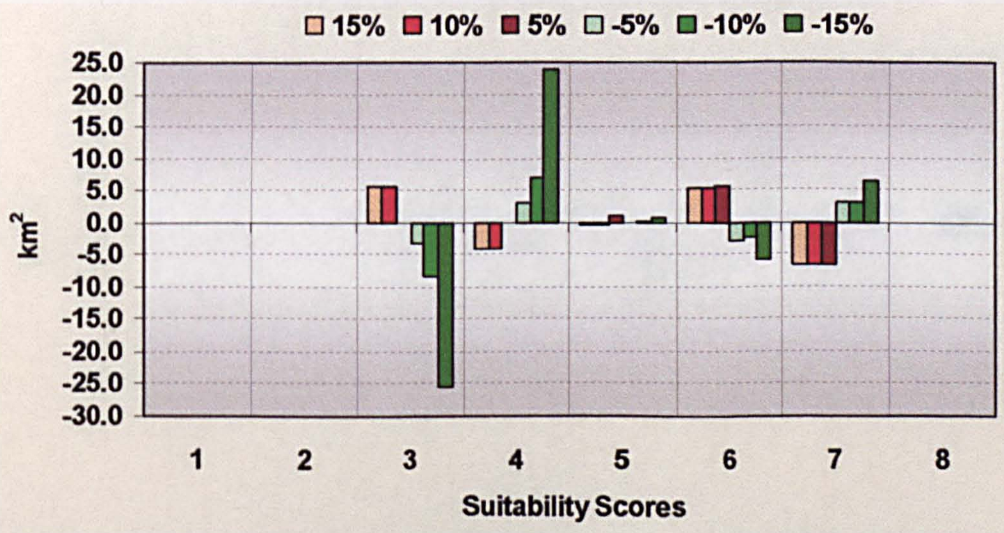

Fig. 6.2: Difference in area for each suitability score between the base line marine environment submodel, when short-term wave values were changed, and the modified percentages.

The sensitivity analysis of the overall model output with the modified short-term wave layers included, found that most of the variation was within the suitability scores 3 to 7 (Table 6.4 and Fig. 6.3). Overall, aggregated negative interval values showed slightly greater variation in area than aggregated positive values, with most of the variation was found on the -15% interval. On the other hand, the positive values did not show much variation. Variation values of +10% and +15% were found to have the same change in area for each of the suitability scores.

Table 6.4: Sensitivity analysis for the overall model output when short-term waves values were changed. All values in km^2.

Suitability Scores	1	2	3	4	5	6	7	8
original	**0**	**0.1**	**26.2**	**78.5**	**121.7**	**41.5**	**7.2**	**0.5**
+ 15%	0	0.1	27.3	78.8	122.6	40.2	6.2	0.5
+ 10%	0	0.1	27.3	78.8	122.6	40.2	6.2	0.5
+ 5%	0	0.1	26.2	79.0	122.9	40.8	6.2	0.5
- 5%	0	0.1	25.8	78.6	121.5	41.1	7.4	1.1
- 10%	0	0.1	25.6	77.9	121.9	41.6	7.5	1.1
- 15%	0	0.1	22.4	80.1	119.9	44.2	7.9	1.1

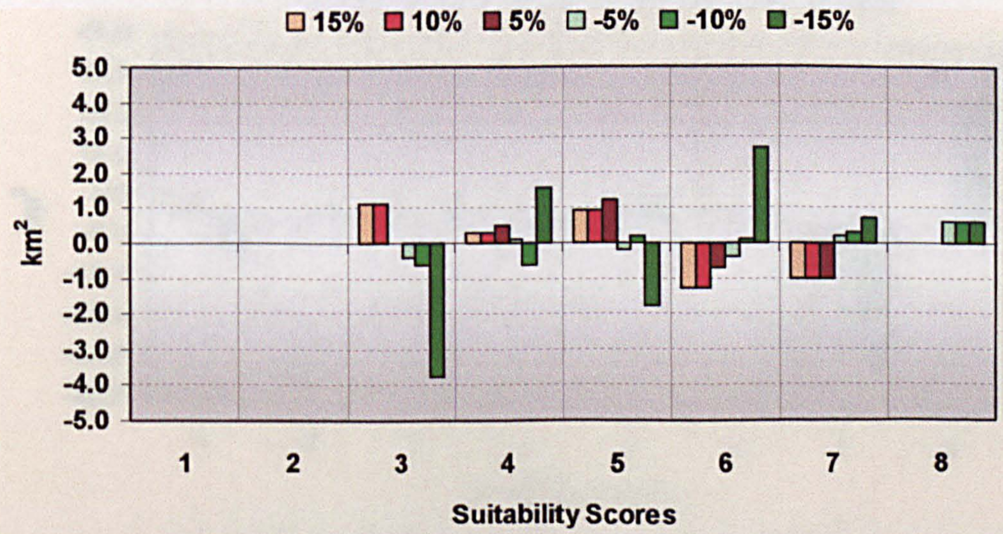

Fig. 6.3: Difference in area for each suitability score between the base line overall model, when short-term wave values were changed, and the modified percentages.

6.3.2 Long-term waves

Sensitivity analysis for the long-term waves layer found that the greatest variation is within in the higher suitability scores (Table 6.5 and Fig. 6.4). Overall, changes in area almost doubled for the aggregated negative values (267 km^2) as compared to the positive values (151 km^2).

Table 6.5: Sensitivity analysis for long-term waves. All values in km^2.

Suitability Scores	1	2	3	4	5	6	7	8
original	**211.9**	**4.5**	**2.9**	**7.2**	**0.0**	**4.4**	**40.0**	**0**
+ 15%	217.0	2.9	7.2	4.4	0	40.1	0	0
+ 10%	217.0	2.9	7.2	0	4.4	8.5	31.6	0
+ 5%	217.0	0	2.9	7.2	4.4	8.5	31.6	0
- 5%	212.3	4.7	0	2.9	7.2	4.4	8.5	31.6
- 10%	204.2	8.1	4.7	2.9	7.2	4.4	8.5	31.6
- 15%	200.9	3.3	8.1	4.7	2.9	7.2	4.4	40.1

Fig. 6.4: Difference in area for each suitability score between the base line long-term waves layer, when long-term wave values were changed, and the modified percentages.

The sensitivity analysis of the marine environment submodel with the modified long-term wave layers included, found most of the variation is to be among the intermediate suitability scores of 6 and 7 (Table 6.6 and Fig. 6.5). The overall changes in area almost doubled for the aggregated negative values (98 km^2) when compared to the aggregated positive values (48 km^2).

Table 6.6: Sensitivity analysis for marine environment submodel when long-term waves values were changed. All values in km^2.

Suitability Scores	1	2	3	4	5	6	7	8
original	**0**	**3.0**	**123.7**	**97.1**	**7.6**	**24.5**	**19.8**	**0**
+ 15%	0	3.0	125.7	98.9	8.1	35.8	4.2	0
+ 10%	0	3.0	125.7	98.9	5.8	24.9	17.4	0
+ 5%	0	3.0	125.6	95.2	9.4	25.2	17.4	0
- 5%	0	3.0	123.7	95.7	7.2	12.9	33.0	0.3
- 10%	0	3.0	120.3	98.1	8.2	12.9	33.0	0.3
- 15%	0	3.0	117.1	97.1	8.5	10.6	39.1	0.3

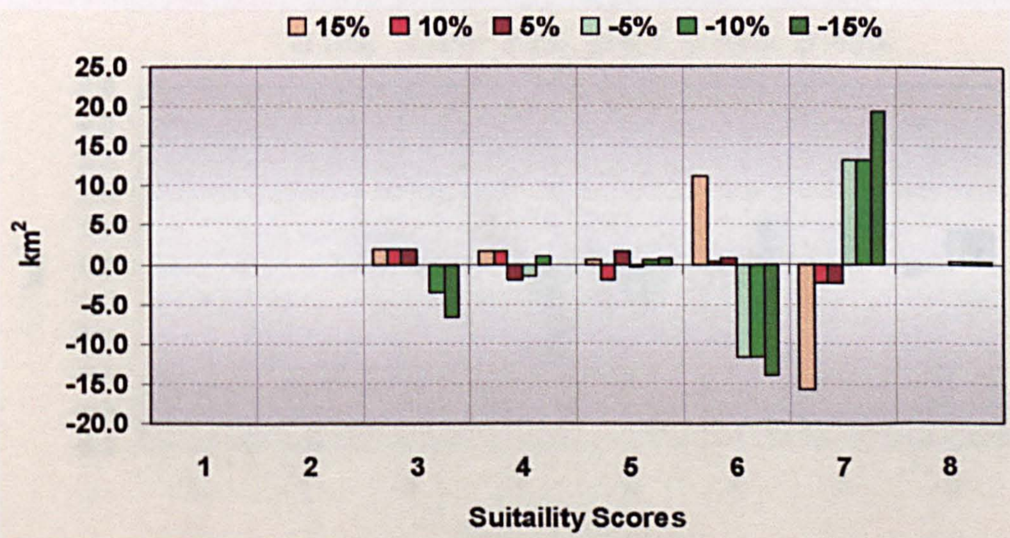

Fig. 6.5: Difference in area for each suitability score between the base line marine environment submodel, when long-term waves values were changed, and the modified percentages.

The sensitivity analysis of the overall model output with the modified long-term wave layers included, indicated that the variation was fairly distributed among the suitability scores of 3 to 8 (Table 6.7 and Fig. 6.6). Generally, aggregated negative interval values showed slightly greater variation in area as compared to the aggregated positive values.

Table 6.7: Sensitivity analysis for the overall model output when long-term waves values were changed. All values in km^2.

Suitability Scores	1	2	3	4	5	6	7	8
original	**0**	**0.1**	**26.2**	**78.5**	**121.7**	**41.5**	**7.2**	**0.5**
+ 15%	0	0.1	27.1	80.4	122.3	40.1	5.6	0.2
+ 10%	0	0.1	27.1	79.5	120.6	40.9	6.9	0.5
+ 5%	0	0.1	26.7	79.0	121.2	41.1	7.0	0.5
- 5%	0	0.1	26.1	78.0	120.8	40.9	8.3	1.4
- 10%	0	0.1	25.8	77.8	120.5	41.7	8.3	1.4
- 15%	0	0.1	25.1	75.7	121.3	42.8	9.2	1.4

Fig. 6.6: Difference in area for each suitability score between the base line overall model, when long-term waves values were changed, and the modified percentages.

6.3.3 Sewage Discharges (change in population)

The sensitivity analysis for the sewage discharges layer due to an increase in the number of people connected to the sewage, found that the greatest variation in the highest suitability score 8 (Table 6.8 and Fig. 6.7). Overall, changes in area more than doubled for the aggregated positive values (8 km^2) as compared to the aggregated negative values (3 km^2). Positive variation values of +10% and +15% were found to have the same changes in area for each of the suitability scores, while all negative variation values showed the same changes in area for the -5% - 10 and -15%.

Table 6.8: Sensitivity analysis for sewage discharges (change in population). All values in km^2.

Suitability Scores	1	2	3	4	5	6	7	8
original	**11.7**	**7.6**	**8.2**	**8.1**	**7.8**	**7.8**	**7.5**	**217.0**
+ 15%	12.2	7.9	8.4	8.3	8.0	7.9	7.6	215.3
+ 10%	12.2	7.9	8.4	8.3	8.0	7.9	7.6	215.3
+ 5%	12.0	7.7	8.3	8.2	7.9	7.8	7.6	216.1
- 5%	11.9	7.6	8.2	8.1	7.7	7.6	7.3	217.3
- 10%	11.9	7.6	8.2	8.1	7.7	7.6	7.3	217.3
- 15%	11.9	7.6	8.2	8.1	7.7	7.6	7.3	217.3

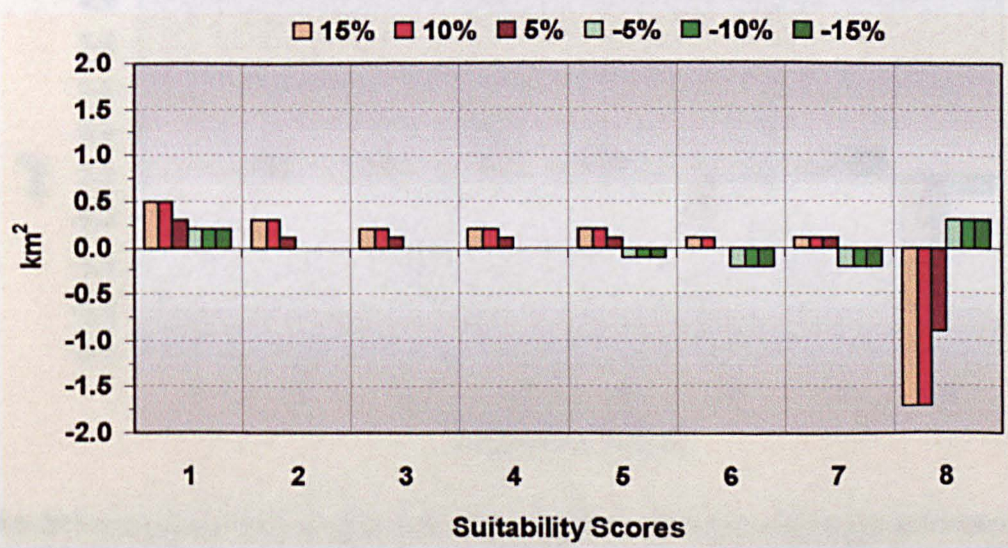

Fig. 6.7: Difference in area for each suitability score between the base line sewage discharges (change in population) layer and the modified percentages.

The sensitivity analysis of the water quality submodel with the modified sewage discharges layers included, found most of the variation to be among the higher suitability scores (Table 6.9 and Fig. 6.8). The overall changes in area more than tripled for the aggregated positive values (7 km^2) as compared to the aggregated negative values (2 km^2).

Table 6.9: Sensitivity analysis for water quality submodel when sewage discharges (change in population) values were changed. All values in km^2.

Suitability Scores	1	2	3	4	5	6	7	8
original	**0**	**2.3**	**4.5**	**15.9**	**12.0**	**51.8**	**32.8**	**156.5**
+ 15%	0	2.5	4.7	16.4	12.3	51.2	32.9	155.8
+ 10%	0	2.5	4.7	16.4	12.3	51.2	32.9	155.8
+ 5%	0	2.3	4.5	16.2	12.2	51.8	32.9	155.8
- 5%	0	2.3	4.5	15.9	12.0	51.7	33.1	156.3
- 10%	0	2.3	4.5	15.9	12.0	51.7	33.1	156.3
- 15%	0	2.3	4.5	15.9	12.0	51.7	33.1	156.3

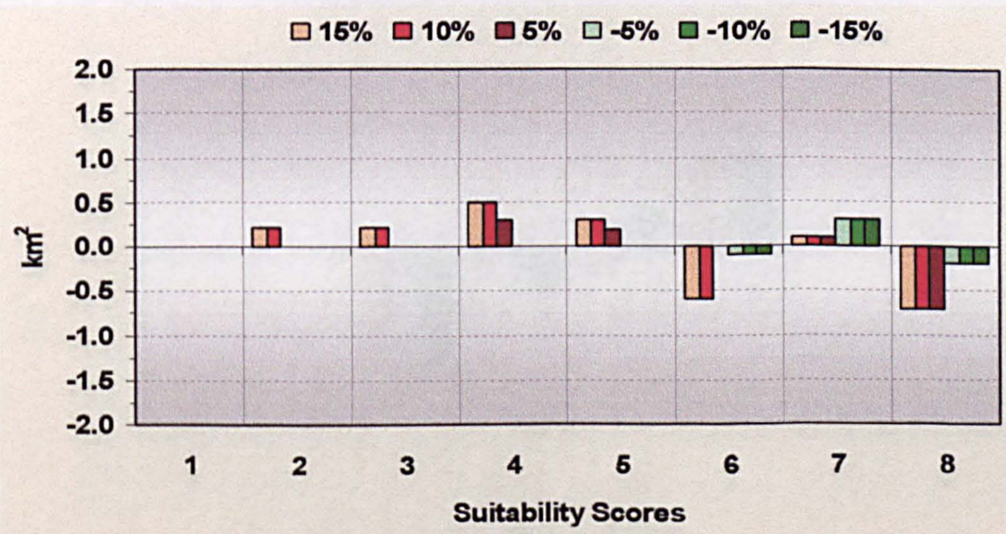

Fig. 6.8: Difference in area for each suitability score between the base line water quality submodel, when sewage discharges (change in population) values were changed, and the modified percentages.

The sensitivity analysis of the overall model output with the modified sewage discharges layers included, found that the variation was distributed between the intermediate suitability scores of 3 to 6 (Table 6.10 and Fig. 6.9). Overall, aggregated negative interval values showed slightly greater variation in area as compared to the aggregated positive values.

Table 6.10: Sensitivity analysis for the overall model output when sewage discharges (change in population) values were changed. All values in km^2.

Suitability Scores	1	2	3	4	5	6	7	8
original	**0**	**0.1**	**26.2**	**78.5**	**121.7**	**41.5**	**7.2**	**0.5**
+ 15%	0	0.1	25	78.7	121.5	42.6	7.2	0.5
+ 10%	0	0.1	25	78.7	121.5	42.6	7.2	0.5
+ 5%	0	0.1	26.2	78.6	121.6	41.5	7.2	0.5
- 5%	0	0.1	25	78.1	122.2	42.6	7.2	0.5
- 10%	0	0.1	25	78.1	122.2	42.6	7.2	0.5
- 15%	0	0.1	25	78.1	122.2	42.6	7.2	0.5

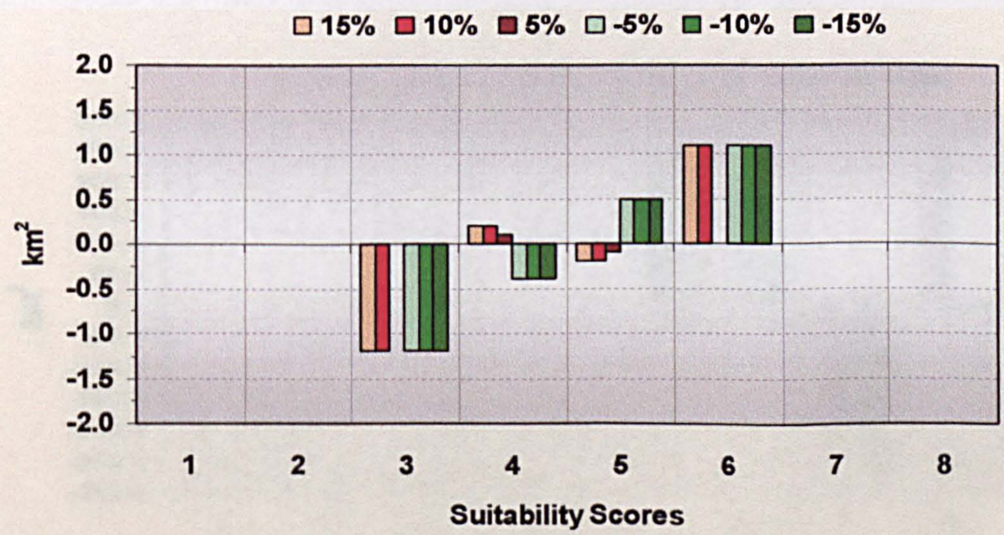

Fig. 6.9: Difference in area for each suitability score between the base line overall model, when sewage discharges (change in population) values were changed, and the modified percentages.

6.3.4 Sea Temperature

Sensitivity analysis indicated that changes in the sea temperature layer had the greatest impact on the predicted suitability area of all the five selected criteria (Table 6.11 and Fig. 6.10). All the changes were found on the higher suitability scores. Aggregated negative interval values showed greater variation in area as compared to the aggregated positive values. Increments of +5% and +10% in sea temperature increased the areas suitable for growing temperate fish, while an increment of +15% was no within the optimum range for growing fish and hence reduced the suitability area. On the other hand, decreases in sea temperature greatly reduced the areas suitable.

Table 6.11: Sensitivity analysis for sea temperature. All values in km^2.

Suitability Scores	1	2	3	4	5	6	7	8
original	**0**	**0**	**0**	**0**	**0**	**0**	**263.6**	**12.0**
+ 15%	0	0	0	0	2.3	76.8	196.6	0
+ 10%	0	0	0	0	0	0	55.9	219.8
+ 5%	0	0	0	0	0	0	10.6	265.1
- 5%	0	0	0	0	0	155.3	120.4	0
- 10%	0	0	0	0	273.9	1.8	0	0
- 15%	0	0	0	0	199.8	75.9	0	0

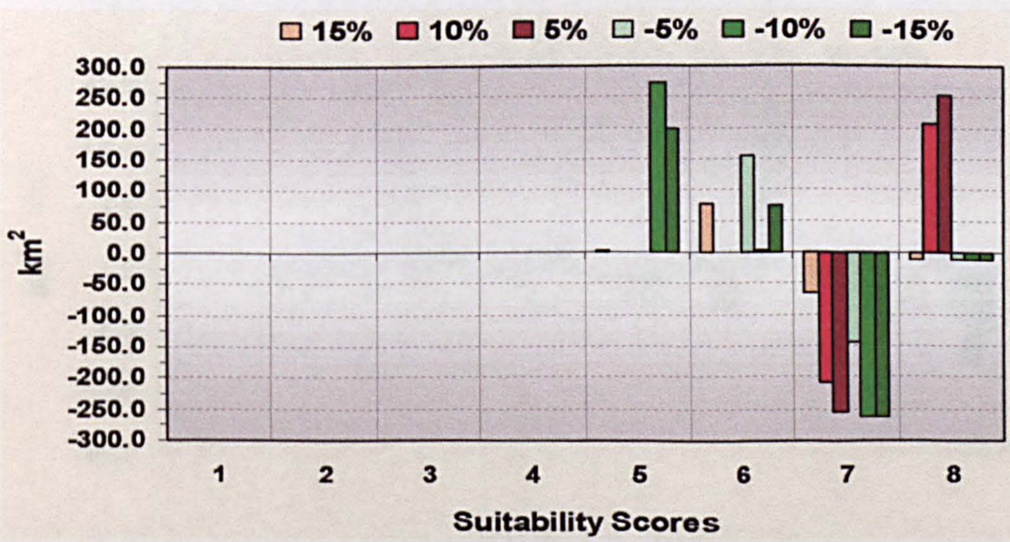

Fig. 6.10: Difference in area for each suitability score between the base line sea temperature layer and the modified percentages

The sensitivity analysis of the water quality submodel with the modified sea temperature layers included, found most of the variation to be among the higher suitability scores of 6, 7 and 8 (Table 6.12 and Fig. 6.11). The sensitivity analysis for the water quality model followed the same trends as the sea temperature analysis. Positive increments in sea temperature up to +10% increased the suitability of the water quality submodel, but were reduced drastically at +15%. Negative increments in sea temperature decreased the suitability area of the water quality submodel. Overall, aggregated negative interval values showed greater variation in area, up to 83 km^2, while the aggregated positive values showed variation up to 51 km^2.

Table 6.12: Sensitivity analysis for the water quality submodel when sea temperature values were changed. All values in km^2.

Suitability Scores	1	2	3	4	5	6	7	8
original	**0**	**2.3**	**4.5**	**15.9**	**12**	**51.8**	**32.8**	**156.5**
+ 15%	0	3.05	5.75	16.35	11.12	55.23	31.06	153.1
+ 10%	0	1.3	4.76	15.25	10.08	48.42	31.71	164.2
+ 5%	0	0.33	5.48	14.73	9.22	48.22	30.64	167.1
- 5%	0	2.79	4.49	16.85	11.03	56.66	31.13	152.8
- 10%	0	3.4	6.24	17.79	9.45	62.79	27.18	148.8
- 15%	0	3.92	6.37	18.03	11.51	65.31	19.11	151.4

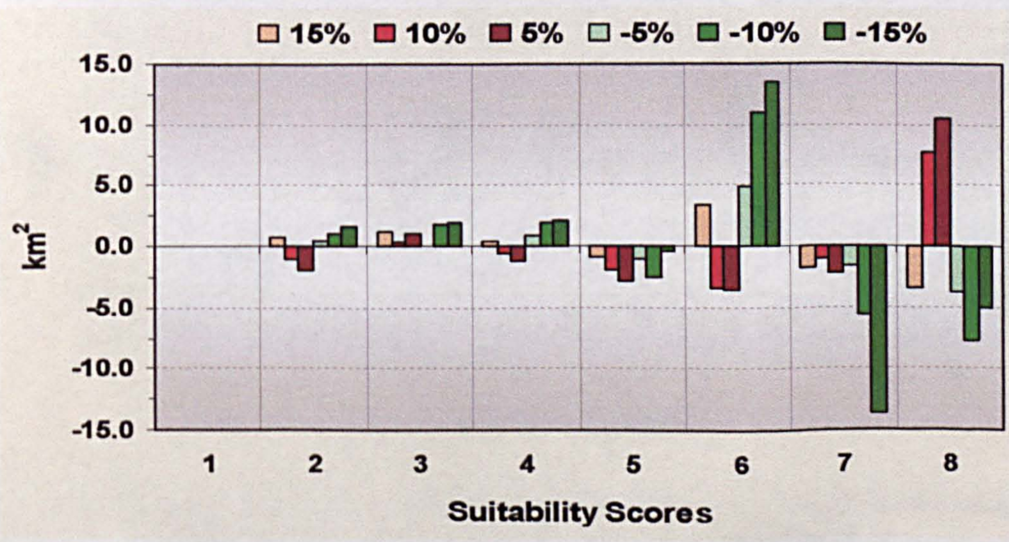

Fig. 6.11: Difference in area for each suitability score between the base line water quality submodel, when sea temperature values were changed, and the modified percentages.

The sensitivity analysis of the overall model output with the modified sea temperature layers included, found that the variation was distributed among the intermediate suitability scores, especially in scores of 3 and 6 (Table 6.13 and Fig. 6.12). In general, aggregated positive interval values showed slightly greater variation in area as compared to the aggregated negative values.

Table 6.13: Sensitivity analysis for the overall model output when sea temperature values were changed. All values in km^2.

Suitability Scores	1	2	3	4	5	6	7	8
original	**0**	**0.1**	**26.2**	**78.5**	**121.7**	**41.5**	**7.2**	**0.5**
+ 15%	0	0.1	25.2	78.8	121.4	42.5	7.1	0.5
+ 10%	0	0.1	24.5	78.6	121.5	43.2	7.2	0.5
+ 5%	0	0.1	24.5	78.6	121.5	43.2	7.3	0.5
- 5%	0	0.1	25.2	78.6	121.7	42.4	7.2	0.5
- 10%	0	0.1	25.7	78.7	121.4	42.2	7.1	0.5
- 15%	0	0.1	26.8	79.1	121.6	40.6	6.9	0.5

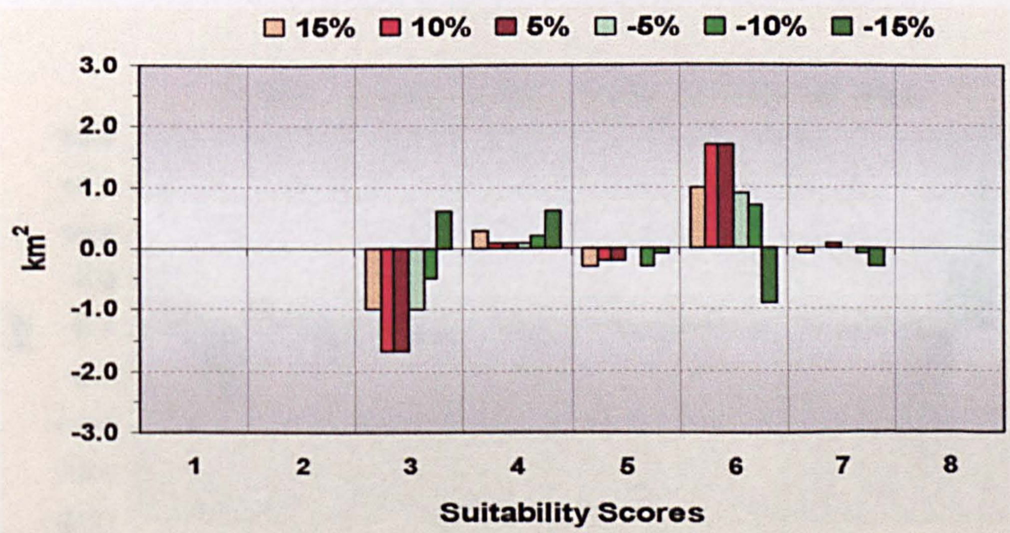

Fig. 6.12: Difference in area for each suitability score between the base line overall model, when sea temperature values were changed, and the modified percentages

6.3.5 Suspended Solids

Sensitivity analysis found that positive increments in suspended solids decreased suitable area for marine fish farming, while the opposite was true for negative increments (Table 6.14 and Fig. 6.13). The greatest variation was found in the score 8, followed by score 1. Aggregated negative interval values showed slightly greater variation in area, up to 61 km^2, while the aggregated positive values showed variation up to 52 km^2.

Table 6.14: Sensitivity analysis for suspended solids. All values in km^2.

Suitability Scores	1	2	3	4	5	6	7	8
original	**32.0**	**10.6**	**11.7**	**11.9**	**11.1**	**9.9**	**9.4**	**179.0**
+ 15%	40.7	13.6	13.5	12.4	11.2	10.6	9.8	163.9
+ 10%	34.8	11.6	12.5	12.5	11.8	10.5	9.5	172.3
+ 5%	33.8	11.2	12.2	12.3	11.8	10.4	9.3	174.8
- 5%	29.3	9.4	10.6	11.2	10.6	9.9	8.9	185.9
- 10%	27.7	9.4	10.8	11.5	11.1	10.2	8.8	186.4
- 15%	24.8	8.1	9.3	10.0	9.8	9.7	9.0	194.9

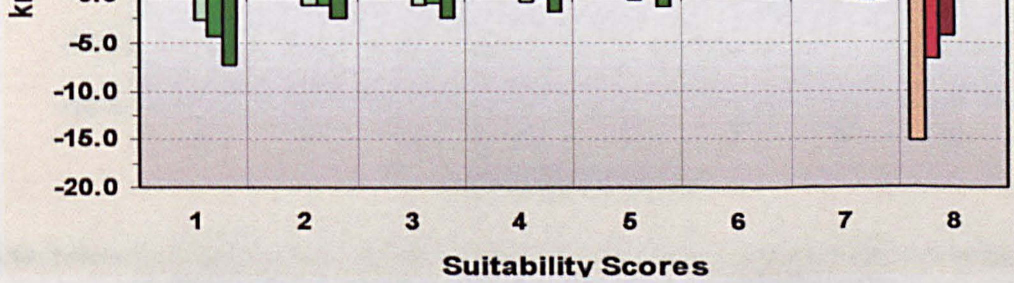

Fig. 6.13: Difference in area for each suitability score between the base line suspended solids layer and the modified percentages

The sensitivity analysis of the water quality submodel with the modified suspended solids layers included, found most of the variation to be among the higher suitability scores of 6 and 8 (Table 6.15 and Fig. 6.14). In general, aggregated negative and positive interval values showed similar variation in area, up to 48 km^2.

Table 6.15: Sensitivity analysis for the water quality submodel when suspended solids values were changed. All values in km^2.

Suitability Scores	1	2	3	4	5	6	7	8
original	**0**	**2.3**	**4.5**	**15.9**	**12.0**	**51.8**	**32.8**	**156.5**
+ 15%	0	2.5	4.8	16.0	12.2	62.3	35.0	142.9
+ 10%	0	2.3	4.7	15.7	12.0	56.3	34.4	150.3
+ 5%	0	2.3	4.7	15.6	12.0	54.9	33.7	152.5
- 5%	0	2.1	4.4	15.2	12.2	49.0	31.3	161.6
- 10%	0	1.8	4.3	14.9	12.6	48.6	32.3	161.2
- 15%	0	1.5	3.8	14.8	13.4	44.2	30.1	167.9

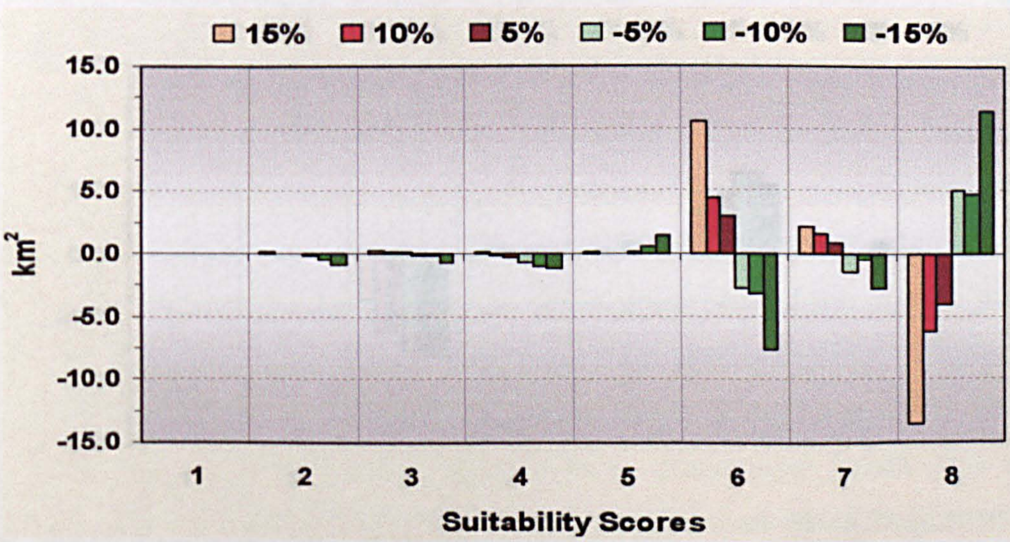

Fig. 6.14: Difference in area for each suitability score between the base line water quality submodel, when suspended solids values were changed, and the modified percentages.

The sensitivity analysis of the overall model output with the modified suspended solids layers included, found the variation to be distributed among the intermediate suitability scores of 3 and 6 (Table 6.16 and Fig. 6.15). Generally, aggregated negative interval values showed slightly greater variation in area as compared to the aggregated positive values.

Table 6.16: Sensitivity analysis for the overall model output when suspended solids values were changed. All values in km^2.

Suitability Scores	1	2	3	4	5	6	7	8
original	**0**	**0.1**	**26.2**	**78.5**	**121.7**	**41.5**	**7.2**	**0.5**
+ 15%	0	0.1	25.5	78.5	121.7	42.2	7.2	0.5
+ 10%	0	0.1	25.0	78.6	121.8	42.4	7.2	0.5
+ 5%	0	0.1	25.0	78.6	121.7	42.5	7.2	0.5
- 5%	0	0.1	24.7	78.4	121.9	42.8	7.2	0.5
- 10%	0	0.1	24.7	78.6	121.8	42.8	7.2	0.5
- 15%	0	0.1	24.6	78.6	121.9	42.6	7.4	0.5

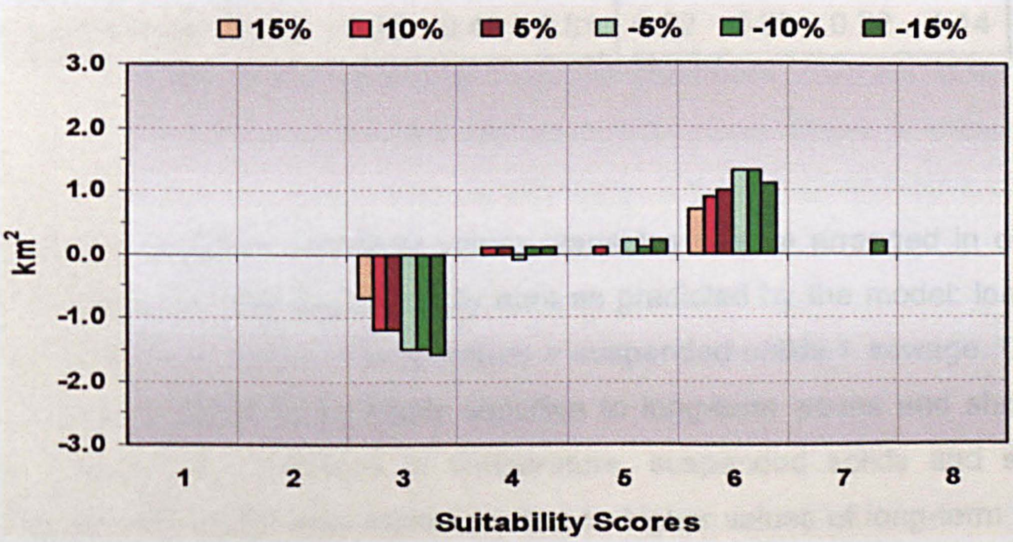

Fig. 6.15: Difference in area for each suitability score between the base line overall model, when suspended solids values were changed, and the modified percentages

6.3.6 Absolute Sensitivity

Absolute sensitivity is a mathematical expression of sensitivity which provides a consistent measure for comparing the five selected model parameters (Shukla, 1998; Malczewski, 1999; Saltelli *et al.*, 2000). The absolute sensitivity (S) is calculated as follows:

$$S = (R_a - R_n)/(P_a - P_n)$$

were R_a and R_n were the model responses for altered and initial parameters respectively, and P_a and P_n were the altered and initial values. The S values for the different parameters were compared to identify the most sensitive parameters (Table 6.17).

Table 6.17: Absolute sensitivity values for different percentages of variations for each of the selected variable.

	15%	10%	5%	Σ	-5%	-10%	-15%	Σ	Σ Total
Short-term waves	0.31	0.46	0.68	1.45	0.38	0.24	0.75	1.37	2.81
Long-term waves	0.45	0.39	0.42	1.26	0.82	0.45	0.57	1.84	3.09
Sewage	0.18	0.27	0.04	0.49	0.64	0.32	0.21	1.17	1.66
Temperature	0.18	0.37	0.76	1.31	0.39	0.18	0.17	0.74	2.05
Suspended Solids	0.10	0.23	0.48	0.81	0.62	0.29	0.22	1.14	1.95

Based on the absolute sensitivity values, variables can be arranged in order of their importance in affecting suitability area as predicted by the model: long-term waves > short-term waves > temperature > suspended solids > sewage. Overall, the model was shown to be highly sensitive to long-term waves and short-term waves, followed by variations in temperature, suspended solids and sewage respectively. The model was more sensitive to higher values of long-term waves, suspended solids and sewage than lower values of these variables. The opposite was true for short-term waves and temperature.

6.4 CONCLUSIONS AND DISCUSSION

The sensitivity analysis carried out in this chapter was aimed at accounting for variability by identifying the sensitivity of the model to the spatial data inputs and to determine their relative criticality. A considerable level of variation was found in the results when the model parameters were varied. The sensitivity analysis shows that the model was especially sensitive to long-term waves and short-term waves, followed by sea temperature, suspended solids and sewage discharges respectively. This was the expected rank, as changes in variables with bigger weights had higher impacts on the overall model output.

Variations in the model output due to changes in sewage discharges (change in population connected) and suspended solids (coming form extreme runoffs) were small, and hence it was concluded that they are not critical variables on the model. Moreover, by the year 2005 no sewage discharges in Tenerife will be allowed without previously being treated (Morales, 1997). This fact will further reduce the possibility of variation in the model's predictions due to changes in this variable.

Although changes in sea temperature impacted the final model output to some extent, its was also considered as non critical. This is because, although the model did change slightly, temperature was still within the very suitable range.

On the other hand, the proposed model for siting marine cages in Tenerife was most affected by wave variations, both long and short-term. This will have a direct effect on the suitable area predicted and also on the cage system of choice, if the wave conditions are not as predicted in this study. If a more conservative estimate was required, to account for the worse case scenario variability, then instead of using the predicted 15-year return period wave to create the extreme wave map as done in this study, alternatively, the value of the upper confidence interval limit could be used to generate this map.

It is concluded that the model presented in this study is robust to changes from uncertainty of the data, processes under study and/or parameterisation of the equations used to describe them. Having said that, it could also be valuable to carry out the wave analysis with longer data sets than the used in this study. Unfortunately, this was not possible at the time of this study because the lack of such information. Nevertheless, the sensitive analysis method used has been criticised for being limited, since it only demonstrates the sensitivity of variations to one variable at a time (Saltelli *et al.*, 2000). However, in the context of this study, where only those single layers which were most likely to influence the final output were of interest, this methodology is appropriate (Lodwick *et al.*, 1990).

Chapter 7

General Discussion

This study focused on the optimisation of offshore marine fish-cage farming in Tenerife, Canary Islands. The main objective was to select the most suitable sites for offshore cage culture. This was accomplished by identifying all possible criteria that influenced the development of marine fish-cage culture within the context of a integrated coastal zone management. Once identified the required data was gathered together, and entered into the GIS system to build up the database. Finally, the database was verified to control the quality of data used, and thus help ensure reliable outcomes. Based on these criteria, three different cage systems were selected and GIS-based models, for each, were developed to select the most suitable sites for developing marine fish cage culture.

To account for possible different points of view relating to the same task of siting marine fish cages, specifically developed questionnaires were used to obtain feed-back from three focus groups, all of whom had relevant but different experience in the field. Sensitivity analysis was used to indicate what criteria are the most or least critical in determining the values of the output map. These critical maps indicate where most or least care may be taken in the input data in order to draw reliable conclusions from the output map, and also to assess the overall robustness of the model.

Areas which were selected as the most suitable for siting cages will benefit from a further study to quantify the dispersive nature of a site, and therefore, assist in predicting possible environmental impacts. For this purpose, a particulate waste distribution model was developed. Although not directly used in this study because lack of current data, it was intended to be used in the last stage of this study. This model could also help regulators to establish the maximum desirable production at a site, and hence, estimate the maximum number of farmed tons and number of cages that a site could support for a sustainable development of the industry in Tenerife.

The aquaculture site selection conducted in this study, also known as zonation, is vitally important as it can greatly influence the economic viability of a venture by determining its capital outlay, running costs, rates of production and mortality factors. It can also resolve conflicts between different coastal activities and users, such as fishing or tourism, making rational and sustainable use of Tenerife's coastal space. Consequently, site selection is considered a key factor if success is to be achieved and a sustainable aquaculture industry is to be established on the island.

The management of aquaculture can be approached in a number of different ways, however, current thinking favours the application of Integrated Coastal Zone Management (ICZM), as presented in this study. Although the development and implementation of ICZM policies is now an established concept and internationally recognised goal, the tools and methodologies for achieving such goals are still under development (Clark 1996; GESAMP, 1996b). It is clear, that for any effective management of the shoreline, it is necessary for the policies to be based on informed decision-making. This in turn requires ready access to appropriate, reliable and timely data and information, in a suitable form for the task at hand (Urbanski, 1999). Since much of this information and data have a spatial component, GIS and related technologies have obvious relevance to the task, as shown in this study. The integration of GIS and environmental modelling has now been accepted as desirable, if not essential for coastal management (Li *et al.*, 2000). Budic (1994) labelled GIS as "revolutionary" in its potential to enhance the planning process itself.

GIS is an information system specifically designed to work with data referenced by spatial or geographic coordinates. In other words, GIS is both a database system with specific capabilities for spatially referenced data, as well as a platform for analytical operations for working with the data (DeMers, 1997). GIS can allow for the analysis of both qualitative and quantitative data, identify associations between components, and therefore, build a "*living database*" with exploratory data analysis, modelling, interpretative and mapping capabilities (Booth, 1998).

There is little doubt that GIS has the potential to greatly contribute to the adoption of an integrated approach towards coastal management problems. However, whilst the use of this technology as a tool for land-based resource management and planning is well established, GIS applications in coastal and aquatic environments are still in their infancy. Moreover, GIS has most often been applied as a tool for mapping rather than modelling

It is clear that aquaculture site selection requires geographically related data and information, with multiple feasible alternatives, which are often conflicting and involving incompatible evaluation criteria. The alternatives are usually evaluated by a number of individuals such as managers, decision makers, or interest groups. These individuals are typically characterized by unique preferences with respect to the relative importance of evaluation criteria. GIS technology offers unique capabilities of automating, managing, and analysing a variety of spatial data for decision-making. At the same time, multicriteria decision-making and a variety of related methodologies offer a rich collection of techniques and procedures to reveal preferences objectively and to incorporate them into GIS-based decision-making.

In this study, GIS was used to perform straightforward database functions as well as to explore functional relationships by querying data in different ways. GIS was applied to combined relevant thematic data layers and explore the possible relationships between them. Statistical testing of observed relationships or correlation between thematic layers were also performed.

Although the implementation and use of GIS-based models for planning and management of aquatic resources is still in its early stages, this study has shown it to be a powerful tool. Nevertheless, GIS is only a tool that provides outputs to a range of input data, it does not provide answers. What it does is to provide an aid to support answers which managers build up with the outputs from the GIS, and perhaps other related material. Also, it is very important to bear in mind that GIS is only as good as the data and conceptual models on which they are based.

Despite its obvious potential benefits and general favourable opinion, it is important to consider whether GIS will make the environmental management process more efficient, cost-effective and productive than more traditional methods. In environmental management, the cost of laborious surveys can be prohibitive particularly when addressing relatively large or inaccessible areas. In such circumstances, a GIS-based approach can be cheaper and more efficient than a traditional field survey based approach. It can also open up opportunities for using alternative source data such as aerial photography or satellite imagery. On the other hand, the lack of readily available, affordable and accurate digital data can mean that a certain amount of hand digitising and ground truthing, to check the quality of the data, is very likely to be necessary, which itself is a time consuming task. In addition, mastering the technology requires time and intensive training to familiarise with the functions of GIS and learn about the logistics of exploiting its capabilities. Hence, the benefits of GIS technology are not attained immediately, the longer a GIS is used, more potential it has to yield benefits.

Some aspects of the present study would not have been possible without GIS. The quantity of factors used would have made the use of more traditional techniques, such as manual map overlay, very difficult. Moreover, some factors, such as the sea temperature layer created in this study, would have been virtually impossible to obtain without the use of satellite information. In addition, relatively simple GIS operations such as the measurement of buffer zones or the generation of a digital elevation model (DEM), become very complicated when done manually with paper maps. It is therefore apparent that appropriate selection of offshore cage site in Tenerife was achieved more quickly and accurately using GIS than it could have been with traditional manual map-making technology.

Decision-making is a process that involves a sequence of activities that begins with problem recognition and ends with recommendations. Although there are numerous alternative ways to organize the sequence of activities in the decision-making process, this study emulated an approach developed by the GISAP group at the Institute of Aquaculture, Stirling, who have been researching the role of GIS for aquaculture support for some years (Aguilar-Manjarrez, 1996; Ross, 1998; Scott and Ross, 1999; Salam, 2000). Decision-making played a key role in this study at all stages of model development. Even before any GIS manipulation took place, decisions had to be made in choosing the factors to be included in the evaluation, the structures of the models and standardisation thresholds.

The framework for spatial multicriteria decision analysis used in this study (Fig. 3.4) began with a recognition and definition of the decision problem. Subsequently, all production functions (factors and constraints) were identified and defined. These were then integrated into a GIS database in the form of thematic layers and later scored for standardization. At this stage, the database was verified by field sampling to establish the quality of data used. The decision maker's preferences were incorporated into the decision model by assigning weights of relative importance to the evaluation under consideration. These, together with the thematic layers, were integrated by using MCE and simple overlays to provide an overall assessment of possible alternatives. Finally, sensitivity analysis was performed to determine the model robustness. The end results of this decision-making process were recommendations, based on the ranking of alternatives and sensitivity analysis, for future action. The integration, manipulations and presentation of the results by means of GIS-based models in this logical flow of steps proved very effective for helping the decision-making process of site selection of this study.

From this study, it is clear that GIS has several advantages for resource management and aquaculture development programme. It not only provided a visual inventory of the characteristic of the environment as thematic layers, but it allowed generation of suitability maps for different culture systems without complex and time-consuming data manipulation. An added advantage of using GIS for this study was the efficiency of integrating a wide range of data and information sources into a compatible format. This study made use of data available in the form of paper maps, tables, charts, satellite images and surveys. The methods used in this study for data capture were very varied, including keyboard entry, manual locating devices (table digitiser and on-screen digitising), automated devices (scanning), or by the importation of existing data files (direct conversion from other digital sources). In this study 31 criteria, 27 factors and 4 constraints, were used. Some of these factors were entered as primary data whereas other were the result of some preliminary data manipulation or modelling. Almost half of the time allocated for this project was used for implementing the GIS database.

It is not always possible to examine all the criteria defined for a project in great detail, and this was the case for the coastal current layer in this study. Information on currents is very important for cage site selection because they control the water exchange rate (replenishment of oxygen and removal of waste metabolites), influence fish behaviour (affecting social hierarchies, growth and growth disparities among stock), contribute towards food losses, and impose additional dynamic loadings on the cage, supporting structures and moorings. Unfortunately, there were no data on coastal currents for Tenerife. The only data available on currents for the Canary Islands region came from global oceanic circulation or from mesoscale studies of the Canary Current. Initially, attempts were made to interpret and interpolate the available Canary Current data to generate a coastal current map. However, as this flow is greatly influenced by local topography and other factors such as tidal currents, local wind driven currents, longshore currents and rip currents (Molina pers. comm.), the current thematic layer was created based on the author's personal knowledge of the study area and the main current flow, the Canary Current. When better information on currents is available, it could be incorporated easily into the model and re-run. In addition, the waste dispersion model developed could be then used for the final site selection and to estimate potential production levels as well as number of farms.

Performing manipulations on maps or raw data that poses error as a result of the data collection leads to error propagation. Most of the data came from reliable sources, such as national and regional institutions with reliable quality standards and were integrated relatively directly into the GIS database. Other data, for example that required in the creation of the sea temperature or suspended solid layers, had to be manipulated prior to its incorporation, hence, increasing the possibility of error propagation.

Some of the sources of error are a product of the measurement instrument, which can be reduced by upgrading the data pre-processing required to generate the thematic layers, as was the case in this study. Whenever possible, the latest state-of-the art methodologies and techniques were used. For example, for the generation of the sea temperature layer, the latest NOAA satellite algorithm and prepossessing techniques was applied. A second possible source of error propagation could be due to the managing of spatial databases. In this case, standard techniques for data manipulation and handling were used to minimize the introduction of errors to the database. Whenever possible, digital data with a quality guarantee was used. In addition, when data capture was necessary, state-of-the-art hardware such as GIS, scanner and digitising table was used to ensure data quality. Moreover, when possible, field trips were carried out for database verification.

The model structure for this study was built based on hierarchical structures (Fig. 3.9), which divided all the criteria into large groupings (or submodels), and further divided them into smaller clusters to obtain the priorities of all elements by means of clustering. Hierarchical structures have been acknowledged as a powerful version of reality when viewing a complex system of interacting components (Saaty, 1977). It was found that this method is by far a more efficient process than treating all the elements together. The same conclusion has also been reached by the GISAP group (Aguilar-Manjarrez, 1996; Salam, 2000) and some other authors (Malczewski, 1999). The criteria used in this study were divided into 8 submodels. By using the GIS-based models structured as hierarchies, the outcome becomes more objective than by using conventional techniques alone.

Although there are similar studies that have used suitability scores of 1 to 4 and 1 to 16 (Aguilar-Manjarrez, 1996; Salam, 2001), in this study a scoring system of 1 to 8 was chosen, 8 being the most suitable and 1 the least, as it was found that the former scoring system gave poor results while the latter was too complicated to use. Nevertheless, based on the experience gained during this study, a scoring scale from 1 to 10 may have been easier and more intuitive to use, as presented by Lowry *et al.* (1995) and Abdel-Kader *et al.* (1998), or from 1 to 100 as presented by Krieger and Mulsow (1990).

It was found that whenever possible, it is best to use threshold values for each of the suitability scores based on those proposed by experts with knowledge of the task at hand as well as the particular study area or literature sources, rather than using a mathematical approach which may not provide a set of threshold limits representative of the problem. Having said that, it will be useful to further investigate the linearity of the selected threshold for some criteria. It may be the case that some criteria thresholds will be more representative if an exponential distribution was used.

The purpose of criterion weighting in this study was to express the importance of each criterion relative to others. From a number criterion-weighting procedures reported in the literature, this study made use of the pairwise comparison method, which has been acknowledged as the most effective technique for spatial decision-making (Eastman *et al.*, 1993; Malczewski *et al.*, 1997a). In this study, the 1-9 scale proposed by Saaty (1997) was used, 1 being least important and 9 the most important. A further advantage of using the IDRISI32 GIS software was that the calculations of the weights using the pairwise comparison method is already incorporated as a built-in decision support module, so avoiding the use of external software and the need to incorporate this information into the GIS-based models.

Although the conclusions and recommendations arising from this study are solely based upon the criteria weights assigned by the author, account was taken of different perceptions by selecting three focus groups and using questionnaires to gather information. The most difficult part of the questionnaires was the completion of the pairwise matrix to calculate the criteria weights. Although a 1 to 9 scale is widely accepted and used by many authors and in commercial software, it was suggested by many of the members of the focus groups that a scale from 1 to 10 would be more intuitive and easier to use for them, as they were more familiar and confident with that approach. Moreover, some decision-makers argued that it was easier for them to directly assign weights to the factors without going through the tedious process of completing the pairwise matrix. Overall, it was found that the choice of weights is crucial to the outcomes and that the wrong weights could be chosen even if the consistency ratio (CR) was within the acceptable limits. This same conclusion has been reached by other authors (Aguilar-Manjarrez and Ross, 1995; Barredo, 1996; Malczewski, 1999).

Aguilar-Manjarrez (1996), Aguilar-Manjarrez and Nath (1998) and Salam (2000) made use of questionnaires together with the pairwise comparison method for assigning weights when dealing with a great number of criteria per model or submodel. However, experience gained from this study suggests that when the number of criteria per group are smaller, questionnaires with direct assignment of weights could better match the decision-maker's preferences rather than using the pairwise method, which is an unfamiliar and confusing technique for many. This, in part, could be the reason for the differences in output predicted by the author and those predicted by the three different focus groups.

Sensitivity analysis was carried out to indicate which layers (criteria) were the most or least critical in determining the values of the final output. This step, although often overlooked, is important because the available information is often uncertain and imprecise due to measurement and conceptual errors, and only limited information may be available on actual errors associated with a particular geographical analysis (Fisher *et al.*, 1997; Arbia *et al.*, 1998; Malczewski, 1999; Li *et al.*, 2000; Woodcock and Gopal, 2000). The model sensitivity was tested by imposing variations on the inputs and the resultant variations computed. A considerable level of variation was found in the results when the model parameters were varied, however, it was concluded that the model presented in this study is robust to changes due to uncertainty in the data, the processes under study and/or parameterisation of the equations used to described them.

The sensitivity analysis conducted in this study was very tedious and time-consuming. Although the GIS software used (IDRISI32) provided some macro modelling facilities, its use is crude and not very effective for this particular task, especially when the models are as numerous and complicated as those presented here. It is hoped, that with the next generation of IDRISI32, this problem will be solved and sensitivity analysis like that presented in this study can be carried out more automatically, faster and efficiently.

This research, and the final outcomes, could benefit for further work and improvements. These include the introduction of data on seabed type, which would be important in deciding the type and cost of moorings, possible indication of the assimilative capacity of the environment, and also could be used as a proxy data for current velocity. With additional time and resources, a more thorough ground truthing design could have been planned. This could include more sampling points as well as more variables sampled. Seasonal variability could also be tested. The developed questionnaires could be used with a greater number of people per focus group. Additionally, the number of focus groups could be expanded to include other views of the same task of siting cages. For example, a tourism industry and a fisherman focus groups could have been added. As previously mentioned, this study could have benefited from the use of current data. This data could have been used in the GIS-based models for the initial siting of cages, as well as their use in the waste dispersion model for the final.

Although the main objective of this study focused on the selection of the most suitable sites for cage farming, if current data were available and hence the waste dispersion model used, the GIS models could have been used to quantify the number of farms and farmed tonnes of fish that the island can potentially support sustainably. To illustrate this point, a simple example is presented using assumptions based on present aquaculture trends in the Canary Islands and standard aquaculture procedures. It was assumed that farms comprised of 12 polyethylene floating cages (gravity cages) of 20 m in diameter and standard mooring systems. Despite the fact that existing farms are composed of rather lower number of cages (2-8), the trend in the Canaries is toward the use of more cages per farm (12). This is because bigger farms are more economical (economics of scale) and area efficient (INSEMAR pers. comm.). A typical system with these characteristics will require a total seabed area of 500 x 300 m, most of which is being used by the moorings (Fig. 7.1).

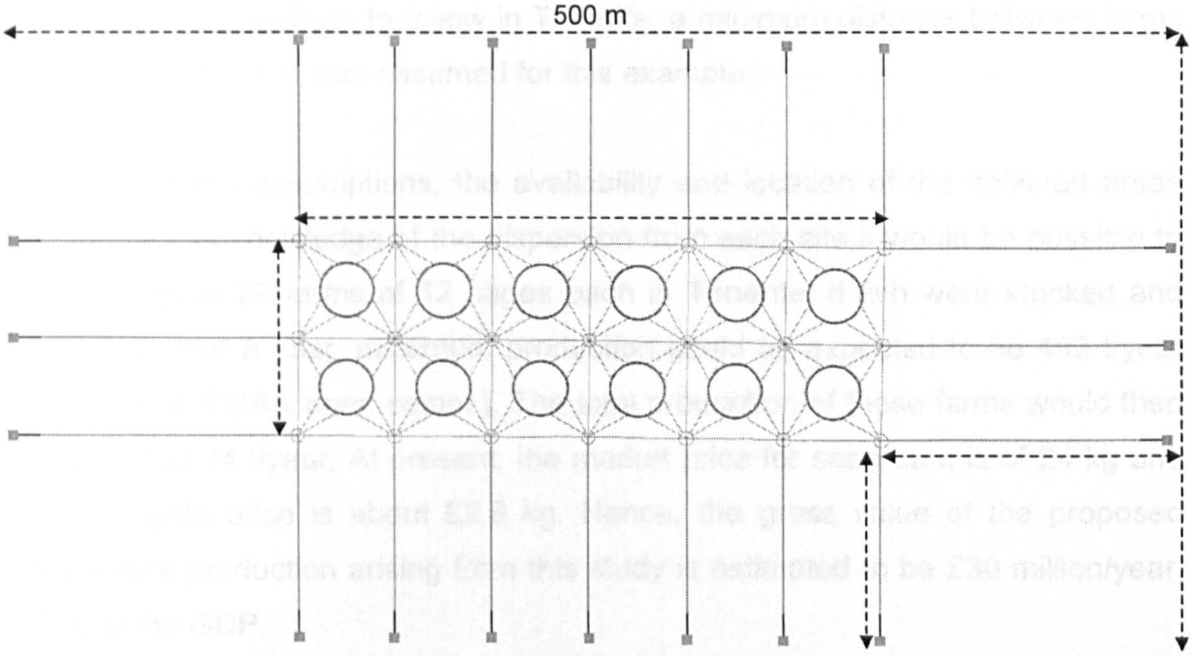

Fig. 7.1: Fish farm composing of 12 polyethylene floating cages of 20 meters in diameter (not to scale). Redrawn with permission from INSEMAR (unpublished data).

Based on data provided by INSEMAR (pers. comm.), the typical growing cycle for seabream to a commercial size of 400 g in Tenerife is about 11-12 months, with total mortality of about 10%. The stocking densities fluctuates around 17 kg/m^3, but never exceed 20 kg/m^3. Temperate species, like seabream, grow faster in the Canaries, as compared to the Mediterranean, due to the warmer average temperatures. At maximum production, a 12 cage farm would be stocked with 1,200,000 fingerlings of 5 g each. Feeding is based on dry pellets and standard aquaculture techniques.

The models identified 37 km^2 of suitable coastal space (sums of scores of 6, 7 and 8) for siting gravity type cages. Nevertheless, it is obvious that farms need to be some distance apart to avoid the risk of diseases contamination and to minimise impacts on the benthos, water column and visually. Also, some space is required for other activities such as navigation. Guidelines on distance restrictions between farms vary greatly between countries, environments, farmed species and systems used. Distance restrictions for marine cage farms are as short as 300 m in New Brunswick (Canada) but up to 8 km in Scotland. As there are currently no regulations or guidelines to follow in Tenerife, a minimum distance between farms (buffer zone) of 5 km was assumed for this example.

Based on these assumptions, the availability and location of the selected areas and the lack of knowledge of the dispersion from each site it would be possible to establish up to 22 farms of 12 cages each in Tenerife. If fish were stocked and harvested once a year, maximum production could be expected to be 492 t/year per farm (INSEMAR pers. comm.). The total production of these farms would then be up to 10,824 t/year. At present, the market price for seabream is of £4 kg and the farm gate price is about £2.8 kg. Hence, the gross value of the proposed aquaculture production arising from this study is estimated to be £30 million/year, 0.5 % of the GDP.

Although the estimated potential value of the aquaculture industry in Tenerife can not compare with the main economical activities, such as the tourism or agriculture which account for a 60% and 10% of the GDP respectively, it could become a complementary sector. In turn, this economical diversification could provide new investments opportunities for other economic sectors that are necessary for the development of aquaculture, such as feed factories, hatcheries, consultancies agencies, insurances, etc. In addition, the development of this industry could be used to reconvert some fishermen into a new, but related, activity which could help this declining sector.

The use of GIS as a management tool has been acknowledged as a very cost-effective way of tackling spatially-related problems. Although this study greatly depended upon the use of GIS, it is nevertheless important to bear in mind that GIS is not only a software in which the operator introduces data for outputs to be obtained. GIS can itself be considered as a virtual environment in which the "real-world" is translated to allow for manipulations and modelling, with the aim of assisting decision-makers in their management strategies.

This study presents a methodology for siting offshore marine fish cages in an integrated, objective and sustainable fashion. Despite the fact that Tenerife was chosen as the study area, the developed methodology could be applied to any other coastal areas worldwide. For some areas, it is most likely that the model assembled in this study could not be applied exactly as presented. Some of the criteria may be of no importance, while perhaps new ones will need to be added. Nevertheless, despite these small differences, the framework and methodology should remain the same independent of the study location. Overall, this study revealed the usefulness of GIS as a coastal aquaculture planning and management tool.

References

Aarsnes, J.V. and Rudi, H. (1990). Current forces on cage, net deflection. In: Engineering for Offshore Fish. Thomas Telford, Great Britain, 137-152 p.

Abdel-Kader, A.F., Nasr, S.M., El-Gamily, H.I. and El-Raey, M. (1998). Environmental sensitivity analysis of potential oil spill for Ras-Mohammed coastal zone, Egypt. Journal of Coastal Research 14, no. 2: 502-10.

Addink, E.A. and Stein, A. (1999). A comparison of conventional and geostatical methods to replace cloud pixels in NOAA-AVHRR images. Int. J. Geographical Information Science 20, no. 5: 961-77.

Aguilar-Manjarrez, J. (1996). Development and evaluation of GIS-based models for planning and management of coastal aquaculture: a case study in Sinaloa, Mexico. PhD Thesis, University of Stirling, 373 p.

Aguilar-Manjarrez, J.A. and Ross, L.G. (1995). Geographical information system (GIS) environmental models for aquaculture development in Sinaloa State, Mexico. Aquaculture International 3, 103-15.

Aguilar-Manjarrez, J. and Nath, S.S. (1998). A strategic reassessment of fish farming potential in Africa. CIFA Technical Paper. No. 32. FAO, Rome,. 170 p.

Alarcon, J.F., and Villanueva, M.L. (2001). Using Geographic Information Systems as a site selection tool for aquaculture. Aquaculture 2001: Book of Abstracts, World Aquaculture Society, 143 J.M Parker Coliseum Louisiana State University Baton Rouge LA 70803 USA, 7.

Alfonso-Carrillo, J. and Gil-Rodriguez, M.C. (1980). Cymodocea nodosa (ucria) ascherson (Zannichelliaceae) y las praderas submarinas o "sebadales" en el Archipielago Canario. Vieraea 8, 365-76.

Altman, D. (1994). Fuzzy set theoretic approach for handling imprecision in spatial analysis. International Journal of Geographical Information Systems 8, no. 3, 271-89.

Anding, D. and Kauth, R. (1970). Estimation of sea temperature from space. Remote Sensing of the Environment 1, 217-20.

Andrew, N.L. and O'Neill, A.L. (2000). Large-scale patterns in habitat structure on subtidal rocky reefs in New South Wales. Marine and Freshwater Research 51: 255-63.

Angell, C.L. (1997). Methods for establishing coastal aquaculture zones in Sri Lanka. FAO, Bangkok (Thailand), 31 pp.

Anon A. (1999). Rock Lobster Assessment Group Workshop. Lobster Res. News: 1-2.

Arbelo, M., Hernández-Leal, J.P., Díaz, F.J., Expósito, F. and Herrera, F. (2000). Efficiency of a global algorithm for retrieving SST from satellites data in a subtropical region. Advances in Space Research 25, no. 5: 1041-1044.

Arbelo, M., Herrera, F., Exposito, F.J., Caselles, V. and Coll, C. (1996). Determination of sea surface temperature using coined TOVS and AVHRR data. Application to the Canary Islands area, Spain. International Journal of Remote Sensing 17, no. 2: 359-71.

Arbia, G., Griffith, D. and Haining, R. (1998). Error propagation modelling in raster GIS: overlay operations. Int. J. Geographical Information Science 12, no. 2: 145-67.

Ardizonne, G.D., Agnesi, S., Biagi, F., Baino, R. and Corsi, F. Geographical information systems and surplus production models: a new model for spatial assessment of demersal resources. Proceedings of the Symposium on Assessment of Demersal Resources by Direct Methods in the Mediterranean and the Adjacent Seas, Pisa (Italy), 18-21 March 1998.

Ardizzone, G.D. and Pelusi, P. (1984). Yield and damage evaluation of bottom trawling on Posidonia meadows. In Boudouresque, C.F., Jeudy de Grissac, A. and Oliver, J. (Eds.), International Workshop on Poseidonia oceanica beds, GIS Posidonie, Marseille, 1, 63-72.

Aristegui, J. (1990). La distribucion de la clorofila a en aguas de Canarias. Boletin Del Instituto Espanol De Oceanografia 6: 61-72.

Aristegui, J., Hernandez-Leon, S., Gomez, S., Medina, M., Ojeda, L. and Torres, S. (1989). Influence of the north trade winds on the biomass and production of neritic plankton around Gran Canaria island. Scientia Marina 53: 223-29.

Aristegui, J., Hernandez-Leon, S., Montero, M.F., Ballesteros, S. and Basterretxea, G. (1992). The biological pump in island-induced eddies. In: Falkowski, P.G., Woodhead, A.D. and Vivirito, K. (Ed.), Primary productivity and biogeochemical cycles in the sea. Plenum, New York, 506 p.

Arístegui, J., Sangrá, P., Hernández-León, S., Cantón, M., Hernández-Guerra, A. and Kerling, J. L. (1994). Island-induced eddies in the Canary Islands. Deep-Sea Research 41, no. 10: 1509-25.

Arístegui, J., Tett, P., Hernández-Guerra, A., Basterretxea, G., Montero, M.F., Wild, K., Sangrá, P., Hernández-Leon, S., Cantón, M., García-Broun, J.A., Pacheco, M. and Barton, E.D. (1997). The influence of island-generated eddies on chlorophyll distribution: a study of mesoscale variation around Gran Canaria. Deep-Sea Research 44, no. 1: 71-96.

Ariz, J., Delgado de Molina, A., Santana, J.C., Arbelo, M., Hernandez, P. and Hererra, F. (1998). Relación entre las capturas de patudo Thunnus obesus (Lowe, 1839), la temperatura superficial y diversos fenómenos mesoescalares, mediante el uso de teledetección infrarroja en el árae de las Islas Canarias durante 1994. Collective Volume of Scientific Papers, Int. Com. Con. Atlan. Tun. (ICCAT), L(1): 393-403.

Arnold, W.S. and Norris, H.A. (1998). Integrated resource management using GIS: Shellfish aquaculture in Florida. Journal of Shellfish Research 17, no. 1: 318.

Arnold, W.S., Norris, H.A. and Berrigan, M.E. (1996). Lease site considerations for hard clam aquaculture in Florida. Journal of Shellfish Research 15, no. 2: 478-79.

Arnold, W.S., White, M.W., Norris, H.A. and Berrigan, M.E. (2000). Hard clam (Mercenaria spp.) aquaculture in Florida, USA: Geographic information system applications to lease site selection. Aquacultural Engineering 23: 203-31.

Aronoff, S. (1989). Geographic information systems: management perspective. WDL Publications, Canada.

Arzul, G., Clemente, A. and Pinier, A. (1996). Effects of phytoplankton growth of dissolved substances produced by fish farming. Aquatic Living Resources 9, no. 2: 95-102.

Baringo, F. (1999). Guía de buceo de Tenerife. PONTO, Sevilla, 189 p.

Barker, C.J. (1990). Classification society rules for fish farms. In: Engineering for Offshore Fish. Thomas Telford, Great Britain, 31-38 p.

Barredo, J.I. (1996). Sistemas de Información Geográfica y evaluación multicriterio en la ordenación del territorio. RA-MA Editorial, Spain, 245 p.

Bartllet, D.J. (1993a). GIS and the Coastal Zone: Past, Present and Future. AGI 3/94.

Bartllet, D.J. (1993b). Coastal zone applications of GIS: Overview. In St Martin, K. (Ed), Explorations in Geographic Information Systems Technology Volumen 3: Applications in Coastal Zone Research and Management. (Worcester, Massachisetts: Clark Labs for Cartographic Technology and Analysis).

Bartllet, D.J. and Carter, R.W.G. (1990). Seaslope ecology: the landscape ecology of the coastal zone. Ekologia (CSFR) 10: 43-53.

Barton, I.J., Zavody, A.M., Brien, M.O., Cutten, D.R., Saunders, R.W. and Llewellyn-Jones, D. T. (1989). Theoretical algorithms fro satellite-derived sea surface temperatures. Journal of Geophysical Research 94, no. D3: 3365-75.

Barton, I.J. (1995). Satellite-derived sea surface temperature: Current status. Journal of Geophysical Research 100: 8777-90.

Basterretxea-Oyarzabal, G. (1994). Influence of the oceanographic mesoescalar structures in the Canary islands region. Thesis. University of Las Palmas de G.C.

Bell, A.K. and Barr, A.G. (1990). Computerised mathematical modelling in the assessment of fish-farming sites. In: Engineering for Offshore Fish. Thomas Telford, Great Britain, 49-61 p.

Benetti, D.D., O'Hanlon, B., Ayvazian, J., Stevens, O., Rivera, J., Palmer, G. and Eldridge, L. (2001). Site assessment criteria for offshore marine fish cage aquaculture. Aquaculture 2001: Book of Abstracts, World Aquaculture Society, 143 J.M Parker Coliseum Louisiana State University Baton Rouge LA 70803 USA, 53.

Beveridge, M. (1996). Cage Aquaculture. Fishing News Books, Great Britain, 346 p.

Bielecka, E., Federowicz-Jackowski, W. and Witkowska, E. (1995). Sequential monitoring of tatra subalpine forests on the basis of cartographic and remotely-sensed data. EURO-MAB IV 21: 119-30.

Biradar, R.S. and Abidi, S.A.H. (2000). Subtle issues in the management of coastal fisheries and aquaculture. Subtle Issues in Coastal Management., Indian Institute of Remote Sensing (NRSA), Dehradun (India), 65-75 pp.

Borgam, L.E. and Resio, D.T. (1977). Extremal Prediction in Wave Climatology. Proceedings, Ports 77, Vol. I, New York, p 394.

Boyer, D.L, Davies, P.A., Holland, W.R., Biolly, F. and Honj, I.H. (1987). Stratified rotating flow over and around isolated 3D topography. Philosophical Transactions of the Royal Society, London. A322, 213-241.

Boyle, P.R., Bailey, N., Fergus, T., Cross, T.F., Cross, E., Boucaud-Camou, H. Troadec, J., Bihan, L., Balguerias, E. and Morais, J. (1998). Cephalopod resources dynamics: patterns in environmental and genetic variation. Third European Marine Science and Technology Conference (MAST Conference), Lisbon, 23-27 May 1998: Project Synopses Vol. 6: Fisheries and Aquaculture (FAIR: 1994-98), Selected Projects From the Research Programme for Agriculture and Fisheries Including Agro-Industry, Food Technology, Forestry, Aquaculture and Rural Development FAIR., European Commission DG 12 Science, Research and Development, Luxembourg (Luxembourg), Vol. 6, Pp. 148-151.

Braun, J.G. (1980). Estudios de produccion en aguas de las Islas Canarias. Boletin Del Instituto Espanol De Oceanografia, 285: 149-54.

Braun, J.G. and Real, F. (1984). Estudios de produccion en la bahia de Antequera: una comparacion con aguas oceanicas. Boletin Del Instituto Espanol De Oceanografia 291: 97-105.

Braun, J.G., De Armas, J.D., Real, F., Escanez, J.E., Villamandos, J.E. Santamaria M.T.G. (1986). Oceanographical conditions in Canary islands waters. Oxygen and nutrients. Int. Counc. Explor. Sea., Hydrogr. Comm., C.M. C:26, pp. 1-8.

Braun, J.G.I., Armas, J.D. and Real, F. 91985).Productividad y biomasa del ultraplancton, nanoplancton y fitoplancton de red en aguas de las Islas Canarias. Boletin Del Instituto Espanol De Oceanografia 2: 192-204.

Braun, J.G., Real, F. and de Armas, J.D. (1982). Production studies in Canary Islands waters. The Canary current: studies of an upwelling system. Hempel International Council for the Exploration of the Sea. Reprint: 11-14 April 1978

Brest, C.L. and Rossow, W.B. (1992). Radiometric Calibration and Monitoring of NOAA AVHRR data for ISCCP, Int. J. Remote Sensing, 13, 235-273.

Brooks, K.N., Ffolliott, P.F., Gregerssen, H.M. and Thames, J.L. (1991). Hydrology and the Management of watersheds. Iowa state University Press, USA, 392 p.

Brown, B., Keats, D.W., Wakibia, J.G. and Anderson. R.J. (1999). Developing community-based seaweed mariculture of *Gracilaria gracilis* on the South African West coast. Conference on Advances on Marine Sciences in Tanzania., IMS, Zanzibar (Tanzania), p. 52.

Brown, R.V., Kahr, A.S. and Peterson, C. (1974). Decision Analysis for the Manager. Holt, Rinehart and Winston Inc., United States of America, 618 p.

Budescu, D.V. and Wallsten, T.S. (1985). Consistency in Interpretation of Probabilistic Phrases . Organizational Behaviour and Human Decision Processes 36: 391-405.

Budescu, D.V., Weinberg, S. and Wallsten, T.S. (1988). Decisions based on numerically and verbally expressed uncertainties. Journal of Experiment Psychology: Human Perception and Performance 14, no. 2: 281-94.

Budic, Z.D. (1993). GIS use among southeastern local governments. URISA Journal 5, no. 1: 17-21.

Budic, Z.D. (1994). Effectiveness of Geographic Information Systems in Local Planning. APA Journal: 244-63.

Bugrova, L. (1996). A comparison of the Financial Feasibility of Three Offshore cage Systems for the Production of sea Bream in the Mediterranean. In: Open Ocean Aquaculture. Proceedings Of An International Conference, May 9-10, 1996, Portland, Maine., 1999, 127-136. USA: New Hampshire/Maine Sea Grant Collage Program.

Bulthuis, D.A. (1983). Effects of in situ light reduction on density and growth of the seagrass Heterozostera tasmanica (Martens ex Aschers) den Hartog in western Port, Victoria, Australia. J. Exp. Mar. Ecol. 61: 91-103.

Burrough, P.A. (1990). Principles of Geographical Information Systems for Land Resources Assessment. Oxford University Press, Great Britain, 194p.

Bushing, W.W. (1997). GIS-based gap analysis of an existing marine reserve network around Santa Catalina Island. Marine Geodesy 20, no. 2-3: 205-334.

Caine, G.C. (1987). Biophysical criteria for siting salmon farms in British Columbia. B.C. Min. Agric. Fish. Food, Aquaculture and Commercial Fisheries Branch.

Cairns, J. and Linfoot, B. (1991). Reasons behind structural failure. Fish Farmer July/August: 55-56.

Campbell, J.B. (1996). Introduction to Remote Sensing. Taylor & Francis, London, 662 p.

Casado, M. J., Barañano, J. R. and Elorriaga, A. G. (2001). Libro Blanco de la Acuicultura en España. Ministerio de Agricultura, Pesca y Alimentación, Centro de Publicaciones, Madrid. 522 p.

Cardone, V.J. (1986). Hidcast of extreme wind, wave, surge and current data offshore Georgia. Oceans 86 Conference: Science Engineering Adventure 1, no. 75-83.

Carlson, P.R., Yabro, I.A. and Barber, T.R. (1994). Relationship of sediment sulfide to mortality of Thalassia testudimun in Florida bay. Bull. Mar. Sci. 54, no. 3: 733-46.

Carter, R.W.G. (1988). Coastal environments: an introduction to the physical, ecological and cultural systems of coastlines. Academic Press, London, 617 p.

Casabianca, M.L., Laugier, T. and Collard, D. (1997). Impact of shellfish farming eutrophication on benthic macrophyte communities in the Thau Lagoon, France. Aquaculture International 5, no. 4: 301-14.

CD-Map (Volumen 1) (1999). Proyecto Anaga, Excmo. Cabildo Insular de Tenerife, Area de Presidencia y Planificacion, S.T. de Planes Insulares.

Charnpratheep, K., Zhou, Q. and Garner, B. (1997). Preliminary landfill site screening using fuzzy geographical information systems. Waste Management & Research 15: 197-215.

Chen, Y.S. (2000). Waste outputs and dispersion around marine fish cages and the implications for modelling. Ph. D. Thesis. University of Stirling, 185 pp.

Chen, Y.S., Beveridge, M.C.M. and Telfer, T.C. (1999). Settling rate characteristics and nutrient content of the faeces of Atlantic salmon (Salmo salar L.) and the implications for modelling of solid wastes dispersion. Aquaculture Research, 30, 395-398

Chenon, F.H., Varet, L,. Loubersac, S,. Grand, G. and Hauti, A. (1992). SIGMA, a GIS of the fisheries and aquaculture territorial department. A tool for a better monitoring of public marine ownerships and pearl oyster culture. Journees Internationales Tenues A Noumea Et A Tahiti, 19-24 Novembre 1990., Orstom, Noumea (New Caledonia): pp. 561-70.

CIATFE (Consejo Insular de Aguas de Tenerife) (1991). Plan Hidrologico Insular de Tenerife. Cabildo Insular de Tenerife, Spain.

Clark, J.R. (1996). Coastal Zone Management Handbook. Lewis Publishers, USA, 704 p.

Clark, R.B. (1998). Marine Pollution. Clarendon Press, Oxford, 161 p.

Clarke, V.A., Ruffin, C.L., Hill, D.J. and Beaman, A.L. (1992). Ratings of orally presented verbal expressions of probability by a heterogeneous sample. Journal of Applied Social Psychology 22: 638-56.

Coche, A.G. (1985.) Soil and freshwater fish culture. FAO, Italy, 174 p.

Cochrane, K.L. (1999). Complexity in fisheries and limitations in the increasing complexity of fisheries management. ICES Journal of Marine Science, 56: 917-26.

Coimbra, J. (2001). GIS-based environmental modelling for management of coastal aquaculture and natural resources: a case study in Baia de Sepetiba, Brazil. NATO Science Series: Series A: Life Sciences, IOS Press, Nieuwe Hemweg 6B Amsterdam 1013 BG The Netherlands, Vol. 314, pp. 261-274, Modern Aquaculture in the Coastal Zone-Lessons and Opportunities.

Coll, C. and Caselles, V. (1994). Analysis of the atmospheric and emissivity influence on the split-window equation for sea surface temperature. International Journal of Remote Sensing 15: 1915-32.

Coll, J.M. (1991). Acuicultura Marina Animal. Ediciones Mundi-Prensa, Madrid.

Cornillon, P., Gilman, C., Stramma, L., Brown, O., Evans, R. and Brown, J. (1987). Processing and analysis of large volumes of satellite-derived thermal infrared data. Journal of Geophysical Research 92: 12,993-13,002.

Corsi, F., Agnesi, S., Schintu, P. and Ardizzone, G. (1996). Geographical Information System (GIS) applied to fisheries data: The case of Italian demersal resources.

Marine Populations Dynamics. Proceedings of the Second Meeting of the DYNPOP Working Group Organized by CIESM and CIHEAM With the Collaboration of the Italian Marine Biology Society (SIBM) and the Institute of Zoology of the University of Genoa (IZUG), Genoa, Italy, 2-5 October 1996.

Cracknel, A.P. (1997). The Advanced Very High Resolution Radiometer. Taylor & Francis Ltd., London, 534 p.

Cromey, C.J, Nickell, T.D. and Black, K.D., (2000) DEPOMOD: A model for predicting the effects of solids deposition from mariculture to the benthos. Scottish Association of Marine Science, Oban. 120 pp.

Czajkowski, K.P., Goward, S.N. and Ouaidrari, H. (1998). Impact of AVHRR filter functions on surface temperature estimation from the split window approach. Int. J. Geographical Information Science 19, no. 10: 2007-12.

Davenport, R., Neuer, S., Hernández-Guerra, A., Ruedas, M.J., Llinas, O., Fischer, G. and Wefer, G. (1999). Seasonal and interannual pigment concentration in the Canary Islands region from CZCS data and comparison with observations from the ESTOC. Int. J. Geographical Information Science 20, no. 7: 1419-33.

De Floriani, L. and Marzano, P. (1994). Line-of-sight communication on terrain models. International Journal of Geographical Information Systems 8: 329-42.

De Leon, A.R. and Braun, J.G. (1973). Ciclo anual de la produccion primaria y su relacion con los nutrientes en aguas Canarias. Boletin Del Instituto Espanol De Oceanografia 167: 1-24.

De Silva, S.S., Amarasinghe, S.U., Nissanka, C., Wijesooriya, A.W. and Fernando, J.M. (2001). Use of geographical information systems as a tool for predicting fish yield in tropical reservoirs: case study on Sri Lankan reservoirs. Fisheries Management and Ecology 8, no. 1: 47-60.

De Vantier, B.A. and Feldman, A.D. (1993). Review of GIS applications in hydrological modelling. Journal of Water Resources Planning and Management 119: 246-61.

DeBarry, P. and Paul, A. (1991). G.I.S. applications in nonpoint source pollution assessment. Proc Natl Conf Hydraul Eng, Asce, New York (USA), p. 882-887.

DeBarry, P.A. and Carrington, J.T. (1990). Computer Watersheds. Civil Engineering (ASCE) CEWRA9 vol. 60, No. 7, p 68-70.

Delgado O., Ruiz, J., Pez, M., Romero, J. and Ballesteros, E. (1999). Effects of fish farming on seagrass (Posidonia oceanica) in a Mediterranean bay: seagrass decline after organic loading cessation. Oceanologica Acta 22: 109-17.

Delgado, O., Grau, A., Pou, S., Riera, F., Massuti, C., Zabala, M. and Ballesteros, E. (1997). Seagrass regression caused by fish cultures in Fornelss bay (Menorca, western Mediterranean). Oceanologica Acta 20, no. 3: 557-63.

DeMers, M.N. (1997). Fundamentals of geographic information systems. John Wiley & Sons, New York, 486 p.

Dennison, W.C. and Alberts, R.S. (1982). Photosynthesis responses of Zostera marina L. (eelgrass) to in situ manipulations of light intensity. Oecologia 55: 269-76.

Diaz Salgado, J, and Lopez Blanco, J. (2000). Assessment of the coastal shrimp aquaculture potential in the Mar Muerto lagoon, using the multicriteria analysis techniques along with a SIG. Investigaciones Geograficas 41: 62-80.

Diaz, C., Galindo, L., Garcia-Montelongo, F., Larrechi, M.S. and Rius, F.X. (1990). Metals in coastal waters of Santa Cruz de Tenerife, Canary Islands. Marine Pollution Bulletin 21, no. 2: 91-95.

Diaz-Diaz, R. (1996). Dinamica de los plaguicidas en el suelo: Evaluacion del riesgo de contaminacion del agua subterranea. Ph.D. Thesis, Departamento De Eadologia y Geologia, Universidad De La Laguna, Tenerife, Spain.

Díaz-Díaz, R.J.E., García Hernández, H. and Loague, K. (1998). Leaching Potentials of Four Pesticides Used for Bananas in the Canary Islands. Journal of Environmental Quality 27: 562-72.

Donnan, D.W. and Davies, J. (1996). Assessing the Natural Heritage Importance of Scotland's Maerl Resource. Partnership in Coastal Zone Management: 533-40.

Dunning, M.S, Sun, K., Danaher, Y. and Fisher, S. (2000). Establishment of a Coastal Habitat Resources Information System (CHRIS) for Queensland. Information Series. Department of Primary Industries (Queensland). Brisbane [Inf. Ser. Dep. Prim. Ind. (Queensl.)], QDPI, Brisbane, Qld. (Australia), pp. 124.

Dyer, R.F. and Forman, E.H. (1991). An Analytic Approach to Marketing Decisions. Prentice Hall: Englewood Cliffs, NJ.

Eason, K. (1988). Information Technology and Organizational Change. Taylor & Francis, London.

Eastman, J.R. (1993). IDRISI version 4.1 update Manual. Clark University Graduate School of Geography, Worcester, MA, USA, 120 P.

Emery, W.J. and Yu, Y. (1997). Satellite sea surface temperature patterns. Int. J. Geographical Information Science 18, no. 2: 323-34.

Emery, W.J., Yu, Y., Wick, G.A., Schluessel, P. and Reynolds, R.W. (1994). Correcting infrared satellite estimates of sea surface temperature for atmospheric water vapour contamination. Journal of Geophysical Research 99: 5219-36.

Epstein, E.F., Hunter, G.J. and Agumya, A. (1998). Liability insurance and the use of geographical information. Int. J. Geographical Information Science 12, no. 3: 203-14.

Erev, I. and Cohen, B.L. (1990). Verbal versus numerical probabilities: Efficiency, biases and the preference paradox. Organizational Behaviour and Human Decision Processes 45: 1-18.

Ervik, A., Hansen, P.K., Aure, J., Stigebrandt, J., Johannessen, P., Jahnsen, T. (1997). Regulating the local environmental impact of extensive marine fish farming: I. The concept of MOM Modelling-Ongrowing fish farms-Monitoring. Aquaculture 158, no. 85-94.

Fairfield, F.M. (1987). Marina planning with Geographic Information Systems. Coastal Zone '87 Proceedings: 1023-30.

Falcon, J.M., Bortone, S.A., Brito, A. and Bundrick, C.M. (1996). Structure of and relationships within and between the littoral, rock-substrate fish communities off four islands in the Canarian Archipelago. Marine Biology 125, no. 2: 215-31.

Fanjul, E.A., Gómez, M., Carretero, J.C., de la Vega, P., Rivero, F.J. (1998). Tide and surge dynamics along the Iberian Atlantic coast. Oceanologica Acta 21 N. 2, 131-143.

Fernández de Puelles, M.L. and Gracía-Braun, J.A. (1989). Dinamica de las comunidades planctonicas en una zona del Atlantico subtropical (Isla de Tenerife). Boletin Del Instituto Espanol De Oceanografia 5: 87-100.

Fernandez-Caldas, E., Tejedor, M.L. and Quantin, P. (1982). Suelos de regiones volcanicas: Tenerife, Islas Canarias. Coleccion Viera y Clavijo VI. Universidad De La Laguna, Tenerife, Spain.

Fiekas, V., Elken, J., Muller, T.J., Aitsam, A. and Zenk, W. (1992). A view of the Canary basin thermocline circulation in winter. Journal of Geophysical Research 97, no. C8: 12,495-12,510.

Findlay, R.H, and Watling, L., (1994). Toward a process level model to predict the effect of salmon net-pen aquaculture on benthos, In B.T. Hargrave [ed.]. Modelling Benthic Impacts of Organic Enrichment from Marine Aquaculture. Canadian Technical Report of Fisheries and Aquatic Sciences, p. 47-78

Fisher, P., Abrahart, R.J. and Herbinger, W. (1997). The sensitivity of two distributed non-point source pollution models to the spatial arrangement of the landscape. Hydrological Processes 11: 241-52.

Foster, M., Petrell, R., Ito, M.R. and Ward, R. (1995). Detection and Counting of Uneaten Food Pellets in a Sea Cage Using Image Analysis. Aquaculture Engineering 14, no. 3: 251-69.

Foucher, E., Thiam, M. and Barry, M. (1998). A GIS for the management of fisheries in West Africa: Preliminary application to the octopus stock in Senegal. South African Journal of Marine Science 20: 337-46.

Fox, W.P. (1990). Modelling of particulate deposition under salmon net-pens. In Final programmatic environmental impact statement. Fish culture in floating net-pens (technical appendices). Washington State Department of Fisheries, USA.

França, G.B. and Cracknell, A.P. (1995). A simple cloud masking approach using NOAA AVHRR daytime data for tropical areas. International Journal of Remote Sensing 16: 1697-705.

Fuchs, J., Martin, J.L.M. and Populus, J. (1998). Assessment of tropical shrimp aquaculture impact on the environment in tropical countries, using hydrobiology, ecology and remote sensing as helping tools for diagnosis. Ifremer, Issy-Les-Moulineaux (France), 263 Pp.

GESAMP (IMO/FAO/UNESCO/WMO/WHO/IAEA/UN/UNEP Joint Group of Expert on the Scientific Aspects of Marine Pollution) (1991). Reducing Environmental Impacts of Coastal Aquaculture. Rep. Stud. GESAMP 47: 39 p.

GESAMP (IMO/FAO/UNESCO/WMO/WHO/IAEA/UN/UNEP Joint Group of Experts on the Scientific Aspects of Marine Pollution) (1997). Towards safe and effective use of chemicals in coastal aquaculture. Rep. Stud. GESAMP 65: 40p.

GESAMP (IMO/FAO/UNESCO/WMO/WHO/IAEA/UN/UNEP Joint Group of Expert on the Scientific Aspects of Marine Pollution) (1996a). Monitoring the ecological effects of Coastal aquaculture Wastes. Rep. Stud. GESAMP 57: 38p.

GESAMP (IMO/FAO/UNESCO/WMO/WHO/IAEA/UN/UNEP Joint Group of Expert on the Scientific Aspects of Marine Pollution) (1996b). The contribution of science to integrated coastal management. Rep. Stud. GESAMP 61: 66p.

Gillespie, S.R. (1999). An empirical approach to estimating GIS benefits. URISA Journal 11, no. 3: 27-34.

Goda, Y. (1977). Numerical experiments on statistical variability of ocean waves. Report of the Port and Harbour Research Institute 16, no. 2: 3-26.

Goda, Y. (1979). A review on Statistical Interpretation of Wave Data. Report of the Port and Harbour Research Institute 18, no. 1: 5-32.

Goda, Y. (1988). On the methodology of selecting design wave height. 21st International Conference on Coastal Engineering: 899-913.

Godschalk, D.R. and McMahon, G. (1992). Staffing the revolution: GIS education for planners. Journal of Planning Education and Research 11, no. 3: 216-26.

Gold, C.M. (1996). An event-driven approach to spatio-temporal mapping. Geomatica 50: 415-25.

Gomm, S. (2001). Integrated Mapping of the UK Marine and Coastal Zone. Proceedings of the GIS Research UK, 9th Annual Conference.

Goodwin, P. and Wright, G. (1992). Decision Analysis for Management Judgment. John Wiley & Sons Ltd., England, 308p.

Gordon, W.R. (1994). A role for comprehensive planning, geographical information system (GIS) technologies and program evaluation in aquatic habitat development. Bulletin of Marine Science 55, no. 2-3: 995-1013.

Gowen, R.J and Bradbury, N.B. (1987). The ecological impact of salmonid farming in coastal waters: a review. Oceanogr. Mar. Biol. Ann. Rev. 25: 563-75.

Gowen, R.J., Bradbury, N.B., Brown, J.R. (1989). The use of simple models in assessing two of the interactions between fish farming and the marine environment. Aquaculture- a Technology in Progress: 1071-80.

Gowen, R.J., Brown, J. R., Bradbury, N.B. and McLusky, D.S. (1988). Investigations into benthic enrichment, hypernutrification and eutrophication associated with mariculture in Scottish coastal waters (1984-1988). Report to the Highlands and Islands Development Board, Crown Estate Commissioners, Nature Conservancy Council, Countryside Commission for Scotland and Scottish Salmon Growers Association. 289 pp.

Gower, J.F.R. (1994). Red tide monitoring using AVHRR HRPT imagery from local receiver. Remote Sensing of Environment 48: 309-18.

Green, N.P.A. (1987). Teach yourself geographical information systems. the design, creation and use of demonstrators and tutors. International Journal of Geographical Information Systems 1: 279-90.

Grita, F. (1998). GIS analysis for the assessment of fish farming potential in the Caribbean. Copescal Tech. Pap, No.10 FAO, Rome (Italy).

Gumbel, E.J. (1958). Statistics of extremes. Columbia Univ Pr, New York.

Günther, H., Hasselmann, S. and Janssen, P.A.E.M. (1991). Wamodel Cycle 4. Technical Report No.4, Deutsche Klimarechenzentrum, Germany (http:// www. dkrz.de/ forschung/reports/report4/wamh-1.html)

Guo, L.S. and He, Y.S. (1999). Integrated Multicriterial Decision Model- a Case Study for the Allocation of Facilities in Chinese Agriculture. J. Agric. Engng Res. 73: 87-94.

Gupta, M.C. (1998). Brackishwater aquaculture site selection using remote sensing & GIS and its impact on environment. Proceedings of the Workshop on Environmental Impact Assessment of Aquaculture Enterprises, Chennai, December 10-12, 1997., Rajiv Gandhi Centre for Aquaculture, Subramaniyapuram (India), pp. 84-109.

Gutman, G.C. (1992). Satellite daytime image classification for global studies of Earth's surface parameters from polar orbiters. International Journal of Remote Sensing 13: 209-34.

Hadrian, D.R., Bishop, I.D. and Mitcheltree, R. (1988). Automated mapping of visual impacts in utility corridors. Landscape and Planning 16, no. 261-282.

Halvorson, H.O. (1997). Addressing public policy issues on scallop aquaculture in Massachusetts. Journal of Shellfish Research 16, no. 1: 287.

Hamm, R.M. (1991). Selection of verbal probabilities: A solution for some problems of verbal probability expression. Organizational Behaviour and Human Decision Processes 48: 193-223.

Hansen, P., Ervik, K., Aure, A., Johannessen, J., Jahnsen, P., Stigebrandt, T., Schaanning, A. (1997). MOM. Concept and Revised Edition of Monitoring Programme 1997. Fisken Og Havet 7. Institute of Marine Research, Bergen, Norway, 51 Pp.

Hansen, P.K., Ervik, A., Schaanning, M,. Johannessen, P., Aure, J., Jahnsen, T. and Stigebrandt, A. (2001). Regulating the local environmental impact of intensive, marine fish farming II. The monitoring programme of the MOM system (Modelling–Ongrowing fish farms–Monitoring). Aquaculture 194: 75-92.

Hargrave, B.T., (1994), A benthic enrichment index, In B.T. Hargrave [ed.]. Modelling Benthic Impacts of Organic Enrichment from Marine Aquaculture. Canadian Technical Report of Fisheries and Aquatic Sciences, p. 79-91.

Hassen, M.B. and Prou, J. (2001). A GIS-based assessment of potential aquacultural nonpoint source loading in an Atlantic bay (France). Ecological Applications 11, no. 3: 88-814.

Håstein, T. (1996). Disease problems, use of drugs, resistance problems and preventive measures in fish farming world wide. Sustainable Fish Farming,. Balkena Publishers, Netherlands, 183-94 p.

Hausenbuiller, R.L. (1985). Soil Science: Principles & Practices. Third Edition. Wm. C. Brown Publishers, Dubuque, Iowa.

Hedrick, R.P. (1998). Relationships of the Host, Pathogen, and Environment: Implications for Diseases of Cultured and Wild Fish Populations. Journal of Aquatic Animal Health 10: 107-11.

Hennessy, M.M., Wilson, L., Struthers, W., and Kelly, L.A. (1996). Waste loadings from two freshwater Atlantic salmon juvenile farms in Scotland. Water, Air and Soil Pollution 86: 235-49.

Hepner, G.F. and Miller, H.J. (1993). Using GIS for environmental assessment. ACSM Bulletin: 42-46.

Hevia, M., Rosenthal, H. and Gowen, R.J. (1996). Modelling benthic deposition under fish cages. Journal of Apply Ichthyology 12, no. 71-74.

Heyman, W.D. and Kjerfve, B. (1999). Hydrological and oceanographic considerations for integrated coastal zone management in Southern Belize. Environmental-Management 24, no. 2: 229-45 .

Hickey, R.J., Bush, D.M. and Boulay, R.S. (1997). GIS Supports Coastal Risk Assessment. GIS World: 54-58.

Hickey, R., Smith, A. and Jankowski, P. (1994). Slope length calculations from a DEM within ARC/INFO grid. Computers, Environment and Urban Systems 18, no. 5: 365-80.

Hill, J.M., Singh, V.P. and Aminian, H. (1897). Computerized Data Base for Flood Prediction Modeling. Water Resources Bulletin 23, no. 1: 21-27.

Hoar, W.S., Randal, D.J. and Brett, J.R. (1979). Fish Physiology Vol. VIII. Academis Press Inc., USA, 786 p.

Holby, O. and Hall, P.O.J. (1994). Chemical fluxes and mass balances in a marine fish cage farm. III. Silicon. Aquaculture 120: 305-18.

Huguenin, J.E. (1997). The design, operations and economics of cage culture systems. Aquacultural Engineering 16: 167-203.

Huizingh, K.R.E. and Vrolijk, H.C.J. (1997). A Comparison of Verbal and Numerical Judgments in the Analytic Hierarchy Process. Organizational Behaviour And Human Decision Processes 70, no. 3: 237-47.

Huizingh, K.R.E. and Vrolijk, H.C.J. (1997). Extending the Applicability of the Analytic Hierarchy Process. Socio-Economic Planning Sciences 31, no. 1: 29-39.

Ibrekk, H.O., Kryvi, H. and Elvestad, S. (1993). Nationwide assessment of the suitability of the Norwegian coastal zone and rivers for aquaculture (LENKA). Coastal Management 21, no. 1: 53-73.

Inoue, H. (1972). On water exchange in a net cage stocked with the fish Kamachi. Bulletin of the Japanese Society of Scientific Fisheries, 44, 659-664.

Institute of Environmental Assessment and The Landscape Institute (1995). Guidelines for Landscape and visual impact assessment. E & FN Spon, Hong Kong, 126 p.

Isaacson, M.S.Q., Asce, M. and MacKenzie, N. (1981). Long-term distributions of ocean waves: a review. Journal Of Waterway, Port, Coastal And Ocean Division 107, no. 2: 93-109.

ISTAC (Canary Institute of Statistics). (1996). Proyecciones de la poblacion; Canarias 1996-2011. Gobierno de Canarias, Spain.

ISTAC (Canary Institute of Statistics). (2001). Gobierno de Canarias, http://www.istac.rcanaria.

Iwana, G.K., Pickering, A.D., Sumpter, J.P. and Schreck, C.B. (1997). Fish Stress and Health in Aquaculture. Cambridge University Press, U.K, 277 p.

Jefferies-Harris, T. and Selwood, J. (1991). Management of marine sand and gravel- A seabed information system. Land and Mineral Surveying 9, no. 2: 6-8.

Jenkins, K.A. and Smith, B.J. (1990). Daytime rock surface temperature variability and its implications for mechanical rock weathering: Tenerife, Canary Islands. CATENA 17, no. 4-5: 449-59.

Joao, E. and Fonseca, A. (1996). Current use of Geographical Information Systems for environmental assessment: A discussion document. LSE Research Papers in Environmental and Spatial Analysis. London School of Economics, London. 36.

Johnston, C.A. (1998). Geographic Information Systems in Ecology. Blackwell Science Ltd., Great Britain, 351 p.

Jones. C. B (1997). Geographical Information Systems and Computer Cartography. Addison Wesley Longman Limited, England, 319p.

Jørgensen, E.S. (1991). Introduction to environmental management modelling. In Application of Ecological Modelling in Environmental Management, ed. P.E. Hansen and S.E. Jørgensen. Elsevier, Amsterdam, 45-98p.

Kapetsky, J.M. (1985). Mangroves, fisheries and aquaculture: selected working papers submitted to the eleventh session of the advisory committee of experts on marine resources research. Supplement. FAO, Rome, Italy, 338p.

Kapetsky, J.M. (1987) Satellite remote sensing to locate and inventory small water bodies for fisheries management and aquaculture development in Zimbabwe. CIFA Occasional Paper, (14), FAO Fisheries Department, Rome, Italy,11p.

Kapetsky, J.M. (1994). A strategic assessment of warm-water fish farming potential in Africa. Technical Paper, 27, FAO, Rome.

Kapetsky, J.M. and Nath, S.S. (1997). A strategic assessment of the potential for freshwater fish farming in Latin America. COPESCAL Technical Paper 128, Rome, FAO.

Kapetsky, J.M. Travaglia, C. (1995). Geographical information systems and remote sensing: an overview of their present and potential applications in aquaculture. In: Nambiar, K.P.P., Singh, T. (Eds.), AquaTech '94: Aquaculture Towards the 21st Century. INFOFISH, Kuala Lumpur, pp. 187-208.

Keeny, R. and Raiffa, H. (1976). Decision with multiple Objectives: Preferences and value trade offs. Wiley and Sons, New York.

Kent, M. (1986). Visibility analysis of mining and waste tipping sites: a review.Landscape and Urban Planning 13: 101-10.

Kent, M. and Coker, P. (1994). Vegetation Description and Analysis. John Wiley & Sons Ltd., England, 363 p.

Kernick, M.L. (2000). Investigation of the solid waste material produced from a European sea bass farm in the Mediterranean. M.Sc. Thesis, Institute of Aquaculture, University of Stirling.

Kertesz, A. (1993). Application of GIS methods in soil erosion modelling. Computers, Environment and Urban Systems 17, no. 3: 233-38 .

Kindwell, K.B. (1998). NOAA Polar Orbiter Data Users Guide (TIROS-N, NOAA-6, NOAA-7, NOAA-8, NOAA-9, NOAA-10, NOAA-11, NOAA-12, NOAA-13 and NOAA-14). NASA, USA.

Kirkwood, C.W. (1997). Strategic decision making: multiobjective decision analysis with spreadsheets. Duxbury Press, Belmont, CA.

Klein, B. and Siedler, G. (1989). On the origin of the Azores Current. Journal of Geophysical Research 94: 6159-68.

Kleindorfer, P.R., Kunreuther, H.C. and Schoemaker, P.J.H. (1993). Decision Sciences An integrative Perspective. Cambridge University Press, United States of America.

Krieger, Y and Sandor, M. (1990). GIS application in marine benthic resource management. GIS for the 1990s, 671-83.

Kulka, D.W. (2001). Distribution of Greenland halibut and by-catch species that overlap the 200-mile limit spatially and in relation to depth-effect of depth restrictions in the fishery. Scientific Council Research Document. Northwest Atlantic Fisheries Organization. 01/40, 42 p.

Kumar, A. and Das, G. (1998). A dynamic runoff model for a Himalayan watershed. International Agricultural Engineering Journal 7, no. 3-4: 201-10.

Lang, L. (1990). Making a GIS dream come true. Planning: 14-20.

Larkun, A.W.D., McComb, A.J. and Shepherd, S.A. (1989). Biology of Seagrasses: A treatise on the biology of seagrasses with special reference to the Australia region. Elsevier, Amsterdam.

Lawless, J. F. (1978). Confidence interval estimation for the Weibull and extreme-value distributions. Technonetrics 20, no. 4: 355-68.

Lawson, T.B. (1995). Fundamentals of Aquacultural Engineering. Chapman & Hall, New York, 335p.

Le Corre, K., Gdir, E.F., Ballester, J.B., Dominguez, J., Lleonart, L., Tunesi, S., Geogakarakos, C., Papaconstantinou, G., Garofalo, L., Orsi, R., and De Metrio, G. (1998). Spatio-temporal analysis of the fisheries resources, their environment and exploitation in the Mediterranean Sea: experimental uses of geographical information systems. 3. European Marine Science and Technology Conference, Lisbon (Portugal), 23-27 May 1998.

Lee, J.S.D. (1998). On applying viewshed analysis for determining least-cost paths on Digital Elevation Models. Int. J. Geographical Information Science 12, no. 8: 891-905.

Leenknecht, D.A., Szuwalski, A. and Sherlock, A.R. (1992). Automated Coastal Engineering System. Technical Reference. Coastal Engineering Research Center, USA.

Lehmann, A. (1998). GIS modeling of submerged macrophyte distribution using Generalized Additive Models. Plant Ecology 139, no. 1: 113-24.

Li, Y., Brimicombe, A.J. and Ralphs, M.P. (2000). Spatial data quality and sensitivity analysis in GIS and environmental modelling: the case of coastal oil spills. Computers, Environment and Urban Systems 24: 95-108.

Lichtenstein, S. & Newman, J.R. (1967). Empirical scaling of common verbal phrases associated with numerical probabilities. Psy Chonomic Science 9, no. 563-564.

Lillesand, T.M. and Kiefer, R.W. (1994). Remote Sensing and Image Interpretation. John Wiley & Sons, USA, 750p.

Linfoot, B.T., Cairns, J. and Poxton, M.G. (1990). Hydrodynamic and biological factors in the design of sea-cages for fish culture. In: Engineering for Offshore Fish. Thomas Telford, Great Britain, 197-210 p.

Llewelyn-Jones, D.T., Minnet, P.J., Saunders, R.W. and Zavody, A.M. (1984). Satellite multichannel infrared measurements of sea surface of the N.E. Atlantic Ocean using AVHRR/2. Quarterly Journal of the Royal Meteorological Society 110: 613-31.

Loague, K. (1991). The impact of land use on estimates of pesticide leaching potential: Assessments and uncertainties. J. Contamin. Hydrol. 8: 157-75.

Loague, K. (1994). Regional scale ground water vulnerability estimates: Impact of reducing data uncertainties for assessments in Hawaii ground water. J. Contamin. Hydrol, no. 605-616.

Lodwick, W.A., Monson, W. and Svoboda, L. (1990). Attribute error and sensitivity analysis of map operations in geographical information systems: suitability analysis. International Journal of Geographical Information Systems 4, no. 4: 413-28.

Løland, G. (1993). Current forces on, and water flow through and around, floating fish farms. Aquaculture International 1: 72-89.

Losada-Rodriguez, M.A., Alejo-Bocanegra, M. and Moriel, M. (1992). Efecto de las olas. Informes de las comisiones sobre el oleaje de los congresos de navegación. MOPT, Spain, 390p.

Loverich, G. (1997). A Summary Of The Case Against The Use Of Gravity Cages In The Sea Farming Industry. Aquaculture Pacific Exchange, Campbell River, British Columbia, Canada.

Lowry, J.H., Miller, H.J. and Hepner, G.F. (1995). A GIS-Based Sensitivity Analysis of Community Vulnerability to Hazardous Contaminants on the Mexico/U.S. Border. Photogrammetric Engineering & Remote Sensing, 61:11, 1347-1359.

Luengo, A.B., Marín, C.B. and Luengo, H.B. (1995). Tenerife y el Mar. Cabildo de Tenerife, Santa Cruz de Tenerife.

Lyon, J.G., Heinen, J.T., Mead, R.A. and Roller, N.E.G. (1987). Spatial data for modeling wildlife habitat. Journal of Surveying Engineering 113, no. 2: 88-100.

Malczewski, J. (1997). Propagation of errors in multicriteria location analysis: a case study. In: Fandel, G. and Gal, T. (Eds.), Multiple criteria decision making. Springer-Verlag, Berlin, 154-155 p.

Malczewski, J. (1999). GIS and multicriteria decision analysis. John Wiley & Sons, New York, 392p..

Manguerra, H.B. and Engel, B.A. (1998). Hydrologic parameterization of watersheds for runoff prediction using SWAT. Journal of the American Water Resources Association, Vol. 34, No. 5, Pp. 1149-1162.

Mann, K.H. (2000). Ecology of Coastal Waters; with implications for management. Blackwell Science, USA, 406p.

Marín, C. and Luengo, A. (1998). Tenerife y el Mar. Tenerife: Cabildo de Tenerife, Santa Cruz de Tenerife, 222p.

Martínez Aranzábal, J. and Martín-Soldevilla, M.J. (1990). Descripción de las funciones de distribución más utilizadas en estudios de clima marítimo. CEDEX, Madrid, 95p.

Martín-Soldevilla, M.J. and Martínez Aranzábal, J. (1990). Análisis medio y extremal del oleaje. CEDEX, Madrid, 72p.

Massam, B.H. (1993). The right place. Longman scientific and Technical, Harlow, Essex, England

Maury, O. and Gascue, D. (1999). SHADYS ('simulateur halieutique de dynamiques spatiales') a GIS based numerical model of fisheries. Example application: the study of a marine protected area. Aquatic Living Resources 12, no. 1: 77-88.

McClain, E.P., Pichel, W.G. and Walton, C.C. (1985). Comparative performance of AVHRR based multichannel sea surface temperatures. Journal of Geophysical Research 90, no. C6: 11587-601.

McGrath, T.S. (1990) Geographic Information Systems applications for recreation management: a case study in the Oregon dunes national recreation area. Master' Thesis, University of Oregon, Eugene, Oregon.

McKenzie, L.J., Roder, C.A., Roelofs, A.J. and Lee Long, W.J. (2000). Post-flood monitoring of seagrasses in Hervey Bay and the Great Sandy Strait, 1999: implications for dugong, turtle and fisheries management. Information Series. Department of Primary Industries (Queensland). Brisbane [Inf. Ser. Dep. Prim. Ind. (Queensl.)], QDPI, Brisbane, Qld. (Australia), pp. 50.

Meaden, G.J. and Kapetsky, J.M. (1991). Geographical information systems and remote sensing in inland fisheries and aquaculture. FAO Fisheries Technical Paper 262. FAO, Rome.

Mendez, S., Pergent, G. and Pergent-Martini, C. (1997). Impact of fish farming facilities on coastal ecosystems. Proceedings of the Third Conference on the Mediterranean Coastal Environment, Qawra, Malta, 197-211.

Miller, G.A. (1956). The Magical Number Seven Plus or Minus Two: Some Limits on Our Capacity for Processing Information. Psychological Review 63: 81-97.

Minnett, P.J. (1990). The regional optimization of infrared measurements of sea surface temperature from space. J. Geophys. Res. 95, no. C8: 13,497-13,510.

Molina, R., Cabanas, J.M. and Laatzen, F.L. (1996). Hidrography and currents in the Canary Region. Cruise Canarias 9205. Boletin Del Instituto Espanol De Oceanografia 12, no. 1: 43-51.

Morales, S.A. (1997). Vertidos al mar; En el año 2005 no se podrán verter aguas residuales sin ser tratadas previamente. Medio Ambiente Canarias, 5.

Morales-Matos, G. and Pérez-González, R. (2000). Gran Atlas Temático de Canaria. Editorial Insular Canarias, S.A., Tenerife, 376p.

Morgan, R.P.C. (1995). Soil Erosion and Conservation. Longman, UK, 198p.

Muir, L.R. and El-Shaarawi, A.H. (1986). On the calculation of extreme wave heights: A review. Ocean Engineering 13: 93-118.

Muzik, I. and Pomeroy, S.J. (1990). A geographic information system for prediction of design flood hydrographs. Canadian Journal of Civil Engineering/Revue Canadienne De Genie Civil 17, no. 6: 965-73.

Muzik, I. (1992). Derivation of unit and flood hydrographs using a GIS. Environmental Monitoring and Assessment 23, no. 1-3: 45-56.

Nackaerts, K., Govers, G. and Orshoven, J.V. (1999). Accuracy assessment of probabilistic visibilities. Int. J. Geographical Information Science 13, no. 7: 709-21.

Nagy, G. (1994). Terrain visibility. Computer & Graphics 18: 763-73.

Nath, S.S., Bolte, J.P., Ross, L.G. and Aguilar-Manjarrez, J. (2000). Applications of geographical information systems (GIS) for spatial decision support in aquaculture. Aquacultural Engineering 23: 233–278.

Nayak, B.U., Chandramohan, P. and Mandal, S. (1990). Evaluation of wave characteristics in the Gulf of Kutch, Gujarat. Indian Journal of Marine Sciences 19: 83-88.

NOAA polar orbiter data users guide (1985). National Environmental Satellite. National Climatic Data Center Satellite Data Service Division U. S. Dep. of Commer. Washington D. C.

OECD (Organization for Economic Co-operation and Development. Coastal zone management. Integrated policies) (1993). OECD, Paris, 125p.

Olivera, F. and Maidment, D. (1998). Geographic information system use for hydrologic data development for design of highway drainage facilities. Transportation Research Record, No. 1625, Pp. 131-138.

Olson, G.W. (1981). Soils and the environment: a guide to soil surveys and their applications. Chapman and Hal,l USA, 178p.

Pacheco, M.M. and Hernández-Guerra, A. (1999). Seasonal variability of recurrent phytoplankton pigment patterns in the Canary Islands area. Int. J. Geographical Information Science 20, no. 7: 1405-18.

Pattiaratchi, C., James, A. and Collins, M. (1986). Island wakes and headland eddies: a comparison between remotely sensed data and laboratory experiments. Journal of Geophysical Research 92: 783-94.

Pena Mendez, E.M., Astorga Espana, M.S. and Garcia Montelongo, F. (1996a). Polychlorinated biphenyls in two mollusc species from the coastof Tenerife (Canary Islands, Spain). Chemosphere 32, no. 12: 2371-80.

Pena-Mendez E.M., Astorga-Espana M.S. and Garcia-Montelongo, F.J. (1999). Interpretation of analytical data on n-alkanes and polynucleararomatic hydrocarbons in Arbacia lixula from the coasts of Tenerife (Canary Islands, Spain) by multivariate data analysis. Chemosphere 39, no. 13: 2259-70.

Pena-Mendez, E., Conde, J.E. and Montelongo, F.G. (1996b). Polycyclic aromatic hydrocarbons and n-alkanes in Osilinusattratus from the coast of Tenerife (Canary Islands). Bulletin of Environmental Contamination and Toxicology 57, no. 5: 803-10.

Penczak, T., Galicka, W., Molinshi, M., Kusto, E. and Zalewski, M. (1982). The enrichment of a mesotrophic lake by carbon, phosphorus and nitrogen from the cage aquaculture of rainbow trout (Salmo gairderi). Journal of Applied Ecology, 19, 371-393.

Penning de Vries, F.W.T., Agus, F. and Kerr, J. (1998). Soil Erosion at multiple scales. CABI Publishing, UK, 390p.

Pereira, J.M.C. and Duckstein, L. (1993). A multiple criteria decision-making approach to GIS-based land suitability evaluation. International Journal of Geographical Information Systems 7, no. 5: 407-24.

Perez-Martinez, O. (1997). Use of Geographical Information Systems (GIS) for modelling waste distribution in cage aquaculture. M.Sc. Thesis, Institute of Aquaculture, University of Stirling.

Pérez, O. M. Telfer T. C. Ross L. G. and Beveridge M. C. M. (in press). Geographical information systems (GIS) as a tool for modelling waste distribution under marine fish cages. Coastal and Estuarine Marine Science.

Petruaskas, C. and Aagaard, P.M. (1970). Extrapolation of historical storm data for estimating design wave heights. Prepr. 2nd Annual Offshore Tech. Conf., OTC 1190.

Philips, M.D. and Beveridge, M. (1986). Cages and the effect on water condition. Fish Farmer: 17-19.

Pierce, G.J., Wang, J., Bellido, J.M., Waluda, C.M., Robin, J.P., Denis, V., Koutsoubas, D., Valavanis, V. and Boyle, P.R. (1998). Relationships between cephalopod abundance and environmental conditions in the Northeast Atlantic and Mediterranean as revealed by GIS. ICES, Copenhagen (Denmark): pp. 22.

Pitz, G.F. and McKillip, J. (1984). Decision analysis for program evaluations. Thousand Oaks, CA: Sage Publications.

Plant, R.A.J. (1998). GIS-based extrapolation of land use-related nitrous oxide flux in the Atlantic zone of Costa Rica. Water, Air, & Soil Pollution 105, no. 1-5: 131-41.

Pond, S. and Pickard, G.L. (1983). Introductory dynamical oceanography. Pergamon Press, New York.

Prabhakara, C., Dalu, G. and Kunde, V.G. (1974). Estimation of sea temperature from remote sensing in the 11 to 13-um window region. Journal of Geophysical Research 79: 5039-44.

Raiffa, H. (1968). Decision Analysis. Addison-Wesly Publishing Company, United States of America

Rao, C.R., Nagaraja, L. and Chen, J. (1994). Post-Launch Calibration of the Visible and Near-Infrared channels of the Advanced Very High Resolution Radiometer on NOAA-7, -9, and -11 Spacecraft, NOAA Technical Report NESDIS 78, 22 pp.

Reyes, J., Sanson, M. and Afonso-Carillo, J. (1995). Leaf phenology, growth and production of the seagrass Cymodocea nodosa at El Medano (south of Tenerife, Canary Islands). Botanica Marina 38, no. 6: 457-65.

Ricketts, P.J. (1992). Current approaches in geographic information systems for coastal management. Marine Pollution Bulletin 25, no. 1-4: 82-87.

Rietveld, P. (1980). Multiple Objective Decision Methods and Regional Planning. North-Holland Publishing Company, Netherlands, 330p.

Roberts, R.J. and Muir, J.F. (1995). 25 years of world aquaculture: Sustainability, a global problem. Sustainable Fish Farming. A.A. Balkena Publishers, Netherlands, 167-81p.

Rodriguez, A.R., Gonzales, S.M.C., Hernandez, H.L.A., Mendoza, J.C.C., Gonzalez, O.M.J., Padron, P.P.A., Cabrera, J.M.T. and Chavez, G.E.V. (1993). Assessment of soil degradation in the Canary Islands (Spain). Land Degradation and Rehabilitation 4, no. 1: 11-20.

Rogers, K.B., and Bergersen, E.P. (1996). Application of geographic information systems in fisheries: Habitat use by northern pike and largemouth bass. Multidimensional Approaches To Reservoir Fisheries Management, AFS, Bethesda, MD (USA), pp. 315-323, American Fisheries Society Symposium, Vol. 16.

Romero, J., Perez, M., Alcoverro, T., Mateo, M.A. and Sanchez-Lizaso, J.L. (1998). Production ecology of Posidonia oceanica (L.) delile meadows in Nueva Tabarca marine reserve: Growth, biomass and nutrient stock along a bathymetric gradient. Oecol. Aquat. 11: 113-23.

Ross, L.G. (1998). The use of geographical information systems in aquaculture: A review. Congreso Nacional De Limnologia. Morelia, Mexico.

Ross, L.G., Mendoza, Q.M.E.A. and Beveridge, M.C.M. (1993). The application of geographical information systems to site selection for coastal aquaculture: an example base on salmonid cage culture. Aquaculture 112, no. 165-178.

Rubec, P.J., Christensen, J.D., Arnold, W.S., Norris, H., Steele, P. and Monaco, M.E. (1998). GIS and modeling: Coupling habitats to Florida fisheries. Journal of Shellfish Research 17, no. 5: 1451-57.

Saaty, T.L. (1977). A scaling Method for Priorities in Hierarchical Structures. Journal of Mathematical Psychology 15: 234-81.

Saaty, T.L. (1980). The analytic hierarchy process. McGraw-Hill, New York, 249p.

Saaty, T.L. (1988). The Analytic Hierarchy process. Typesetters Ltd., Becceles, Suffolk.

Saaty, T.L. (1994). Fundamentals of Decision Making and Priority Theory with the AHP. RWS Publications, Pittsburgh, PA, U.S.A.

Salam, A.M. and Ross, L.G. (2000). Optimizing site selection for development of shrimp(*Penaeus monodon*) and mud crab (Scylla serrata) culture in Southwestern Bangladesh. Proceedings of GIS'2000, 14th Annual Conference on Geographic Information Systems. Toronto, Canada, 13-16 March'2000.

Salam, M.A. (2000). The potential of geographical information system-based modelling for aquaculture development and management in south western Bangladesh. Ph.D. Thesis, University of Stirling, pp. 318.

Saltelli, A., Chan, K. and Scott, E.M. (2000). Sensitivity Analysis. JohnWiley & Sons Ltd., Great Britain, 475p.

Samuelsen, O.B. (1992). The fate of antibiotics/chemotherapeuthics in marine aquaculture sediments, Problems of Chemotherapy in Aquaculture, pp. 162-73.

Sánchez-Lizaso, J.L., Guillen-Nieto, J.E. and Ramos-Espla, A.A. (1990). The regression of Poseidonia oceanica meadows in El Campello (Spain), Rapp. Comm. Int. Mer. Medit. 32 (7).

Sanz, J.L., Lobato, A., Acosta, J. and Herranz, P. (1997). The S.I.G.M.A.Z.A.L. project. A marine geographical information system. Proceedings of the 18th ICA/ACI International Cartographic Conference Volumen 4, no. Tockolm, Sweden: 2271-75.

Sanz, J. L., Lobato, A. B. and Tello, O. (1999). Problems on the definition and the meaning of some attributes in a GIS for the management of regulated coastal areas. Coast GIS '99. Brest, France. September 1999.

Sasamal, S.K. (1999). Sea surface temperature of the North Indian Ocean during April 1998. Int. J. Geographical Information Science 20, no. 13: 2485-90.

Sasowsky, K.C and Gardner, T.W. (1991). Watershed configuration and geographic information system. Water Resources Bulletin 27, no. 1: 7-18.

Saunders, R.W. (1986). An automated scheme for the removal of cloud contamination from AVHRR radiances over western Europe. International Journal of Remote Sensing 7, no. 7: 867-86.

Saunders, R.W. and Kriebel, K.T. (1988). An improved method for detecting clear sky and cloudy radiances from AVHRR data. International Journal of Remote Sensing 9, no. 1: 123-50.

Schaller, J. (1992). GIS application in environmental planning and assessment. Comput. Environ. and Urban Systems 16: 337-53.

Schippers, P., Verboom, J., Knaapen, J.P. and van Apeldoorn, R.C. (1996). Dispersal and habitat connectivity in complex heterogeneous landscapes: An analysis with a GIS-based random walk model. Ecography 19, no. 2: 97-106.

Schmidt, A.R. and Romack, R.D. (1991). Development and Organization of a Geographic Information System Data Base and its Application to Investigation of Rainfall/Runoff-Model Parameters in Illinois. Books and Open File Report Section, USGS, Box 25425, Denver, CO 80225. USGS Open-File Report 91-209, 52p.

Schultz, G.A. (1993). Application of GIS and remote sensing in hydrology. IAHS Publications 211: 127-40.

Scott, P.C. and Ross, L.G. GIS-based modelling for prediction of coastal aquaculture development potential and production output for Baía de Sepetiba Brazil. Coast GIS '99. Brest, France. September 1999.

Scott, P.C., Cansado, S. and Ross, L.G. (1998). A GIS-assisted mollusc culture potential determination for Sepetiba Bay, Brazil. GIS98. Lisbon. Portugal.

Scottish Executive (1999). Policy Guidance Note: Locational Guidelines for the Authorisation of Marine Fish farms in Scottish Waters. Scottish Executive, Edinburgh. pp.152.

SCS (Soil Conservation Service) (1973). A method for estimating volume and rate of runoff in small watersheds. ASDA, USA.

Sebastini, M., Sambrano, A., Villamizar, A. and Villalba, C. (1989). Cumulative impact and sequential geographical analysis as a toll for land use planning. A case study: Laguna La Reina, Muranda State, Venezuela. Journal of Environmental Management 29: 237-48.

Shenoi, S.C. (1999). On the suitability of global algorithms for the retrieval of SST from the north Indian Ocean using NOAA/AVHRR data. Int. J. Geographical Information Science 20, no. 1: 11-29.

Shepherd, J. and Bromage, N. (1995). Intensive Fish Farming. Blackwell Science, Great Britain, 404p.

Shepherd, S.A., McComb, A.J., Bulthuis, D.A., Neverauskas, V., Steffensen, D.A. and West, R. (1989). Decline of seagrasses. In: Larkun, A.W.D., McComb, A.J. and

Shepherd, S.A. (Eds.), Biology of Seagrasses: A treatise on the biology of seagrasses with special reference to the Australia region. Elsevier, Amsterdam.

Short, F.T., Burdick, D.M. and Kaldy III, J.E. (1995). Mesocosm experiments quantify the effects of eutrophication on eelgrass, Zostera marina, Limnol. Oceanogr. 40, no. 4: 740-749.

Shukla, S., Mostaghimi, S., Shanholtz, V.O. and Collins, M.C. (1998). A GIS-based modeling approach for evaluating groundwater vulnerability to pesticides. Journal of the American Water Resources Association 34, no. 6: 1275-93.

Silvert, W. (1992). Assessing environmental impacts of finfish aquaculture in marine waters. Aquaculture 107: 67-79.

Silvert, W. (1994). Modelling benthic and impacts of organic matter loading. In Modelling Benthic Impacts of Organic Enrichment from Marine Aquaculture, ed. B.T. Hargrave, pp. 1-18. Canadian Technical Report of Fisheries and Aquatic Sciences, Canada.

Simon, H.A. (1960). The new science of management decision. Harper & Row, New York, 175p.

Simpson, J.J. and Humphrey, C. (1990). An automated cloud screening algorithm for daytime advanced very high resolution radiometer imagery. Journal of Geophysical Research. C. Oceans 95, no. 8: 13459-81 .

Slaattelid, O.H. (1990). Model test with flexible, circular floats for fish farming. In: Engineering for Offshore Fish. Thomas Telford, Great Britain pp 93-106.

Smith, R.D., Dennison, W.C. and Alberte, R.S. (1984). Role of seagrasses photosynthesis in root aerobic processes. Plant Physiology 74: 1055-58.

Soil Survey Division Staff (USA Department of Agriculture) (1993). Soil survey manual. USDA, Washington DC, 437p.

Sowles, J.W., Churchill, L. and Silvert, W. (1994). The effect of benthic carbon loading on degradation of bottom conditions under farm sites. In B.T. Hargrave [ed.]. Model Benthic Impacts of Organic Enrichment from Marine Aquaculture. Canadian Technical Report of Fisheries and Aquatic Sciences, p. 31-46

Stewart, R.H. (1985). Methods of satellite oceanography. University of California Press, Berkely.

Stone, D.R. and Johnson, R.J. (1959). A study of words indicating frequency. Journal of Educational Psychology 50: 224-227.

Stramma, L. (1984). Geostrophic transport in the warm Water Sphere of the eastern subtropical North Atlantic. Journal of Marine Research 42: 537-58.

Stramma, L. and Siedler, G. (1988). Seasonal changes in the North Atlantic subtropical gyre. Journal of Geophysical Research 93: 8111-18.

Stuebe, M., Johnston, M. and Douglas, M. (1990). Runoff volume estimation using GIS techniques. Water Resour Bull, Vol. 26, No. 4, Pp. 611-620.

Taranto, T.J., Jacobs, D.R., Skewes, T.D. and Long, B.G. (1997a). Torres Strait reef resources: maps of percentage cover of algae and percentage cover of seagrasses. CSIRO, Cleveland, Qld. (Australia), 63p.

Taranto, T.J., Jacobs, D.R., Skewes, T.D. and Long, B.G. (1997b). Torres Strait reef resources: maps of holothurian abundance (hectare). CSIRO, Cleveland, Qld. (Australia), 44p.

Telfer, T.C. (1995). Modelling of environmental loading: a tool to help fish cage managers. Aquaculture News, 20, 17.

Terrados, J.C.M., Duarte L., Kamp-Nielsen, N.S.R., Agawin, E., Gacia, D., Lacap, M.D., Fortes, J., Borum, M., Lubanski, T., and Greve. L. (1999). Are seagrass growth and survival constrained by the reducing conditions of the sediment?. Aquatic Botany 65: 175-97.

Theriault, S., and Tremblay, C. (1999). The use of GIS with modeling a watershed. Canadian Water Resources, Vol. 24, No. 1, 35-52.

Thom, H.C.S. (1973). Extreme wave height distributions over oceans. Proceedings ASCE 99, no. WW3: 355-74.

Thornthwaite, C.W. and Mather, J.R. (1957). Instructions and tables for computing potential evapotranspiration and the water balance. Drexel Institute of Technology, Publications in Climatology, Centerton, N.J., V. 10, No. 3, 311p.

Thriscutt, A.M., Lobsiger, U. and Levesque, S. (1997). High resolution airborne digital imagery for aquaculture site monitoring. Proceedings of the huntsman marine science centre symposium coldwater aquaculture to the year 2000, 109p.

Tovar, A., Moreno, C., Manuel-Vez, M.P., Garcia-Vargas, M. (2000). Environmental impacts of intensive aquaculture in marine waters. Water Research 34, no. 1: 334-42.

Treweek, J. (1999). Ecological Impact Assessment. Blackwell Science, UK, 351p.

Triantaphyllou, E. and Mann, S.H. (1995). Using the Analytic Hierarchy Process for Decision Making in Engineering Applications: Some Challenges. International Journal of Industrial Engineering: Applications and Practice 2, no. 1: 35-44.

Triantaphyllou, E., Lootsma, F.A., Pardalos, P.M. and Mann, S.H. (1994). On the Evaluation and Application of Different Scales For Quantifying Pairwise Comparisons in Fuzzy Sets. Multi-Criteria Decision Analysis, 3: 1-23.

Troell, M. and Berg, H. (1995). Cage fish farming in the tropical Lake Kariba; impact and biogeochemical changes in sediment. 55.

Turner, R. (1991). In at the deep end. Fish Farmer July/August: 48-49.

Udouj, T.H. and Scott, H,D. (1999). Simulated phosphorus and sediment loadings in two representative subbasins of the Illinois River. Journal of Soil Contamination , Vol. 8, No. 4, pp.

Urbanski, J. A. (1999). The use of fuzzy sets in the evaluation of the environment of coastal waters. Int. J. Geographical Information Science 13, no. 7: 723-30.

US Army Corps of Engineers, (1984). Shore Protection Manual. US Government Printing Office, Washington DC.

USDA-SCS (U.S. Department of Agriculture, Soil Conservation Service) (1986). Urban hydrology for small watersheds. Tech. Release 55.

Van Rompaey, A.J.J., Govers, G. and Baudet, M. (1999). A strategy for controlling error of distributed environmental models by aggregation. Int. J. Geographical Information Science 13, no. 6: 577-90.

Vazquez, J., Perry, K. and Kilpatrick, K. (1998). NOAA/NASA AVHRR Oceans Pathfinder Sea Surface Temperature Data Set User's Reference Manual Version 4.0. Web page,http://podaac.jpl.nasa.gov/pub/sea_surface_temperature/avhrr/pathfinder/doc/usr_gde4_0_toc.html.

Victorov, S.V. (1996). Regional Satellite Oceanography. Taylor & Francis, Great Britain, 306p.

Wadsworth, R. and Treweek, J. (1999) Geographical Information Systems for Ecology. Addison Wesley Longman, Harlow.

Walls, A.V. (1996). The application of GIS as a modelling tool in the environmental management marine aquaculture. M.Sc. Thesis, Institute of Aquaculture, University of Stirling.

Walton, C.C. (1988). Nonlinear multichannel algorithm for estimating sea surface temperature with AVHRR satellite data. Journal of Applied Meteorology 27: 115-24.

Walton, C.C., McClain, E.P. and Sapper, J.F. (1990). Recent changes in satellite based multichannel sea surface temperature algorithms. Marine Technology Society Meeting, MYS' 90, Washington D.C.

Warren-Hansen, I. (1982). Report on EIFAC on fish farm effluents. In Evaluating matter discharged from trout farming, Ed. J.S. Alabaster,. EIFC Technical. Papers, 57-63 p.

Warwick, J.J. and Haness, S.J. (1994). Efficacy of ARC/INFO GIS application to hydrologic modeling. J. Water Resour. Plan. Manage 120, no. 3: 366-81.

Wei, G., Panchang, V.G. and Pearce, B.R. (1990). Some numerical models for predicting wave conditions around aquaculture sites. In: Engineering for Offshore Fish. Thomas Telford, Great Britain, 119-135p.

Weston, D.P. (1990). Quantitative examination of macrobenthic community changes along an organic enrichment gradient. Marine Ecology Progress Series 61: 233-44.

Wheatley, D. (1995). Cumulative viewshed analysis: a GIS-based method for investigating intervisibility, and its archaeological application. In Archaeology and geographical information systems edited by G. Lock and Z. Stancic. Taylor & Francis, London, 171-185p.

Wilkinson, G.G. (1996). A review of current issues in the integration of GIS and remote sensing data. International Journal of Geographical Information Systems 10, no. 1: 85-101.

Williams, J.R. (1975). Sediment routing for agricultural watersheds. Water Resour. Bull. 11, no. 5: 965-74.

Williams, J.R. and Berndt, H.D. (1977). Sediment yield prediction based on watershed hydrology. Trans. ASAE 20, no. 6: 1100-1104.

Willinsky, M.D. and Huguenin, J.E. (1996). Conceptual, engineering and operational frameworks for submersible cage systems. In: Open Ocean Aquaculture. Proceedings Of An International Conference, May 9-10, 1996, Portland, Maine., 1996, 41-92. USA: New Hampshire/Maine Sea Grant Collage Program.

Wilson, C.A., Roberts, H.H. and Supan, J. (2000). MHACS: Marine habitat acoustic characterization systems. A program for the acquisition and interpretation of digital acoustics to characterize marine habitat. Journal of Shellfish Research 19, no. 1: 627-28.

Wilson, C.A., Roberts, H.H., Supan, J. and Winans, W. (1999). The acquisition and interpretation of digital acoustics for characterizing Louisiana's shallow water oyster habitat. Journal of Shellfish Research 18, no. 2: 730-731.

Wischmaier, W.H., Johnson, C.B. and Cross, B.V. (1971). A soil erodibility nomograph for farmland and construction sites. Journal of Soil and Water Conservation 26: 189-93.

Wischmeier, W.H. and Smith, D.D. (1978). Predicting rainfall erosion losses, a guide to conservation planning. U.S. Dept. Agric., Agric. Handbook No. 537, USA.

Wolansky, E., Imberger, J. and Heron, M.L. (1984). Island wakes in shallow coastal waters. J. Geophys. Res. 89: 10533-69.

Woodcock, C.E. and Gopal, S. (2000). Fuzzy set theory and thematic maps: accuracy assessment and area estimation. Int. J. Geographical Information Science 14, no. 2: 153-72.

Wright, D. and Bartlett, D. (2000). Marineand Coastal Geographical Information Systems. Taylor & Francis, London, 319p.

Wright, D.J. (1999). Spatial reasoning for marine geology and geophysics. In marine and Coastal Geographical Information Systems. Ed. Wright, D. and Bartlett, D., Taylor & Francis, London, 319p.

Wright, D.J. and Goodchild, M.F. (1997). Data from the deep implications for the GIS community. Int. J. Geographical Information Science 11, no. 6: 523-28.

Yamaguchi, M. Tsuchiya Y. and Shibano T. 1978. Analysis of extreme wave statistics with hindcasted data for 80 years. Proc. 25th Coastal Engg. Conf. in Japan: 70-74.

Zar, J.H. (1999). Biostatistical Analysis. Prentice-Hall Inc., USA, 662.

Zhang, H., Haan, C.T. and Nofziger, D.L. (1990). Hydrologic modelling with GIS: an overview. Applied Engineering in Agriculture ASAE, 6: 453-58.

Zhou, Q. (1998). Exercise 8. Environmental Modelling. http://geog.hkbu.edu.hk/QZone/Teaching/GEOG3142/exer08.html#l andsystems.

Zimmer, A.C. (1983). Verbal vs. numerical processing of subjective probabilities. In Scholz, R. W. (Ed.), Decision Making Under Uncertainty. North-Holland, Amsterdam 328-330.

Appendix 1

Runoff Curve Numbers

Table A1.1: Runoff curve numbers for urban areas[1].

COVER DESCRIPTION		CURVE NUMBERS FOR HYDROLOGIC SOIL GROUP			
Cover type and hydrologic condition	**Average percent impervious area[2]**	**A**	**B**	**C**	**D**
Fully developed urban areas (vegetation established)					
Open space (lawns, parks, golf courses, cemeteries, etc.)[3]:					
Poor condition (grass cover <50%)		68	79	86	89
Fair condition (grass cover 50%to 75%)		49	69	79	84
Good condition (grass cover >75%)		39	61	74	80
Impervious areas:					
Paved parking lots, roofs, driveways, etc. (excluding right-of-way)		98	98	98	98
Streets and roads:					
Paved; curbs and storm sewers (excluding right-of-way)		98	98	98	98
Paved; open ditches (including right-of-way)		83	89	92	93
Gravel (including right-of way)		76	85	89	91
Dirt (including right-of-way)		72	82	87	89
Western desert urban areas:					
Natural desert landscaping (pervious areas only)[4]		63	77	85	88
Artificial desert landscaping (impervious weed barrier, desert shrub with 1-to 2-inch sand or gravel mulch and basin borders)		96	96	96	96
Urban districts:					
Commercial and business	85	89	92	94	95
Industrial	72	81	88	91	93
Residential districts by average lot size:					
1/8 acre or less (town houses)	65	77	85	90	92
1/4 acre	38	61	75	83	87
1/3 acre	30	57	72	81	86
1/2 acre	25	54	70	80	85
1 acre	20	51	68	79	84
2 acres	12	46	65	77	82
Developing urban areas					
Newly graded areas (pervious areas only, no vegetation)[5]	77	86	91	94	
Idle lands (CN 's are determined using cover types similar to those in table 2-2c).					

1 Average runoff condition, and Ia =0.2S.

2 The average percent impervious area shown was used to develop the composite CN 's. Other assumptions are as follows: impervious areas are directly connected to the drainage system, impervious areas have a CN of 98, and pervious areas are considered equivalent to open space in good hydrologic condition. CN 's for other combinations of conditions may be computed using figure 2-3 or 2-4.

3 CN 's shown are equivalent to those of pasture. Composite CN 's may be computed for other combinations of open space cover type.

4 Composite CN 's for natural desert landscaping should be computed using figures 2-3 or 2-4 based on the impervious area percentage (CN =98) and the pervious area CN. The pervious area CN 's are assumed equivalent to desert shrub in poor hydrologic condition.

5 Composite CN 's to use for the design of temporary measures during grading and construction should be computed using figure 2-3 or 2-4 based on the degree of development (impervious area percentage) and the CN 's for the newly graded pervious areas.

Table A1.2: Runoff curve numbers for cultivated agricultural lands[1].

Cover description			Curve numbers for hydrologic soil group			
Cover type	Treatment[2]	Hydrologic condition[3]	A	B	C	D
Fallow	Bare soil	—	77	86	91	94
	Crop residue cover (CR)	Poor	76	85	90	93
		Good	74	83	88	90
Row crops	Straight row (SR)	Poor	72	81	88	91
		Good	67	78	85	89
	SR +CR	Poor	71	80	87	90
		Good	64	75	82	85
	Contoured (C)	Poor	70	79	84	88
		Good	35	75	82	86
	C +CR	Poor	69	78	83	87
		Good	64	74	81	85
	Contoured &terraced (C&T)	Poor	66	74	80	82
		Good	62	71	78	81
	C&T+CR	Poor	65	73	79	81
		Good	61	70	77	80
Small grain	SR	Poor	65	76	84	88
		Good	63	75	83	87
	SR +CR	Poor	64	75	83	86
		Good	60	72	80	84
	C	Poor	63	74	82	85
		Good	61	73	81	84
	C +CR	Poor	62	73	81	84
		Good	60	72	80	83
	C&T	Poor	61	72	79	82
		Good	59	70	78	81
	C&T+CR	Poor	60	71	78	81
		Good	58	69	77	80
Close-seeded or broadcast legumes or rotation meadow	SR	Poor	66	77	85	89
		Good	58	72	81	85
	C	Poor	64	75	83	85
		Good	55	69	78	83
	C&T	Poor	63	73	80	83
		Good	51	67	76	80

1 Average runoff condition, and Ia =0.2s

2 Crop residue cover applies only if residue is on at least 5% of the surface throughout the year.

3 Hydraulic condition is based on combination factors that affect infiltration and runoff, including (a) density and canopy of vegetative areas, (b) amount of year-round cover, (c) amount of grass or close-seeded legumes, (d) percent of residue cover on the land surface (good =20%), and (e) degree of surface roughness.

Poor: Factors impair infiltration and tend to increase runoff.
Good: Factors encourage average and better than average infiltration and tend to decrease runoff.

Table A1.3: Runoff curve numbers for other agricultural lands[1].

COVER DESCRIPTION		CURVE NUMBERS FOR HYDROLOGIC SOIL GROUP			
Cover type	**Hydrologic condition**	**A**	**B**	**C**	**D**
Pasture, grassland, or range —continuous forage for grazing.[2]	Poor	68	79	86	89
	Fair	49	69	79	84
	Good	39	61	74	80
Meadow —continuous grass, protected from grazing and generally mowed for hay.	—	30	58	71	78
Brush —brush-weed-grass mixture with brush the major element.[3]	Poor	48	67	77	83
	Fair	35	56	70	77
	Good	30[4]	48	65	73
Woods —grass combination (orchard or tree farm).[5]	Poor	57	73	82	86
	Fair	43	65	76	82
	Good	32	58	72	79
Woods.[6]	Poor	45	66	77	83
	Fair	36	60	73	79
	Good	30[4]	55	70	77
Farmsteads —buildings, lanes, driveways,— and surrounding lots.	—	59	74	82	86

1 Average runoff condition, and Ia ,=0.2S.
2 *Poor*: <50% ground cover or heavily grazed with no mulch.
Fair: 50 to 75% ground cover and not heavily grazed.
Good: >75% ground cover and lightly or only occasionally grazed.
3 *Poor* <50% ground cover.
Fair: 50 to 75% ground cover.
Good: >75% ground cover.
4 Actual curve number is less than 30; use CN =30 for runoff computations.
5 CN 's shown were computed for areas with 50% woods and 50% grass (pasture) cover. Other combinations of conditions may be computed from the CN 's for woods and pasture.
6 *Poor*: Forest litter, small trees, and brush are destroyed by heavy grazing or regular burning.
Fair: Woods are grazed but not burned, and some forest litter covers the soil.
Good: Woods are protected from grazing, and litter and brush adequately cover the soil.

Table A1.4: Runoff curve numbers for arid and semiarid rangelands[1].

COVER DESCRIPTION		CURVE NUMBERS FOR HYDROLOGIC SOIL GROUP			
Cover type	**Hydrologic Condition**[2]	**A**[3]	**B**	**C**	**D**
Herbaceous —mixture of grass, weeds, and low-growing brush, with brush the minor element.	Poor		80	87	93
	Fair		71	81	89
	Good		62	74	85
Oak-aspen —mountain brush mixture of oak brush, aspen, mountain mahogany, bitter brush, maple, and other brush.	Poor		66	74	79
	Fair		48	57	63
	Good		30	41	48
Pinyon-juniper —pinyon, juniper, or both; grass understory.	Poor		75	85	89
	Fair		58	73	80
	Good		41	61	71
Sagebrush with grass understory.	Poor		67	80	85
	Fair		51	63	70
	Good		35	47	55
Desert shrub —major plants include saltbush, greasewood, creosotebush, blackbrush, bursage, palo verde, mesquite, and cactus.	Poor	63	77	85	88
	Fair	55	72	81	86
	Good	49	68	79	84

1 Average runoff condition, and I_a ,=0.2S. For range in humid regions, use Table A1.3.
2 Poor:<30% ground cover (litter, grass, and brush overstory).
Fair: 30 to 70% ground cover.
Good: >70% ground cover.
3 Curve numbers for group A have been developed only for desert shrub.

Appendix 2
Weights Questionnaire

QUESTIONNAIRE OF WEIGHTING PROCEDURE FOR MARINE CAGE SITE SELECTION IN TENERIFE

The main objective of this project is to select the best sites for marine fish-cage farming of actual commercialised species (*Sparus aurata* and *Dicentrarchus labrax*) and potential local species (*Sarpa salpa*, *Pagrus pagrus* and *Diplodus sargus cadenati*) in Tenerife.

Site selection is a key factor in any aquaculture operation if success is to be achieved and also, if sustainability is desirable. The correct choice of site in any aquatic farming operation is vitally important since it can greatly influence economic viability by determining capital outlay, and by affecting running coasts, rates of productions and mortality factors. Moreover, it can solve conflicts between different coastal activities, such as fishing, tourism, aquaculture, etc., making a rational and sustainable use of the coastal space.

The first prerequisite for sustainable aquaculture is an adequate aquaculture resource allocation system (zonation). Such a system should be implemented within the context of an integrated planning approach (Integrated Coastal Zone Management) rather than simply creating a series of regulations to avoid environmental deterioration.

Name and Field of expertise

1. IDENTIFIED THOSE VARIABLES AND CONSTRAINTS YOU CONSIDER MOST IMPORTANT FOR MARINE CAGE CULTURE IN TENERIFE.

Variables or factors: a factor enhances or detracts from the suitability of a specific alternative under consideration. It is therefore measured as a continue scale. (temperature, salinity, oxygen, etc)

Constraints: a constraint serves to limit the alternatives under consideration. In other words, cage culture CAN NOT be sited regardless of their potential suitability. (e.g. military areas)

1.1 List the factors or variables you consider most important for siting marine cage culture in Tenerife?

1	
2	
3	
4	
5	
6	
7	
8	
9	

1.2 List the constraints you consider most important for siting marine cage culture in Tenerife?

1	
2	
3	
4	
5	

2. PROVIDE A RANK SCORE TO THE FOLLOWING FACTORS ACCORDING TO THE MOST IMPORTANT OR LEAST IMPORTANT.

1 DISTANCE FROM BEACHES	
1 LENGTH	
2 WIDTH	
3 COMPOSITION (SAND, GRAVEL, ETC)	
4 RATE OF OCCUPATION	
5 RATE OF URBANISATION	
OTHERS:	
OTHERS:	

2 FISHERIES	
1 FINGERLING ACCUMULATION	
2 PELAGIC FISH	
3 RASAS (BAJAS)	
OTHERS:	
OTHERS:	

3 INFRASTRUCTURE	
1 HARBOURS (FISHING REFUGES AND PIERS)	
OTHERS:	
OTHERS:	

4 MARINE ENVIRONMENT	
1 BATHYMETRY	
2 CURRENTS	
3 WAVES SHORT TERM	
4 WAVES LONG TERM	
OTHERS:	
OTHERS:	

5 NAUTICAL SPORTS	
1 SCUBA-DIVING SITES	
2 SCUBA-DIVING IN SINGULARITY MARINE HABITATS SITES	
3 SHIPWRECKED BOATS SITES	
4 UNDERWATER FISHING SITES	
5 WINDSURF SITES	
6 LITTORAL SAILING SITES	
OTHERS:	
OTHERS:	

6 WATER QUALITY	
1 SEWAGE DISCHARGES	
2 TEMPERATURE	
3 SUSPENDED SOLIDS	
OTHERS:	
OTHERS:	

3. COMPLETE THE FOLLOWING PAIR-WISE MATRIX ACCORDINGLY TO THE RELATIVE IMPORTANCE OF EACH FACTOR WITH RESPECT OF THE OTHERS.

1/9	1/8	1/7	1/6	1/5	1/4	1/3	1/2	1	2	3	4	5	6	7	8	9
Extremely very strong strongly moderately																
⇐ Less Important								More Important ⇒								

Pairwise comparisons matrix.

	Length	Width	Composition	Occupation	Urbanisation
Length	1				
Width		1			
Composition			1		
Occupation				1	
Urbanisation					1

Pairwise comparisons matrix for fishing submodel.

	Fingerling accumulation	Pelagic accumulation	Rocky platforms
Fingerling accumulation	1		
Pelagic accumulation		1	
Rocky platforms			1

Pairwise comparisons matrix for infrastructure submodel.

	Ports	Freezing Industry
Ports	1	
Freezing Industry		1

Pairwise comparisons matrix for the marine environment submodel and Corelsa® cage system.

	Bathymetry	Seabed Slope	Currents	Waves short term	Waves long term
Bathymetry	1				
Bathymetry Slope		1			
Currents			1		
Waves short term				1	
Waves long term					1

Pairwise comparisons matrix for nautical sports submodel.

	Scuba-diving	Scuba-diving in particular marine habitats	Shipwrecked boats	Spearfishing	Windsurfing	Near-shore sailing
Scuba-diving	1					
Scuba-diving in particular marine habitats		1				
Shipwrecked boats			1			
Spearfishing				1		
Windsurfing					1	
Near-shore sailing						1

Pairwise comparisons matrix fro water quality submodel.

	Sewage	Temperature	Suspended solids
Sewage	1		
Temperature		1	
Suspended solids			1

Pairwise comparisons matrix for Corelsa® cages.

	Beach	Fisheries	Infrastructure	Marine Env.	Nautical Sports	Water Quality	Viewshed
Beach	1						
Fisheries		1					
Infrastructure			1				
Marine Env.				1			
Nautical Sports					1		
Water Quality						1	
Viewshed							1

Appendix 3

Waste Dispersion Model

Perez O M, Telfer T C, Beveridge M C M and Ross L G. (in press). Geographical Information Systems (GIS) as a simple tool for modelling waste distribution under marine fish cages. Estuarine, Coastal and Shelf Science.

ABSTRACT

Deposition of particulate organic waste from marine fish farm cages on to seabed sediments can cause major changes to the benthic ecosystem. Validated spatial models are considered as the most cost-effective tools for predicting environmental impacts. An improved version of an existing predictive particulate waste distribution model for farmed Atlantic salmon (*Salmo salar* L.) is presented, which uses Geographic Information Systems (GIS) combined with a spreadsheet. The model presented uses existing distribution algorithms but also incorporates functions to calculate feed loading for all the cages within a pontoon independently, spreads the input load over the whole cage area and simulates post-depositional distribution of the carbon. The model uses approximate estimates of feed and faecal waste derived from dietary considerations (mass balance model) and separate, unique settling velocities for waste feed and faecal particles. The model incorporates values of current speed and direction recorded over spring and neap tides. Output from the model is in the form of a contour plot of organic carbon (g C m-2), showing distribution of the particulate organic carbon material as deposited on the seabed. During this study using hydrographic data collected from near a fish farm, the model predicted a smooth gradient of sediment carbon concentrations which decreased with distance from the cages. Model performance was validated using measured levels of sediment carbon, and showed a significant correlation between predicted and actual sediment loading ($R = 0.7$; $P < 0.01$). The differences between predicted and measured quantities of carbon found at some sampling stations are likely to be due to processes not included in the model, such as small differences in bathymetry, differences in bottom type which may have increased or decreased the carbon distribution through saltation, or natural variation in the sediment composition.

INTRODUCTION

The rapid expansion and development of the aquaculture industry has increased environmental concerns and questions about possible ecological impacts. Environmental managers, and especially regulators, have pointed out the necessity of minimising environmental impacts if productivity in the new industry is to be sustainable (e.g. Scottish Executive, 1999). However, a complete reduction to zero of wastes discharged from marine fish cages is not possible for present culture systems, from either a technological or an economical point of view. There are many forms of wastes produced as a consequence of the transformation of any natural resource into a marketable product, and this is as true for marine fish aquaculture as other forms of resource utilisation. However, of all the possible wastes released by marine fish farming to the environment, particulate organic waste in the form of uneaten feed and faeces are usually the most significant fraction (Beveridge, 1996). This material, which generally settles on the seabed near to the cages, provides a net input of organic carbon and nitrogen to the sediments, thus the accumulation of waste can cause major changes in the benthic community and may exceed the environment's capacity to bioprocess this material (Findlay and Watling, 1994; GESAMP, 1996; Gowen and Bradbury, 1987; Gowen et al., 1988; Hargrave, 1994). Moreover, environmental deterioration due to high organic matter concentrations in the sediments may affect the health of farmed fishes and hence profitability (Beveridge, 1996; GESAMP, 1991b). Modelling of input and distribution of wastes and discharges is a cost-effective tool that can assist in the prediction of future impacts and aid decision-makers.

It is not possible to describe, explain or predict ecosystem behaviour without knowing how ecosystem components are distributed in time, space or with respect to each other ("what is where?") and understanding the relationships and processes that explain their distribution and behaviour ("why is it there?"). As well as requiring knowledge of spatial distribution and relationships, the ability to make reliable predictions ("what happens if?") often demands knowledge about temporal trends. GIS are powerful tools that can be used to organise and present spatial data in a way that allows effective environmental management planning. Spatial modelling using GIS is now under development with encouraging results (Corwin and Wagenet, 1996; Sunday-Tim, 1996). However, further investigation is required before this can be fully integrated into environmental planning, particularly for coastal zone management. The success of GIS for modelling purposes stems from their capacity for fast image generation and manipulation, the flexibility to run alternative scenarios, statistical analysis of the image and generation of sophisticated output which helps visual interpretation of results. Distribution models for organic waste from aquaculture can be used to predict possible impacts on the environment, helping environmental regulators to make informed decisions when licensing new marine fish farm developments and granting consents to discharge waste. Some models have been developed to forecast loading and distribution of particulate waste carbon from fish farms (Fox, 1990; Gowen et al., 1989; Hevia et al., 1996; Silvert, 1992; Silvert, 1994; Telfer, 1995), but only DEPOMOD has undergone substantial validation (C. Cromey, pers. comm).

This paper describes the development of GIS spatial modelling techniques with a pre-existing particulate distribution model for farmed Atlantic salmon (Salmo salar L.) (Telfer, 1995; V. Walls, pers. comm.), which is based on distribution equations developed by Gowen et al. (1989). The GIS based model was validated using field data and fish production information from a salmon farm in Scotland.

MODEL DEVELOPMENT

There are three main stages within this model; quantification of the waste material (uneaten feed and faces) using mass balance techniques, calculation of the distribution of the waste components using Gowen's formula (Gowen et al., 1989), and calculation and generation of the final contour distribution diagrams. The first two submodels are run in a spreadsheet and the third is carried out using GIS software.

Mass Balance

The quantities of waste released to the environment, particulate organic carbon in form of uneaten feed and faecal material, are calculated using a mass balance model (Fig.1). The expected fish production during a set period of time is multiplied by the expected food conversion ratio (FCR) for that period. In the present model, the percentage of water in the feed is assumed to be 8% (Findlay, 1994) while that of carbon in the feed is assumed to be 46% (Penczak et al., 1982). From the feed given to the fish, 90% is consumed and the remaining 10% is lost as uneaten feed (Hargrave, 1994). It is assumed here that 50% of the consumed carbon is respired (Gowen et al., 1988) and that 14% is incorporated into body tissues (Chen, 2000), although it is important to bear in mind that mass balance quantities for organic carbon flux for cage salmonid production vary from author to author (e.g. Gowen et al., 1989; Hevia et al., 1996; Silvert, 1994; Telfer, 1995). Carbon in faecal material is calculated as the difference between carbon consumed and carbon used for respiration and growth.

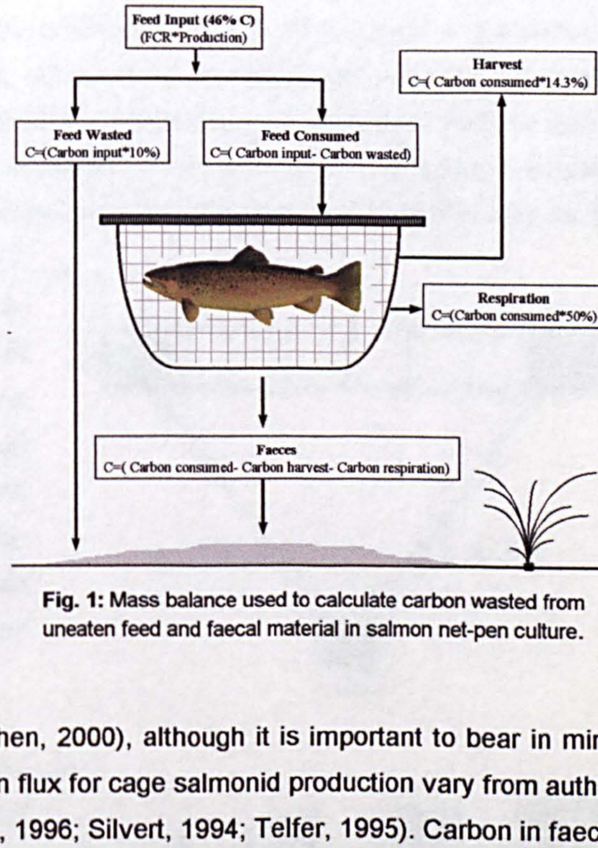

Fig. 1: Mass balance used to calculate carbon wasted from uneaten feed and faecal material in salmon net-pen culture.

Distribution Equation

The horizontal distribution of a particle (X and Y components for each cage of the farm) is calculated using the equations of Gowen et al., (1989) (see Equations 1 and 2). The depth under the cage (d), the mean current speed (V), current direction (θ), settling velocity (u) and position of each cage (x, y) are site specific measured quantities. For modelling purposes, the farm is located in the middle of a 500 by 500 cell array, each cell representing 1 m2.

$$X = \frac{d * V\sin\theta}{u} + x \qquad (1)$$

$$Y = \frac{d * V\cos\theta}{u} + y \qquad (2)$$

Because wastes fall more or less vertically through the cage (Inoue, 1972), the source of distribution was assumed to be from the depth corresponding to the bottom of cage. The same equation is used to calculate the distribution of both uneaten feed and faeces, but different settling velocities are assigned to each; 0.128 ms-1 and 0.04 ms-1 respectively (Warrer-Hansen, 1982; Chen et al., 1999).

Geographical Information Systems (Idrisi32)

The carbon deposition co-ordinates calculated with Gowen's formula (Gowen et al., 1989) and their associated carbon values are exported to Idrisi32 GIS software. Interpolation between values is then undertaken by the GIS program to generate a complete surface. This technique is a particular strength of using GIS for modelling purposes, in that small or sparse data sets can be used to produce a complete map. However, the nature of the interpolation process means that the carbon quantities are over-estimated which requires correction later in the model. The reason for sparse number of data points used for modelling, and the need to interpolate to smooth the data, is that the current readings, speed (V) and direction (θ), are taken at regular intervals over a defined time period (e.g. 1 hour). During that period (t0) all the carbon produced is assumed to settle in one location (X0,Y0) and during the subsequent hour (t1) in another location (X1,Y1). In reality, the process of moving from one location to another is done gradually and the carbon is dispersed over all locations, not only at the initial and end locations, as illustrated in Fig. 2a.

Most models assume a single point as the source of carbon output from a cage (feed and faeces), usually the cage centre. To eliminate this assumption, predicted carbon values allocated on the seabed are spread over an area equal to the cage area by applying a filter within Idrisi (Fig. 2b).

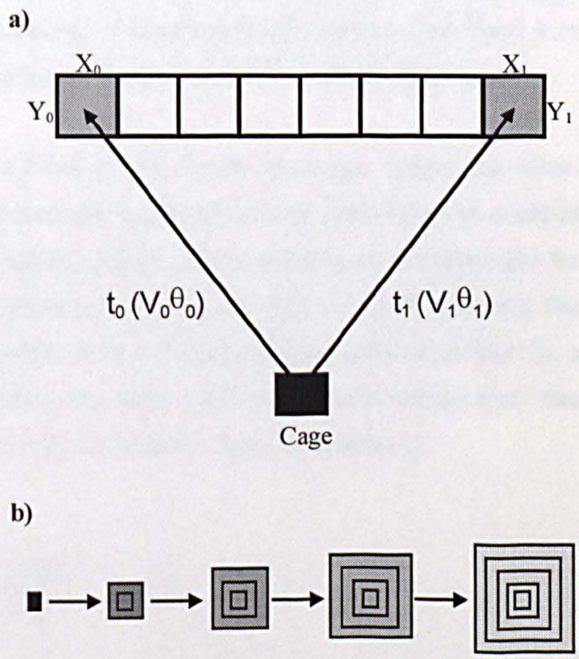

Fig. 2: The process of carbon allocation by spreadsheet (a) and the consecutive filtering technique to spread carbon into an area similar to the cage area (b).

Variations in initial distribution of waste and post-deposition changes in carbon are considered by using a second filtering technique within IDRISI, which redistributes the amount of carbon from each cell into the eight surrounding cells by a predetermined percentage, which differs between the relatively dense feed and lighter faeces. Each cell represents 1m2, hence the final area affected from each of the initial cells is 9 m2 (Fig. 3a, b, c).

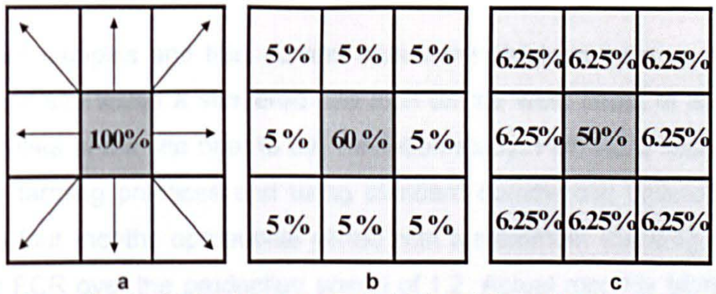

Fig. 3: Sequence of steps involved in "carbon spreading". (a) the original cell as predicted from Gowen's equations, (b) spread of carbon from uneaten feed to surrounding cells, (c) spread of faecal carbon to the surrounding cells.

The filter structure is based upon theoretical work (Chen, 2000). Pellets and faecal matter travel along the sediment by saltation (rolling, sliding or hopping) when current speeds attain a critical value, defined here as the velocity that causes 50% of the pellets to move. Distance travelled and number of re-suspended particles are site specific. Although this final GIS filter has minimal impact on modelled carbon distribution, as shown by sensitivity analysis with and without the filter, it is included to give a more realistic picture of the processes involved in the final carbon distribution.

Finally, it is necessary to correct the carbon quantities in the resultant image, which are over-estimated due to the interpolation process. Interpolation generates additional data between a set of known values. However, it does not reduce the original carbon concentrations to compensate for this, which means that the model assumes that there is considerably more carbon entering the sediment than there really is. The correction is achieved by multiplying the resultant output by a correction factor (CF), which is calculated by dividing the total predicted waste carbon from the mass balance (feed and faeces) by the total carbon in the resultant image (Equation 3).

$$CF = \frac{\text{Total predicted waste carbon (kg)}}{\text{Waste carbon in the image (kg)}} \qquad (3)$$

MODEL VALIDATION

Introduction

A mathematical model is an approximation of the real world and thus its predictions are inherently uncertain. The uncertainty results from lack of knowledge of natural processes, lack of quantity and quality of data, and also from the assumptions within the model. All are potential sources of error, which decrease the accuracy of prediction. Models, therefore, require validation in order to establish agreement between predictions and observations. Model validation is accepted as being achieved when the model output compares favourably with "real" environmental data (e.g. measured carbon, biological data) from an independent location (GESAMP, 1991a).

Sample site

A set of sediment samples and tidal current data were obtained from an Atlantic salmon (Salmo salar L.) sea cage site within a sheltered sea loch on the west coast of Scotland. There were no fish farming activities at the site prior to the validation study. Fish were reared according to current Scottish salmon farming practices and using standard commercial pelleted feeds. The validation was based on a four months operational period with a maximum standing biomass of 172.5 t fish and an average FCR over the production period of 1.2. Actual monthly biomass values were used in the model validation.

Field measurements

Sediment samples were taken twice approximately 4 months after production began by the farm operator at the stations shown in Fig. 4. Samples included those from two reference stations at a distance >500 m from the farm but in the same depth and a similar sediment type. Carbon content of sediment grab samples were determined by an ignition technique (Holme and McIntyre, 1971). Current velocity and direction were measured adjacent to the cage in mid-water, as surface currents are attenuated by the cage structure and the bottom currents are of greater importance in re-suspension and the final allocation of the wastes than in the initial horizontal distribution. Current velocity and direction were measured using Valeport BFM308 current meters over a 12-hour neap and 12-hour spring tide. Recordings were made every 10 minutes over a 1-min averaging period.

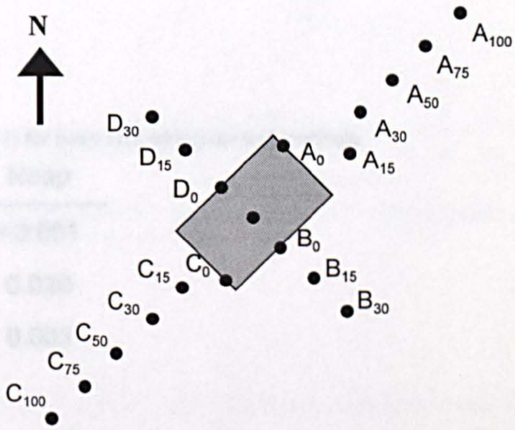

Fig. 4: Position of the sediment sampling stations in relation to the fish cages (redrawn SEPA, unpublished data). Transects are labelled by letter and distance (m) from the cage block edge.

Statistical comparison method

To assess how predicted carbon compared with actual values measured in the field, a Pearson correlation test (2-tailed) was performed between output from the model and measured levels of carbon for all sampling stations along the four transects.

RESULTS

Water current data, speed and direction at neap and spring tides recorded at the farm location are shown in Fig. 5a and 5b. Both, neap and spring tide currents flowed predominantly in north-east and south-west directions, with the neap tide currents being the faster. Table 1 shows the minimum, maximum and mean current speeds for neap and spring current readings.

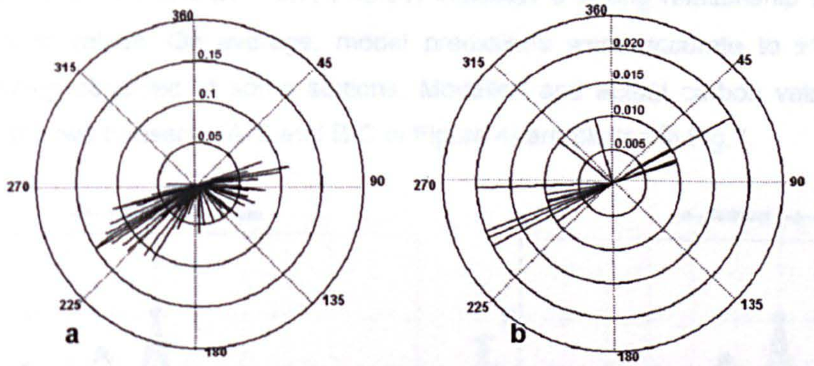

Fig. 5: Polar diagrams of current speed (m/s) and direction (degrees true north) during the spring (a) and neap (b) tide periods.

Table 1: Minimum, maximum and mean current speeds (m s-1) for neap and spring current readings.

	Spring	Neap
Min.	<0.001	<0.001
Max.	0.160	0.020
Mean	0.076	0.003

The final output from the model is a contour map showing the distribution of particulate organic carbon deposited on the seabed. Figure 6 shows the carbon distribution predicted by the model to which the measured background carbon value has been added (1.353 kg C m-2). The farm comprised 18 cages located in two rows of 9. The depth under the cages was 15 m. From the mass balance calculations 35.4 t of carbon were wasted, 10.3 and 25.0 t due to uneaten feed and faeces respectively. The carbon was distributed mainly in NE and SW directions. The highest concentrations were located under the cage, reaching values of 12 kg C m-2. The concentration of carbon decreased as the distance from the cage increased.

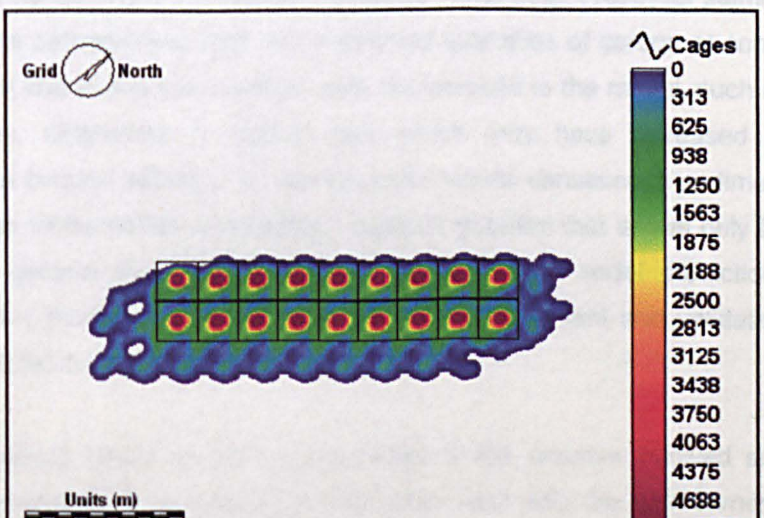

Fig. 6: Contour model for fish farm site showing distribution of organic waste carbon input (g C/m2) to the sediment over a 4-month simulation.

The Pearson correlation test (R = 0.7; P<0.01) indicates a strong relationship between modelled and real carbon values. On average, model predictions were accurate to ±18%, 0% to 40% differences being observed at some stations. Modelled and actual carbon values from the field survey along the two transects (A-C and B-C in Figure 4) are plotted in Fig.7.

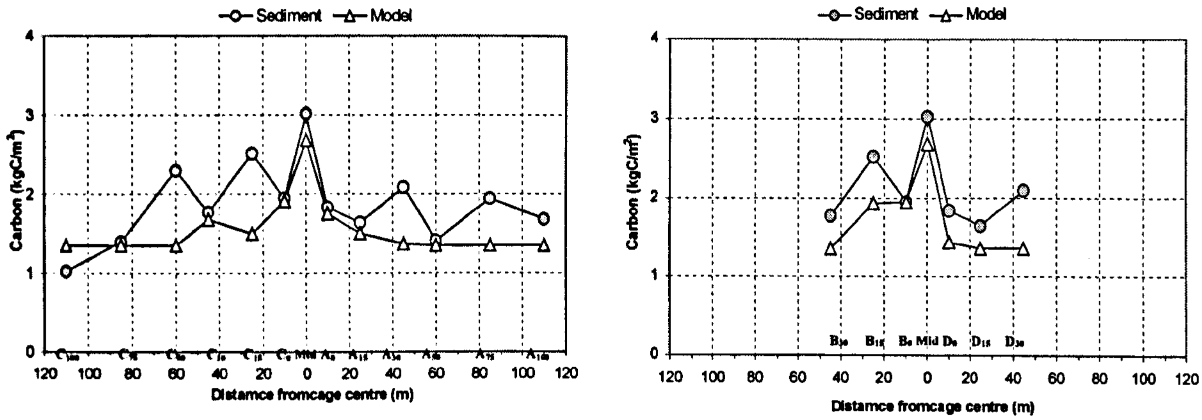

Fig. 7: Comparison between predicted carbon quantities corrected for background value and actual field measurements along the longest transect A to C (a) and transect B to D (b).

DISCUSSION

The results indicate that the modelled outputs of distribution concur with sediment measurements (Fig. 7). The model predicted a smooth gradient of sediment carbon concentrations which decrease with distance from the cages, as did the benthic enrichment model of Hevia et al. (1996) for salmon cages in Norway. The differences between predicted and measured quantities of carbon at some sampling stations may have been due to processes which were not included in the model, such as small differences in bathymetry, differences in bottom type which may have increased or decreased the carbon distribution through saltation, or unpredictable natural variations in sediment composition. Predictions from the model reflect a smoother, idealised gradient that allows only for input from fish wastes and a general background carbon level. Although, model predictions generally agree with field data the model would benefit from further development and validation under different hydrodynamic and fish farm production scenarios.

Models are based upon assumptions based on both a knowledge of the process involved and personal judgement of their importance, their relation to each other and with the environment. Because assumptions carry an inherent risk of inaccuracy, it is desirable both to reduce their use to a minimum and to identify their impact on overall predictions in order to understand and interpret model outputs. Possible sources of inaccuracy in the present model are the lack of consideration of environmental capacity and the assumption that all carbon wastes from the cages settle on the seabed, where none is degraded or consumed by invertebrates and wild fish. Although it is likely that this will vary with location, the present GIS model considers post-deposition movement of carbon, and has eliminated some assumptions from previously used modelling techniques. Furthermore, few data are needed to run the model, so reducing costs of field surveys.

Although the model has only been developed for particulate carbon, the distribution of any other solid material from a fish farm, such as N, P or in-feed chemotherapeutants, can also be modelled, providing accurate data on inputs that are available.

Potential applications for the model are within Environmental Impact Assessment (EIA), design of monitoring programmes, site selection, farm management and rapid generation of "what if?" scenarios. An environmental management plan should include an EIA and this often requires the use of predictive models to quantify significant potential impacts and design a monitoring programme (GESAMP, 1996). Numerical models, such as described here, have the potential to generate quantitative predictions and are therefore a useful tool in quantifying impacts of cage aquaculture wastes. Moreover, Jørgensen, (1991) suggested that the use of validated models to predict environmental impacts was the most cost-effective approach. Models can also be used to allocate development areas (zonation) or for comparison of outputs at different sites by modelling the waste deposition pattern for any given production level. Similarly, the maximum desirable production at a site can be established. However, any modelling-based predictions must be tested by monitoring (GESAMP, 1991a; Silvert, 1992; Sowles et al., 1994).

Environmental models remain insufficiently developed to be used as the sole tool to predict impacts in the environment. They are complementary to field surveys and risk assessment. It is important to be aware of the influence of site characteristics on the interpretation of model outputs. Natural processes are site specific and carbon inputs that may cause problems at one site may not pose a problem at another (Findlay and Watling, 1994).

ACKNOWLEDGEMENTS

We thank the Scottish Environment Protection Agency for the use of their field data in the model validation. This work was carry out as part of a training project financed by the EC under the FAIR program (GT 973516). TCT and MCMB acknowledge the assistance of the CRAFT FAIR project CT-98-9201. The authors would like to acknowledge V. Walls for her contribution to this research

REFERENCES

Beveridge, M.C.M. 1996 *Cage Aquaculture (2^{nd} edition)*. Fishing News Books, Oxford, 346 pp.

Chen, Y.S., Beveridge, M.C.M. and Telfer, T.C. 1999. Settling rate characteristics and nutrient content of the faeces of Atlantic salmon (*Salmo salar* L.) and the implications for modelling of solid wastes dispersion. *Aquaculture Research*, **30**, 395-398

Chen, Y.S. 2000 Waste outputs and dispersion around marine fish cages and the implications for modelling. Ph. D. Thesis. University of Stirling, 185 pp.

Corwing, D.L., and Waganet 1996 Applications of GIS to the modelling of nonpoint source pollutants in the Vadose Zone: A Conference Overview. Journal of Environmental Quality, 25, 403-409.

Findlay, R.H. and Watling, L. 1994 Toward a process level model to predict the effect of salmon net-pen aquaculture on benthos. In *Modelling Benthic Impacts of Organic Enrichment from Marine Aquaculture*, ed. B.T. Hargrave, pp. 47-78. Canadian Technical Report of Fisheries and Aquatic Sciences, Canada.

Fox, W.P. 1990 Modelling of particulate deposition under salmon net-pens. *In Final programmatic environmental impact statement*. Fish culture in floating net-pens (technical appendices). Washington State Department of Fisheries, USA.

GESAMP (IMO/FAO/UNESCO/WMO/WHO/IAEA/UN/UNEP Joint Group of Expert on the Scientific Aspects of Marine Pollution) 1991a Coastal Modelling. *GESAMP Reports and Studies* No. **43**, 192 pp.

GESAMP (IMO/FAO/UNESCO/WMO/WHO/IAEA/UN/UNEP Joint Group of Expert on the Scientific Aspects of Marine Pollution) 1991b Reducing Environmental Impacts of Coastal Aquaculture. *GESAMP Reports and Studies No.* **47**, 39 pp.

GESAMP (IMO/FAO/UNESCO/WMO/WHO/IAEA/UN/UNEP Joint Group of Expert on the Scientific Aspects of Marine Pollution) 1996 Monitoring the ecological effects of Coastal aquaculture Wastes. *GESAMP Reports and Studies No.* **57**, 38 pp.

Gowen, R.J. and Bradbury, N.B. 1987 The Ecological Impacts of Salmonid Farming in Coastal Waters: A Review. *Oceanography Marine Biology Annual Review*, **24**, 563-575.

Gowen, R.J., Brown, J.R., Bradbury, N.B. and McLusky, D.S. 1988 Investigations into benthic enrichment, hypernutrification and eutrophication associated with mariculture in Scottish coastal waters (1984-1988). Report to the Highlands and Islands Development Board, Crown Estate Commissioners, Nature Conservancy Council, Countryside Commission for Scotland and Scottish Salmon Growers Association. 289 pp.

Gowen, R.J., Bradbury, N.B. and Brown, J.R. 1989 The use of simple models in assessing two of the interactions between fish farming and the marine environment. In *Aquaculture-a biotechnology in progress*, ed. N. De Pauw, E., Jaspers and N. Wilkins, pp. 1071-1080. European Aquaculture Society, Belgium.

Gowen, R.J., Smyth, D. and Silvert, W. 1994 Modelling the spatial distribution and loading of organic fish farm waste to the seabed. In *Modelling Benthic Impacts of Organic Enrichment from Marine Aquaculture*, ed. B.T. Hargrave, pp. 19-30. Canadian Technical Report of Fisheries and Aquatic Sciences, Canada.

Hargrave, B.T. 1994 A benthic enrichment index. In *Modelling Benthic Impacts of Organic Enrichment from Marine Aquaculture*, ed. B.T. Hargrave, pp. 79-91. Canadian Technical Report of Fisheries and Aquatic Sciences, Canada.

Hevia, M., Rosenthal, H. and Gowen, R.J. 1996 Modelling benthic deposition under fish cages. *Journal of Applied Ichthyology*, **12**, 71-74.

Holme, N.A, and McIntyre, A.D. 1971 *Methods for the Study of marine Benthos*. Blackwell Scientific Publications, Oxford, 334 pp.

Inoue, H. 1972 On water exchange in a net cage stocked with the fish Kamachi. Bulletin of the Japanese Society of Scientific Fisheries, **44**, 659-664.

Jørgensen, E.S. 1991 Introduction to environmental management modelling. In Application of Ecological Modelling in Environmental Management, ed. P.E. Hansen and S.E. Jørgensen, pp. 45-98. Elsevier, Amsterdam.

Penczak, T., Galicka, W., Molinshi, M., Kusto, E. and Zalewski, M. 1982 The enrichment of a mesotrophic lake by carbon, phosphorus and nitrogen from the cage aquaculture of rainbow trout (*Salmo gairderi*). *Journal of Applied Ecology*, **19**, 371-393.

Scottish Executive. 1999 *Policy Guidance Note: Locational Guidelines for the Authorisation of Marine Fish farms in Scottish Waters*. Scottish Executive, Edinburgh. pp.152.

Silvert, W. 1992 Assessing environmental impacts of finfish aquaculture in marine waters. *Aquaculture*, **107**, 67-79.

Silvert, W. 1994 Modelling benthic and impacts of organic matter loading. In *Modelling Benthic Impacts of Organic Enrichment from Marine Aquaculture*, ed. B.T. Hargrave, pp. 1-18. Canadian Technical Report of Fisheries and Aquatic Sciences, Canada.

Sowles, J.W., Churchill, L. and Silvert, W. 1994 The effect of benthic carbon loading on degradation of bottom conditions under farm sites. In *Modelling Benthic Impacts of Organic Enrichment from Marine Aquaculture*, ed. B.T. Hargrave, pp. 31-46. Canadian Technical Report of Fisheries and Aquatic Sciences, Canada.

Sunday-Tim 1996 Coupling Vadose Zone Models with GIS: Emerging Trends and Potent Bottlenecks. *Journal of Environmental Quality*, **25**, 535-544.

Telfer, T.C. 1995 Modelling of environmental loading: a tool to help fish cage managers. *Aquaculture News*, **20**, 17.

Warren-Hansen, I. 1982 Report on EIFAC on fish farm effluents. In *Evaluating matter discharged from trout farming*, ed. J.S. Alabaster, pp. 57-63. EIFC Technical. Papers.